NUREG–1464

NRC Iterative Performance Assessment Phase 2

Development of Capabilities for Review of a Performance Assessment for a High–Level Waste Repository

U.S. Nuclear Regulatory Commission

Office of Nuclear Material Safety and Safeguards

Office of Nuclear Regulatory Research

Center for Nuclear Waste Regulatory Analyses

AVAILABILITY NOTICE

Availability of Reference Materials Cited in NRC Publications

Most documents cited in NRC publications will be available from one of the following sources:

1. The NRC Public Document Room, 2120 L Street, NW., Lower Level, Washington, DC 20555-0001
2. The Superintendent of Documents, U.S. Government Printing Office, P. O. Box 37082, Washington, DC 20402-9328
3. The National Technical Information Service, Springfield, VA 22161-0002

Although the listing that follows represents the majority of documents cited in NRC publications, it is not intended to be exhaustive.

Referenced documents available for inspection and copying for a fee from the NRC Public Document Room include NRC correspondence and internal NRC memoranda; NRC bulletins, circulars, information notices, inspection and investigation notices; licensee event reports; vendor reports and correspondence; Commission papers; and applicant and licensee documents and correspondence.

The following documents in the NUREG series are available for purchase from the Government Printing Office: formal NRC staff and contractor reports, NRC-sponsored conference proceedings, international agreement reports, grantee reports, and NRC booklets and brochures. Also available are regulatory guides, NRC regulations in the *Code of Federal Regulations*, and *Nuclear Regulatory Commission Issuances*.

Documents available from the National Technical Information Service include NUREG-series reports and technical reports prepared by other Federal agencies and reports prepared by the Atomic Energy Commission, forerunner agency to the Nuclear Regulatory Commission.

Documents available from public and special technical libraries include all open literature items, such as books, journal articles, and transactions. *Federal Register* notices, Federal and State legislation, and congressional reports can usually be obtained from these libraries.

Documents such as theses, dissertations, foreign reports and translations, and non-NRC conference proceedings are available for purchase from the organization sponsoring the publication cited.

Single copies of NRC draft reports are available free, to the extent of supply, upon written request to the Office of Administration, Distribution and Mail Services Section, U.S. Nuclear Regulatory Commission, Washington, DC 20555-0001.

Copies of industry codes and standards used in a substantive manner in the NRC regulatory process are maintained at the NRC Library, Two White Flint North, 11545 Rockville Pike, Rockville, MD 20852-2738, for use by the public. Codes and standards are usually copyrighted and may be purchased from the originating organization or, if they are American National Standards, from the American National Standards Institute, 1430 Broadway, New York, NY 10018-3308.

NUREG–1464

NRC Iterative Performance Assessment Phase 2

Development of Capabilities for Review of a Performance Assessment for a High–Level Waste Repository

Manuscript Completed: August 1994
Date Published: October 1995

Editors:
R. G. Wescott, M. P. Lee, N. A. Eisenberg
Office of Nuclear Material Safety and Safeguards

T. J. McCartin
Office of Nuclear Regulatory Research

Nuclear Regulatory Commission
Washington, D.C. 20555-0001

and

R. G. Baca
Center for Nuclear Waste Regulatory Analyses
San Antonio, TX 78228–0510

ABSTRACT

In order to better review a potential license application to construct and operate a geologic repository for spent nuclear fuel and high-level radioactive waste (HLW), the Nuclear Regulatory Commission staff (and its contractor) has expanded and improved its capability to conduct performance assessments. This report documents the demonstration of the second phase of this capability. The demonstration made use of the scenario selection procedure developed by Sandia National Laboratories to provide a set of scenarios, with corresponding probabilities, for use in the consequence analysis of a potential HLW disposal site in unsaturated tuff. Models of release of radionuclides from the waste form and transport in ground water, air and by direct pathways provided preliminary estimates of releases to the accessible environment for a 10,000 year period. The input values of parameters necessary for the consequence models were sampled numerous times using Latin Hypercube Sampling from assumed probability distributions. The results from the consequence models were then used to generate Complementary Cumulative Distribution Functions (CCDFs) for either release to the accessible environment or effective dose equivalents to a target population. CCDFs were calculated for probabilistically significant combinations (scenarios) of four disruptive events; drilling, pluvial climate, seismicity and magmatism. Sensitivity and uncertainty analyses of the calculated releases and effective dose equivalents were also used to determine the importance of the parameters. Because of the preliminary nature of the analysis and the lack of an adequate data base, the results and conclusions presented in this report should be carefully interpreted. They should not be misconstrued to represent the actual performance of the proposed Yucca Mountain repository nor serve as an endorsement of the methods used.

Table of Contents

	Page
Abstract	iii
Executive Summary	xxi
Table Showing English/Metric System Conversion Factors	xxviii
Acknowledgments	xxxi
1 Introduction *M.P. Lee/NMSS, R.G. Wescott/NMSS, N.A. Eisenberg/NMSS, and J.S. Trapp/NMSS*	1–1
1.1 NRC'S Iterative Performance Assessment Program	1–1
1.1.1 Background	1–1
1.1.2 Objectives	1–1
1.1.3 Regulatory Basis for IPA	1–2
1.1.4 Steps in Performing a Total-System Performance Assessment	1–3
1.2 IPA Phase 2: Overview	1–5
1.2.1 Purpose and Scope	1–5
1.2.2 IPA Organization and Staffing	1–6
1.2.3 Quality Assurance	1–6
1.2.4 Approach and Content of the Report	1–9
1.2.5 Improvements Since Phase 1	1–10
1.3 Description of the Modeled System	1–15
1.3.1 Site Description	1–15
1.3.2 Repository Description (Including the Waste Package and Contained Waste Form)	1–18
1.3.3 IPA Phase 2 System Model and Methodology	1–20
2 Total-System Performance Assessment Computer Code *R.W. Janetzke/CNWRA and B. Sagar/CNWRA*	2–1
2.1 Operational Description	2–1
2.1.1 Introduction	2–1
2.1.2 Code Organization	2–1
2.1.3 TPA Module Descriptions	2–3
2.1.4 Data Handling and Control	2–7
2.1.5 Sampled vs. Global Data	2–8
2.2 Improvements and Changes Since IPA Phase 1	2–8
2.3 Conclusions and Suggestions for Future Work	2–10
3 Scenario Analysis Module *J.R. Park/NMSS, J.S. Trapp/NMSS, A–B Ibrahim/NMSS, M.P. Miklas/CNWRA, and N.A. Eisenberg/NMSS*	3–1

Table of Contents (continued)

		Page
3.1	Introduction	3–1
3.2	Description of the SNL Scenario Selection Procedure	3–1
3.2.1	Step No. 1—Identification of Events and Processes	3–2
3.2.2	Step No. 2—Classification of Events and Processes	3–2
3.2.3	Step No. 3—Screening of Events and Processes	3–2
3.2.4	Step No. 4—Combination of Events and Processes into Scenarios	3–2
3.2.5	Step No. 5—Screening of Scenarios	3–3
3.3	IPA Phase 2 Scenario Development Using the SNL Methodology	3–3
3.3.1	Identification and Classification of Events and Processes	3–3
3.3.2	Screening of Events and Processes	3–5
3.3.2.1	Rationales Used to Screen Events and Processes	3–6
3.3.2.2	Rationales Used to Retain Events and Processes for Further Consideration	3–7
3.3.3	Combination of Events and Processes into Scenario Classes	3–28
3.3.4	Screening of Scenario Classes	3–33
3.4	Discussion of Results	3–33
4	Flow and Transport Module *T.J. McCartin/RES, W.H. Ford/NMSS, R.G. Wescott/NMSS, and R. B. Codell/NMSS*	4–1
4.1	Introduction: Consequence Models for Flow and Radionuclide Transport	4–1
4.2	Flow and Radionuclide Transport Model for Ground-Water Releases	4–1
4.2.1	Site Concepts	4–1
4.2.2	Recent Modeling Studies	4–10
4.2.3	Site Conceptual Model	4–12
4.2.3.1	Stratigraphy	4–12
4.2.3.2	Boundary Conditions	4–19
4.2.3.3	Site Parameters	4–26
4.2.4	Computational Model Description	4–31
4.2.4.1	Computational Strategy	4–31
4.2.4.2	Selection and Development of Computational Model(s)	4–31
4.2.4.3	Site Representation	4–36
4.3	Flow and Radionuclide Transport Module for Gaseous Releases	4–38
4.3.1	Governing Equations	4–38
4.3.2	NRC Model	4–41
4.3.3	Application to Yucca Mountain	4–42
4.3.4	Parameters and Modeled Results	4–42

Table of Contents (continued)

Page

4.4 Flow and Transport Auxiliary Analyses 4–45

4.4.1 Evaluation of the SNL Technology: Testing of the *DCM3D* Computer Code ... 4–53
B. Sagar/CNWRA, L. Tweedy/SwRI, T.J. McCartin/RES, and A.B. Gureghian/CNWRA

4.4.2 Evaluation of the K_d Assumption 4–53
J.W. Bradbury/NMSS

4.4.3 Regional Flow Analysis 4–55
M.P. Ahola/CNWRA

4.4.4 Effects of Stratification, Dip of Strata, and Sub-Vertical Faults 4–59
A.C. Bagtzoglou/CNWRA

4.4.5 Exploration of Dual-Continum Flow Modeling Concepts 4–60
W.H. Ford/NMSS

4.4.6 Release and Transport of Potentially Gaseous Radionuclides Other than ^{14}C during Volcanism and Normal Operations 4–61
R.B. Codell/NMSS

4.4.7 Evaluation of USGS Ground-Water Modeling for the Region That Includes Yucca Mountain 4–62
N.M. Coleman/NMSS

4.4.8 Modeling Saturated Flow to the Accessible Environment 4–62
W.H. Ford/NMSS

4.4.9 Geochemical Model for ^{14}C Transport in Unsaturated Rock 4–63
R.B. Codell/NMSS and W.M. Murphy/CNWRA

4.4.10 The Exchange of Major Cations at Yucca Mountain 4–63
H.M. Astwood/NMSS

4.4.11 Considerations in Modeling Infiltration at Yucca Mountain 4–64
J.A. Pohle/NMSS and T.J. McCartin/RES

4.4.12 Comparison of *NEFTRAN II* to *UCBNE41* 4–65
M.R. Byrne/NMSS

4.5 Conclusions and Suggestions for Further Work 4–66

5 Source Term Module 5–1
R.B. Codell/NMSS, J.C. Walton/CNWRA[1], and B. Sagar/CNWRA

5.1 Introduction 5–1

5.2 Overall Structure of the Source Term Code 5–1

5.2.1 Conceptual Model 5–1

5.2.2 Input to and Output from *SOTEC* 5–2

5.2.3 Structure of Calculations 5–2

5.2.4 Radionuclide Inventory 5–5

5.3 Waste Package Environment 5–5

5.3.1 Introduction 5–5

[1]Now with the Department of Civil Engineering at the University of Texas, El Paso.

Table of Contents (continued)

		Page
5.3.2	Thermal Environment	5–5
5.3.3	Hydrologic Environment	5–6
5.3.4	Interaction of Liquid Water with Waste Form: Direct Contact	5–7
5.3.5	Ensemble Averaging	5–7
5.3.6	Geochemical Environment	5–8
5.4	Waste Package Failure Modes	5–8
5.4.1	Corrosion Models	5–8
5.4.1.1	General Corrosion	5–8
5.4.1.2	Crevice Corrosion	5–9
5.4.1.3	Pitting Corrosion	5–9
5.4.2	Temperature Model for Source Term	5–9
5.4.2.1	Introduction	5–9
5.4.2.2	Heat Transfer in Yucca Mountain	5–10
5.4.2.3	Thermal Loading of the Repository	5–10
5.4.2.4	NRC Temperature Model	5
5.4.2.5	Use of the Temperature Model	5–15
5.4.2.6	Extent of Possible Errors in NRC Temperature Model	5–15
5.5	Structural Failure Models	5–15
5.5.1	Introduction	5–15
5.5.2	Buckling Evaluation	5–16
5.6	Waste Dissolution and Radionuclide Releases	5–16
5.6.1	Introduction	5–16
5.6.2	Waste Dissolution	5–18
5.6.2.1	Effective Waste Package Failure Time	5–18
5.6.2.2	Solubility Limited Release	5–20
5.6.2.3	Advective Mass Transfer	5–20
5.6.2.4	Diffusive Mass Transfer	5–20
5.6.2.5	Treatment of Colloids	5–21
5.6.3	Calculations of Gaseous Releases of ^{14}C	5–21
5.6.3.1	Introduction	5–21
5.6.3.2	Prompt Release Fraction	5–22
5.6.3.3	Cladding Integrity	5
5.6.3.4	Release of ^{14}C from Oxidation of Cladding	5
5.6.3.5	Release from UO_2	5–25

Table of Contents (continued)

		Page
5.7	Source Term Auxiliary Analyses	5–31
5.7.1	Ensemble Averaging for Source Term Parameters *R.B. Codell/NMSS*	5–36
5.7.2	Release and Transport of Potentially Gaseous Radionuclides Other than ^{14}C during Volcanism and Normal Operations *R.B. Codell/NMSS*	5–36
5.8	Conclusions and Suggestions for Further Work	5–37
6	Disruptive Consequence Analysis	6–1
6.1	Overall Approaches for Treating Consequences of Disruptive Events *P.C. Lichtner/CNWRA, R.D. Manteufel/CNWRA, and R.B. Codell/NMSS*	6–1
6.2	Treatment of Climate *M.P. Miklas/CNWRA*	6–2
6.3	Improved Drilling Model and Code *N.A. Eisenberg/NMSS and J.R. Firth/NMSS*	6–2
6.3.1	Introduction	6–2
6.3.2	Model for Release of Radionuclides from the Rock Column	6–3
6.3.3	Consequences	6–4
6.3.4	Hit Probability	6–5
6.3.5	Radionuclide Inventory Determination	6–5
6.3.6	Overview	6–7
6.4	Improved Seismic Scenarios Model and Code *R.B Codell/NMSS, N.A. Eisenberg/NMSS, A.A. O'Campo/SwRI, and C.J. Freitas/SwRI*	6–7
6.4.1	Introduction	6–7
6.4.2	Response of Waste Package to Seismic Shaking	6–7
6.4.3	Waste Package Fragility	6–10
6.4.4	Computational Algorithm for Seismic Failure of Waste Packages	6–10
6.4.5	Estimating Probability of Seismic Failure Scenario	6–11
6.5	Improved Magmatic Scenarios Model and Code *R.G. Baca/CNWRA, R.D. Manteufel/CNWRA, C.S. Lin/SwRI, and R. Drake/SwRI*	6–13
6.5.1	Introduction	6–13
6.5.2	Relevant Literature	6–14
6.5.3	Description of Modeling Approach	6–15
6.5.3.1	Introduction	6–15
6.5.3.2	Simulation Procedure	6–15
6.5.3.3	Assumptions and Limitations	6–18
6.5.3.4	Summary	6–18
6.6	Overall Conclusions and Suggestions for Further Work	6–19

Table of Contents (continued)

		Page
7	Dose-Assessment Module *R.B. Neel/NMSS*	7-1
7.1	Background	7-1
7.2	Basis for the Calculation of Human Exposures in IPA Phase 2	7-1
7.2.1	Concept of the "Reference Biosphere"	7-1
7.2.2	Similarity to Assumptions in 40 CFR Part 191	7-2
7.2.3	Similarity to the Approach Taken by BIOMOVS	7-2
7.3	Computer Code Selected for Dose Assessment	7-2
7.3.1	Overview of *DITTY*	7-2
7.3.2	General Approach to Dose Calculations in *DITTY*	7-3
7.3.3	Calculation of Total Dose in *DITTY*	7-3
7.3.4	Selection of *DITTY* Model Parameters	7-5
7.4	Differences From Internal Dosimetry Models in ICRP-30	7-5
7.5	Selection of DCFs for this Study	7-5
7.5.1	DCFs for Ingestion and Inhalation	7-5
7.5.2	DCFs for External Exposure	7-6
7.6	Selection of Parameters for the Ingestion Pathways	7-6
7.6.1	Drinking-Water Parameters	7-6
7.6.2	Food-Transfer Parameters	7-6
7.6.3	Growing-Season Parameters	7-7
7.6.4	Irrigation Rate for Crops	7-7
7.6.5	Crop Yields	7-7
7.7	Selection of Parameters for the Inhalation Pathways	7-8
7.7.1	Meteorological Data	7-8
7.7.2	Regional Population Distribution at Yucca Mountain	7-8
7.8	Application of the Dose-Assessment Methodology to Yucca Mountain: Biosphere Scenarios	7-8
7.8.1	Application of the "Critical-Group" Concept	7-8
7.8.2	Hypothetical Biosphere Scenario: Waterborne Release	7-8
7.8.3	More Realistic Biosphere Scenario: Waterborne Release	7-11
7.8.4	Hypothetical Biosphere Scenarios: Airborne Releases	7-11
7.9	Conclusions and Possible Considerations for Future Dose Assessments	7-12
7.9.1	Conclusions	7-12
7.9.2	Considerations for Future Dose Assessments	7-12

Table of Contents (continued)

		Page
8	Sensitivity and Uncertainty Analysis *V. Colten-Bradley/NMSS, R.B. Codell/NMSS, and M.R. Byrne/NMSS*	8–1
8.1	Introduction	8–1
8.2	Overview of Techniques and Methods	8–1
8.2.1	Background	8–1
8.2.2	IPA Phase 1 Sensitivity and Uncertainty Analyses	8–1
8.2.2.1	Sensitivity Analyses	8–1
8.2.2.2	Uncertainty Analyses	8–2
8.2.3	Techniques	8–2
8.3	Selection of Most Influential Independent Parameters	8–2
8.3.1	Subset Selection by Stepwise Regression Analysis	8–2
8.3.2	Compartmental Component Analysis	8–7
8.3.2.1	Contribution of Individual Nuclides to *Normalized Release* and *Effective Dose Equivalent*	8–8
8.3.2.2	Releases by Pathway	8–8
8.3.3	Significance of Independent Parameters—Kolmogorov-Smirnov Test and Sign Test	8–8
8.3.3.1	The Kolmogorov-Smirnov Test	8–14
8.3.3.2	The Sign Test	8–14
8.4	Sensitivity Analysis	8–14
8.4.1	Introduction	8–14
8.4.2	Estimation of Sensitivities by Regression Analysis	8–17
8.4.2.1	Standardization	8–17
8.4.2.2	Rank Transformation	8–17
8.4.3	Estimation of Sensitivities by Differential Analysis	8–17
8.4.4	Comparison of Sensitivity Coefficients Estimated from Regression and Differential Analyses	8–18
8.4.5	Model Sensitivity Analysis	8–18
8.4.5.1	CCDF Sensitivity	8–18
8.4.5.2	Sensitivity of Results to Number of Vectors	8–19
8.5	Uncertainty Analysis	8–20
8.6	Emulation of the Total-System Performance Assessment Model Using Multilinear Regression	8–24
8.6.1	Estimation of the Response	8–24
8.6.2	Evaluation of the Goodness of Fit	8–26

Table of Contents (continued)

Page

8.6.2.1 Correlation Coefficient 8–26
8.6.2.2 Mallows' C_p Statistic 8–26

8.7 Sensitivity and Uncertainty Auxiliary Analyses 8–29
Y.T. Wu/CNWRA, A.B. Gureghian/CNWRA, and R.B. Codell/NMSS

8.8 Conclusions and Suggestions for Further Work 8–30

9 Analytical Results 9–1
R.G. Wescott/NMSS, R.B. Codell/NMSS, and V. Colten-Bradley/NMSS

9.1 Introduction and Caveats Concerning the Results of IPA Phase 2 9–1
9.2 Conditional CCDFs and Exceedance Probability Curves 9–2
9.2.1 Construction of the CCDFs 9–2
9.2.1.1 Conditional CCDFs 9–2
9.2.1.2 Screened Conditional CCDFs 9–2
9.2.1.3 Total CCDF 9–2
9.2.1.4 "Hair" Diagrams 9–3

9.2.2 Conditional CCDFs for Various Scenario Classes ..... [illegible]
9.2.3 Basic Scenarios ..... [illegible]

9.3 Total System CCDF 9–13
9.4 Differences Between IPA Phases 1 and 2, and Comparison of Results 9–13
9.4.1 Improvements in IPA Phase 2 Likely to Affect Results 9–13
9.4.1.1 Scenarios 9–13
9.4.1.2 Pathways 9–13
9.4.1.3 Source Term 9–18

9.4.2 Possible Reasons for Differences in Results 9–18
9.4.3 Conclusions 9–20

9.5 Effects of Modeled Performance of Natural and Engineered Barriers on Total System Performance 9–20
9.5.1 Effect of Travel Time of Water through Geosphere 9–21
9.5.2 Effect of Release Rate from the EBS 9–23
9.5.3 Effect of Waste Package Lifetime 9–23
9.5.4 Effects of the Performance of All Natural and Engineered Barriers 9–23

9.6 Illustration of Individual Annual Dose Calculation 9–23
M.R. Byrne/NMSS

9.7 Summary and Conclusions ..... [illegible]

10 Conclusions and Recommendations ..... [illegible]
IPA Phase 2 Staff

Table of Contents (continued)

		Page
10.1	Introduction	10–1
10.2	Evaluation of IPA Phase 2 Methodology and Scientific Bases for Analyses	10–1
10.2.1	Adequacy of Methodology	10–1
10.2.2	Adequacy of Scientific Basis for the IPA Phase 2 Analyses	10–3
10.2.3	Conclusions Regarding IPA Phase 2 Methodology and Analyses	10–3
10.3	Insights and Conclusions from IPA Phase 2	10–4
10.3.1	Significant Insights and Conclusions from Model Development and from the Sensitivity and Uncertainty Analyses	10–4
10.3.2	Insights and Conclusions Regarding System and Subsystem Performance	10–6
10.4	Recommendations	10–8
10.4.1	Recommendations for Additional Scientific Input	10–8
10.4.2	Recommendations Regarding Modeling Improvements and Supporting Analyses in NRC's IPA Activities	10–9
10.4.2.1	TPA Computer Code	10–9
10.4.2.2	Scenario Analysis Module	10–9
10.4.2.3	Flow and Transport Module	10–10
10.4.2.4	Source Term Module	10–11
10.4.2.5	Disruptive Consequence Analysis	10–12
10.4.2.6	Dose Assessment Module	10–13
10.4.2.7	Sensitivity and Uncertainty Analysis	10–13
11	References	11–1

Figures

1–1	Components of a Total–System Performance Assessment	1–4
2–1	Flow Diagram Showing the Elements of the Total-System Performance Assessment Computer Code	2–2
3–1	Potential Combinations of Two Releases and Three Transport Phenomena	3–4
3–2	Calderas of the Southwest Nevada Volcanic Field near Yucca Mountain	3–9
3–3	Proposed Crater Flat Volcanic Zone	3–11
3–4	Proposed Area of Most Recent Volcanism	3–12
3–5	Postulated AMRV and "High-Risk" Zones	3–13
3–6	Basic Steps in a Probabilistic Seismic Hazard Analysis	3–19
3–7	Annual Probability of Exceedance versus Peak Ground Acceleration for Several Faults near Yucca Mountain	3–20
3–8	Comparison of Annual Probability of Exceedance versus Peak Ground Acceleration by Location of Faults	3–21

Figures (continued)

		Page
3–9	Annual Probability of Exceedance of Peak Surface Rupture Displacement for the Paintbrush Canyon, Midway Valley, Bow Ridge, Ghost Dance, and Sever Wash Faults	3–22
3–10	Precipitation and Temperature Variation over the Past 45,000 Years in the Vicinity of the Nevada Test Site	3–26
3–11	Combinations of Events and Processes into Scenario Classes	3–30
3–12	Probabilities of Scenario Classes for IPA Phase 2 Generated by Combinations of Probabilities of Occurrence of Constituent Events and Processes	3–31
3–13	Scenario Classes with Generated Probabilities Greater than 1×10^{-4} in 10,000 Years	3–32
4–1	Location of the Yucca Mountain Site	4–2
4–2	East-West Geologic Cross-Section for the Yucca Mountain Site	4–3
4–3	Locations of Faults, Drill Holes, and Generated Cross-Sections	4–4
4–4	Cross-Section L–L′	4–6
4–5	Hypothetical Example of a "Combined" Transport Stratigraphy that Accounts for Hydrologic and Geochemical Stratification	4–11
4–6	Location of Seven Selected Boreholes Used to Define the Hydrogeologic Units for Seven Repository Sub-Areas	4–[illegible]
4–7	Depiction of Changes, in Hydrogeologic Units, along the Surface of the Water Table from beneath the Proposed Repository to the Accessible Environment	4–17
4–8	Depiction of Changes, in Hydrogeologic Units, along the Surface of the Water Table, under Pluvial Conditions that was Used for the Saturated Zone Model	4–21
4–9	Depiction of the Assumed Radionuclide Plume Width Used for Calculating Concentrations at a Well Located at the Accessible Environment Boundary	4–24
4–10	Graphical Representation of the Correlation Length of a Hydrogeologic Unit and its Relationship to the Calculation of a Representative Conductivity	4–27
4–11	Illustration of a Representative Flow Path for a Sub-Area of the Repository, Assuming One-Dimensional Flow in Both the Saturated and Unsaturated Zones	4–32
4–12	Depiction of the Hydrologic Units and Boundary Conditions Used to Evaluate the Spatial Variation of Percolation at the Repository Depth	4–35
4–13	Depiction of the Multiple Transport Paths, Based on Four Different Hydrogeologic Units and the Indicated Combinations of Fracture and Matrix Flow	4–38
4–14	^{14}C Module Logic Diagram	4–43
4–15	Modeled Repository Section	4–44
4–16	Vapor Flux at Ambient Conditions	4–46
4–17	Vapor Flux at 500 Years after Permanent Closure of the Geologic Repository	4–47
4–18	Vapor Flux at 5,000 Years After Permanent Closure of the Geologic Repository	4–48
4–19	Vapor Flux at 10,000 Years After Permanent Closure of the Geologic Repository	4
4–20	Paths and Travel Times for Design Thermal Loading	4–[illegible]

Figures (continued)

		Page
4–21	Paths and Travel Times for 2 × the Design Thermal Loading	4–51
4–22	Paths and Travel Times for .5 × the Design Thermal Loading	4–52
4–23	Location of Recharge and Discharge Areas for the Regional Model	4–57
4–24	Water-Table Rise at Yucca Mountain as a Function of Increased Recharge Rate	4–58
4–25	Maximum Water-Table Rise at Yucca Mountain as a Function of Intrusive Dike Orientation	4–58
4–26	Discharge Rates for ^{243}Am Computed By *NEFTRAN II* and *UCBNE41* in a Benchmarking Exercise	4–67
4–27	Discharge Rates for ^{239}Pu Computed By *NEFTRAN II* and *UCBNE41* in a Benchmarking Exercise	4–68
4–28	Discharge Rates for ^{235}U Computed By *NEFTRAN II* and *UCBNE41* in a Benchmarking Exercise	4–69
5–1	*SOTEC*—Source Term Code Input and Output Files	5–3
5–2	*SOTEC* Code	5–4
5–3	Representation of Waste Package Canisters and Waste Emplacement Panels in Temperature Model	5–11
5–4	Grouping of Waste Package Canisters and Waste Emplacement Panels in Temperature Model	5–13
5–5	Dissolved Radionuclide-Release Model	5–17
5–6	Locations of Radionuclides in Spent Nuclear Fuel	5–19
5–7	^{14}C Gaseous Release Model	5–26
5–8	Fit of Temperature Difference between Waste Package Container Skin and Maximum Fuel	5–29
5–9a	Model-Prototype Comparison, 250°C	5–32
5–9b	Model-Prototype Comparison, 225°C	5–32
5–9c	Model-Prototype Comparison, 200°C	5–33
5–9d	Model-Prototype Comparison, 195°C	5–33
5–9e	Model-Prototype Comparison, 175°C	5–34
5–9f	Model-Prototype Comparison, 155°C	5–34
5–9g	Model-Prototype Comparison, 130°C	5–35
5–9h	Model-Prototype Comparison, 109°C	5–35
6–1	Representation of Waste Package Canister for Improved Seismic Scenarios Model	6–8
6–2	Waste Package Canister Thickness versus Time for Seven Repository Sub-Areas for the Base Case Scenario	6–12
6–3	Configuration of the Geologic Repository in the Magmatic Scenarios Simulation	6–16
7–1	Human Exposure Pathways in the Accessible Environment, as Calculated by the *DITTY* Computer Code	7–4

Figures (continued)

		Page
7–2	Estimated Population Distribution in the Vicinity of Yucca Mountain, Nevada	7–9
8–1	Example Boxplot Showing Interquartile Region, the Whiskers at 1.5 × and Outliers in the Distribution	8–7
8–2	Absolute Contributions to *Normalized Release* by Selected Radionuclides, Base Case Scenario	8–9
8–3	Absolute Contributions to *Effective Dose Equivalent* by Selected Radionuclides	8–10
8–4	Absolute Contributions to *Normalized Release* by Selected Radionuclides, Fully Disturbed Scenario	8–11
8–5	Absolute Contributions to *Effective Dose Equivalent* by Selected Radionuclides, Fully Disturbed Scenario	8–12
8–6	Fractional Contributions to *Normalized Release* by Geosphere Pathway	8–13
8–7	Distribution Functions used in the Kolmogorov-Smirnov Test	8–15
8–8	Maximum Spurious Correlations among Independent Parameters versus Correlations between Model Output and Independent Parameters for 100 Vectors	8–21
8–9	Maximum Spurious Correlations among Independent Parameters versus Correlations between Model Output and Independent Parameters for 400 Vectors	8–22
8–10	Sensitivity of Base Case Scenario CCDF to the Number of Vectors	8–23
8–11	Plot of Residuals from Multilinear Regression as a Test for Heteroscedasticity	8–25
8–12	Plot of Predicted Response from Multilinear Regression Analysis versus *Normalized Release* Calculated by the TPA Computer Code, Base Case Scenario	8–27
8–13	Comparison of CCDFs for Predicted Response from the TPA Computer Code, Base Case Scenario	8–28
9–1	Conditional CCDFs for *Normalized Release* for Basic Scenarios	9–5
9–2	Conditional CCDFs for *Effective Dose Equivalent*	9–6
9–3	Scenario Plot of Pluvial Scenario versus Base Case Scenario	9–7
9–4	Scenario Plot of Drilling Scenario versus Base Case Scenario	9–9
9–5a	Scenario Plot of Seismic Scenario versus Base Case Scenario	9–10
9–5b	Scenario Plot of Seismic Scenario versus Base Case Scenario (Liquid Releases Only)	9–11
9–6	Scenario Plot of Magmatic Scenario	9–12
9–7a	Total CCDF for *Normalized Release* from Significant Scenarios	9–14
9–7b	Total CCDF for *Effective Dose Equivalent* from Significant Scenarios	9–15
9–8a	"Hair Diagram" Showing All *Normalized Release* Vectors	9–16
9–8b	Percentile Values of Release Vectors from "Hair Diagrams"	9–17
9–9	Comparison of CCDFs for IPA Phase 1 and Phase 2 Results	9–19
9–10a	Scatter Plots of Liquid Travel Times	9–23
9–10b	CCDF Sensitivity Plot for "Fastest" Liquid Travel Time	9–24

Figures (continued)

		Page
9–11	CCDF Sensitivity Plot for Release Rate from EBS	9–25
9–12a	Distribution of Waste Package Failure Times for Base Case Scenario	9–26
9–12b	CCDF Sensitivity Plot for Waste Package Failure Times for Base Case Scenario	9–27
9–12c	CCDF Sensitivity Plot for Waste Package Failure Times for Base Case Scenario (Gaseous Release Only)	9–28
9–12d	Scatter Plots of Releases to Environment versus Waste Package Failure Times for Base Case Scenario	9–29
9–12e	Scatterplots of EBS Release Rates versus Time of Release for Base Case Scenario	9–30
9–13	CCDF Sensitivity Plot for All 10 CFR Part 60 Subsystem Requirements	9–31
9–14	Illustration of Annual Individual Dose Calculation	9–32
10–1	CCDF for Dissolved Radionuclides, Base Case Scenario	10–5

Tables

1–1	Staff Participating in the IPA Phase 2 Scenario Analysis	1–7
1–2	Staff Participating in the Analysis of Scenarios used in the IPA Phase 2 Consequence Analysis	1–8
1–3	IPA Phase 1 Recommendations Implemented during IPA Phase 2	1–11
3–1	Initial Set of Potentially Disruptive Events and Processes	3–6
3–2	Significant Earthquakes in or near the Southern Great Basin ($M \geq 6.5$)	3–16
3–3	Significant Earthquakes in or near the Southern Great Basin ($M \geq 4.0$)	3–17
3–4	Scenario Classes Remaining after Screening	3–33
4–1	Summary of Hydrogeologic Properties of Hydrogeologic Units within the Unsaturated Zone at Yucca Mountain	4–7
4–2	Summary of Hydrogeologic Characteristics, as Determined through Laboratory and Field Measurements, of Major Stratigraphic Units in the Vicinity of Yucca Mountain	4–8
4–3	Elevations and Distances for Boreholes in the Vicinity of Yucca Mountain that Were Used to Define Hydrogeologic Units for the Unsaturated Flow Model	4–13
4–4	Hydrogeologic Unit Thickness and Location of Water Table for Boreholes in the Vicinity of Yucca Mountain	4–14
4–5	Hydrogeologic Unit Thickness to be Used in the Unsaturated Flow Model	4–16
4–6	Length of Hydrogeologic Unit Sequences along the Saturated Flow Paths for Each of the Seven Repository Sub-Areas	4–18
4–7	Hydrogeologic Unit Thickness to be Used in the Unsaturated Flow Model	4–20

Tables (continued)

		Page
4–8	Length of Hydrogeologic Unit Sequences along the Saturated Flow Paths for Each of the Seven Repository Sub-Areas	4–22
4–9	Permeability Zones Used to Determine the Range of Radionuclide Plume Depths for Transport in Fractures within the Saturated Zone	4–25
4–10	Matrix Representative Conductivities and Permeabilities for the Indicated Hydrogeologic Units and the Values Used to Calculate the Representative Values Based on 100 Data Realizations and the Calculational Approach Presented in Figure 4–10	4–28
4–11	Fracture Representative Conductivities and Permeabilities for the Indicated Hydrogeologic Units and the Values Used to Calculate the Representative Values Based on 100 Data Realizations and the Calculational Approach Presented in Figure 4–10	4–30
4–12	Hydrogeologic Parameters Used for Simulating Two-Dimensional Flow with *DCM3D*, to Analyze the Spatial Distribution of Percolation at the Repository Depth	4–34
4–13	Distribution of Percolation for the Seven Repository Sub-Areas, as Depicted in Figure 4–6	4–35
4–14	Variation of Matrix Flux versus the Total Flux for Each of the Hydrogeologic Units Simulated at Yucca Mountain	4–3
4–15	Selected Hydrologic Parameters for Yucca Mountain	4–45
4–16	Results of K_d Simulations	4–55
5–1	Initial Radionculide Inventory	5–5
5–2	Adjusted ^{14}C Content in Spent Nuclear Fuel	5–23
5–3	Diffusion of $^{14}CO_2$ from Surface Oxide	5–24
5–4	Model Parameters from Manual Identification	5–31
6–1	List of Disruptive Events, Their Corresponding LHS Parameters, and Whether Release of Radionuclides Associated with the Event Occurs Directly or Indirectly	6–3
6–2	The Distribution of Waste Packages by Repository Sub-Area	6–4
6–3	Parameters Used in the *SEISMO* Code	6–8
8–1	Scenario Classes Modeled in the IPA Phase 2 Analysis	8–3
8–2	Results of Stepwise and Multilinear Regression: *Normalized Release* for Base Case Scenario	8–4
8–3	Results of Stepwise and Multilinear Regression: *Effective Dose Equivalent* for Base Case Scenario	8–5
8–4	Results of Stepwise and Multilinear Regression: *Normalized Release* for Fully Disturbed Scenario	8–
8–5	Results of Stepwise and Multilinear Regression: *Effective Dose Equivalent* for Fully Disturbed Scenario	8–6

Tables (continued)

		Page
8–6	Important Variables Selected by the Kolmogorov-Smirnov and Sign Tests for the Base Case Scenario at the 0.05 Level of Significance	8–16
8–7	Comparison of First Derivatives of *Normalized Release* by Regression and Differential Analysis	8–19
9–1	Estimated Probabilities for the Scenario Classes Modeled in the IPA Phase 2 Analysis	9–3

Appendicies

A.	Latin Hypercube Sampled Input Parameters *IPA Phase 2 Staff*	A–1
B.	Hydrologic and Radionuclide Transport Data for the Ground-Water Pathway *T.J. McCartin/RES and J.W. Bradbury/NMSS*	B–1
C.	Evaluation of the Sandia National Laboratory Methodology: Testing of the *DCM3D* Computer Code *B. Sagar/CNWRA, L. Tweedy/SwRI, T.J. McCartin/RES, and A.B. Gureghian/CNWRA*	C–1
D.	K_d Approximation Testing *J.W. Bradbury/NMSS*	D–1
E.	Regional Flow Analysis *M.P. Ahola/CNWRA and B. Sagar/CNWRA*	E–1
F.	Effects of Stratification, Dip of Strata, and Sub-Vertical Faults *A.C. Bagtzoglou/CNWRA, R. Ababou/CNWRA, and B. Sagar/CNWRA*	F–1
G.	Exploration of Dual-Continum Flow Modeling Concepts *W.H. Ford/NMSS*	G–1
H.	Release and Transport of Potentially Gaseous Radionuclides Other than ^{14}C during Volcanism and Normal Operations *R.B. Codell/NMSS*	H–1
I.	Evaluation of U.S. Geological Survey Ground-Water Modeling for the Region that Includes Yucca Mountain *N.M. Coleman/NMSS*	I–1
J.	Modeling Saturated Zone Flow to the Accessible Environment *W.H. Ford/NMSS*	J–1
K.	Geochemical Model for ^{14}C Transport in Unsaturated Rock *R.B. Codell/NMSS and W.M. Murphy/CNWRA*	K–1
L.	The Exchange of Major Cations at Yucca Mountain *H.M. Astwood/NMSS*	L–1
M.	Ensemble Averaging for Source Term Parameters *R.B. Codell/NMSS*	M–1

EXECUTIVE SUMMARY

1 Introduction and Background

Phase 2 of the Nuclear Regulatory Commission Iterative Performance Assessment (IPA) program is the second major effort undertaken by the NRC staff and its contractor, the Center for Nuclear Waste Regulatory Analyses (CNWRA), to demonstrate the capability to review a performance assessment for a proposed geologic repository for spent nuclear fuel and high-level radioactive waste (HLW) at Yucca Mountain, Nevada. The primary objective of the IPA program is to develop, maintain, and enhance the NRC staff capability to review effectively performance assessments submitted for support of the U.S. Department of Energy's (DOE's) prelicensing activities such as site characterization, and for the license application. Additional and related objectives include:

- Evaluating the ongoing DOE site characterization program (including field studies, laboratory studies, and analyses, and interim performance assessments generated by DOE or its contractors).
- Evaluating the implementability of the 10 CFR Part 60 performance objectives.
- Providing input to the ongoing evolution of the radiation protection standard for the geologic repository, set forth by the U.S. Environmental Protection Agency (EPA) in 40 CFR Part 191, which is incorporated by reference in 10 CFR Part 60.
- Providing input to regulatory guidance and other regulatory products related to performance assessment, especially the staff's License Application Review Plan (LARP).
- Assisting in the definition of the Office of Nuclear Material Safety and Safeguards (NMSS) technical assistance and research programs in the area of HLW.

IPA Phase 1, completed in 1990 and published in 1992, was performed jointly by staff members from NMSS and the Office of Nuclear Regulatory Research. IPA Phase 2 involved considerably more sophistication in model and computer code development than Phase 1, including: (1) the preparation of an executive module to control and operate the computational modules comprising the total-system performance assessment (TPA) computer code; (2) the use of a much more mechanistic and detailed source term model and computer code; (3) more refined modeling of flow and transport in both saturated and unsaturated media, including the addition of gas flow to the transport analysis; (4) the inclusion of seismic and magmatic disruptive scenarios; and (5) the addition of a dose assessment capability. Many of the improvements to the IPA Phase 2 analysis were based, in part, on the preliminary recommendations made as a result of the insights gained from the Phase 1 effort. Planning for IPA Phase 2 began before the publication of the Phase 1 results. The IPA Phase 2 technical work began in 1991, was completed in 1993, and the documentation and review process continued into 1994.

It should be noted that the results presented in the following chapters have had limited formal review, are based on numerous simplifying assumptions, and use only limited site-specific data; thus, the numerical results should not be taken as representative of the performance of the proposed repository at Yucca Mountain, Nevada. The analysis is also replete with uncertainties regarding conceptual models for consequences and scenarios. In the conduct of this limited study, the authors did not encounter any definitive indications that the EPA standard could not be implemented. However, because of the incomplete scenario analysis in this demonstration, not all aspects of the EPA standard were tested (e.g., the difficulties in estimating scenario probabilities). Therefore, taking these tentative results of a preliminary analysis out of context, or separating these tentative results from these caveats, may lead to the inappropriate interpretation and use of the results.

Finally, this report should be considered as an interim demonstration of some of the methods that the NRC staff might use to review a performance assessment submitted by DOE as part of any potential license application. Thus, at the conclusion of some future phase of the IPA

effort, instruction to the NRC staff on which specific compliance determination methods will be used to review a DOE performance assessment will be developed and documented in the LARP. In the future, this work may also aid in developing guidance to DOE.

2 Purpose

As noted above, the primary purpose of IPA Phase 2 was to improve the capability of the NRC staff to conduct and evaluate calculations of key aspects of a total-system performance assessment for a proposed geologic repository. An independent assessment capability is considered to be an important aspect of the licensing review to be conducted by the NRC staff. Specific goals of IPA Phase 2 were to:

- Use the Tuff Performance Assessment Methodology developed by the Sandia National Laboratories (SNL);
- Provide for preliminary dose assessment capability;
- Provide a gas source term and transport capability;
- Provide an executive module to control run parameters;
- Improve the existing IPA source term code;
- Include the saturated zone in the evaluation of the ground-water pathway; and
- Include more disruptive scenarios in the performance assessment.

In addition, IPA Phase 2 achieved some worthwhile secondary goals, including:

- Limited evaluation of existing analytical tools to conduct a performance assessment (both methodologies and computer codes);
- Obtaining insight into the needs for the improvement of existing, or the development of new methodologies;
- Providing insights into the needs of site characterization; and
- Providing a smooth transition of contractor support from SNL to the CNWRA.

3 Scope

The scope of IPA Phase 2 consisted of the same basic steps as were performed for Phase 1 including: system and subsystem definitions; scenario analysis; and consequence analysis, including disruptive scenarios, analyses of results, and documentation. The IPA Phase 2 study included many improvements over Phase 1, which expanded the scope and are discussed in Section 1.2.5 of this report. The auxiliary analyses performed for IPA Phase 2 were performed by both NRC and CNWRA technical staff members and supported modeling in the areas of regional hydrology, site infiltration analysis, model testing, geochemistry, and source term.

The results of IPA Phase 2 included total and conditional complementary cumulative distribution functions (CCDFs) for summed normalized releases to the accessible environment and effective dose equivalents for the exposed population. Maximum concentrations of radionuclides in ground water were not compared with drinking water standards, and maximum doses to individuals were only calculated approximately. Screening analyses were performed, with the results of the calculations, to investigate the relationship between subsystem performance and overall system performance. Recommendations in the areas of additional scientific input (research), modeling improvements, and supporting analyses were formulated from the IPA Phase 2 work. The results of the sensitivity and uncertainty analyses were also factored into the recommendations.

Development of all total-system performance assessment (TPA) computational modules, supporting analyses, and analyses of results are documented in the IPA Phase 2 report. In addition, the values of parameters used, including the statistical distributions, are included in the appendices.

4 Elements of the IPA Phase 2 Total-System Performance Assessment

This report is largely structured along the same lines used to conduct IPA Phase 2, as noted below:

TPA Computer Code Development

The TPA computer code described in Chapter 2 consists of an *executive module* and several computational modules, which are linked together to calculate, in a Monte Carlo probabilistic manner, the total-system performance of a geologic repository. Both cumulative releases to the accessible environment and radiologic population dose are computed. In addition to controlling the execution of the various modules, the executive module computed the total CCDF by combining the results from the consequence modules and the probabilities of various scenario classes, which were determined separately. The TPA *executive module* also controlled data transfer between modules, including: (a) global data common to all modules; (b) sampled data, parameters sampled from a Latin Hypercube Sampling (LHS) module (see Appendix A); and (c) special input files for the various scenarios or particular consequence modules. The modular construction of the systems code is expected to allow for relatively easy modification or replacement of the various consequence modules, without changing the overall structure of the TPA computer code.

Scenario Analysis

Scenario analysis is comprised of scenario identification, scenario screening, and estimates of scenario probabilities. As noted in Chapter 3, four fundamental events were combined to form 16 mutually exclusive scenario classes. These fundamental events are: (1) change to a pluvial climate; (2) human intrusion by exploratory drilling; (3) seismic disruption; and (4) magmatic disruption. Only four scenarios classes were selected for inclusion in the simulations to estimate the radionuclide release CCDF representing repository performance. Of the remaining 11 scenario classes, another 5 were included in the simulations for the purpose of comparing undisturbed repository performance with disruptions caused by single disruptive events.

Flow and Transport Analysis

The flow and transport analysis described in Chapter 4 consisted of constructing models of radionuclide transport from the source term through both liquid and gaseous pathways. For the liquid pathways, the repository was divided into seven distinct regions, to represent the spatial variability. Radionuclide transport in ground water was assumed to be vertical in the unsaturated zone and primarily horizontal along the water table in the saturated zone. Thus, a water transport pathway, for a particular region, consisted of a series of individual one-dimensional segments, each representing a hydrologic unit associated with that region. The matrix-fracture flow characteristics of these one-dimensional flow paths, used for the TPA code simulations, were based on a detailed modeling of unsaturated flow, using a dual-continuum approach, to represent the fracture and matrix system. Gaseous transport was modeled in two dimensions, using the time-varying temperature distribution which resulted from the repository thermal loading to determine a set of time-dependent velocity fields. Time-varying releases of ^{14}C from the source term model were tracked from the repository to the atmosphere, to determine the release over the performance assessment period and to provide input to the dose assessment model. The TPA system code provided sampled hydrologic parameters (described in Appendices A and B) to both the liquid- and the gas-transport models, for each simulation.

Source Term Analysis

The source term module described in Chapter 5 mechanistically modeled the interaction between waste packages and their immediate environment. Failure of waste package containers was modeled as occurring in three categories: (1) due to initial defects; (2) via corrosion of the waste package, followed by buckling; and (3) failures due to disruptive events. The initiation of corrosion was assumed to require the presence of water in the liquid state, which in turn was assumed to depend on whether the temperature computed for a location had dropped below the boiling point. After initiation, corrosion proceeded according to sampled corrosion parameters supplied by the TPA system code. Modeling of spent nuclear fuel

alteration, dissolution, and near-field transport (the last two processes for releases in the liquid pathway only) was employed to determine the time-varying liquid and gaseous releases for use by the transport models.

Disruptive Consequence Analysis

Disruptive consequence modeling described in Chapter 6 estimated the effects of four disruptive events on the performance of the geologic repository. The drilling model assumed a random process to determine the number, location, and time-of-drilling for boreholes, and whether a waste package canister was hit for each simulated borehole. Excavated waste or contaminated rock provided a surface release for transfer to the total release and dose calculations. The seismo-mechanical model determined waste package failure of the corrosion-weakened waste package canisters from a randomly-sampled earthquake acceleration and supplied the information to the source term code, to calculate releases. The magmatic model randomly selected the time of the magmatic event, its size, location, and orientation. Distributions for these parameters were based on geologic evidence. The intersection of these magmatic features, both dikes and cones, with the repository layout, determined the amount of the emplaced inventory contributing to the releases to the accessible environment (either to the groundwater or surface, or, in the case of extrusive magmatic events, airborne release). Climate change was modeled by a shift in the distribution assumed for infiltration, and the depth to the water table under the repository horizon.

Dose Assessment

A dose assessment capability was included as part of the TPA system code activity; this assessment capability is described in Chapter 7. The dose assessment provided estimates of population and individual effective dose equivalent for each simulation. The dose model employed a static biosphere and determined dose to humans from five exposure pathways: (1) inhalation; (2) air submersion; (3) ingestion of vegetable crops; (4) ingestion of animal products; and (5) ground-shine. Dose related parameters were not sampled in the analyses.

Sensitivity and Uncertainty Analysis

With the simulation results from nine scenario classes and 400 realizations from the sampled parameters, sensitivity and uncertainty analyses were performed. These analyses included regression and differential analyses described in Chapter 8 of this report. The regression analyses included stepwise regression analysis to identify the most significant parameters and the construction of linear and transformed regression models, to test the ability of regression modeling to emulate the performance calculation with a limited set of parameters. A number of coefficients were computed from the regression analysis, to represent sensitivity and uncertainty. Differential analysis was performed using additional system code runs with selected input parameters (without sampling). Sensitivity and uncertainty parameters were calculated directly and compared with those determined from the regression analysis.

Analytical Results

Analyses of the results of the TPA system code simulations also included scatter plots of the releases from various disruptive scenarios compared with the base case releases; sensitivity plots showing the sensitivity of the CCDF to various screening criteria; and histograms of calculated parameters such as approximations to waste package failure times and ground-water travel times. These analyses are presented primarily in Chapter 9 of this report.

Fourteen auxiliary analyses were also conducted to support the tasks listed above. Most of the auxiliary analyses support modeling in the areas of regional hydrology, local infiltration, geochemistry, and radionuclide transport. These analyses provided inputs to the performance assessment consequence models such as the transport characteristics of flow paths, elevation of the pluvial case water table, and geochemical parameters for liquid and gas transport. Other analyses supported the source term model by determining volatile radionuclides that could be released during a magmatic event, and providing a basis for using a representative waste package for the source term for each of the seven repository regions modeled. The results of these analyses are summarized in Chapters 4, 5, and 8. Details regarding how 12 of the 14 auxiliary analyses were conducted are described in detail as

Appendices C to M of this report. Also described in the text of the report are other short analyses, as well as analyses that have been published elsewhere.

5 Overall System and Subsystem Performance Assessment Results

The results of the TPA computer code simulations using the parameter distributions provided in Appendix A of this report and the scenario probabilities provided in Chapter 3 are presented in Chapter 9 in Figures 9-7a, 9-7b, 9-8a, and 9-8b. The results as shown in these figures indicate non-compliance with the EPA release standard, where the probability of release exceeding the EPA limit is greater than 0.1. Median population *Effective Dose Equivalents* exceed 10^5 person-rems. The dominant contributor to the EPA *Normalized Release* is ^{14}C, primarily in the gaseous pathway. The primary contributor to population dose is from the liquid pathway and the ingestion of beef raised on a farm 5 kilometers from the repository. Major radionuclides identified as contributing to dose include ^{94}Nb, ^{210}Pb, ^{243}Am, and ^{237}Np.

NRC's subsystem performance requirements (10 CFR 60.113)* are designed to add to the confidence that the overall system requirements will be met. Even though no direct quantitative correlation between subsystem requirements and the overall system requirement is stipulated in the NRC regulation, an effort was made to determine how subsystem performance contributed, to or was related to, overall system performance. For these analyses, only the CCDF of normalized release was used. Four measures of liquid or hydraulic travel times were considered: (1) fastest path; (2) average; (3) most flux; and (4) flux weighted. Evaluation of each of these potential measures showed that long hydraulic travel times were generally correlated with smaller cumulative releases. However, the nature of the travel time distribution for the fastest path and most flux were such that most travel times were 800 and 1200 years. The distribution for average and flux-weighted travel times showed no vectors with travel times less than 10,000 years. For these reasons, the appropriateness of any given criterion was not directly evaluated. The relationship between release and waste package lifetime was found to be strong, with significant sensitivity of the CCDF to waste package lifetimes in the 300 to 1000-year range. Little correlation was found between the EBS release rate criterion and the normalized EPA release. Meeting the EBS release rate criterion alone did not guarantee a normalized EPA release less than 1.0. The correlation of consequences with various potential measures of subsystem performance is discussed in Section 9.5 of this report.

*The regulations in 10 CFR 60.113 establish specific performance objectives for the following repository subsystems: (1) the engineered barrier system (EBS); and (2) the geologic setting.

6 Insights and Conclusions From Model Development and the Sensitivity and Uncertainty Analyses

The most significant information gained from the IPA Phase 2 study was determined to be insights and conclusions regarding the evaluation of the IPA Phase 2 methodology and analyses, aspects of the site and repository design that might be important to performance, and the results of the overall system and subsystem performance assessments. These items are discussed in more detail in Chapter 10 of this report.

In regard to the adequacy of the IPA Phase 2 methodology, it was concluded that although the methodology can and must be improved as performance assessments become more detailed and sophisticated, the present methodology is adequate to identify important parameters and processes, gain insights regarding model development and repository performance, and evaluate research and technical assistance needs.

The scientific basis for analysis, that is the published information regarding the site and repository design, was not considered adequate to represent the performance of the repository in regard to compliance. For this reason, the most important information gained from the performance calculations is considered to be the identification of important parameters and processes and the relative effects of events and criteria on the CCDFs.

Significant insights and conclusions from model development and the sensitivity and uncertainty analysis include the following:

- The fractured unsaturated matrix of the site can greatly influence repository performance

by providing pathways for fast transport of liquids and vapor. The fractured unsaturated matrix is also difficult to model realistically.

- Percolation rate was identified as the most important parameter, from the sensitivity-uncertainty analysis in scenarios where there was a distribution of both matrix and fracture flow (the non-pluvial scenario classes).

- Abstracted flow models used in IPA Phase 2 probably do not include all of the important characteristics of the flow system and should be supported by three-dimensional, non-isothermal, two-phase models.

- Fracture geochemistry appears to be more important than geochemistry for the matrix for gas and liquid transport.

- Corrosion- and dissolution-related parameters were found to be important, in all scenario classes, for dose and release.

- Near-field hydrothermal processes may greatly influence container lifetime in terms of wetting time and corrosion rate.

- Repository heat load is likely to be an important parameter and should be evaluated in terms of performance sensitivity, in future IPA analyses.

- Uncertainty regarding the probability and consequences of the existing model, for magmatism, justifies more sophisticated modeling efforts.

7 Recommendations

Recommendations for additional scientific input generally follow the insights and conclusions determined from model development and the sensitivity and uncertainty analyses. These recommendations described in Section 10.4.1 of this report include:

- Research regarding fracture-matrix hydraulic and geochemical interactions, including those affecting gas transport, should be undertaken or continued.

- Regional hydrogeology will have to be understood sufficiently to determine the effects of disruptive events on site water levels and hydrologic boundary conditions.

- A relationship correlating percolation with precipitation at the site needs to be developed by DOE. This may allow the incorporation of expert judgment or future climate modeling into the estimation of the base case and pluvial climate percolation range and distribution.

- The effects of high humidity and/or water with high ionic strength on waste package corrosion need to be quantitatively understood for incorporation into the waste package failure component of the source term model.

- Realistic source term modeling will require input from near-field hydrothermal research, which may need to consider alternative waste package designs and placement configurations.

- Research in magmatism, including the role o volatiles, multiple dike intrusions, pre-existing geologic structure, and uncertainty in geochronological data, needs to be undertaken.

In Section 10.4.2 of this report, additional recommendations resulting from the IPA Phase 2 work are listed by chapter. The types of recommendations vary, from being very model-oriented, in the modeling chapters (4 to 6), to requiring additional analyses or procedures such as in Chapters 2, 7, and 8. The recommendations for modeling improvements and/or supporting analysis by chapter are:

- Recommendations concerning the TPA computer code (Chapter 2) included better adherence to software quality assurance procedures, the need for greater model abstraction, and need for the TPA computer code be continually upgraded.

- Recommendations in the area of scenario analysis (Chapter 3) consisted of the need to reassess staff judgments and probabilities assumed in the screening of events and

processes, and the need to examine partitioning of scenario classes.

- Flow and transport recommendations (Chapter 4) include model improvements in the area of unsaturated flow, including more complex modeling of fracture-matrix interactions, two-phase fluid movement, and the effects of fracture imbibition on percolation. Also recommended is a closer examination of hydrogeologic features and heterogeneity in the unsaturated zone, to find possible fast pathways or "short circuits." The recommendations also call for improvements in saturated zone modeling, after evaluating more alternative approaches and adding more output (from intermediate calculations) to the computer models, to better interpret results.

- Source term recommendations (Chapter 5) include modeling improvements in the waste package area, such as near-field hydrothermal and heat transfer modeling, more mechanistic corrosion models, and more realistic waste package failure models. Also included in the source term recommendations were improvements in the release modeling, such as accounting for spatial and temporal variability, improved gaseous ^{14}C releases, and improved dissolution modeling.

- Recommendations associated with disruptive consequence modules (Chapter 6) include the need to improve the drilling, seismic, and volcanism models. There is also a recommendation to include recently obtained information from expert judgment in the pluvial climate consequence simulations.

- Dose assessment recommendations (Chapter 7) include improvements to the input and means of presentation of the *DITTY* code results, and the need to perform sensitivity and uncertainty analysis on the dose assessment parameters. It is also recommended that other dose assessment codes be evaluated, as well as methods employed by international organizations.

- Recommendations from the area of sensitivity and uncertainty analysis (Chapter 8) consist of developing techniques specifically for evaluating probabilistic quantities and the need to incorporate correlation between parameters into the regression model.

TABLE SHOWING ENGLISH/METRIC SYSTEM CONVERSION FACTORS

The preferred system of measurement today is the "Systèm Internationale" or the metric system. However, for some physical quantities, many scientists and engineers prefer the familiar and continue to use the English system (foot-pound units). With few exceptions, all units of measure cited in this report are usually in the metric system.

The following table provides the appropriate conversion factors to allow the user to switch between these two systems of measure. Not all units nor methods of conversion are shown. Unit abbreviations are shown in parentheses. All conversion factors are approximate.

QUANTITY	*TO INCH–POUND UNITS*	*FROM METRIC UNITS*[1]	*CONVERSION FACTOR*[2]
		SPACE AND TIME	
length	statute mile (mi) foot (ft) inch (in)	kilometer (km) meter (m) centimeter (cm)	0.6214 3.2808 0.3937
area	square mile (mi^2) acre square foot (ft^2) square inch (in^2)	square kilometer (km^2) square kilometer square meter (m^2) square centimeter (cm^2)	0.3861 247.1 10.7639 0.1550
volume	cubic yard (yd^3) cubic foot (ft^3) cubic inch (in^3)	cubic meter (m^3) cubic meter liter (l) centimeter (cm^3)	1.3080 35.3147 0.0353 0.0610
velocity	feet/second (ft/sec)	meters/second (m/sec)	3.2808
acceleration	feet/square second (ft/sec^2)	meters/square second (m/sec^2)	3.2808
		MECHANICS	
mass (weight)	pounds (lb) short ton	kilogram (kg) metric ton (t)	2.2046 1.1023
density	pounds/cubic foot (lbs/ft^3)	kilograms/cubic meter (kg/m^3)	0.0624
force	pound-force (lbf)	Newton (N) dyne (dyn)	0.2248 $.2248 \times 10^5$
pressure	atmosphere (atm) pound-force/square foot (lb/ft^2)	kilopascal (kPa) dyne/square centimeter (dyn/cm^2)	0.0099 0.0021
power	horsepower (hp)	kilowatts (kW)	1.3405
work	footpound-force (ft-lbf)	joule (J)	0.7376
		HEAT	
temperature	degrees Fahrenheit (°F)	degrees Celsius (°C) degrees Kelvin (°K)	°F = 1.8°C + 32 °F = 1.8°K - 459.67
		IONIZING RADIATION	
activity (of a radionuclide)	curie (Ci)	megabecquerel (MBq)	2.7027×10^{-5}
absorbed dose	rad	gray (Gy)	100
dose equivalent	rem	sievert (Sv)	100

[1]Not all metric units are shown. Most metric units can be arrived at by multiplying the value by 10^n.

[2]Multiply quantity in metric units by the appropriate conversion factor to obtain inch-pound units. For additional unit conversions, refer to C.J. Pennycuick, *Conversion Factors: SI Units and Many Others*, Chicago, The University of Chicago Press, 1988.

ACKNOWLEDGMENTS

The editors and authors (cited in the "Table of Contents," by Chapter/Section) gratefully acknowledge the many contributions made by other Office of Nuclear Material Safety and Safeguards and the Office of Nuclear Regulatory Research (RES) management and staff, the Office of the General Counsel, and the Center for Nuclear Waste Regulatory Analyses (CNWRA) which have been incorporated into the text of this report. In this regard, L.R. Abramson/RES, L.E. Lancaster/RES, T. Margulies/RES (now with the U.S. Environmental Protection Agency), R.W. Janetzke/CNWRA, and R.D. Manteufel/CNWRA, deserve special recognition. Special thanks are also to the following individuals for their comments and/or reviews of specific chapters of this report: K.R. Hooks/NMSS—Chapter 1; H.K. Manaktala/CNWRA and T.M. Ahn/NMSS—Chapter 5; P.C. Lichtner/CNWRA and R.D. Manteufel/CNWRA—Chapter 6; J.P. Kotra/NMSS—Chapter 7; and B. Mason/Southwest Research Institute and M.G. Bradley/Freddie Mac—Chapter 8. Ellen Kraus provided editorial guidance, M. Linda McKenzie prepared the manuscript for publication, and Lionel J. Watkins supervised the preparation of the illustrations. Overall publication direction was provided by JoAnn Resner.

1 INTRODUCTION

1.1 NRC's Iterative Performance Assessment Program

1.1.1 Background

Work performed under the first demonstration of the staff's capability to execute critical parts of a performance assessment for a geologic repository for high-level radioactive waste (HLW)[1] was intended as an initial step in a sequence of planned iterative performance assessments (IPAs) to be undertaken by the U.S. Nuclear Regulatory Commission staff and its contractor—the Center for Nuclear Waste Regulatory Analyses (CNWRA). This report describes the results of the second phase (designated "IPA Phase 2") of the continuing demonstration of the development of the NRC staff's capability to review a performance assessment for a geologic repository. This capability helps the NRC staff assess whether the U.S. Department of Energy's (DOE's) site characterization activities are adequate, during the pre-licensing phase, and, later, helps the staff review a potential license application to construct a geologic repository for HLW.

As its name indicates, IPA involves repeated iterations directed at improving both the NRC staff's capability for reviewing DOE's demonstration of repository performance and the staff's understanding of combined systems and events and processes that are key to repository performance. Performance assessment of a geologic repository, like other systematic safety-assessment methodologies, benefits substantially by being conducted in an iterative manner, primarily because the lessons learned regarding modeling improvements, data needs, and methodology can be addressed in subsequent iterations.

1.1.2 Objectives

Under Section 114(d)(2) of the Nuclear Waste Policy Act of 1982 (NWPA), as amended (Public Law 97-425), the Commission is required to issue a final decision on the issuance of a construction authorization for a geologic repository for HLW no later than 3 years after DOE's license application is submitted, although the Commission may extend this deadline for 12 months, for good cause, in accordance with the NWPA, as amended. Meeting this schedule depends greatly on the following: (1) early and open pre-licensing consultation between NRC and DOE on the information that would be needed for licensing; (2) adequate DOE site characterization plans and activities; (3) DOE's submission of a complete and high-quality license application; and (4) effective NRC staff preparation for the license application review process, by having its technical assessment capability in place.

The overall objective of NRC's IPA program, therefore, is to maintain and enhance the staff capabilities necessary to support these geologic repository program activities. During the **pre-licensing phase**, the specific objectives of NRC's IPA program thus include:

- Evaluating the ongoing DOE site characterization program (including field studies, laboratory studies, and analyses, and interim performance assessments generated by DOE or its contractors).
- Evaluating ways to implement the 10 CFR Part 60 performance objectives.
- Providing input to the ongoing evolution of the radiation protection standard for the geologic repository, set forth by the U.S. Environmental Protection Agency (EPA) in 40 CFR Part 191 (*Code of Federal Regulations*, Title 40, "Protection of Environment") which is incorporated by reference in 10 CFR Part 60.
- Providing input to regulatory guidance and other regulatory products related to performance assessment, especially the Draft License Application Review Plan (see NRC, 1994).
- Assisting in the definition of the Office of Nuclear Material Safety and Safeguards

[1]As used in this document, HLW includes spent nuclear fuel and transuranic wastes, unless otherwise specifically stated.

(NMSS) technical assistance and research programs in the area of HLW.

Additional specific objectives of NRC's IPA program, during the **licensing phase**, include:

- To provide an independent calculation of key aspects of DOE's total-system performance assessments submitted as part of a license application.
- To probe DOE's assessment for potential weakness, based on a familiarity with the methods, data, and assumptions used in the performance assessments.

1.1.3 Regulatory Basis for IPA

NRC's basic licensing and related regulatory authority are provided by the Atomic Energy Act of 1954 (Public Law 83-703), as amended. This authority applies to certain facilities of DOE (as successor to the Energy Research and Development Administration) under Section 202 of the Energy Reorganization Act of 1974 (Public Law 93-438). Congress further defined NRC's role, as it relates to the disposal of HLW in geologic repositories, in NWPA and the Nuclear Waste Policy Amendments Act of 1987 (Public Law 100-203).

Section 121(a) of NWPA, as amended, called for EPA to promulgate generally applicable environmental standards for the management, storage, and disposal of HLW. In addition, NWPA prescribed (Section 121(b)) that the EPA standards be implemented by NRC as part of the procedural and technical regulations it was to promulgate for the licensing of geologic repositories for the disposal of HLW. The EPA promulgated its standard in the form of 40 CFR Part 191 (EPA, 1985);[2] the NRC standard is in the form of 10 CFR Part 60 (NRC, 1981 and 1983).

40 CFR Part 191 establishes containment requirements that limit releases of radioactive material to the "accessible environment" (10 CFR 60.2), weighted by a factor approximately proportional to radiotoxicity, and integrated over a period of time (10,000 years is the current regulatory requirement) after permanent closur of the geologic repository.[3]

10 CFR Part 60 incorporates 40 CFR Part 191 as the overall performance requirement for a geologic repository. The requirements in 10 CFR 60.112 set an overall system performance objective that amounts to meeting EPA's containment requirements, whereas certain other sections (10 CFR 60.113) set forth subsystem performance objectives. (The use of subsystem performance objectives is consistent with the Commission's multiple barrier, defense-in-depth concept and contributes to developing reasonable assurance that the EPA standards will be met.)

40 CFR Part 191 specifies three broad quantitative performance requirements for the overall geologic repository system:[4]

- Limits on the cumulative release of radioactivity at the boundary of the accessible environment over 10,000 years (40 CFR 191.13—containment requirements).
- Limits on dose to individuals for the first 1000 years (40 CFR 191.15—individual protection requirements).
- Limits on permissible concentrations of radionuclides in special sources of ground water for the first 1000 years (40 CFR 191.16—ground-water protection requirements).

As for the subsystem performance objectives, the regulations in 10 CFR 60.113 establish specific performance objectives for the following repository subsystems: (1) the EBS and (2) the

[2]40 CFR Part 191 was vacated by the U.S. Court of Appeals for the First Circuit and remanded to the EPA for further consideration.

[3]Currently, a revised set of standards specific to the Yucca Mountain site is being developed in accordance with the provisions of the Energy Policy Act of 1992. The Energy Policy Act of 1992 (Public Law 102-486), approved October 24, 1992, directs NRC to promulgate a rule, modifying 10 CFR Part 60 of its regulations, so that these regulations are consistent with EPA's public health and safety standards for protection of the public from releases to the accessible environment from radioactive materials stored or disposed of at Yucca Mountain, Nevada, consistent with the findings and recommendations made by the National Academy of Sciences, to EPA, on issues relating to the environmental standards governing the Yucca Mountain repository. It is assumed that the revised EPA standards for the Yucca Mountain site will not be substantially different from those currently contained in 40 CFR Part 191, particularly as they pertain to the need to conduct a quantitative performance assessment as the means to estimate postclosure performance of the repository system.

[4]As used here, the repository system refers to the combination of: (i) emplaced wastes; (ii) the engineered barrier system (EBS); (iii) the engineered disposal facility; and (iv) the geologic medium surrounding the geologic repository operations area (GROA) facility (i.e., within the controlled area).

geologic setting. These performance objectives require the following:

- Substantially complete containment of waste in the waste packages for a minimum period of 300 to 1000 years after closure (10 CFR 60.113(a)(1)(ii)(A)).
- Controlled fractional release rate from the EBS, based on the inventory at 1000 years after closure (10 CFR 60.113(a)(1)(ii)(B)).
- Pre-waste-emplacement ground-water travel time (GWTT) of at least 1000 years (10 CFR 60.113(a)(2)).

Because the EPA standard is probability-based, the demonstration of compliance must also be probability-based. However, a probabilistic evaluation is useful regardless of the nature of the standard because of large uncertainties. Accordingly, the measure of total system performance for a geologic repository can be expressed by the complementary cumulative distribution function (CCDF) for cumulative normalized radioactive releases to the accessible environment over 10,000 years. The representation of repository performance by a CCDF incorporates:

- Consideration of the various parameters affecting the performance of the geologic repository; and
- Consideration of a range of anticipated and unanticipated processes, conditions, and events that could affect future geologic repository performance.

In conducting a total-system performance assessment, the analysis needs to account for the various uncertainties that are inherent in those processes, conditions, and events considered. The present performance assessment approach undertaken by the staff in its IPA effort incorporates both parameter uncertainty and scenario probability into a single CCDF. Alternative representations show the entire set of single-vector CCDFs or single conditional CCDFs for each scenario. Both of these alternatives are capable of representing parameter uncertainty and scenario probability as separate factors.

1.1.4 Steps in Performing a Total-System Performance Assessment

The general approach to developing and analyzing a total-system performance assessment can be defined by the following steps, outlined below, and shown in Figure 1–1. For both the IPA Phase 1 and Phase 2 efforts, all these steps were performed to various levels of detail.

Step No. 1—System Description

The repository is broken into its component parts for the purposes of modeling. These components include the waste form, the mined geologic repository system (including the engineered barriers such as the waste package), and the portion of the geosphere surrounding the geologic repository through which the radionuclides, in time, may migrate. The system description therefore should include information that supports the development of models describing repository performance, and should identify data and parameters for the models used to support the *Scenario Analysis* (Step No. 2—described below).

Step No. 2—Scenario Analysis

Scenarios representing alternative possible future states of the environment, as they reflect the repository, are identified and screened. For this analysis, scenarios are formulated based on classes of events and processes external to the repository system. (Events and processes internal to the repository system are treated in the *Consequence Analysis* (Step No. 3—described below).) Probabilities were estimated for the selected scenarios.

Step No. 3—Consequence Analysis (release, transport, and dose modeling)

Models are developed to describe the performance of the subsystems of the geologic repository and are linked to describe overall performance. Overall repository performance, in terms of cumulative releases of radionuclides to the accessible environment, over a specified time period (in

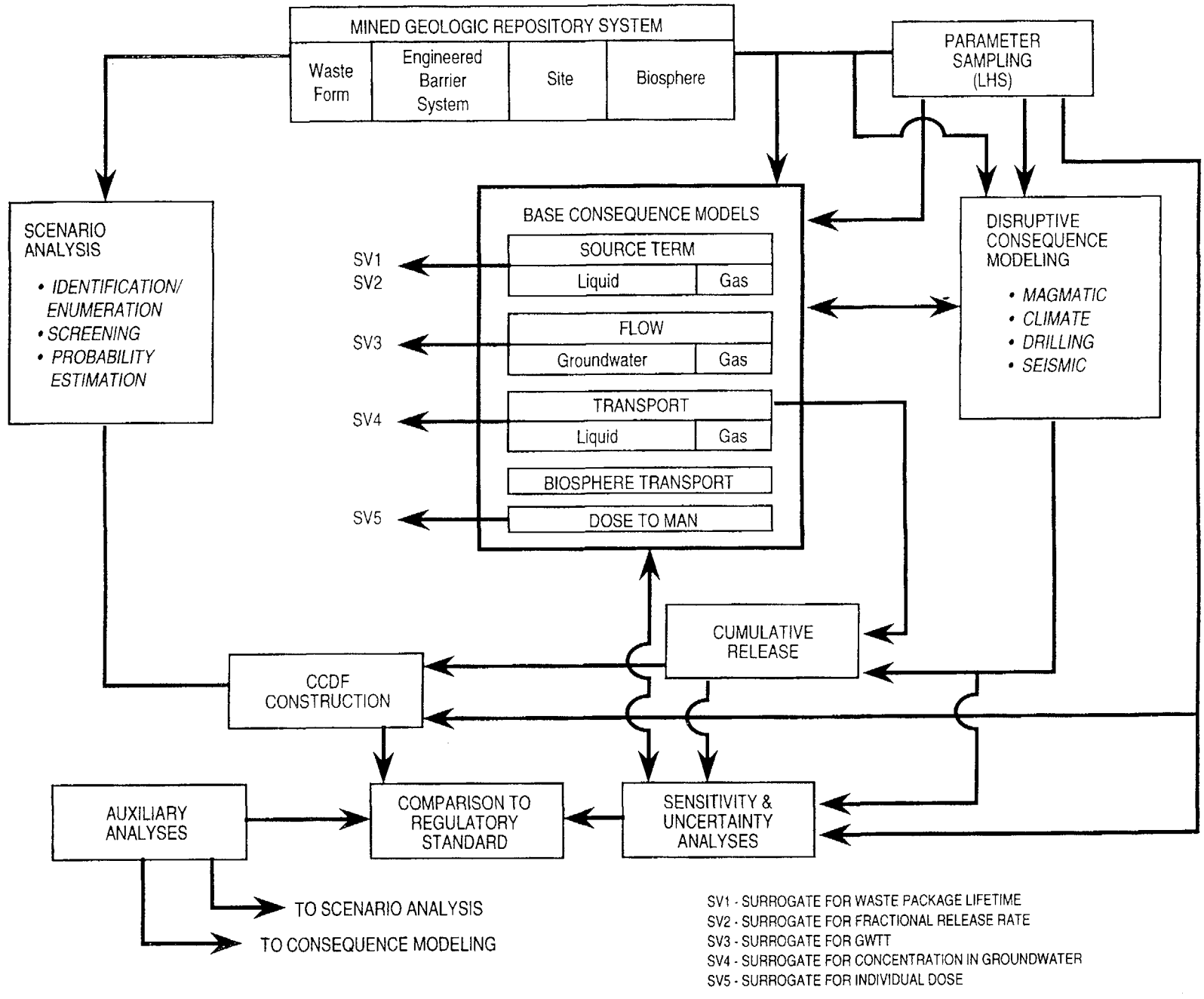

Figure 1–1 Components of a total-system performance assessment

this study, 10,000 years), is calculated for each scenario, using numerous simulations of possible ranges of parameter values. In addition to the CCDF for cumulative releases (Step No. 4), other types of system performance measures, such as maximum doses to individuals, can also be considered.

Step No. 4—Probabilistic Performance Measure Calculation (the CCDF)

For each scenario identified in Step No. 2, the consequences, in terms of normalized cumulative releases of radionuclides to the environment over a specified period of time, are calculated and the results displayed in a plot of total releases versus the probability that such consequences are exceeded (i.e., the CCDF of total releases to the accessible environment for 10,000 years, normalized by the EPA release limit for each radionuclide and summed over all contributing pathways). The total results incorporating scenario probability are compared with release limits established by the EPA standard.

Step No. 5—Sensitivity and Uncertainty Analysis

A sensitivity analysis is conducted to evaluate the fractional change in calculated results caused by incremental changes in the values of input parameters and data. An uncertainty analysis is also conducted to quantify the uncertainty in performance estimates in terms of the major sources of uncertainty, in input parameters. Uncertainty in modeling, however, including conceptual model uncertainty and uncertainty regarding the probability of future states, was not quantified in either IPA Phase 1 or Phase 2.

Step No. 6—Documentation

Documentation is developed to clarify the assumptions used in the analysis, their bases, and the implications of their uses. An important aspect is documentation of auxiliary analyses, which evaluate the adequacy of the consequence modules and the assumptions underlying them, synthesize data into parameters, and provide other insights.

1.2 IPA Phase 2: Overview

1.2.1 Purpose and Scope

As noted earlier, the primary purpose of IPA Phase 2 was to enhance and improve the capability of the NRC staff to conduct and evaluate calculations of key aspects of repository performance by performing a limited total-system performance assessment. It is believed that the NRC staff's capability to perform an independent assessment will be an important aspect of its licensing review. The specific goals of IPA Phase 2 were to:

- Use the Tuff Performance Assessment Methodology developed by Sandia National Laboratories (SNL);
- Provide for a preliminary dose assessment capability;
- Provide a gas source term and transport capability;
- Provide an executive module to control run parameters;
- Improve the existing IPA source term code;
- Include the saturated zone in the evaluation of the ground-water pathway; and
- Include consideration of additional disruptive scenarios.

In addition, IPA Phase 2 achieved some worthwhile secondary goals, including:

- Limited evaluation of existing analytical tools for conducting a performance assessment (both methodologies and computer codes); and
- Insight into the need for the improvement of existing methodologies or the development of new ones.

IPA Phase 2 also provided a smooth transition of contractor support from SNL to the CNWRA.

The scope of IPA Phase 2 consisted of the same basic steps (described in Section 1.1.4) as were performed for IPA Phase 1, including: *system description, scenario analysis, consequence analysis,*

CCDF calculation, and documentation. The IPA Phase 2 study included many improvements, over IPA Phase 1, which expanded the scope and are discussed in Section 1.2.5. The auxiliary analyses undertaken for IPA Phase 2 were performed by both NRC (NMSS and the Office of Nuclear Regulatory Research (RES)) and CNWRA technical staff members, and supported modeling in the areas of regional hydrology, site infiltration analysis, model testing, geochemistry, and source term.

The results computed in the total-system performance assessment included total and conditional CCDFs for summed normalized releases and effective dose equivalents for the exposed population. Maximum concentrations of radionuclides in groundwater were not compared with drinking water standards and maximum doses to individuals were only calculated approximately. Screening analyses were performed, with the results of the calculations, to investigate the relationship between subsystem performance and total system performance. Recommendations in the areas of additional scientific input (research), modeling improvements, and supporting analyses were formulated from the IPA Phase 2 work. The results of the sensitivity and uncertainty analyses were also factored into the recommendations.

Development of all computational modules, supporting analyses, and analyses of results are documented in the IPA Phase 2 report. In addition, the values of parameters used, including the statistical distributions, are included in the appendices.

1.2.2 IPA Organization and Staffing

NRC staff members from both NMSS and RES, and the CNWRA participated in IPA Phase 2. The technical staff involved in IPA Phase 2 came from all three organizations. To coordinate the efforts of the three participating organizations, the organizers designated a technical project manager from NMSS (M. Lee), and three technical coordinators: one respectively from NMSS (R. Wescott succeeding N. Eisenberg); RES (T. McCartin); and the CNWRA (R. Baca succeeding B. Sagar). The assignment of staff to the technical efforts in Phase 2 was done regardless of organizational affiliations and focused on individual technical capabilities.

The project manager and technical coordinators facilitated communication among the various task leaders and technical participants. The technical coordinators also proposed plans for technical activities, schedules, and staffing for IPA Phase 2, for approval by the IPA Management Board. The IPA Management Board was comprised of M. Federline (NMSS) (succeeding R. Ballard); M. Silberberg (RES/Waste Management Branch (WMB)); and B. Sagar, succeeding W. Patrick (CNWRA).

Each of the six major divisions of technical activity was assigned to a working group with a designated task leader. The principal staff (including task leads) assigned to each of these working groups is indicated in the "Table of Contents" of this report: these staff were responsible for conducting the respective analyses and documenting the results. The specific staff responsible for the TPA module development is described in Section 2.1.3 of this report.

However, other NMSS, RES/WMB, and CNWRA staff made substantial contributions during the formative stages of the IPA Phase 2 analysis, as indicated below. Those additional staff members that participated in the initial scoping deliberations for the scenario analysis described in Section 3.3 of this report are listed in Table 1-1. Similarly, in Chapter 5 ("Source Term Module"), important contributions to the analysis were made by: P. Nair, G. Cragnolino, and N. Sridhar of the CNWRA; T. Torng of the Southwest Research Institute (SwRI); and K. Chang and N. Eisenberg of NMSS. Finally, in Chapter 6 ("Disruptive Consequence Analysis"), the Phase 2 analysis benefited from contributions made by those additional staff listed in Table 1-2.

1.2.3 Quality Assurance

The following discussion is intended to briefly outline the quality assurance (QA) measures applied to the software for the IPA Phase 2 computational modules.

As noted earlier, IPA Phase 2 was performed jointly by NMSS, RES, and CNWRA staff. IPA

Table 1–1 Staff Participating in the IPA Phase 2 Scenario Analysis

Individual/Organization	*Discipline(s)*
G. Birchard/RES	geochemistry
J. Bradbury/NMSS	geochemistry
P. Brooks/NMSS	performance assessment
R. Cady/RES	waste package/engineered barrier system
K. Chang/NMSS	waste package/engineered barrier system
D. Chery/NMSS	hydrology, climatology
R. Codell/NMSS	performance assessment
N. Eisenberg/NMSS	performance assessment
B. Gureghian/CNWRA	hydrology, climatology
R. Hofmann/CNWRA	geophysics
A–B Ibrahim/NMSS	geophysics
H. Lefevre/NMSS	economic geology
L. Kovach/RES	geology, volcanism
T. McCartin/RES	hydrology
M. Miklas/CNWRA	geology/climatology
E. O'Donnell/RES	geology
G. Stirewalt/CNWRA	geology
J. Park/NMSS	performance assessment
J. Trapp/NMSS	geology
D. Turner/CNWRA	geology

Table 1–2 Staff Participating in the Analysis of Scenarios used in the IPA Phase 2 Consequence Analysis

Scenario Class	*Analysis Team*/Organization*
Climate	**M. Miklas/CNWRA** J. Park/NMSS N. Eisenberg/NMSS B. Sagar/CNWRA
Drilling	**N. Eisenberg/NMSS** J. Firth/NMSS A. Drake/CNWRA C. Frietas/SwRI J. Park/NMSS B. Sagar/CNWRA
Seismicity	**N. Eisenberg/NMSS** R. Codell/NMSS K. Chang/NMSS A. Chowdhury/CNWRA D. Dancer/NMSS C. Frietas/SwRI A–B Ibrahim/NMSS P. Nair/CNWRA B. Sagar/CNWRA
Volcanism	**R. Baca/CNWRA** L. Abramson/RES L. Lancaster/RES R. Codell/NMSS R. Drake/SwRI N. Eisenberg/NMSS L. Kovach/RES T. Margulies/RES J. Park/NMSS B. Sagar/CNWRA J. Trapp/NMSS C. Lin/SwRI

*Bold type designates principal investigator.

Phase 2 planning and development was performed in accordance with QA guidelines established in the draft IPA Phase 2 Program Plan. The computer programming performed was under the controls of the CNWRA's QA program to avoid the necessity of developing equivalent NMSS/RES procedures for this activity. The CNWRA's implementing procedure in the area of computer codes is Technical Operating Procedure (TOP)-018 (CNWRA, 1991). This procedure imposes methods for configuration management of the scientific and engineering software (e.g., computer codes) acquired, developed, and/or modified and used by NMSS, RES, and CNWRA staff. The procedure is intended to ensure the integrity of such codes by maintaining an auditable and traceable record of any needed changes.

It should be noted that QA requirements contained in TOP-018 conform to the broader QA guidance contained in NUREG-0856 (Silling, 1983). NUREG-0856 recommends guidelines for DOE to use when preparing the documentation for scientific and engineering software used in those analyses submitted in support of any DOE license application for a geologic repository for HLW.

However, it should be noted that Users' Guides for all computational modules are planned and/or under development at this time, to satisfy the requirements of TOP-018.

1.2.4 Approach and Content of the Report

An interdisciplinary, integrated approach was used to conduct the IPA Phase 2 analyses. Working groups or teams of NMSS, RES, and CNWRA staff were organized that roughly correspond to the methodological steps for a performance assessment shown in Figure 1-1. In IPA Phase 2, the areas of investigation included:

- Scenario analysis and selection;
- Simulation of ground-water flow and radionuclide transport;
- Calculation of radionuclide source terms;
- Analysis of disruptive events;
- Modeling of radioactive transport to the biosphere; and
- Analysis of the sensitivity and uncertainty in data, models, and performance estimates.

This report is largely structured along the same lines used to organize the work. Chapters 2 through 8 of this report describe the work performed by the various working groups, as noted below:

Chapter	*Title*
2	"Total-System Performance Assessment Computer Code"
3	"Scenario Analysis"
4	"Flow and Transport Module"
5	"Source Term Module"
6	"Disruptive Consequence Analysis"
7	"Dose Assessment Module"
8	"Sensitivity and Uncertainty Analysis"

A computer code was used to provide the computational algorithms to estimate values of the various performance measures and to performing the calculations leading to an estimate of the CCDF for normalized release and dose.[5] This computer code takes into account a number of the interactions studied among subsystems, components, future states, and processes associated with the geologic repository. Chapter 2 of this report provides a description of this computer code.

One of the IPA Phase 2 activities was a demonstration of the estimation of the total system performance measure (cumulative releases to the accessible environment), as well as some calculation of estimates of those measures related to the performance of natural and engineered barriers. Analytical results from the IPA Phase 2 demonstration and analysis are presented in Chapter 9.

[5]The concepts of normalized release and dose are described in Sections 9.2.1 and 9.2.3, respectively.

Chapter 10 ("Conclusions and Recommendations for Further Work") presents some preliminary thoughts on the adequacy of the staff's current performance assessment capability, as well as some recommendations on the direction of future NRC IPA efforts.

Finally, auxiliary analyses were conducted as part of the investigations described above to examine specific processes and factors that may be important to total system performance. Auxiliary analyses support the performance assessment by using more detailed models to:

- Provide greater insight into cause-and-effect relationships;
- Evaluate conservatism of model assumptions;
- Evaluate alternate modeling approaches; and/or
- Interpret field and laboratory data.

Summary descriptions of these auxiliary analyses are given in Chapters 4, 5, and 8.

1.2.5 Improvements Since Phase 1

The following discussion summarizes the improvements achieved during IPA Phase 2 in the staff capability to execute a performance assessment for a geologic repository for HLW. This summary is structured along the same lines used to organize the work. It should be noted, though, that some of these improvements were based, in part, on the preliminary recommendations made as a result of the insights gained from the IPA Phase 1 effort (see "Preliminary Suggestions for Further Work" in Codell *et al.*, 1992). The suggestions for technical improvements were grouped into three categories:

- Suggestions to improve or extend the modeling capability for reviewing performance assessments;
- Suggestions for refining or adding auxiliary analyses to help better evaluate the performance estimates; and
- Suggestions for refinements or additions to the scientific bases, including the methodologies available and field and laboratory data, for arriving at estimates of repository performance.

Table 1–3 summarizes the IPA Phase 1 recommendations and the extent to which these recommendations were treated in IPA Phase 2. However, some of these recommendations were not implemented, and to the extent that they still apply, they are discussed in Chapter 10 of this report. Refer to Chapters 2 through 8 of this report for a more detailed discussion of these improvements.

Total-System Performance Assessment (TPA) Computer Code (Chapter 2)

In IPA Phase 1, the staff developed a system code to process externally generated information needed to construct the CCDF to represent the performance of the geologic repository for a limited set of scenario classes. In IPA Phase 2, the staff developed a more sophisticated computer code to control the flow of data to and from the computational modules and the sequencing of their execution. This arrangement is believed to offer advantages in eliminating potential data transfer errors and provides an easier means of making changes that affect several modules.

The principal features of the staff's more sophisticated computer code in IPA Phase 2 are:

- The execution of the various scenarios is performed under the control of the TPA executive module, with consistent data (including sampled variables) provided automatically to all the consequence modules; and
- The system executive is responsible for invoking modules automatically and processing release values to construct a CCDF for each run (by nuclide, pathway, zone, module, vector, scenario, and overall, as specified).

In summary, the IPA Phase 1 analysis relied heavily on manual manipulation of files rather than the relatively high degree of automation provided by the system driver for Phase 2.

Scenario Analysis (Chapter 3)

As noted above, only a limited set of scenario classes was considered in IPA Phase 1. These

Table 1-3 IPA Phase 1 Recommendations Implemented during IPA Phase 2

IPA Phase 1 Recommendation	*Implementation in IPA Phase 2*[6]	*Section of IPA Phase 2 Report*
Improvements and Extensions to Modeling:		
General		
Add the capability for modeling additional scenario classes.	Limited	Sections 6.2 and 6.4
Control the CCDF generation with the system code, using the consequence codes as subroutines, instead of generating data sets external to the system code.	Full	Chapter 2
Acquire, test, and evaluate codes that SNL developed for a repository in the unsaturated zone.	Full	Chapter 4, Appendices C, G, and J
Evaluate additional computer codes, which could not be acquired and evaluated during the IPA Phase 1 effort, to determine whether existing codes can meet the NRC modeling needs, or whether additional code development is needed.	Limited	Chapter 4, Appendices C, G, and J
Explore, with the CNWRA, the adaptation of the Fast Probabilistic Performance Assessment methodology to generate the total system CCDF.	Limited	Section 8.8
Perform a sensitivity analysis, using both drilling and groundwater transport parameters.	No longer applicable	——
Flow and Transport		
Refine groundwater modeling (e.g., by considering more dimensions).	Limited	Chapter 4
Incorporate a model of gas-pathway transport in the calculation of the CCDF.	Full	Section 4.3
Include flow and transport through the saturated zone.	Full	Chapter 4
Use a more sophisticated computational model for transport through partially saturated, fractured rock.	Limited	Chapter 4

[6]"Limited" and "full" are relative terms intended to convey the degree of modeling improvement between IPA Phase 1 and Phase 2. The term "limited" suggests only marginal modeling improvement over IPA Phase 1, whereas "full" suggests significant modeling improvement over IPA Phase 1.

Table 1-3 (continued)

IPA Phase 1 Recommendation	*Implementation in IPA Phase 2*	*Section of IPA Phase 2 Report*
Source Term		
Attempt to develop or use a previously developed mechanistic model of waste-package failure.	Limited	Chapter 5
Treat the repository as a source of radionuclides distributed in time and space.	Full	Chapters 4 and 5
Improvements and Extensions to Auxiliary Analyses:		
Perform detailed geochemical analyses to investigate the use of K_ds in estimating radionuclide transport.	Limited	Appendix D
Evaluate the importance of thermally and barometrically driven air flow on repository performance at Yucca Mountain.	Limited	Sections 4.3, 5.4.2, and 5.6.3
Perform detailed hydrologic analyses for Yucca Mountain, to provide a better input to the transport analysis and to examine, in more detail, various alternative hypotheses regarding hydrology at Yucca Mountain.	Limited	Appendices E and I
Recommendations for Additional Scientific Input:		
Develop and demonstrate a mathematically rigorous, scientifically robust method for scenario analysis.	Limited	Chapter 3
Obtain geoscience input for modeling volcanism.	Full[7]	Section 6.4
Obtain geoscience and hydrologic input for modeling faulting, uplift, and subsidence at Yucca Mountain.	Limited	Section 6.2, Appendices F and H
Obtain field and laboratory data on the transport of gaseous radionuclides, especially ^{14}C, at Yucca Mountain.	Limited	Sections 4.3 and 5.6.3, Appendix H

[7]Despite implementation of this IPA Phase 1 recommendation in Phase 2, the staff believes that significant additional work in this area is still needed. See Sections 6.4 and 6.6 for the staff's specific recommendations.

classes were the exploratory drilling (human intrusion) and climate change (pluvial) events leading to four scenario classes. However, for the IPA Phase 2 analysis, the staff applied the SNL scenario selection methodology for use in the consequence analysis of a potential HLW disposal site (see Cranwell *et al.*, 1990). Based on the staff evaluation and modification of the SNL methodology, four scenarios of fundamental events were considered (climate change, seismicity, magmatism, and human intrusion) from which 16 scenario classes resulted.

Flow and Transport Module (Chapter 4)

The IPA Phase 1 effort identified and accounted for a number of important attributes of the Yucca Mountain site (e.g., stratigraphic changes below the repository in the unsaturated zone and differences between matrix and fracture flow). The IPA Phase 2 effort not only has maintained the important attributes identified in the Phase 1 study but has added further modeling complexity such as:

- The number of zones used to represent the repository was increased from four to seven;
- Saturated zone pathways to the accessible environment;
- Calculation of radionuclide concentration for dose assessment; and
- Distribution of mass flux between the fracture and matrix continua.

The additional detailed model complexity is expected to provide further insights into the performance of fractured rock as geologic barrier, data requirements, and the capabilities of the computational methods.

The flow and transport module in IPA Phase 2 built upon the Phase 1 effort. Three transport pathways were considered in IPA Phase 2 (i.e., gaseous, aqueous, and direct) compared with two transport pathways (i.e., both aqueous and direct) in IPA Phase 1. The flow and transport module in IPA Phase 2 provided for treatment of:

- Steady-state liquid phase transport (advection, dispersion, decay, and sorption); and
- Time-varying gas-phase transport (advection, decay, temperature effects, and equilibrium speciation)

Source Term Module (Chapter 5)

Because the modeling of waste-package failure was nonmechanistic and rudimentary in IPA Phase 1, improvement to this aspect of repository performance was sought in Phase 2. The model used by the staff to calculate the source term in IPA Phase 1 was implemented in the *NEFTRAN* (**NE**twork **F**low and **TRAN**sport) computer code developed by SNL (see Longsine *et al.*, 1987). In Phase 1, radionuclide releases were modeled to occur only after failure of the waste package, characterized as a single failure time for the entire repository. The principal features of the staff's source term analysis are discussed below.

In IPA Phase 2, the analysts developed a new computer code to calculate the source term. The *SOTEC* (**S**ource **T**erm **C**ode) module (see Sagar *et al.* (1992)) deals with the calculation of aqueous and gaseous radionuclide time- and space-dependent source terms for the geologic repository. It does so by considering the variations in those physical processes expected to be most important for the release of radionuclides from the EBS. The repository radionuclide inventory was reduced to 20 radionuclides for consideration in the analysis. (The screening process, which selected the more significant radionuclide contributors to the performance measures of interest, is discussed in Section 5.2.4.)

Three primary calculations are done in *SOTEC*: (a) failure of waste packages because of a combination of corrosion processes and mechanical stresses; (b) the leaching of spent nuclear fuel and migration of radionuclides from the EBS; and (c) the release of $^{14}CO_2$ gas from the oxidation of UO_2 and other components in spent nuclear fuel and hardware.

Disruptive Consequence Analysis (Chapter 6)

The ability of the undisturbed repository system to isolate HLW may be modified by a number of disruptive events. These events, individually and

in combination, have the potential to alter the repository performance in several different ways. They may result in direct releases of radionuclides to the accessible environment or modification of the undisturbed release process.

In IPA Phase 1, the staff developed a model and corresponding computer code to treat the disruptive consequences of human intrusion to geologic repository performance by exploratory drilling. In IPA Phase 2, the number of disruptive consequences considered was increased. In addition to the base case (e.g., no disruptive events), the IPA Phase 2 analysis considered four classes of fundamental causative events: pluvial climate change, human intrusion (including exploratory drilling), seismic effects, and magmatic events, for a total of 16 mutually exclusive scenario classes.

Dose Assessment Module (Chapter 7)

A major difference between the IPA Phase 1 and IPA Phase 2 studies was the addition of a dose assessment capability into the TPA computer code in IPA Phase 2. In IPA Phase 2, human exposures were evaluated using a dose assessment software package entitled *DITTY* (Dose Integrated for Ten Thousand Years—see Napier *et al.*, 1988; pp. 3-16—3-18) that was obtained from the Pacific Northwest Laboratories.

Sensitivity and Uncertainty Analysis Module (Chapter 8)

As noted above, performance assessments for a geologic repository will be based on conceptual models that, in part, are based on empirical data embodied as computer programs. Because of the inherent variably of the empirical data and the description of processes included in the models, the predicted performance will be uncertain. An important part of conducting an IPA for a geologic repository therefore is quantifying the sensitivity of the results to the values of the input parameters, and the uncertainty associated with the probabilities of occurrence of credible scenarios.

In IPA Phase 1, the staff performed a statistical analysis of the liquid-pathway calculations using several techniques including Latin Hypercube Sampling (LHS) and regression analysis methods (see Section 9.5 ("Sensitivities and Uncertainties for Liquid-Pathway Analysis") in Codell *et al.*, 1992). In the IPA Phase 2 study, the capability t perform a statistical analysis of the total-system performance assessment results was expanded through the application of statistical techniques, in addition to regression analysis. The LHS scheme was used to sample input parameters for the source term, flow, and transport models, and disruptive consequences affecting the performance of the geologic repository.

Auxiliary Analyses (Chapters 4, 5, and 8)

In IPA Phase 1, four distinct auxiliary analyses were performed:

- The potential for non-vertical flow;
- The sampling requirements for CCDF generation;
- The consequences of $^{14}CO_2$ gaseous releases; and
- The statistical analysis of available hydrologic data for input to flow and transport models

For the IPA Phase 2 analysis, the following 14 additional auxiliary analyses were performed:

In Chapter 4:

- An evaluation of the *DCM3D* computer code for the analysis of three-dimensional ground-water flow;
- An evaluation of the distribution coefficient (K_d) approximation for radionuclide retardation;
- An analysis of a regional ground-water flow model for Yucca Mountain;
- An evaluation of the effects of layering, dipping, angle, and faulting on two-dimensional (2-D), variably saturated flow;
- A *DCM3D* dual-continuum flow modeling demonstration;
- An analysis of $^{14}CO_2$ transport;
- An evaluation of U.S. Geological Survey (USGS) regional flow modeling for the Yuc Mountain region;

- An evaluation of saturated zone flow modeling exercise, using *DCM3D*;
- Considerations in modeling infiltration at Yucca Mountain;
- An analysis of the exchange of major cations at Yucca Mountain; and
- A comparison of *NEFTRAN II* to the *UCBNE41* transport code.

In Chapter 5:

- Ensemble averaging for source term parameters; and
- An analysis of the release and transport of gaseous radionuclides other than ^{14}C.

In Chapter 8:

- An evaluation of several methods of sensitivity and uncertainty analyses.

Many additional, smaller-scope auxiliary analyses were performed as part of developing the computational modules or other aspects of the IPA Phase 2 analysis. These analyses are given limited documentation in this report in the respective chapters in which they occur.

1.3 Description of the Modeled System

As noted in Section 1.1, the first step in a total-system performance assessment is to develop a system description of the geologic repository that includes information to support development of models describing repository performance and to determine assumptions and parameters on which the models depend. In this manner, the geologic repository is broken into its component parts for the purposes of modeling. These components include the waste form, the mined geologic repository system, and the portion of the geosphere surrounding the geologic repository through which the radionuclides, in time, migrate. The following descriptions of the site and the geologic repository (including the waste package) (Sections 1.3.1 and 1.3.2, respectively), are condensed from the 1988 Site Characterization Plan (SCP) (DOE, 1988) and other relevant sources. These descriptions provided the bases for the conceptual models (described in Section 1.3.3) used in the IPA Phase 2 analysis described in subsequent chapters.

1.3.1 Site Description

Although the performance assessment methodology chosen is generic, the transport models, disruptive scenarios, and biological pathways are, to a large part, site-specific. The following is a brief description of the Yucca Mountain site geology, hydrology, mineral resource potential, and climatology—with an indication of where, in the report, each was factored into the IPA Phase 2 analysis. Except as otherwise noted, the following general description of the site geology has been condensed from Chapter 1 ("Geology") of DOE's 1988 SCP.

The Yucca Mountain Site is located in Nye County, which is in southern Nevada, approximately 160 kilometers northwest of Las Vegas. The site (by definition, the location of the controlled area) is entirely located on Federal land managed by DOE and the Bureau of Land Management, whereas the extreme northern portions of the site lie within, or abut, Nellis Air Force Range. Yucca Mountain is located in the southern part of the Great Basin, the northernmost subprovince of the Basin and Range Physiographic Province. Generally this province is characterized by more or less regularly spaced sub-parallel ranges and intervening alluviated basins formed through extensional faulting. The site region is generally arid, with sparse vegetation and low population density.

Yucca mountain itself is an irregularly shaped upland 6- to 10-kilometers wide and about 40-kilometers long. The crest of the mountain ranges between altitudes of 1500 and 1930 meters, about 650 meters higher than the floor of Crater Flat to the west. The physiographic features of the mountain are dominated by a sub-parallel series of *en-echelon*, north-trending ridges and valleys controlled by steeply dipping faults. Fault blocks are tilted eastward so that, in general, the fault-bounded west-facing slopes are generally high and steep, whereas the east-facing slopes are more gentle and deeply dissected by a sub-parallel system of linear valleys. The mountain is bounded by Crater Flat on the west, by Jackass Flat-Fortymile Wash on the east and southeast, the Amargosa Desert to the south, and by the Timber Mountain Caldera complex to the north.

The surface and near surface stratigraphy at Yucca Mountain is comprised of a gently dipping sequence of Miocene ash-flow tuffs, lavas, and volcanic breccias more than 1800 meters thick, and flanked by younger alluvial deposits of late Tertiary and Quaternary age.

The rock unit being considered for a repository is a densely welded ash-flow tuff of the Topopah Spring Member of the Paintbrush Tuff. Although the Paintbrush Tuff regionally is composed of six major ash-flow tuffs and three related lava-flow sequences, at Yucca Mountain only four ash-flow tuffs are recognized. In the general area of the proposed repository, this unit ranges in thickness from approximately 300 meters to almost 600 meters, generally thickest in the north and thinning to the south and east. The Topopah Spring Member is the lowermost member of the Paintbrush Tuff and is the thickest unit in the area of the repository, ranging in thickness from 287 meters (drill hole USW G-2) to 369 meters (drill hole USW H-1). This member is comprised of seven recognizable units, which in ascending order are: the lower nonwelded to moderately welded zone (13 to 42 meters thick); the basal vitrophyre (10 to 25 meters thick); the lower nonlithophysal zone (27 to 56 meters thick); the lower lithophysal zone (43 to 117 meters thick); the middle nonlithophysal zone (20 to 50 meters thick); the upper lithophysal zone (54 to 96 meters thick); and the caprock zone (39 to 62 meters thick). In ascending order, above this unit, are three ash-flow tuffs: the Pah Canyon, Yucca Mountain Member, and the Tiva Canyon Member. The Pah Canyon and Yucca Mountain Members are relatively thin units in the area of the repository reaching a combined thickness of only slightly greater than 100 meters in the area of USW G-2, while normally having a combined thickness of 20 to 30 meters. These units are non-existent in the area of drill hole UE-25p#1. The Tiva Canyon Member is the youngest bedrock unit present over much of the site region, thickening southward from about 90 to nearly 140 meters in the central part of Yucca Mountain and then thinning southward again to about 125 meters. Ten informal map units have been recognized in the Tiva Canyon Member. In ascending order these are: the columnar unit, the hackly unit, the lower lithophysal unit, the red clinkstone, the gray clinkstone, the rounded step, the lower cliff, the upper lithophysal, the upper cliff and, the cap rock unit. The relative proportion of the various units changes from north to south, with the lithophysal units representing about 30 percent of the Tiva Canyon in the northern reaches and only about 10 percent to the south.

Although the Tiva Canyon represents the youngest identified, exposed unit of the Paintbrush Tuff in the Yucca Mountain area, a nonwelded ash-flow and ash-fall tuff has been identified in the subsurface, in the vicinity of the proposed location of the surface facilities. It is possible that this material, which reaches a maximum thickness of 61 meters, is the lateral equivalent of the Pinyon Pass and Chocolate Mountain members of the Paintbrush Tuff.

The Rainier Mesa Member of the Timber Mountain Tuff is locally present above the Tiva Canyon in the lower reaches of Solitario Canyon, in core from boring UE-25p#1, and in Trench 14 on the west side of Exile Hill. This suggests that the Rainier Mesa Member was present as a very thin unit above the Tiva Canyon and has subsequently been eroded, or that this member was only deposited in the lower elevations. The youngest volcanic rocks that have been identified to date, at Yucca Mountain, itself, are basaltic dikes located at the northern reaches of Solitario Canyon, where they are implaced along a fault zone.

The basaltic dikes at the northern reaches of Solitario Canyon have been interpreted by Crowe *et al.* (1983, p. 24) as part of the oldest of three main episodes of basaltic volcanism that has occurred in the Yucca Mountain region after the period of explosive silicic activity responsible for the thick tuff accumulations. This first episode involved bimodal basalt-rhyolite eruptions from approximately 11 to 8 million years before present (mybp). The second phase of basaltic eruptions, the older rift basalts, range in age from 9 to 6.5 million years and include the basalts of Rocket Wash and Pahute Mesa. The third episode of basaltic activity, which has continued into the late Quaternary, occurred after a pause in volcanic activity from about 6.5 to 4.1 mybp and includes the basalts of Buckboard Mesa, Crater Flat, and Lathrop Wells. More detail regarding magmatic activity and how it was factored into the IPA

Phase 2 analysis may be found in Section 3.3.2.2(A) of this report.

Below the Paintbrush Tuffs are the rhyolite lavas and tuffaceous beds of the Calico Hills. In outcrop, this unit comprises a sequence of ash-flow and ash-fall tuffs, volcanoclastic sediments, and rhyolitic lavas. In the northern reaches of Yucca Mountain, this entire unit is zeolitized, but in the southern reaches (near drill holes USW GU–3 and USW G–3) it remains vitric. Underlying the Calico Hills unit are 1000 or more meters of older tuffs and volcanogenic rocks above the pre-volcanic units.

The subsurface extent of pre-volcanic rocks in the Yucca Mountain area is poorly known; however, based on the results from drill hole UE–25p#1, it is known that carbonate rocks of the Silurian-age Lone Mountain Dolomite and Roberts Mountain Formation are present. These rocks comprise part of the lower carbonate aquifer, a regional aquifer used in many parts of Nevada as a primary water-supply source. Based on gravity data, it is suggested that the prevolcanic rocks are approximately 3000 meters thick; however, it is not known if these units are entirely upper Proterozoic and Paleozoic strata, or if younger, post-Silurian units are found beneath the vocanics. It is suggested, based on aeromagnetic data, that the northern portions of Yucca Mountain may be underlain by the Mississippian Eleana Formation (Bath and Jahren, 1984).

Unconsolidated deposits in the region of Yucca Mountain consist primarily of colluvium, alluvium, eolian sand, lacustrian deposits, and playa deposits. In the general site area colluvium, alluvium, and sand deposits are the primary materials found. The thickness of these units is extremely variable, ranging from 0 meters thickness, over much of Yucca Mountain, to in excess of 1000 meters in the center of the surrounding basins.

The main structural grain at Yucca Mountain, as seen from aerial photographs, is a pronounced north-south trending linear fabric defined by parallel, east-tilted fault blocks. In general, the repository block is considered to be a block outlined by faults, with the Solitario Canyon fault to the west, the Drill Hole Wash structure to the northwest, and a zone of imbricate faults to the east and southeast. This relatively simple pattern becomes complex on closer inspection, as all ridge-bounding faults in this area appear to be connected to adjacent faults, most commonly by short, northwest, trending fault splays (O'Neil *et al.*, 1992). The generally north-trending faults primarily display a down-to-the-west sense of fault displacement, but also have a component of left-lateral slip that is displayed by offset stream channels and *en-echelon* fault splays, commonly linked by pull-apart grabens (*op cit.*). Therefore, although the structure can generally be described as a series of high-angle faults believed to merge downward into a detachment system reflective of the extensional mechanism that appears predominant in this region, the actual structural domain is more complex. In general, from north to south, the structural pattern appears younger and displays a clockwise rotation of structure that may be as large as 30 degrees, since the middle Miocene. Although faults are generally displayed as simple lines on maps and cross-sections, detailed field mapping is showing that these fault zones are extremely complex. Ongoing work by Spengler (1993[8]), indicates, for example, that the Ghost Dance Fault, which has 38 meters of displacement along the southeastern margin of the perimeter drift, is a zone of many small faults, with a mapped width of over 200 meters.

Within the Yucca Mountain Region, 32 faults have been mapped that display Quaternary displacement. These include faults such as: the Solitario Canyon Fault, with over 500 meters of mapped displacement; the Paintbrush Canyon Fault, with over 200 meters displacement; and the Bow Ridge Fault, with over 220 meters of displacement. Although the mapped displacement, per event, on the units, is generally on the order of a few centimeters, this normally only includes the vertical component of displacement, so the amount of total displacement for each episode of faulting is poorly constrained. Based on ongoing work by DOE, it appears that the recurrence interval on the various faults is on the order of 50 to 100,000 years for earthquakes of

[8]Spengler, R.W., "Resolution of the Stratigraphic and Structural Settings and Mineral Resource Potential of Yucca Mountain," Unpublished USGS Presentation at DOE/NRC Technical Exchange on Geophysics Integration, Las Vegas, Nevada, June 8, 1993.

approximate magnitude 6.5. (Whitney, 1993[9]). This value would appear to be in the same general range as the "minimum maximum credible earthquake" of dePolo (1993). That the Yucca Mountain area is tectonically active has been demonstrated by the Little Skull Mountain earthquakes or the recent Rock Valley earthquakes. More detail regarding seismic activity and how it was factored into the IPA Phase 2 analysis may be found in Section 3.3.2.2(B) of this report.

A significant aspect of locating a repository at Yucca Mountain is the thickness of the unsaturated zone, allowing the construction of a repository from 180 to 400 meters above the water table. The water table forms the upper boundary of a tuff aquifer that is part of the Alkali Flats-Furnace Creek ground-water subbasin. A major discharge point of the basin is Franklin Lake Playa, at Alkali Flats, in California, through evapotranspiration. Another possible discharge point is at springs in Death Valley near Furnace Creek Ranch. More detailed information regarding the ground-water hydrology of the site and how it was factored into the performance assessment may be found in Section 4.2 and Appendices B, C, E, I, and J of this report.

There are no perennial streams in the vicinity of Yucca Mountain. The springs in Oasis Valley, the Armagosa Desert, and Death Valley are the only reliable sources of surface water in the Alkali Flats Subbasin. Most of the water discharged by the springs travels only a short distance before evaporating or infiltrating into the ground. Floods may occur in the arroyos during heavy rain storms.

The dominant cations in the Yucca Mountain ground water are sodium, calcium, potassium, and magnesium. Sodium is the most abundant cation, accounting for 65 to 95 percent of the cations present. Minerals with high sorption capacity, zeolites, and clays are present along potential ground-water flow paths beneath the repository site. More detailed information regarding the site geochemistry and how it was factored into the IPA Phase 2 analysis can be found in Appendices D, K, and L of this report.

Yucca Mountain is located in a natural, resources-rich geologic region; however, site characterization activities to date have not disclosed any direct evidence of significant mineral or petroleum reserves at Yucca Mountain. Ground water and zeolites are possible resources known to be present at the site; however, they are more economically available elsewhere than in the Yucca Mountain region. More detail regarding the potential for economic mineral resources at Yucca Mountain, and how exploration for such resources was factored into the IPA Phase 2 analysis, may be found in Section 3.3.2.2(D) of this report.

Finally, the present climate at the Yucca Mountain site is classified as a mid-latitude desert climate. Temperatures approach 49°C in the summer time, and the annual precipitation is less than 0.15 meters. The skies are generally clear throughout the year with low relative humidity. During the fall, winter, and early spring, the predominant winds are from the north. During the late spring and summer, the winds shift to a predominantly south to southwesterly direction. More detailed information regarding climate and how it was factored into the performance assessment may be found in Section 3.3.2.2(C) of this report. Information concerning growing season and sources of meteorological data can be found in Sections 7.7 and 7.8 of this report.

1.3.2 Repository Description (Including the Waste Package and Contained Waste Form)

As with the site, knowledge of the design of the geologic repository is also necessary to develop the performance assessment methodology and to construct the proper models. The following is a brief description of the GROA underground facility, the waste package disposal container and contained waste form, and emplacement method, as described in Chapters 6 and 7 ("Conceptual Design of the Repository" and "Waste Package," respectively) of the 1988 SCP, and indicates where these descriptions are factored into the IPA Phase 2 analysis.

The GROA underground facility, where the final emplacement of the nuclear waste would occur, is planned to be constructed at a depth of about 300

[9]Whitney, J. W., "Integration of the Geophysical Studies with Activities in the Tectonics Program," Unpublished USGS Presentation at DOE/NRC Technical Exchange on Geophysics Integration, Las Vegas, Nevada, June 8, 1993.

meters below the eastern flank of Yucca Mountain. The host rock is sufficiently thick over a large enough area to accommodate up to 70,000 metric tons equivalent of waste. Existing information about the site indicates that an area of 848 hectares could be available for waste emplacement; 558 hectares will be used under current plans. The main component of the underground facility is the emplacement panel. Each panel would be about 430 meters wide and about 460 to 980 meters long. The present preliminary layout calls for 18 emplacement panels based on a design areal power density of 57 kilowatts (kW)/acre.[10] Each panel would contain a number of emplacement drifts. The capacity and the layout of the underground facility are factored into the source term analysis described in Chapter 5 of this report. The anticipated thermal loading of the geologic repository is also an input to the source term analysis, as well as the analysis of gas transport examined in Section 4.3 of this report.

The waste package design is expected to consist of the waste form and the disposal container, and is the principal engineered barrier. The principal waste forms will be either spent nuclear fuel from commercial nuclear power reactors or vitrified waste (glass) from both defense and commercial sources, although other waste forms may be disposed of at the proposed site.[11] The reference spent nuclear fuel is 10 years-old with a thermal decay power of about 3.3 kW/waste package (see DOE, 1988; p. 7-29). The gamma dose rate at the surface of the waste package for spent nuclear fuel is about 50,000 rads per hour, and the neutron flux rate is about 10,000 neutrons per square centimeter per second. The vitrified waste will have a thermal power level of about 200 to 470 watts per waste package. The gamma dose at the surface of the waste package is about 5500 rads per hour, and the neutron flux rate will be low. Slightly different assumptions were used for the radionuclide inventory (see Barnard *et al.*; pp. 4-13—4-14 and 6-1—6-16). However, for the purposes of this analysis, only spent nuclear fuel was considered. How the age and composition of the waste forms was factored into the source term analysis is discussed in Chapter 5 of this report.

A key component of the waste package is an overpack container for both the spent nuclear fuel and vitrified waste forms. The reference material for the waste package is stainless steel, with an outside diameter of about 0.66 meters (for stainless steel), and a length of about 3.20 meters for vitrified waste, and 4.7 meters for spent nuclear fuel. The container has a thickness of 0.95 centimeters. After the waste form is loaded into the waste package, the container will be filled with argon gas, and the top will be welded on the container. The loaded waste package would weigh from 2700 to 6300 kilograms, depending on the quantity of waste. The weight, construction, and size of the disposal container are factored into the performance analysis in the seismic scenarios analysis discussed in Section 6.4 of this report.

In the SCP conceptual design, it was assumed that the waste packages would be emplaced in vertical boreholes drilled into the floors of the waste-emplacement drifts. In the vertical emplacement mode, the boreholes, about 7.6 meters deep and about 0.76 meters in diameter, would be drilled vertically into the floor of the emplacement drifts, and a single waste package would be emplaced in each borehole. The container will rest on a support plate inserted into the bottom of the vertical borehole, and the borehole would be lined with a metal casing starting at the top of the hole and extending past the top of the waste package. A metal plug will be inserted on top of the container, to provide shielding from radiation, and crushed tuff would be packed around and on top of this plug and closed with a metal cover. The emplacement hole, its orientation, and geometry are factored into the analysis of the source term discussed in Chapter 5 and the seismic scenarios model discussed in Section 6.4.

Section 60.111(b) requires that the GROA be designed so that the emplaced waste be retrievable at any time up to 50 years after the start of waste emplacement operations. A "caretaker" period of 24 years will begin after the waste emplacement period of 26 years. At the end of the caretaker period, after confirmatory tests of repository performance (10 CFR 60.137), the GROA would be prepared for permanent closure by backfilling the underground facility, and

[10] 57 kW/acre is used in this report for easy comparison with the SCP, rather than the metric equivalent of 141 kW/hectare.

[11] Other waste forms that may possibly be disposed of in a geologic repository include low-level, greater-than-Class-C, or transuranic wastes.

permanently sealing the shafts and ramps. Presently proposed concepts for sealing shafts include surface barriers, shaft fill, settlement plugs, and stationary plugs. The backfill would consist of tuff excavated during the construction of the underground facility.

1.3.3 IPA Phase 2 System Model and Methodology

The base case system model used in IPA Phase 2 was comprised of subsystem and process models (or modules). The major subsystems modeled were the waste package and EBS, the local hydrosphere, and a postulated biosphere. Major processes modeled separately were water percolation, gas transport, and ground-water transport. Disruptive events that were considered to act on the system model were pluvial climate change, seismicity, human intrusion, and magmatism.

For the liquid source term and transport (Section 4.2), the site was conceptualized as a layered stratigraphy, and the repository and water pathways were divided into seven distinct columns. These columns helped take into account the variation in stratigraphic sequences and thickness, differences in unsaturated and saturated pathway distances, and temperatures within the repository. Auxiliary analyses conducted with a 2–D dual continuum representation of the repository cross-section (Appendices C and G) were used to determine how percolation from rainfall should be distributed among the seven sub-areas (columns) as well as determine the distribution of flow between rock fractures and matrices in the unsaturated portion of the pathways. The source term module, described in Chapter 5, considers the environment of the waste package and near-field, including the EBS. When disruptive events are not present, the source term module uses repository zone temperature as an indicator of whether each particular zone is wet or dry. After the initial dry-out period in each zone, corrosion is calculated as a function of environmental conditions. When the wall thickness from corrosion is thin enough to result in failure of the waste package canister, water is assumed to enter the canister and the waste dissolution process is assumed to begin. There is also a small quantity of packages assumed to have initial defects which did not require corrosion before dissolution and release could take place. Transport out of the waste package canister by advection and diffusion is calculated as a function of the fracture flow rate into the zone and the results are passed on to the liquid flow and transport module. In the transport model, *in-situ* matrix and fracture velocities and matrix geochemical retardation are used to determine the time-varying amounts of radionuclides reaching the biosphere (e.g., the accessible environment).

In regard to gas source term and transport (Section 4.3), the site was also conceptualized as a layered stratigraphy; however, the site and repository were not subdivided into sub-areas. Yucca Mountain and the repository were modeled as a 2-D cross-section with a time-varying temperature distribution. The temperature distribution was calculated based on conductive heat transfer, taking into account the repository thermal loading and the heat transfer properties of the rock. The gas source term which results from initial defects and corrosion (in the absence of disruptive events), was assumed to be evenly distributed throughout the repository. A model employing many simplified assumptions was developed to determine the velocity vectors throughout the cross-section at various times throughout the performance assessment period. The gas source term releases were tracked through the repository, using these time-varying velocity vectors, and reduced for radioactive decay, in accordance with their travel time (including geochemical retardation) to the surface (e.g., the accessible environment).

To simulate the performance of the repository system under the influence of credible external events, mutually exclusive scenario classes were developed (Chapter 6). For calculation of dose and release within various scenario classes, the base case system model parameters and logic were changed to account for the disruptive event or combination of events being modeled. For scenario classes involving the climate change, the water table was raised and infiltration was sampled from a different distribution than was used for the normal climate. Scenario classes involving drilling allowed damage to emplaced waste packages and also added a pathway (the borehole) as a direct pathway to the accessible environment. Scenario classes involving seismicity required the interaction of a seismic canister failure module with the source term module. The source term module calculates waste package

thicknesses, based on corrosion processes, and combines this information with seismic acceleration probability data from the seismic module to determine when and if a waste package should fail. No changes in the existing pathways or the addition of new pathways is assumed to be caused by seismicity. For classes involving volcanism, the repository is assumed to be in the possible path of intrusive and extrusive volcanic events. The intrusive events are assumed to be underground magma intrusions that damage waste packages but don't provide an additional pathway to the surface. Extrusive events are assumed to entrain a portion of the repository waste and carry it directly to the surface, resulting in an airborne release.

After the transport of radionuclides to the accessible environment (biosphere), as a function of time, is determined, the radionuclides from the various pathways are accumulated, to determine the cumulative release, for comparison with the EPA standard and to calculate the cumulative population dose (Chapter 6). The biosphere used for the dose calculation is assumed to be a 2700-acre farm, with three people maintaining a year-round residence and 177 people off site eating beef cattle, which grazed on the farm, for the waterborne dose; and 22,200 persons in the region for the airborne dose. The dose was calculated in 70-year (lifetime) intervals and accumulated. After completion of the runs and construction of the CCDFs (for both release and dose) sensitivity and uncertainty analyses were performed.

The system code was run 400 times for each modeled scenario class. Over two hundred parameters were sampled for some of the classes. The sampling was performed using the LHS routine. Because of the large uncertainty in both site parameters and process parameters, probability distributions were determined for hydrologic characteristics of the individual geologic strata, corrosion parameters, percolation distribution parameters, and scenario-related parameters, as well as other site- and process-related parameters.

2 TOTAL-SYSTEM PERFORMANCE ASSESSMENT COMPUTER CODE

2.1 Operational Description

2.1.1 Introduction

In IPA Phase 1, the U.S. Nuclear Regulatory Commission staff developed its own system code to process information needed to generate the complementary cumulative distribution function (CCDF) representative of the performance of the geologic repository, for a limited set of scenario classes, using preliminary data and numerous assumptions (see Chapter 4 ("System Code"), in Codell *et al.*, 1992). However, in IPA Phase 2, the staff developed a more sophisticated model and computer code to represent the performance of a geologic repository. The principal features of the staff's improved computer code, designated the total-system performance assessment (TPA) computer code, are discussed below.[1]

The main objectives of the TPA computer code are to develop the computational algorithms for estimating compliance with the performance objectives set forth in 10 CFR Part 60. When fully developed, the TPA computer code will permit estimates of overall system (10 CFR 60.112) and subsystem (10 CFR 60.113) performance, as a function of the specific characteristics of the proposed repository site and design. Such computations take into account the complex interactions among site and design subsystems, components, future states, and processes. Accordingly, the NRC staff expects to use the TPA computer code to review critical aspects of the performance assessment contained in a U.S. Department of Energy (DOE) license application, and as a basis for interactions related to the sufficiency of DOE's site characterization program during the pre-licensing period.

A complete description of the TPA computer code is available in the Center for Nuclear Waste Regulatory Analyses (CNWRA) document 93-017 (Sagar and Janetzke, 1993). The requirements for the code were developed early in the design process (see Appendix C ("Requirements Document for TPA Computer Code") in Sagar and Janetzke (1993)). The TPA computer code was developed using software utilities designed to increase the productivity of the developers and the quality of the final product. One of these was the "preFOR" FORTRAN preprocessor utility, which is described in CNWRA 91-003 (Janetzke and Sagar, 1991a).

2.1.2 Code Organization

The diverse nature of the physical processes present in the natural system being simulated requires that theories from many disciplines be integrated into an overall system model. The TPA program is designed to simulate the behavior of a geologic repository located in a partially saturated medium; both the natural system and the engineered barriers are accounted for in the program design. The evolutionary change in the natural system is described in terms of disruptive scenarios which, in addition to a parametric description of the changed state, also has a probability of occurrence attached to it. Consequently, the TPA computer code is designed as a set of consequence modules largely independent computational units, with their execution controlled by a system manager or executive module. Figure 2-1 shows schematically the data flow and execution dependencies of the subprocesses of the TPA computer code.

Almost all the concepts necessary to model a repository system are included in modules that are controlled by the *executive module* (also referred to as the *system executive* or *executive*). However, the implementation of these modules is kept flexible so that various scenarios may be simulated. In other words, no specific conceptual model is embedded in the *executive module*, except for the fact that the general approach of scenario analysis is adopted. In the scenario approach, the future state of the repository system is defined by a set of parameters whose values are chosen from specified probability distributions. This set of parameters is assumed to be independent of time for a particular scenario, although this is not strictly required for the scenario approach. A different scenario is defined, if parameter values change within the time span of interest (e.g., 10,000 years). In the analyses conducted so far, disruptions defining

[1]The principal features of the staff's advanced model for a geologic repository that forms the basis for this improved computer code are discussed in Chapters 3 through 7.

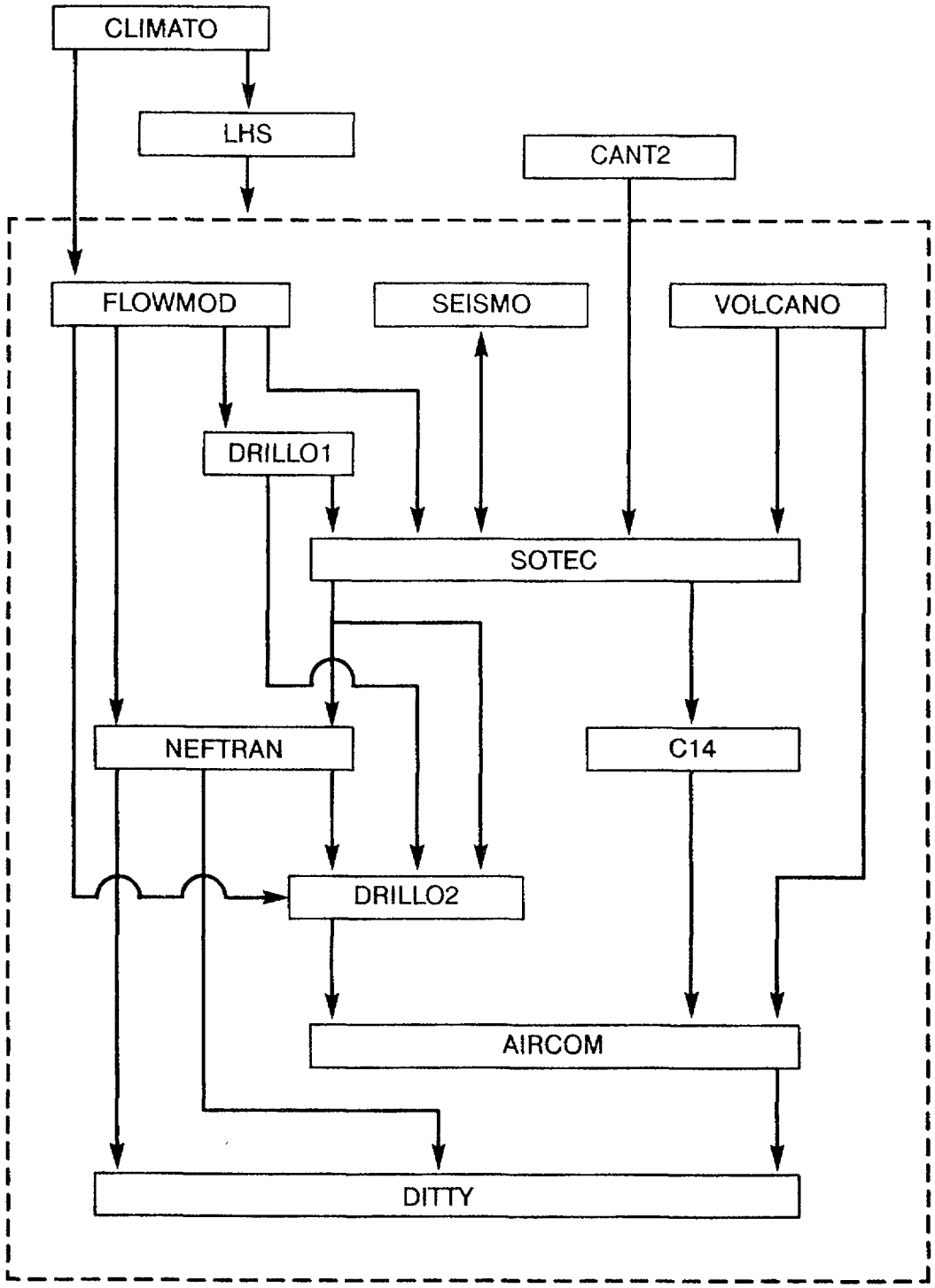

Figure 2–1 Flow diagram showing the elements of the total-system performance assessment computer code (These elements are described in Section 2.1.3. The dashed line shows which elements are controlled by the *executive module*, described in Section 2.1.2.)

scenarios occur at a specified time and the disturbed state then remains constant, which is probably reasonable for every scenario except those involving pluvial climate.

Automated features included in the system facilitate the unattended running of a set of multiple scenarios with associated output.

The TPA computer code consists of four basic parts:

- The system manager or *executive module*;
- Algorithm(s) to sample from statistical distributions;
- Algorithm(s) to model future states or scenarios; and
- Algorithms to model internal repository system processes such as source term, transport, and consequences.

Consequences are quantified in terms of cumulative releases and dose-to-man. In addition, algorithms to compute sensitivities and perform uncertainty analyses are executed separately as an auxiliary process (see Chapter 8).

Although not depicted in the figure, the *executive module* of the TPA computer code acts as the controller for the overall computer code and executes the consequence modules in the desired sequence and ensures that appropriate values of the common parameters are passed to the appropriate consequence modules. The *executive module* controls the sequence of execution of various modules, transfers data to other modules, and controls data transfer from one module to another. Authored principally by R. Janetzke and B. Sagar at the CNWRA, the *executive module* of the TPA computer code currently consists of about 21,000 lines of FORTRAN, whereas the complete system code (including all modules) is about 85,000 lines (see Sagar and Janetzke, 1993). The total execution time for one realization of all consequence modules on the Cray computer was about 100 seconds.

The programs for the consequence modules are also referred to as subprocesses in the sense that together they provide the complete process for describing the behavior of the repository. The consequence modules are designed to be executed either as part of a TPA computer code or independently. The standard documentation prepared for these programs will also apply to their use in the TPA computer code, with minor modifications to input and output procedures, which are explained in CNWRA 91-009 (Sagar and Janetzke, 1991). The TPA computer code uses a dedicated subroutine to handle the setup and initiation of each subprocess. An additional subroutine is required to read any results that may be provided to the *executive* by a particular subprocess. The subprocess is created as the result of a CALL to a utility routine, which is specific to the operating system. This CALL is the mechanism that starts the subprocess. Control is returned to the *executive module* at the end of the execution of the subprocess.

The subprocess for obtaining samples from specified statistical distributions is based on the Latin Hypercube Sampling (LHS) method (see Iman and Shortencarier, 1984). Other programs used as subprocesses include algorithms for computing flow fields, estimation of doses, and calculation of consequences of scenarios such as human intrusion. Modules to calculate sensitivities of the final results (e.g., CCDF) to selected parameters are implemented as external auxiliary processes.

The TPA *executive* code is maintained in the CNWRA configuration management system (TOP-018; CNWRA, 1982), and is fully compliant with it.

2.1.3 TPA Module Descriptions

As noted above and illustrated in the figure, the TPA computer code is organized into a number of modules that perform specific computational functions. A brief description of each of the TPA computer code modules is provided below, in alphabetical order.

AIRCOM—This module is mainly utilitarian in nature and does not perform any calculations relative to the physics of the overall geologic repository system, except for the introduction of fractions of contaminated soil that become airborne and respirable for the drilling and volcanic disruptive events. Its main purpose is to merge the various airborne release data files (*VOLCANO, DRILLO,* and *C14*) into one file in

the proper format for use by the dose module—*DITTY* (**D**ose **I**ntegrated for **T**en **T**housand **Y**ears; see Napier *et al.*, 1988), as discussed below, and at greater length in Chapter 7.

In IPA Phase 2, contaminated soil or gaseous $^{14}CO_2$ was assumed to be transported to the ground surface above the repository as a result of disruption of the geologic repository itself, either by human intrusion or by an extrusive volcanic event. In this analysis, only a fraction of this surface radioactivity was assumed to become available for transport by the air pathway to members of the public beyond the controlled area (10 CFR 60.2) of the geologic repository. The fractions of the radioactivity that were assumed to become airborne were stored in the *AIRCOM* module. All the airborne radioactivity was assumed to be respirable (whether in the solid, liquid, or gaseous states). Any radioactivity that did not become airborne was considered to remain undisturbed at the point of release to the above-ground surface.

The *AIRCOM* values were used as inputs to the files used by DITTY, to calculate the exposure of the regional population, or that part of the farm family, to airborne radioactivity released from the geologic repository. First, the *DRILLO*, *VOLCANO*, and *C14* modules were used to calculate the quantities of contaminated soil or gaseous ^{14}C released to the ground surface at various times during the 10,000-year study (as determined by LHS sampling of appropriate model parameters). Next, these quantities were multiplied by the corresponding airborne fractions in *AIRCOM* to generate the input values (curies per year released to air) for use by the *DITTY* module, to calculate dose.

This module was developed by A. O'Campo of the Southwest Research Institute (SwRI).

CLIMATO—This module is a place holder for a future climate-related constituent of a disruptive event. In IPA Phase 2, climate change is treated by specifying climate-dependent infiltration rate and water table position for use in the *FLOWMOD* transport module (see Section 6.2).

CANT2—The time-dependent temperature of the surface of a waste package is calculated in *CANT2*. Developed by R. Codell (NMSS), the *CANT2* module is based upon an analytic solution of the linear heat conduction equation, by the principle of superposition assuming, a finite number of heat sources. In IPA Phase 2, the repository is assumed to consist of seven regions or sub-areas, each repository sub-area comprised of several waste emplacement panels. The main purpose of *CANT2* is to predict the temperature of a representative waste package in each of the seven repository sub-areas needed for the source term module—*SOTEC* (**S**ource **T**erm **C**ode)—to determine the time at which liquid water can come into contact with the waste packages. The output is written to a file, which is read by the *SOTEC* module. *SOTEC* also uses this temperature for the temperature-dependent parts of the source term model (e.g., the *C14* release module).

In IPA Phase 2, none of the parameters used by *CANT2* is considered random; these parameters also did not vary with disruptive scenarios. Consequently, *CANT2* is executed only once, and the resulting temperatures are used by all the vectors of all the scenarios.

C14—In IPA Phase 2, $^{14}CO_2$ is considered to be the only radionuclide that can be transported in the gaseous phase. *C14* calculates the travel time and decay of $^{14}CO_2$ releases from the source term module. Authored by R. Wescott (NMSS) and R. Codell this module uses an independently calculated time-varying far-field temperature field, to determine time-dependent gas velocities. *C14* uses the equations of flow, hydrologic parameters from the LHS sampling module, and the time varying temperature field induced by the spent nuclear fuel, to calculate a time varying gas velocity field from the water table to the atmosphere. Releases from the source term are tracked through this field and reduced by radioactive decay taking into account retardation of $^{14}CO_2$, because of the interaction of the host rock and water. The amount of $^{14}CO_2$ released from the repository, as calculated by the source term module, *SOTEC*, is provided to *C14* as an input. The resulting releases to the atmosphere are then passed to the *AIRCOM* module in terms of curies/year, as points in time from repository closure to the end of the period of regulatory interest, for the purposes of performance assessment.

This module is discussed at greater length in Chapter 4.

DITTY—The transport of radioactivity to the biosphere is modeled in the *DITTY* module. *DITTY* estimates the time integral of collective dose over a 10,000-year duration for releases (or concentrations) of radionuclides to the accessible environment. In IPA Phase 2, the exposure pathways of interest included: the atmosphere, land surfaces, the top 15 centimeters of surface soil, vegetation, animal products (milk, beef), and drinking water. (Aquatic pathways were not considered.) The annual releases to the air or water pathways over the 10,000-year period of interest were provided as input to *DITTY* by other consequence modules, in the form of average annual concentrations. The values for these concentration-time pairs were obtained as outputs directly from *NEFTRAN* or indirectly from *C14*, *DRILL02*, and *VOLCANO*, via the *AIRCOM* module.

Developed originally for the Hanford site, this code was obtained from the Battelle Pacific Northwest Laboratories (PNL) in Richland, Washington. This module considers both air and liquid transport pathways and calculates both the individual and population doses. The *DITTY* module is designed to deal with both acute and chronic releases, and annual, committed, or accumulated doses can be calculated. Several of the Hanford site-specific data coded in *DITTY* were modified. A second generation of dose calculation codes, *GENII*, which includes the original *DITTY* code, is currently available from PNL. For conceptual models included in *DITTY* and its user's manual, see Napier *et al.* (1988).

This module is discussed at greater length in Chapter 7.

DRILLO1—In IPA Phase 2, the human intrusion disruptive event is stipulated to consist of drilling initiated above the geologic repository. The location of boreholes and the timing of drilling are assumed to be random (see Appendix H ("Analysis for Drilling Scenario") in Codell *et al.* (1992)). Although a random spatial distribution may not be physically realizable, it is used here for simplicity. The drill bit can either hit a waste package directly or it may only penetrate contaminated rock. Radioactive material may be brought to the surface, in either case.

Authored by N. Eisenberg (NMSS), J. Firth (NMSS), and C. Freitas (SwRI), the *DRILLO1* module uses sampled data on the seven repository sub-areas and the distribution of waste packages. This information is used, for each borehole, to determine the region where the borehole is located and whether a waste package was struck during the drilling event. These results are then used by *DRILLO2* to determine the consequences. The calculated number of direct hits and their times of occurrence are also supplied to the *SOTEC* module, for inclusion in the calculation of a source term.

DRILLO2—Consequences from the drilling disruptive events identified in *DRILLO1* are calculated in *DRILLO2*. A drill bit hitting a waste package directly or penetrating contaminated rock is assumed to lift a certain portion of the radionuclide inventory to the ground surface. The inventory in a waste package and in the rock surrounding waste packages is as a function of time, and is used by *DRILLO2*, to determine consequences. A small percentage of the radioactive material brought to the surface is assumed to be particulate material that becomes airborne. This information is then provided to the *AIRCOM* module, for calculation of the respirable fraction of the human dose in *DITTY*. The *DRILLO2* module was authored by N. Eisenberg, J. Firth, and C. Freitas.

The detailed features of the *DRILLO* modules are discussed in Frietas *et al.* (1994).

FLOWMOD—The computational module entitled *FLOWMOD* determines the hydrologic flow regime that provides ground-water flux for use in the source term module (*SOTEC*) and transport pathways and properties for use in the transport module—*NEFTRAN* (**NE**twork **F**low and **TRAN**Sport). The primary functions within *FLOWMOD* are the determination of: (a) the spatial distribution of ground-water flux; (b) the quantity of flow in the matrix and the fracture; (c) fluid velocities; and (d) saturation-dependent retardation coefficients. The computational demands of solving partially saturated flow in fractured tuff precluded a direct solution of the flow equation; therefore, a table interpolation scheme was used to determine spatial distribution

of flow and the quantity of matrix versus fracture flow. The tables used for these interpolations were based on the results, using a dual-continuum approach, as set forth in the *DCM3D* computer program (see Updegraff *et al.*, 1991) for simulating Yucca Mountain. The interpolation scheme made use of sampled data for the infiltration rate and the hydraulic properties of the matrix and fractures.

FLOWMOD uses these relationships to determine the mass fluxes and particle travel times for each of the stratigraphic units comprising a certain number of vertical columns corresponding to each of the geologic repository sub-areas (seven in IPA Phase 2). The *DCM3D* computer program is not a part of the TPA computer code. It was executed separately to create the input data for *FLOWMOD*. This module was developed by T. McCartin (RES) and W. Ford (NMSS).

This module is discussed at greater length in Chapter 4.

LHS—The TPA user can specify various parameters pertaining to any number of consequence modules to be sampled where statistical distributions represent uncertainty. The *LHS* module uses the sampling method of Iman and Shortencarier (1984) to create equally likely parameter vectors. Although only uncorrelated parameters were used in IPA Phase 2 calculations, the *LHS* module is designed to sample from correlated parameters also. Two aspects of the *LHS* module to be noted are: (a) all sampled parameters, irrespective of which consequence module they belong to, are sampled at one time; and (b) for the analysis of any one scenario, a single call to the *LHS* module provides all the vectors or realizations.

The computer program for the LHS was obtained from the Sandia National Laboratories (SNL), under contract to NRC. The detailed features of the *LHS* module are discussed in Sagar and Janetzke (1993).

NEFTRAN—The far-field transport of radionuclides is treated in the *NEFTRAN* module. The initial version of the code used during IPA Phase 1 was obtained from SNL (see Longsine *et al.*, 1987) under an NRC research contract. In IPA Phase 2, the staff used an improved version designated *NEFTRAN II* (see Olague *et al.*, 1991).

The *NEFTRAN* module simulates the transport of radionuclides in the aqueous phase away from the geologic repository, and calculates the integrated discharge of radionuclides, over 10,000 years, at the boundary of the accessible environment and the time-varying concentration of radionuclides (used in the calculation of the dose) at the boundary of the accessible environment. In the simulation of radionuclide transport, the following two primary factors are accounted for in the *NEFTRAN* simulations: (a) element-specific retardation of radionuclides, based on the geologic unit and the degree of saturation; and (b) multiple flow paths, to represent the possible dual flow paths caused by fracture and matrix flow. As shown in Figure 2–1, the pore velocities calculated by *FLOWMOD* are provided as input to *NEFTRAN*. In *NEFTRAN*, the transport domain is considered to be made up of one-dimensional (1–D) transport paths, along which the convection-diffusion equation is solved semi-analytically by the distributed velocity method (DVM). Details of the DVM are availabl in Olague *et al.* (1991).

This module is discussed at greater length in Chapter 4.

SEISMO—The *SEISMO* module calculates the probabilities of failures of waste packages, because of a seismic event. The probability of occurrence of an event of certain magnitude is considered to be time-dependent. To simplify the analysis, a seismic hazard curve representing time-dependence of earthquake magnitudes (peak accelerations) at a certain probability level (e.g., 95 percent) is first obtained. This curve is obtained from a family of postulated plots between the occurrence probability versus earthquake magnitude for a set of fixed time periods. Based on the structural properties of the container material, a fragility curve representing a relation between peak acceleration and the critical container wall thickness is derived. The actual container wall thickness, for waste packages, as affected by corrosion processes, is obtained from *SOTEC* as a function of time, which produces a time history of nominal wall thickness, when considering the undisturbed case. Any time the critical wall thickness obtained from the fragility curve is greater than the actual thickness

produced by the *SOTEC*, failure occurs. The number of such failures is fed back to *SOTEC* for calculation of the source term. This module was authored by N. Eisenberg, R. Codell, and C. Freitas.

This module is discussed at greater length in Chapter 6.

SOTEC—deals with the calculation of aqueous and gaseous radionuclide time- and space-dependent source terms for the geologic repository. It does so by considering the variations in those physical processes expected to be important for the release of radionuclides from the engineered barrier system. As mentioned above, ^{14}C is the only radionuclide that is treated in the gaseous phase in IPA Phase 2. However, all radionuclides, including ^{14}C, are considered in the aqueous phase. As shown in the figure, *SOTEC* provides the aqueous, gaseous, and direct radionuclide releases to the geosphere transport modules—*C14, DRILLO2, NEFTRAN, SEISMO,* and *VOLCANO*.

Three primary calculations are done in *SOTEC*: (a) failure of waste containers because of a combination of corrosion processes and mechanical stresses; (b) the leaching of spent fuel; and (c) the release of $^{14}CO_2$ gas from the oxidation of UO_2 and other components in the spent nuclear fuel and hardware. In Version 1.0 of *SOTEC* (Sagar *et al.*, 1992), general corrosion, pitting, and crevice corrosion are modeled, based on a temperature-dependent corrosion potential. The temperatures obtained in *CANT2* are provided as inputs to *SOTEC*. Leaching rates are considered to be either solubility limited or congruent to UO_2 rates. This module was authored by B. Sagar, R. Codell, J. Walton (CNWRA), and R. Janetzke. More details are available in Sagar *et al.* (1992).

This module is discussed at greater length in Chapter 5.

VOLCANO—Consequences caused by magmatic events are calculated in the *VOLCANO* module. This module was developed by R. Baca (CNWRA), L. Lancaster (RES), R. Drake (CNWRA), and C. Lin (SwRI), and is based on the work of Margulies *et al.* (1992). In the geometric approach followed in *VOLCANO*, Monte Carlo sampling is used to generate a volcanic event randomly in a rectangular region surrounding the repository horizon. Random sampling is used to specify: (a) the location of the sampled volcanic eruption; (b) the nature (intrusive, leading to dike formation and extrusive, leading to dike and/or cone formation) of the volcanic event; (c) the dimensions of the dike or cone; and (d) the orientation of the dike. From the area of the geologic repository intercepted by dikes and cones, the numbers of waste packages failed by the magmatic event are determined assuming all intercepted waste packages have failed. This information is used in *SOTEC*. When the volcanic event is extrusive, the contents of the failed waste packages are assumed to be released to the accessible environment (direct release), and a fraction of this is assumed to be ejected to the atmosphere, which is then used in *AIRCOM* to calculate human dose, and in the *executive module*, to calculate the total release. A more detailed description of the *VOLCANO* module is given in Lin *et al.* (1993).

This module is discussed at greater length in Chapter 6.

Finally, all the consequence modules used for the TPA system code are maintained under the CNWRA configuration management system (TOP-018), and will be fully compliant with it upon the receipt of *User Guides* for *CANT2, FLOWMOD, C14, DRILLO, SEISMO,* and *AIRCOM*.

2.1.4 Data Handling and Control

The input/output (I/O) files for the TPA system code can generally be divided into four different types:

- Input;
- Temporary (used for the duration of the current scenario);
- Reusable (used for more than one scenario); and
- Output.

The input files include the TPA input file, LHS standard input file, and standard input files for each of the consequence modules. The TPA input file is prepared in a free-format style. That is, the

input values are associated with keywords rather than with fixed column positions in the input file. This was implemented using a set of standard FORTRAN routines described in CNWRA 91-005 (Janetzke and Sagar, 1991b).

The temporary files include the files generated by the TPA computer code for the purpose of transmitting control parameters to an external module. These typically contain global parameters (parameters that are common to more than one module) which can override the parameters read from the module's standard input file. The temporary files receive their names from the TPA *executive module* and are overwritten for each new vector processed. In general, only the programmer (and not the end user) needs to access the temporary files.

The reusable files are those on which intermediate results from various consequence modules are written. The data in these files may be processed later by other modules.

The output files include the output file of the TPA computer code itself, standard output files of each one of the consequence modules, error log files, and specially formatted files, for external utilities such as the TECPLOT graphics utility (Amtec Engineering, 1984).

Names of all files except the temporary files can be read as part of the input. The format-free input process of the TPA *executive* is explained in Sagar and Janetzke (1993).

2.1.5 Sampled vs. Global Data

Many of the consequence modules require some of their input parameters to be sampled from a certain statistical distribution over a range with known end points. This feature is adapted in a common manner for all of the computational modules involved. The *LHS* module is used to generate the **sampled data** for all of the parameters, and for all vectors of a given scenario. A standard *LHS* input file is created with distribution specifications for all of the parameters. Appendix A lists the distribution and range specifications for the *LHS*-sampled input parameters used in the IPA Phase 2 analysis. The *LHS* module then produces a single output file, containing a data set for each vector. When a consequence module begins execution, it reads this file sequentially until it finds the correct vector and then reads the entire parameter set for that vector. The consequence module must then select its parameters from this set, as specified in a "map" file, which identifies the location of each parameter.

When the modules are executed in a stand-alone mode, sampled parameters are not used, and all the necessary control input is provided via the standard input file. In the TPA computer code, however, the sampled data must override any values provided in the standard input file. This is done by ensuring that the sampled data are read after the standard input file is read, and before any quantities are derived from them.

One of the primary requirements of the simulation process is that parameters that are common to many subprocesses be specified consistently. Since the design of the TPA software is such that all the subprocesses can run independently, this consistency is maintained through the temporary global data files, which transmit data from the *executive* to the consequence modules. These data files contain parameters in a fixed order, and the corresponding consequence module must follow this order when extracting the parameters from the file. This process is completely automated and does not require manipulation by the user.

2.2 Improvements and Changes Since IPA Phase 1

IPA Phase 1 included releases only via the water pathway and direct drilling pathway. Release and transport of ^{14}C in the gas phase were considered only in an auxiliary analysis, and not in the evaluation of risk. The source term module was a version of the module already existing in *NEFTRAN*, modified somewhat for consideration of unsaturated flow.

The analysis of the liquid phase release and transport to the accessible environment considered the following mechanisms:

- One-dimensional steady-state flow and transport through the unsaturated zone, through four parallel columns consisting of multiple layers of rock under the influence o. normal and pluvial rates of water infiltration.

- Waste form dissolution, based on the quantity of water that could enter the waste package container.
- An empirical failure-time distribution for the waste package canisters. All waste packages canisters were considered to fail simultaneously.
- Direct release of a portion of the waste brought to the surface in drill cuttings.

IPA Phase 1 considered four scenarios:

- Normal infiltration, no drilling;
- Normal infiltration with drilling;
- Pluvial infiltration, no drilling; and
- Pluvial infiltration with drilling.

The normal infiltration cases considered 500 vectors each. The pluvial scenarios considered only 98 vectors, because of a problem with long run times. There were a total of 29 radionuclides initially included in the analysis. Results of the scenarios were used to generate the conditional CCDFs for each scenario, and combined with scenario probabilities to produce an overall CCDF. The input and output vectors were also used to generate sensitivity analyses, using multiple linear regression and several other techniques.

The IPA Phase 1 analysis relied heavily on manual manipulation of files, rather than the relatively high degree of automation provided by the system driver for Phase 2. The *LHS*, *NEFTRAN*, and sensitivity/uncertainty analyses were submitted manually and used by the analyst in sequence. By contrast, in IPA Phase 2, the staff developed a more sophisticated model and computer code to represent the performance of a geologic repository. The principal features of the staff's advanced model were:

- The geologic repository is represented by seven repository sub-areas.
- Three transport pathways were considered—gaseous, aqueous, and direct.
- Treatment of mechanistic models of waste package failure (including a specified number of early failures).
- Consideration of four disruptive events—climate change, seismic shaking, human intrusion (including exploratory drilling), and magmatic eruption—for a total of 16 probability combinations.
- Considered only 20 radionuclides, on the basis of screening.

The principal features of the staff's more sophisticated computer code in IPA Phase 2 are:

- The execution of the various scenarios is now performed under the control of the TPA *executive module*, with consistent data provided automatically to all of the consequence modules.
- The *system executive* is responsible for the invocation of the modules and the reading of the release values after each module is run. It is designed to calculate the CCDF for releases by nuclide, pathway, repository sub-area, scenario, and overall.

Although both internal and external modes[2] are available for the TPA *executive module*, the internal mode is preferred. This mode ensures that all the modules receive the same input data automatically. The individual modules obtain much of their control and data information from the *system executive*; therefore the *executive* exercises a degree of precision when invoking the module to execute a particular scenario or vector. The communication mechanism used for this is formatted ASCII files. These files are called global data files, since much of the content is common to the consequence modules.

All the sampled parameters from all of the modules are generated during a single run of the *LHS* module code, and then each module can select its sampled parameters from the file, using identical techniques. A mapping file serves to aid

[2]"Internal" versus "external" refers to the manner of code execution and the time at which the output files from the consequence modules are generated. In the internal mode, consequence modules are run and cumulative radionuclide releases calculated as the system code is executed. In the external mode, the modules are separate from the system code, and as a result, the cumulative releases can be generated and placed in files at any time before iteration of the system code.

the module in extracting the correct parameters from the *LHS* output file, since the *LHS* program does not organize its output with keys for each parameter. The map file contains the exact location of each sampled parameter for a given computational module.

As noted above, in IPA Phase 2, the repository was divided into additional zones (now seven), and the normalized release values were stored separately for each repository sub-area, as well as each of the 20 nuclides. Moreover, as discussed in Section 2.1.3, several new scenario and consequence modules were added to the system code, namely seismicity, volcanism, $^{14}CO_2$ gas flow, and dosimetry.

Finally, the TPA *executive* can produce a CCDF plot in the TECPLOT format for each scenario, as well as a total CCDF for all of the scenarios, from the single internal array that stores the normalized release values from all of the consequence modules.

2.3 Conclusions and Suggestions for Future Work

A number of conclusions and recommendations for further work can be drawn from the design, development, and execution of the TPA computer code (including its modules), during IPA Phase 2. Several of these conclusions and recommendations were first proposed following IPA Phase 1, but not fully implemented during Phase 2. To the extent that these conclusions and recommendations still apply, and should continue to be considered in future IPA work, they are repeated below.

1—The process of abstraction.

Deriving simple, efficient computational modules (and attendant computer codes) from more complete and complex models, to represent the performance of components of the repository system for use in probabilistic simulations, is an issue that requires more focus and analysis. As noted in IPA Phase 1, general approaches for achieving satisfactory computational speed, while maintaining an appropriate degree of physical representativeness, need to be evolved; this still continues to be the case, based on the staff's Phase 2 work.

For example, in IPA Phase 2, the staff discovered that significant modification (simplification) had to be done to the original design concepts during the eventual implementation of the TPA computer code. As noted earlier, the computational requirements of modules became prohibitive, and significant simplifications were required in order to achieve acceptable execution times. Hence, it is recommended that more attention be paid to the appropriateness of abstracting the complicated phenomena, to achieve efficient mathematical models. Moreover, it is recommended that the TPA computer code (and its modules) be considered a dynamic entity, and modifications should readily be pursued, to achieve a more effective TPA computer code.

Finally, considering that the connection between more representative codes and the simpler codes used to demonstrate compliance is likely to be a major issue in licensing, the staff continues to believe that the abstraction process may be a subject suitable for the development of regulatory guidance in the future.

2—Software documentation.

During the development of several computational modules, a number of difficulties were encountered related to software quality assurance (QA), including the lack of: documented module designs, module integration designs, and documented module testing. Hence, it is recommended that more attention in the future be paid to QA procedures.

3—Continue to evaluate additional computer codes, that could not be acquired and evaluated during the IPA Phase 1 or Phase 2 efforts, to determine whether existing codes can meet the NRC modeling needs, or whether additional code development is needed.

As summarized in Section 2.1.3 and noted in subsequent chapters of this report, several computer codes that appeared to be promising in terms of providing missing parts of the analysis, and that offered improved treatment of certain aspects of modeling, were evaluated for use in the IPA Phase 2 demonstration. These codes included *BIGFLOW* (Ababou and Bagtzoglou, 1993), *DITTY, DCM3D* (Updegraff *et al.*, 1991), *MODFF* (Torak, 1992), *NEFTRAN, PHREEQE* (Parkhur *et al.*, 1980), *PHREEQM* (Nienhuis and Appelo, 1990), and *UCBNE41* (Lung *et al.*, 1987).

However, the staff believes that there are additional computer codes that need to be evaluated that might provide some additional assistance to the staff in its performance assessment efforts. Some of the codes that might be worthwhile investigating in the future are: *TOUGH* (Pruess, 1987), *TOSPAC* (Dudley *et al.*, 1988), *AREST* (Apted *et al.*, 1989), and *EBSPAC* (see Sridar *et al.*, 1993).

3 SCENARIO ANALYSIS MODULE[1]

3.1 Introduction

In IPA Phase 1, a general approach to scenario development was identified, but, because of resource constraints, implemented only to a limited extent (see "Methodology for Scenario Development," in Codell *et al.*, 1992, pp. 31–39). Therefore, to identify scenarios for that effort, a less systematic, more expedient approach was taken. That approach involved selecting two classes of events (climate change/pluvial conditions and human intrusion by exploratory drilling) for the analysis, in part, because the modeling variations needed to accommodate these events in the consequence analysis were not excessive. The probability of occurrence for exploratory drilling was determined by following the guidance provided by the U.S. Environmental Protection Agency (EPA), in Appendix B of 40 CFR Part 191[2] (*Code of Federal Regulations*, Title 40, "Protection of Environment") (see EPA, 1993; 58 *FR* 7936). The probability of climate change/ pluvial conditions was determined arbitrarily. A recommendation arising from the IPA Phase 1 effort was to develop and demonstrate a mathematically rigorous, scientifically robust method for scenario analysis (see Codell *et al.*, 1992, p. 91).

In IPA Phase 2, the staff has applied the Sandia National Laboratories (SNL) scenario selection procedure to generate scenarios for use in the IPA Phase 2 consequence analysis. The SNL methodology has been applied by the SNL staff to hypothetical basalt and salt sites, and by international organizations involved in the geologic disposal of high-level radioactive waste (HLW). This section briefly summarizes the SNL procedure and then documents the development of a final set of scenario classes and corresponding probability estimates for use in the IPA Phase 2 effort.

In this analysis, a "scenario" is defined as any postulated future sequence of events and processes (EPs) external to the repository system which is sufficiently credible to warrant consideration of its projected effect on repository performance. These sequences represent some of the potential ways in which the repository system environment might evolve. Such alternate evolutions may result from the occurrence of natural phenomena and/or from human-initiated activity, and could affect the release and transport of radionuclides from the repository to the accessible environment. A "scenario class" is a unique combination of processes and/or events without regard to the order in which they occur.

3.2 Description of the SNL Scenario Selection Procedure

The SNL scenario selection methodology (Cranwell *et al.*, 1990) consists of a five-step process that, when completed, provides a set of scenarios, with corresponding probabilities, for use in the consequence analysis of a potential HLW disposal site. These steps are:

No. 1. Identification of those EPs deemed to be potentially disruptive of long-term isolation of HLW at a disposal site.

No. 2. Classification of these EPs.

No. 3. Screening of these EPs, using well-defined criteria.

No. 4. Formation of scenarios by combining the EPs remaining after screening.

No. 5. Screening of these scenarios, using well-defined criteria.

[1]The figures shown in this chapter present the results from a demonstration of staff capability to review a performance assessment. These figures, like the demonstration, are limited by the use of many simplifying assumptions and sparse data.

[2]Currently, a revised set of standards specific to the Yucca Mountain site is being developed in accordance with the provisions of the Energy Policy Act of 1992. The Energy Policy Act of 1992 (Public Law 102–486), approved October 24, 1992, directs NRC to promulgate a rule, modifying 10 CFR Part 60 of its regulations, so that these regulations are consistent with EPA's public health and safety standards for protection of the public from releases to the accessible environment from radioactive materials stored or disposed of at Yucca Mountain, Nevada, consistent with the findings and recommendations made by the National Academy of Sciences, to EPA, on issues relating to the environmental standards governing the Yucca Mountain repository. It is assumed that the revised EPA standards for the Yucca Mountain site will not be substantially different from those currently contained in 40 CFR Part 191, particularly as they pertain to the need to conduct a quantitative performance assessment as the means to estimate postclosure performance of the repository system.

3.2.1 Step No. 1—Identification of Events and Processes

The initial step in the SNL procedure is the identification of EPs that are considered to be potentially disruptive of waste isolation at the particular HLW disposal site in question. These EPs, which should be as comprehensive and complete as possible, are identified by persons knowledgeable in the fields of earth science and waste management and would include both natural and human-induced phenomena. The use of generic lists of EPs (e.g., see International Atomic Energy Agency (IAEA), 1981) can help to ensure that important site-specific phenomena are not overlooked.

3.2.2 Step No. 2—Classification of Events and Processes

The second step in the methodology is the categorization of the EPs. This can be accomplished using any of a number of different classification schemes. Criteria for classification might include:

- The origin and physical characteristics of the EPs (i.e., natural, human-initiated, or waste-/repository-induced);
- The manner of influence the EPs have on the repository system and surrounding geology (e.g., whether they affect near-field or far-field processes or phenomena);
- The time of occurrence (e.g., between 0 to 100, 101 to 1000, or 1001 to 10,000 years); and
- The probability of occurrence (e.g., likely, unlikely but possible, or very unlikely).

The classification of EPs provides an opportunity to ensure that important phenomena are not omitted, and as such, this step is iteratively linked with Step No. 1. In addition, this particular step also imparts an initial organization to the collection of EPs, which is needed to begin developing and analyzing potential scenarios.

3.2.3 Step No. 3—Screening of Events and Processes

Given the potentially large collection of EPs that could be identified and the correspondingly large number of scenarios that could be formed from these EPs, it is essential that the analysis focuses on those EPs that are sufficiently credible to warrant consideration so that the task of scenario identification (and the subsequent consequence analysis) remains tractable. Therefore, using well-defined criteria, it should be possible to eliminate some of the identified and classified EPs from further consideration. Basic screening criteria include:

- The physical reasonableness of occurrence of the EP at the site;

  EPs whose occurrence are impossible because of the characteristics of the waste, facility, or site can be removed from the analysis, based on a lack of physical reasonableness.

- The probability of occurrence of the EP; and

  EPs with very low probabilities of occurrence also can be screened from further consideration. The value used as the criterion for screening should be consistent with the appropriate regulations. For example, EPA guidance in 40 CFR Part 191 is such that categories of EPs estimated to have less than 1 chance in 10,000 of occurring over 10,000 years need not be considered.

- The potential consequences associated with the EP's occurrence.

  EPs may be screened if their occurrence has insignificant potential effects on the natural properties of the site (e.g., the hydraulic head distribution). Such a judgment would require flow and thermomechanical analyses to be made. In addition, EPs with similar consequences may be grouped together as long as their probabilities are appropriately combined.

3.2.4 Step No. 4—Combination of Events and Processes into Scenarios

In the fourth step, the EPs remaining after screening are combined into scenarios. These scenarios are formed using a logic diagram or similar device, to ensure that all possible combinations of the EPs are identified and examined. The number of scenarios developed will depend on the numb of EPs available (i.e., if n phenomena remain following initial screening, then 2^n scenarios are possible). For example, in Figure 3-1, five EPs

(designated *R1, R2, T1, T2,* and *T3*) are linked to form 32 (2^5) scenarios, where, under the SNL procedure, each specific path through the tree is called a "scenario."

In Figure 3-1, one of the combinations is labeled "base case." Under the SNL methodology, the base case scenario represents an initial conceptualization of the disposal system, which includes the characteristics of the geologic site, the underground facility, and the emplaced waste (Bonano *et al.*, 1989). In this scenario, all components of the engineered barrier system (EBS), consisting of the underground facility and the waste packages (10 CFR Part 60.2), are assumed to perform as designed, undisturbed by external phenomena (e.g., igneous activity, exploratory drilling). As shown in the figure, other scenarios will be perturbations to these nominal conditions (Cranwell *et al.*, 1990).

3.2.5 Step No. 5—Screening of Scenarios

The newly-formed scenarios are then screened using criteria similar to those applied in the initial screening of the EPs: physical reasonableness, probability, and potential consequences. Screening based on physical reasonableness, for example, would eliminate incompatible combinations of various EPs.

Provided that the EPs are mutually independent (i.e., the occurrence or non-occurrence of one EP has no influence on the subsequent occurrence or non-occurrence of another EP and vice versa), individual scenario probabilities can be calculated by multiplying the likelihoods of the different EPs comprising the scenario. If the EPs are not mutually independent, then conditional probabilities are used. The probability value used should be consistent with appropriate regulations.

Scenarios can be screened if there are no consequences associated with their occurrence. Consequences, in this case, refer to either radionuclide discharges to the accessible environment or to the health effects resulting from such releases.

3.3 IPA Phase 2 Scenario Development Using the SNL Methodology

The development of scenario classes for IPA Phase 2, using the SNL methodology, was conducted by the IPA staff over a period of several months. Bonano *et al.* (1990) present the process of formalizing the elicitation and use of expert judgment in the performance assessment of HLW repositories in deep geologic formations. However, this *formal* process was not followed in the collection and use of the opinions expressed in the staff discussions. Instead, an *informal* approach was taken in which open discussions of the potentially disruptive EPs, their possible effects on the system, and their relative likelihoods were combined with more detailed individually-submitted written information on the same topics, with documentation of the staff member's reasoning, supported by appropriate references and/or general principles.

3.3.1 Identification and Classification of Events and Processes

Before identifying an initial set of potentially disruptive phenomena for consideration, the boundaries of the repository system first were defined. In an approach similar to that taken in the IPA Phase 1 scenario development effort (Codell *et al.*, 1992; pp. 31-32), these boundaries were chosen to be largely coincident with those of the accessible environment. For this analysis, the repository system was defined as extending 5 kilometers horizontally from the outer perimeter of the proposed repository, and vertically from the land surface to a depth just below the current water table.

Phenomena initiated beyond these boundaries were classified as external perturbations of the system, even if the effects of the phenomena occurred within the repository. Thus, for example, fault displacement in the repository would be classified as an external event, because the tectonic forces responsible for initiating the movement can be considered external to the system. Exploratory drilling would be classified as an external event for similar reasons. Phenomena, such as waste canister corrosion and borehole seal degradation, on the other hand, occur within the system boundaries, and thus would be classified as internal processes. Under this classification, external phenomena were retained for consideration in the scenario analysis, whereas

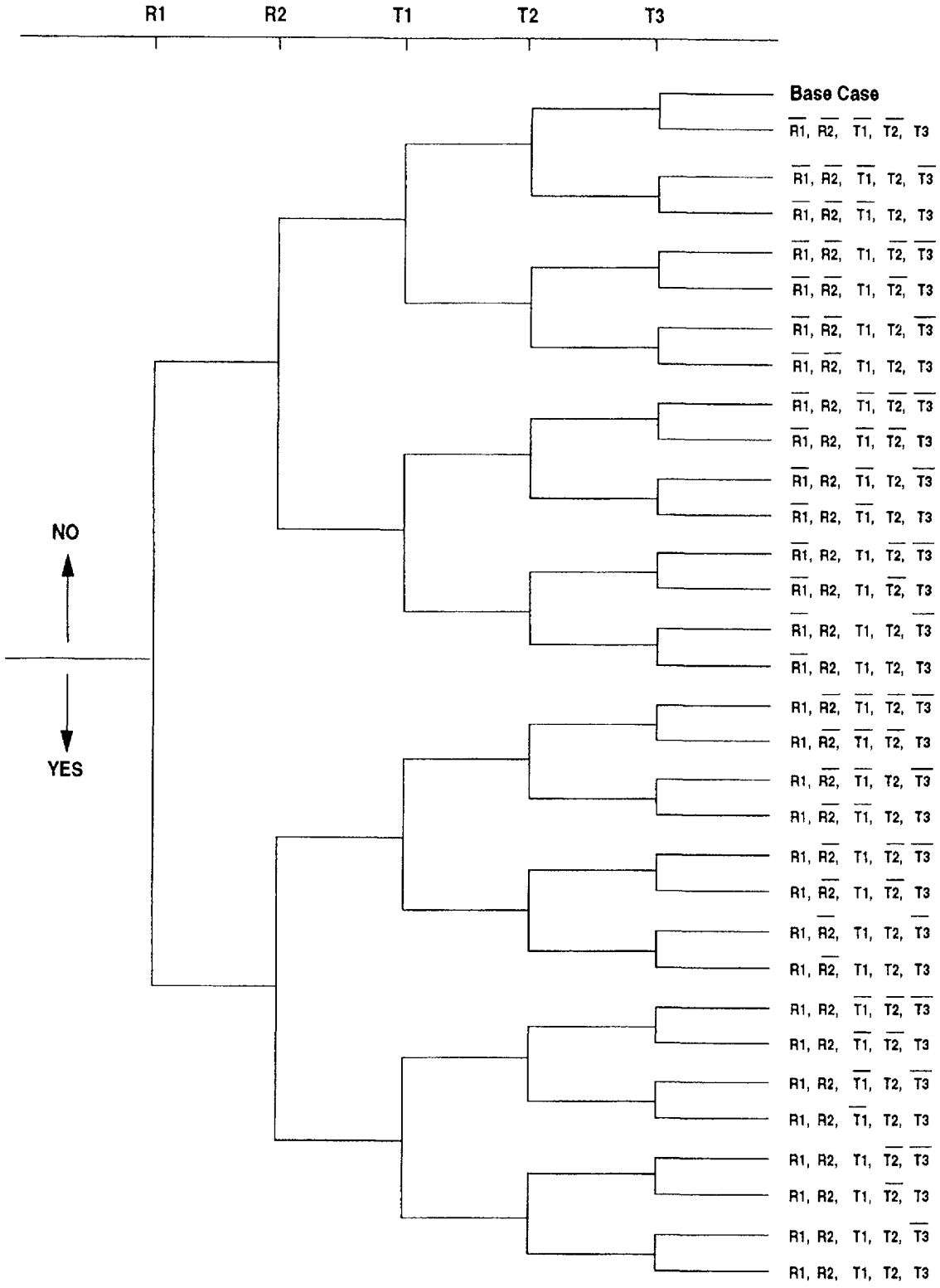

Figure 3–1 Potential combinations of two releases (R) and three transport (T) phenomena (Adopted from Cranwell *et al.* (1990))

internal events and processes, including features of the site (e.g., faults), were assumed to be incorporated into the models and data bases used to describe the system. This approach differs from that proposed by Cranwell *et al.* since they include internal processes and features (e.g., borehole seal degradation, faults) in their scenario analysis (Cranwell *et al.*, 1990; pp. 26, 44–53).

As discussed previously in Codell *et al.* (1992; pp. 31–32), the approach adopted here differs from those proposed by other analysts. Hodgkinson and Sumerling (1990), for example, describe a scenario development approach in which no distinction is made between "internal" phenomena and those occurring outside the repository. Under this scheme, processes such as waste canister corrosion would be combined into scenarios for analysis, and as a result, their list of "events, features, and processes," incorporating both internal and external phenomena, contains nearly 150 entries. Even after screening of these entries, the number of scenarios that could be constructed would be quite formidable. The approach chosen for the IPA Phase 2 analysis greatly reduces the number of scenarios that can be generated, and thus the complexity of the total-system performance assessment.

For the IPA Phase 2 scenario analysis, an initial set of potentially disruptive EPs (Table 3-1) was compiled from similar lists of those considered:

- In the IPA Phase 1 scenario analysis (Codell *et al.*, 1992);
- In the SNL work of Cranwell *et al.* (1990); and
- From the generic list of EPs assembled by the IAEA (1981).

This list should not be considered complete nor comprehensive; further work may identify additional EPs that warrant at least initial consideration within a scenario analysis for the Yucca Mountain site.

It is important to note that these EPs can be considered as "categories" of events and processes since, implicitly, the entire range of possible manifestation styles, locations, and times (i.e., "subevents" and "subprocesses") is contained under each identified EP. In keeping the detail for the EPs at this broad level, the staff considers that the EPA screening criteria based on probability (i.e., less than 1×10^{-4} over 10,000 years) can be applied more appropriately. Also, because categories of EPs are being considered, classes of scenarios, rather than explicitly-defined individual scenarios, will be produced by this analysis. Consequence modeling of individual scenarios representing the scenario classes generated through this procedure is discussed in the following chapters.

3.3.2 Screening of Events and Processes

All three of the screening criteria (i.e., physical reasonableness, probability of occurrence, and potential consequences) identified in Section 3.2.3 were used to screen the initial set of EPs for this analysis. Flow and thermodynamic calculations, suggested by Cranwell *et al.* (1990), were not used in screening based on potential consequences, primarily because the numerical computer codes necessary for such analyses were not available. Instead, screening on this criteria was based on staff judgment.

After screening, six EPs remained for staff consideration:

- Igneous Activity—Intrusive
- Igneous Activity—Extrusive
- Faulting
- Seismicity
- Climate Change
- Exploratory Drilling

For this scenario development effort, these six EPs were further reduced to four by combining "Intrusive" and "Extrusive Igneous Activity," and "Faulting" and "Seismicity," into single EPs. In addition, with respect to a Faulting/Seismicity EP, consequence analysis modeling for IPA Phase 2 focused solely on the effects of seismicity, and therefore, the final set of EPs to be combined into scenarios for IPA Phase 2 was:

- Igneous Activity
- Seismicity
- Climate Change
- Exploratory Drilling

Table 3–1 Initial Set of Potentially Disruptive Events and Processes

Natural Events and Processes	*Human–initiated Events and Processes*
A. Igneous Activity	A. Climate control (e.g., greenhouse effect)
1. Extrusive	B. War
2. Intrusive	C. Nuclear weapon testing at Nevada Test Site
B. Tectonic Activity	D. Exploratory drilling for natural resources
1. Regional uplift	E. Mining
2. Regional subsidence	1. Surface-based (open pit)
3. Seismicity	2. Underground shafts and drifts
4. Faulting	F. Large-scale alterations to hydrology (e.g., dams)
C. Climatic Conditions	
1. Current climate—extreme phenomena	
2. Climate change	
D. Other	
1. Sea level change	
2. Tsunamis/seiches	
3. Meteorite impact	

3.3.2.1 Rationales Used to Screen Events and Processes

The rationales used to screen particular initial EPs from further consideration in IPA Phase 2 are discussed next. These rationales are necessarily preliminary and will need to be revisited when the appropriate models, codes, and data are available for this purpose.

1. Regional uplift/subsidence

Potential consequences associated with the occurrence of these initial EPs were deemed to be insignificant. The proposed repository will lie approximately 300 meters below the ground surface and about 180 to 400 meters above the regional water table, whereas rates of regional vertical tectonic movement are estimated to be less than 3 centimeters/1000 years (DOE, 1988b; p. 1–28). Therefore, regional uplift/subsidence alone would appear to have negligible direct effects on repository performance over the 10,000-year period of regulatory interest. The potential impacts of erosion, both regional denudation and local incision, associated with current and projected climatic conditions, should be examined, if necessary, in future analyses.

2. Current climate (extreme phenomena)

This initial EP was screened because such phenomena would be included under the current climate conditions, which are part of the base-case scenario class.

3. Sea level changes

This initial EP was screened because of insignificant potential effects on repository performance. Yucca Mountain and vicinity are part of the Death Valley internally-drained groundwater basin system, and therefore, significant sea level changes would not affect the stream baselines or the water-table elevation (Ross, 1987). In addition, changes in the sea level are related to global phenomena and processes, such as climatic variations and plate tectonics. Site performance may be more sensitive to these processes instead.

4. Tsunamis/seiches

These initial EPs were screened because of the low probability of occurrence at the site. Yucca Mountain is located several hundred miles from the Pacific Ocean, in an arid climate, and is not overlain by large bodies of surface-water necessary for seiche formation (DOE, 1988a; p. 29).

5. Meteorite impact

This initial EP was screened because of the low probability of its occurrence at the site. Various studies have calculated the likelihood of a meteorite impact sufficient to disturb a repository at depth to be in the range of 10^{-13}/square kilometer/year (Cranwell *et al.*, 1990).

6. Climate control

This initial EP was subsumed under the initial EP: "Climate Change," because consequences associated with its occurrence would be similar to those associated with natural climatic changes.

7. War

Disruption of a repository at Yucca Mountain would likely require the direct impact of a thermonuclear weapon; however, Yucca Mountain does not appear to be a prime candidate for such a focused attack. In addition, any radioactive release associated with the breaching of the repository would be a minor consideration in a war in which nuclear weapons were employed. For these reasons, this initial EP was screened from further analysis.

8. Nuclear weapon testing at the Nevada Test Site (NTS)

Subsurface testing of nuclear weapons by the U.S. government has been conducted at the NTS to the north and northeast of Yucca Mountain. Currently, however, no weapon tests are being conducted because of the U.S. self-imposed moratorium against such testing, which extends until 1996. Should subsurface nuclear weapon testing be resumed in the future, any effects on site performance in response to the detonation of these weapons would be experienced in terms of seismicity. For this reason, this initial EP was subsumed under the initial EP: "Seismicity."

9. Mining

Mining for mineral resources at Yucca Mountain could involve either surface (e.g., open pit) or subsurface techniques (e.g., shafts and/or drifts). The seismic effects of surface and subsurface mining operations would not appear to have a significant effect on the post-closure performance of a mined geologic repository at Yucca Mountain (Raney, 1990a). The possible impacts of an open pit mine as a potential site of localized infiltration should be examined, if necessary, in future analyses. Subsurface techniques used to exploit a proposed mineral deposit below the repository horizon could result in the repository being intersected. If the repository were intersected, it is assumed that those engaged in such mining activities would recognize the incompatibility of the wastes with their exploration, seal the mined openings, and abandon their activities.

10. Human-initiated large-scale alterations to hydrology

Large-scale alterations to the groundwater hydrology could involve the construction of dams to surface flow or of irrigation systems for farming. The construction of a dam in the Yucca Mountain area would appear to be unlikely, given the arid regional climate and the lack of significant perennial streams in the area (DOE, 1988a; p. 29). The use of ground water for irrigation could have the net effect of lowering the water table, and thus, increasing the thickness of the unsaturated zone beneath the repository. This might be beneficial to site performance. Therefore, this initial EP was screened from further analysis.

3.3.2.2 Rationales Used to Retain Events and Processes for Further Consideration

The events and processes retained for consideration after screening are described in detail next. For each EP, the following is provided: (1) a description of the EP for the Yucca Mountain region; (2) a short summary discussion of potential impacts on repository performance; (3) a discussion of some current issues in estimating probabilities for the particular EP; and (4) the approach (and results) used in IPA Phase 2 for estimating the probability of occurrence for the EP.

1. Igneous activity (Intrusive and Extrusive)

Description: In the Yucca Mountain region, volcanic activity approximately 16 million years

ago (Ma), produced several large caldera complexes located to the north and west of the proposed site (e.g., Timber Mountain Caldera) (Figure 3–2). These calderas are associated chiefly with the explosive eruptions of silicic volcanic rocks. Yucca Mountain is underlain by a sequence of these silicic rocks from about 1,000 to 3,000 meters thick, consisting mainly of welded and non-welded ash-flow and air-fall tuffs (DOE, 1988a; p. 17). Volcanic flows and breccias commonly occur underground in the northern part of Yucca Mountain but are rare in the southern part.

Approximately 6 to 8 Ma, the volcanic activity in the region changed into a more quiescent basaltic-flow type, characterized by low volume eruptions of short duration (DOE, 1988a; p. 18). Within a 30 kilometer radius of the proposed repository site, 29 post-caldera basaltic vents can be identified (Crowe *et al.*, 1992). In addition, within the immediate vicinity of Yucca Mountain, basaltic dikes are exposed in the northern reaches of Solitario Canyon, borings in the vicinity of Yucca Mountain have occasionally intersected basalt, and further away, relatively extensive basaltic intrusions have been mapped in the area of Paiute Mesa. The youngest basalt-type volcanic feature in the area, located at the southern edge of Crater Flat, is the Lathrop Wells cinder cone, which may have originally formed approximately 130,000 years ago, with possible further eruptions up to as recently as 20,000 years ago (DOE, 1988a; p. 18).

At present, there is considerable debate concerning the age of the volcanic features in the Yucca Mountain region. The variance in the opinions stems from differences in both methods of evaluation and interpretations of available data (see Crowe *et al.*, 1995). The difference is greatest for the youngest features, such as the Lathrop Wells cone, and decreases as older and older material is evaluated.

Potential impacts on radionuclide release and transport: Depending on its location and magnitude, igneous activity could directly or indirectly affect the waste isolation capabilities of a proposed repository at Yucca Mountain. Direct impacts could result from the intersection of the repository by intruding igneous bodies. Such intersections could severely disrupt the EBS through:

- Mechanical disruption of the underground facility and redistribution of the local stress regime;
- Contact of the magma with the waste package canisters,[3] which may result in displacement, fracturing, and shearing of the canisters (in addition to thermal and chemical alterations);
- Entrainment of the potentially damaged waste packages in the rising magma body; and
- Potential release of radionuclides at the surface associated with volcanic activity.

Indirect impacts of igneous activity on repository performance could include:

- Formation of a regional hydrothermal circulation system, if the intrusive body were large enough;
- Creation of barrier(s) to ground-water flow, possibly leading to a temporary or permanent change in the water-table elevation;
- Alteration of regional percolation and ground-water flow paths;
- Thermal and geochemical alteration and degassing associated with the magmatic fluids;
- Localization of surface infiltration due to volcanic eruptions; and
- Creation of preferential radionuclide release pathways associated with accompanying fracturing and seismicity.

Probability of occurrence considerations: Estimates of the occurrence of future igneous activity require numerous assumptions concerning the temporal and spatial variability of such activity. To begin addressing such questions of variability, data collected through a program of regional and site surface and subsurface investigations must be available. These data should include the locations, distribution, and physical characteristics of the magmatic features (actual and inferred) in the area, as well as the ages of these various features.

[3]The term "waste package" is used here synonymously with "container" and "canister."

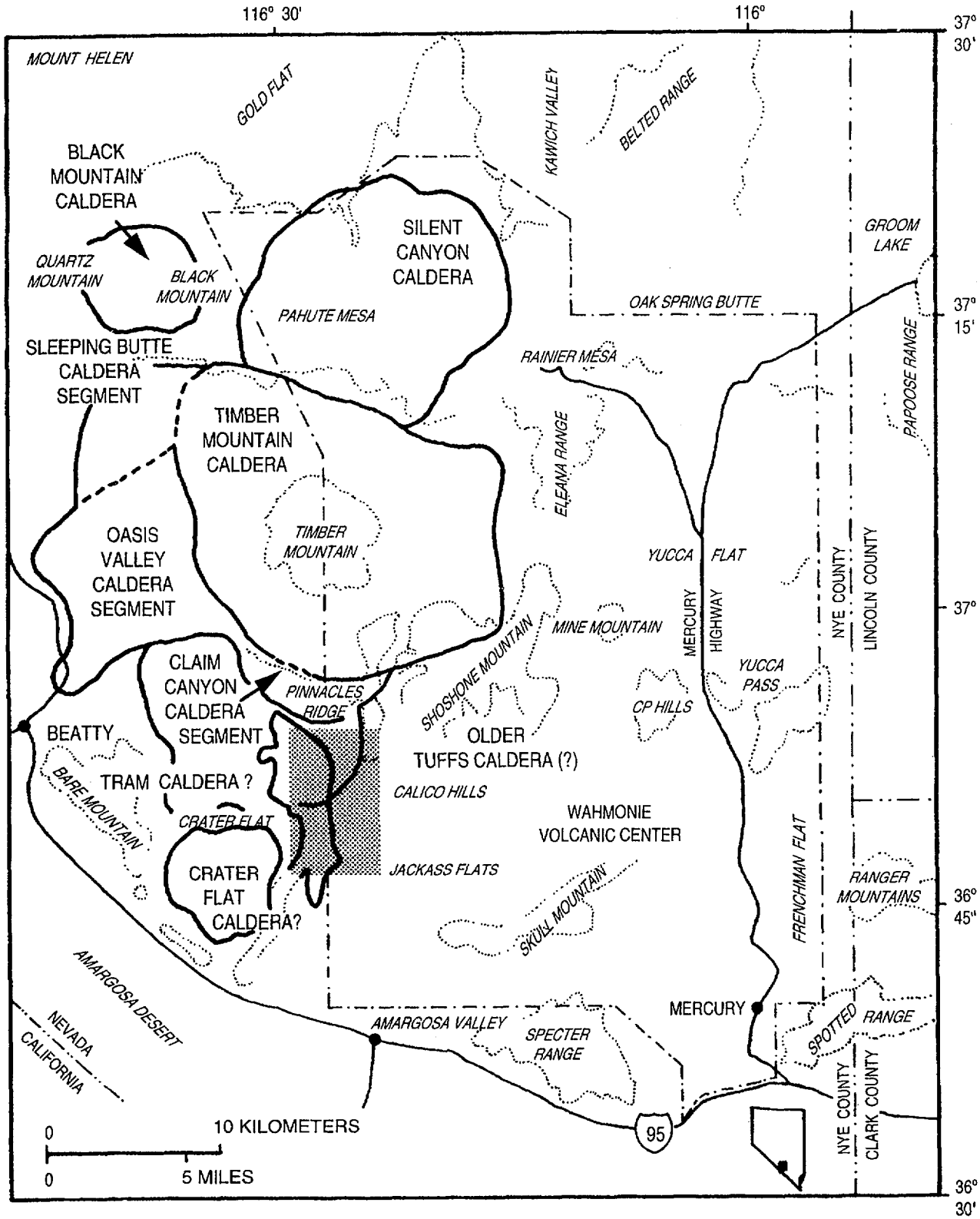

Figure 3–2 Calderas of the Southwest Nevada volcanic field near Yucca Mountain (Modified from Maldonado and Koether (1983))

The program of investigations must also address the extent to which some phenomena may still be present and undetected, taking into account the degree of resolution achieved by the investigations.

The development of a predictive model of future igneous activity for Yucca Mountain requires a description of the igneous "life history" (past, present, and future) for the region, based on interpretations of the collected data and calculated age dates. Various conceptual models based on these interpretations would be necessary, in areas such as:

- The region likely to host potential future igneous activity;
- The mechanics of magmatic emplacement (e.g., mantle-derived magma vs. crustal magma chamber; the rate of magma production in the subsurface; the amount of magma necessary for intrusive or extrusive activity); and
- The cyclic nature of the magmatism in the region (e.g., waxing/waning, monocyclic/polycyclic, relationship of local region to a larger region).

To determine the parameters required for igneous activity probability calculations, it is necessary to define a particular region in which the appropriate data would be gathered. The definition of such regions will need to be based on an understanding of the relationship, both temporal and spatial, between the regional tectonic features (e.g., variously oriented fault zones) and identified and inferred intrusive and volcanic features. Several studies have attempted to do this for the Yucca Mountain region (e.g., Crowe *et al.*, 1982; Crowe and Perry, 1989; and Smith *et al.*, 1990). Crowe and Perry (1989), for example, defined the Crater Flat Volcanic Zone (CFVZ) in their attempt to identify a region potentially more likely to host future volcanic activity (Figure 3–3). The northwest-trend of Quaternary-age volcanic cones (recognized and inferred) and lava flows in the CFVZ is thought to be related to a strike-slip fault beneath Crater Flat and the Amargosa Valley postulated by Schweickert (1989). Smith *et al.* (1990) identified a larger region, the "Area of Most Recent Volcanism" (AMRV), based primarily on the age of the various volcanic centers in the Yucca Mountain region (i.e., including only those younger than 4.5 Ma) (Figure 3–4). Within the AMRV, Smith *et al.* defined narrow north-northeast-trending "high-risk" zones corresponding to cinder-cone alignment orientations that they hypothesize may develop as a result of structural control (Figure 3–5).

Once an appropriate region has been defined, magma production rates may be estimated from the calculated volume of magma extruded at the surface over a particular time period. These production rates have been used to determine the recurrence time for the formation of representative volumes of past magmatic cycles in the Yucca Mountain region (Crowe *et al.*, 1982; and Crowe and Perry, 1989). Based on the available data, Crowe *et al.* (1982) suggest that there has been a decrease in the volume of volcanism (i.e., erupted volumes) through time in the NTS region. Magma production rates based on estimated surface magma volumes may not accurately reflect "true" production rates, because the calculations ignore the subsurface component of the igneous activity Shaw (1987) has proposed that, in general, only about one-third of the total magma production is reflected at the surface.

To adequately assess the risk to a proposed repository site from future igneous activity, it is also important to determine whether there is a cyclic nature to the activity in the region (i.e., whether activity is waxing or waning, monocyclic or polycyclic, and if so, where in the cycle(s) the region is presently). Ideally, this assessment will be based on a relatively complete understanding of the complex processes involved in magma generation at depth and the controls on the magma's ascent to the surface or near subsurface. Lacking this understanding, other methods of describing the expression of igneous activity have been used. The potential rates of future volcanic activity for the Yucca Mountain region have been estimated using both counts of volcanic centers within a particular age range, and examination of magma production rates (Crowe *et al.*, 1982; Crowe and Perry, 1989; and Margulies *et al.*, 1992).

Crowe *et al.* (1982) used the rates of activity to calculate the range in the probability of volcanic

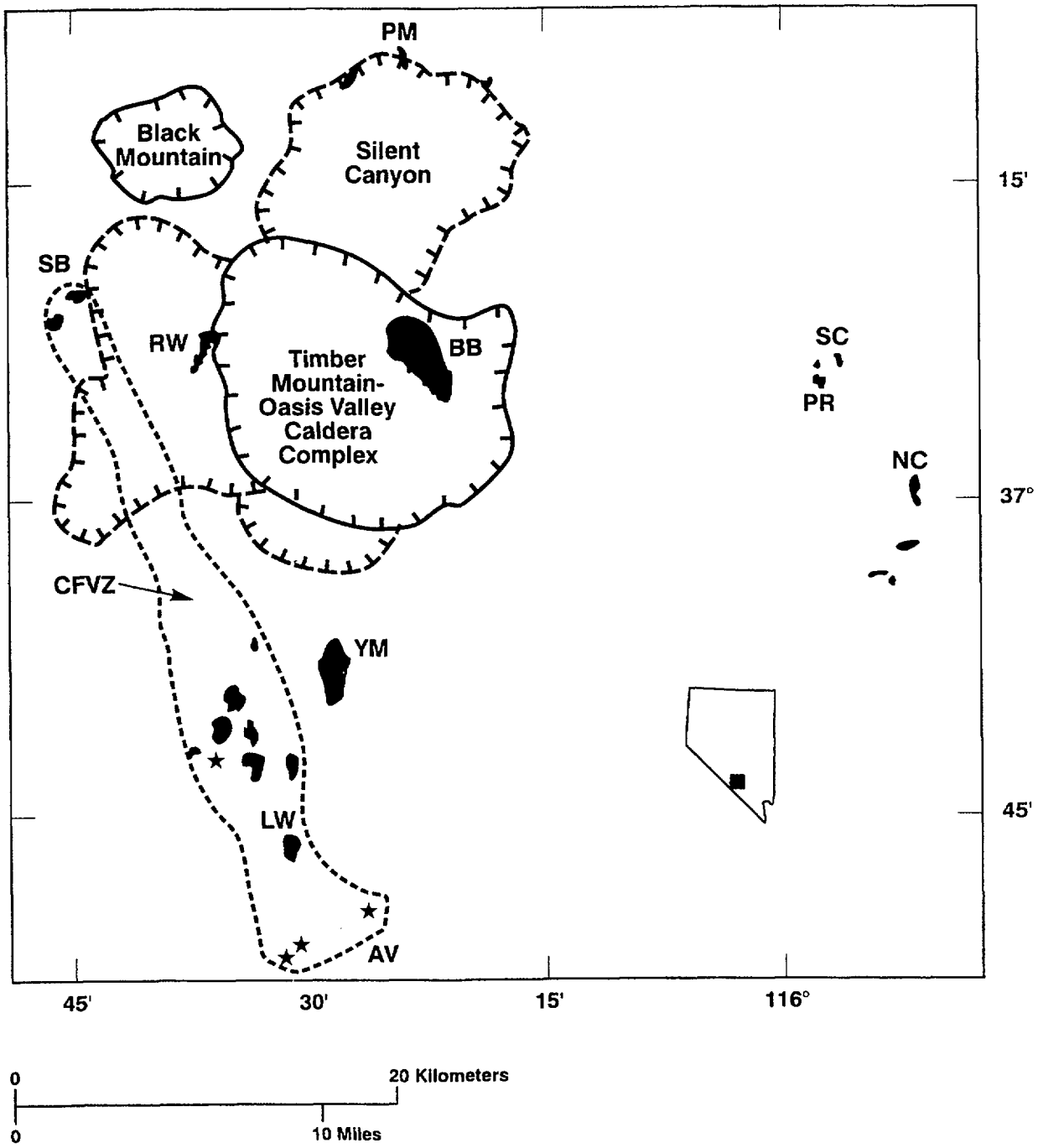

Figure 3–3 **Proposed Crater Flat volcanic zone (CFVZ)** (Generalized geologic map shows the distribution of the youngest episodes of basaltic volcanism in the Yucca Mountain region including outlines of major silicic caldera complexes. **AV:** Aeromagnetic anomalies of Amargosa Valley; **BB:** Buckboard Mesa basalt; **LW:** Lathrop Wells volcanic center; **NC:** Nye Canyon basalt; **PM:** Pahute Mesa basalt; **PR:** Paiute Ridge basalt; **RW:** Rocket Wash basalt; **SB:** Sleeping Butte volcanic centers; **SC:** Scarp Canyon basalt; **YM:** Yucca Mountain; and ***:** Inferred buried basalt centers or intrusive rocks. Modified from Crowe and Perry (1989, p. 328))

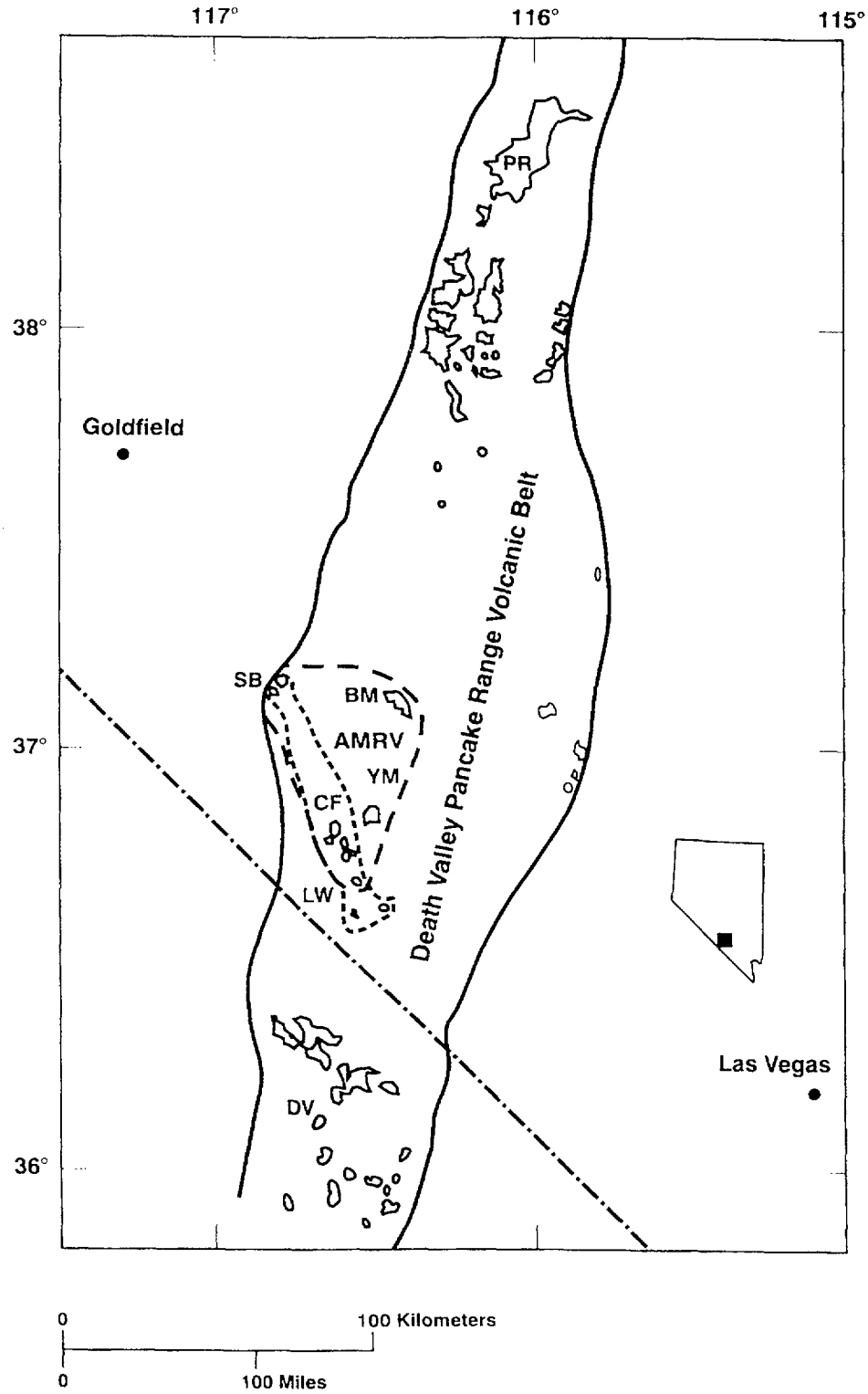

Figure 3–4 **Proposed area of most recent volcanism (AMRV)** (Volcanic areas are as follows: **BM:** Buckboard Mesa; **LW:** Lathrop Wells; **CF:** Crater Flat; **DV:** Death Valley; **PR:** Paiute Ridge; **SB:** Sleeping Butte; and **YM:** Yucca Mountain. Adopted from Smith *et al.* (1990).)

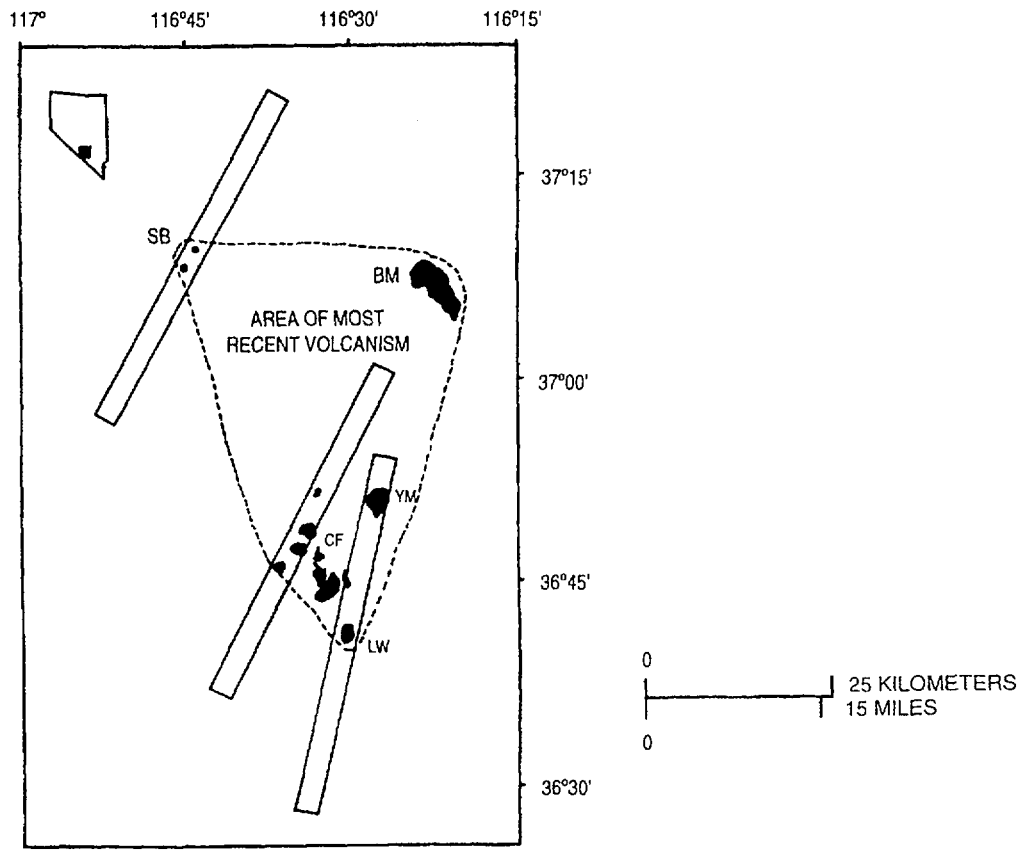

Figure 3–5 Postulated AMRV and "high-risk" zones (designated by rectangles) (Volcanic areas are as follows: **BM:** Buckboard Mesa; **CF:** Crater Flat; **LW:** Lathrop Wells; **SB:** Sleeping Butte; and **YM:** Yucca Mountain. Adopted from Smith *et al.* (1990).)

disruption of the proposed repository site. In determining these probabilities, Crowe *et al.* assumed a simple (homogeneous) Poisson distribution in time and space, such that the rate of magmatic eruption over time is constant and individual eruptive events occur independently. The calculated probabilities ranged from 3.3×10^{-10} to 4.7×10^{-8} per year, depending on:

- Whether the rate was determined from vent counts or magma production rates; and
- The region defined for the calculation.

The basic model proposed by Margulies *et al.* (1992) also assumed a temporally and spatially homogeneous Poisson distribution for volcanic centers. The recurrence rate in the model was estimated by summing the number of volcanos within the AMRV proposed by Smith *et al.* (1990), and dividing this number by the area of the AMRV and the time interval over which the vents have been active. The probability of an igneous event at Yucca Mountain was estimated to be 1.7×10^{-4} over 10,000 years. Margulies *et al.* also examined the effects of:

- A spatially varying recurrence rate, with zones of "enhanced magmatism" within the given region; and
- A change in the rate of occurrence of igneous activity for the region at a given time.

Homogeneous Poisson models, however, may not be appropriate for use in probability calculations for the Yucca Mountain region, because such models do not accurately describe volcano distributions, are unlikely to reflect accurately the probability of future volcanic activity, and may underestimate the probability of volcanic events. Statistical tests, such as the Hopkins F-test and the Clark-Evans test, indicate that, spatially, volcanos in the region do not have a homogeneous Poisson distribution (Connor and Hill, 1993). In addition, several investigators have argued that temporally homogeneous Poisson

models are inappropriate for volcanic fields in general and the probability of future volcanic events in the Yucca Mountain region in particular (Ho *et al.*, 1991; Ho, 1990, 1992; McBirney, 1992; and Sheridan, 1992). Additionally, the scarcity of and the uncertainty in the data for the region may not support the use of a simple Poisson model for predicting future volcanism in the area. For these reasons, employing such models to predict the future occurrence of volcanic activity may underestimate the risk of volcanism for the proposed Yucca Mountain repository site.

Probability for IPA Phase 2. As just discussed, a homogeneous Poisson model does not adequately describe the distribution of existing volcanic cones in the Yucca Mountain region. A model to estimate the probability of volcanic disruption of the proposed site will need to reflect the statistically significant amount of vent clustering in the region. In the IPA Phase 2 analysis, the staff based its probability estimate on the work of Connor and Hill (1993), who used a nonhomogeneous Poisson model calculated by near-neighbor methods to estimate the probability of volcanic disruption within an 8 square-kilometer area, over the next 10,000 years in the Yucca Mountain region. Assuming a late Quaternary recurrence rate of 7 ± 2 volcanos/million years, they estimated a probability of disruption of between 8.0×10^{-5} to 3.4×10^{-4} in 10,000 years, with most estimates between 1×10^{-4} and 3×10^{-4}. For the purposes of this scenario analysis effort, a probability equal to 1.5×10^{-4} over 10,000 years will be used.

Given that the probability of volcanic disruption in the vicinity of the repository is taken to be 1.5×10^{-4}, the probability of such a disruption per unit area (i.e., per square kilometer), p_v, is equal to 1.875×10^{-5}. Next, for the consequence modeling of the effects of igneous activity on repository performance (see Section 6.4), the likelihood of an intrusive dike was assumed to be 10 times that of a volcanic eruption. Therefore, the probability of an igneous event (formation of a volcanic cone or an intrusive dike) per unit area in the next 10,000 years is:

$$\overline{P_m} = 11 p_v \cong 2.1 \times 10^{-4} \quad . \qquad \textbf{(3–1)}$$

In estimating the consequences of igneous activity, a simulation area, A_s, bounding the repository site was assumed to ensure that any potential modeled igneous activity intercepting the repository will be included in the analysis. The size and shape of this area are not related to geologic structure in the region, but were solely based on the distribution of dike sizes assumed for the consequence analysis. The simulation area encompasses a 12- by 12-kilometer area around the repository.

Therefore, for the IPA Phase 2 scenario analysis, the probability of igneous activity within the simulation area over the next 10,000 years is:

$$P_m = \overline{P_m} A_s \cong 0.03 \, . \qquad \textbf{(3–2)}$$

This scenario probability is higher than probabilities estimated previously for the repository area (e.g., Crowe *et al.*, 1982; and Margulies *et al.*, 1992) because of a combination of factors. First, a nonhomogeneous Poisson model, rather than a homogeneous Poisson model, was used. Secondly, the probability of occurrence of an intrusive dike (assumed to be ten times that of a volcanic event) was included in the estimate. Finally, the region for which the probability estimate applies is a simulation area that bounds the repository and which is some 18 times larger than the repository area. It is also important to note, however, that because the simulation area is large enough to include all modeled igneous activity that may intercept the repository, a significant number of igneous events may not do so, and therefore, as modeled in the consequence analysis, such events may have no impact on repository performance. As a result, the probability of igneous activity directly affecting the repository is actually less than the given value.

As a final note, although the use of nonhomogeneous Poisson models can address the tendency of volcanic centers to cluster within a volcanic field through time, estimations of the probability of future volcanic activity (and intrusive activity, as well) will need to take into account additional geological information (e.g., pre-existing tectonic structure, strain rate) before more refined assessments of the probability of such activity can be made with confidence (Connor and Hill, 1993).

2. *Seismicity*

Description: Yucca Mountain is located in the Basin and Range tectonic province that

constitutes the southwestern portion of the North American crustal plate. The Basin and Range is characterized by more or less regularly spaced northerly-oriented subparallel mountain ranges and intervening alluvium basins formed by extensional faulting. The faulting in southern Nevada occurred mainly in response to the tectonic activity that has occurred in the Basin and Range over the last 15 million years (DOE, 1988a; p. 18).

Faults in the Yucca Mountain region can be grouped into three major systems depending upon their orientation: northwest (e.g., the Yucca Wash fault); northeast (e.g., the Rock Valley Fault zone); and north to northeast (e.g., the Solitario Canyon and Ghost Dance faults). Detachment faults have been postulated in many recent models of tectonism for the Yucca Mountain region (e.g., Scott and Rosenbaum, 1986).

Yucca Mountain is composed of a series of north-trending structural blocks that have been tilted eastward along west-dipping, high-angle normal faults. The proposed repository block is bounded by faults: on the west by the Solitario Canyon fault, on the northeast by the Drill Hole Wash structure, and on the east and southeast by the western edge of an imbricate normal fault zone. The Ghost Dance fault transects the proposed location for the underground repository. The faults at Yucca Mountain include both local faults related to the formation of calderas and longer regional faults of the Basin-and-Range type (DOE, 1988a; p. 20).

The site is in a region of diffuse seismicity (earthquake activity). In the past 150 years, eight major earthquakes (with magnitudes of 6.5 or more) have occurred within about 400 kilometers of Yucca Mountain. The nearest was the 1872 Owens Valley earthquake (estimated magnitude of about 8.25) some 145 kilometers west of Yucca Mountain. Although, in some instances, earthquake epicenters in the southern Great Basin appear to be related to mapped faults and regional structures, in the vicinity of Yucca Mountain, generally it has not been possible to correlate earthquakes with specific faults or tectonic structures (*op cit.*, p. 22).

Most of the major faults in the area of Yucca Mountain have experienced displacement during the Quaternary Period. Relatively moderate seismic activity continues today along strike-slip fault zones northwest, southwest, and southeast of Yucca Mountain, and there is evidence that seismic activity with associated surface fault displacements have occurred during this century in the Walker Lane shear zone (Yount *et al.*, 1993) which may extend through the site. Tables 3–2 and 3–3 (modified after DOE, 1988b; p. 1–166) provide a listing of recorded earthquakes of magnitude 4.0 or greater that have occurred in or near the Southern Great Basin since 1857. Meremonte and Rogers (1987) documented all historical Southern Great Basin earthquakes (i.e., from 1868 to 1978).

Studies of tectonic and stress regimes in the Yucca Mountain region are not complete, but they suggest the region is characterized by northwesterly extension, with normal and strike-slip faulting. The chief sources of information on the stress pattern are:

- *In-situ* stress measurements;
- Calculated earthquake focal mechanisms; and
- The orientation and nature (i.e., sense of movement) of the regional and local faults.

Large uncertainties exist in the assessment of the earthquake potential of geologic structures and seismogenic zones in the Southern Great Basin. These are caused, in part, by:

- The sparse historical record (past 150 years) of seismicity in the region;
- An equivocal association of historical earthquakes with mapped tectonic structures;
- Large uncertainties associated with critical fault parameters (e.g., fault segmentation, slip rate);
- Uncertainty associated with estimated recurrence intervals on local faults;
- The potential for earthquake activity to be both temporally and spatially clustered in the Basin and Range Province;

Table 3–2 Significant Earthquakes in or near the Southern Great Basin (Modified from DOE (1988b, pp. 1–166 – 1–167).)

Date	*Name or Region*	*Magnitude (M) (Richter Scale)*	*Distance from Yucca Mountain (km)*
Earthquakes of $M \geq 6.5$ within 400 km of the Yucca Mountain Site			
9 Jan 1857	Fort Tèjon	8 1/4	300
26 Mar 1872	Owens Valley	8 1/4	150
21 Dec 1932	Cedar Mountain	7.3	202
21 Jul 1952	Kern County	7.7	267
6 Jul 1954	Rainbow Mountain	6.8	331
24 Aug 1954	Rainbow Mountain	6.8	331
16 Dec 1954	Fairview Peak	7.2	276
16 Dec 1954	Dixie Valley	6.9	323
28 Jun 1992	Landers, CA	7.5	300

Table 3–3 Significant Earthquakes in or near the Southern Great Basin (Modified from DOE (1988b, pp. 1–166 – 1–167).)

Date	*Name or Region*	*Magnitude (M) (Richter Scale)*	*Distance from Yucca Mountain (km)*
Selected Earthquakes of $M \geq 4.0$ within 100 km of Yucca Mountain Site			
28 Mar 1934	Gold Flat	4.5	52
13 Jun 1939	Northern Death Valley	5.0	73
14 Jun 1945	Last Chance Range	5.0	96
30 Aug 1948	Amargosa Desert	4.0	42
13 Jan 1950	Dome Mountain	4.1	19
16 Jun 1951	Eleana Range	4.5	72
28 Jan 1959	Skull Mountain	4.0	23
27 Mar 1961	Skull Mountain	4.4	28
6 Jan 1969	Pahute Mesa	4.5	44
10 Jan 1969	Pahute Mesa	4.6	32
5 Aug 1971	Massachusetts Mountain	4.5	42
15 Feb 1973	Ranger Mountains	4.0	49
12 Jun 1973	Pahute Mesa	4.5	43
28 Oct 1975	Timber Mountain	4.0	30
8 Jan 1976	Pahute Mesa	4.6	52
7 Feb 1976	Pahute Mesa	4.8	52
29 Jun 1992	Little Skull Mountain	5.6	30
30 May 1993	Rock Valley	4.0	35

- The potential for earthquake activity outside of the southern Great Basin to initiate earthquakes in or near the site; and

- Large uncertainties associated with conceptual models of faulting at the site, including the potential for coupling of earthquakes with igneous activity.

Potential impacts on radionuclide release and transport: Faulting and seismicity in the Yucca Mountain region could have significant effects on waste isolation. Displacement along the Ghost Dance Fault could potentially shear waste packages, exposing the contents of the packages to transport. In addition to the potential shearing, canisters away from the movement will experience the effects of the accompanying seismic wave, which could include:

- The shaking of the waste packages in their emplacement holes, possibly damaging or even rupturing the canisters; and

- The loss of the air gap because of spalling of material into the emplacement hole.

Host rock material filling an emplacement hole will alter the stress distribution on the waste package and could provide an avenue for water to come into contact with the waste package, thus increasing the probability of corrosion and the potential for failure.

Fault movement and accompanying seismicity could affect the hydrologic system in the Yucca Mountain region, through:

- Creation, destruction, or modification of barriers to ground-water flow;

- Alteration of the fracture network and thereby the flow paths for infiltrating waters; and

- Seismic pumping leading to short-term changes in the water-table elevation (Carrigan *et al.*, 1991).

Repeated seismicity passing through the site could have pronounced effects on waste package lifetimes, especially as the packages age.

Probability of occurrence considerations: A probabilistic seismic hazard analysis provides the frequency distribution of earthquake ground motion (i.e., it develops an estimate (annual probability of occurrence) of earthquakes greater than a given reference earthquake). The annual probability that the peak ground acceleration, A, will exceed a certain acceleration, a, at a given site is defined mathematically by:

$$P(A > a) = \int_m \int_r P(A > a \mid m,r)\, F_{sm}(m) F_{sr}(r)\, dm\, dr, \qquad (3\text{–}3)$$

where $P\{A > a \mid m,r\}$ is the probability that the acceleration A is greater than a, for an earthquake of magnitude m at a distance r, and F_{sm} and F_{sr} are the probability distance functions for magnitude and density, respectively. Figure 3–6 shows the three basic inputs (Step Nos. 1 to 3 in the figure) needed to calculate the probabilistic seismic hazard (Step No. 4).

The development of a probabilistic model for seismic and fault hazards requires data and assumptions concerning such parameters as: fault rupture lengths, fault slip rates, earthquake magnitude distributions, geometry of the seismic source zones, and attenuation of the seismic waves.

Within the last decade, different probabilistic seismic hazard methodologies have been developed. The principal methodologies were those developed to assess the seismic hazard for nuclear power reactors in the eastern U.S. (e.g., Electric Power Research Institute (EPRI), 1986; and Bernreuter *et al.*, 1989); however, the applicability of these methodologies for an HLW repository in the western U.S. has yet to be determined. The seismic hazard model and the basic methodology to estimate seismic hazards at a site have been described in detail by Cornell (1968, 1971), McGuire (1976), and Algermissen *et al.* (1982).

The initial step in conducting a seismic hazard analysis for a site is the definition of a seismic hazard model. To define such a model, it is necessary to:

- Identify the seismic source zones;
- Describe the magnitude recurrence model;

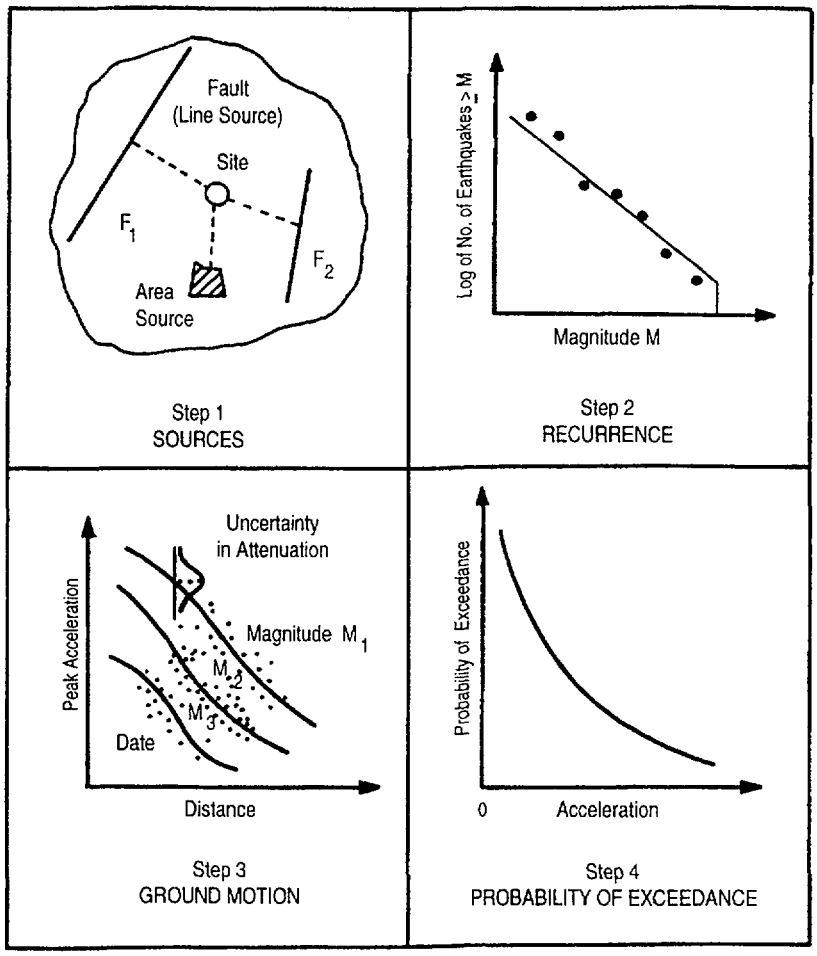

Figure 3–6 **Basic steps in a probabilistic seismic hazard analysis** (Adopted from the TERA Corporation (1978).)

- Describe the ground attenuation model; and
- Identify the fault slip rate.

After obtaining this information (Step Nos. 1 through 3 of Figure 3–6), the probability of exceeding a certain acceleration or a certain fault displacement value can be calculated (Step No. 4). Software programs developed by EPRI (1986) or Bernreuter *et al.* (1989) can be used to calculate the seismic hazards.

Figures 3–7 to 3–9 present results for seismic hazard and fault displacement analyses conducted for the Yucca Mountain region from the work of URS/John A. Blume & Associates (1987). These results are based on a sparse data set, the Campbell attenuation model for Utah (Campbell *et al.*, 1982) was used, and a specific slip rate was assumed. The results presented here will likely change as site characterization continues and adequate data for use in determining slip rates and the attenuation model become available.

Probability for IPA Phase 2: For the purposes of estimating a probability, seismicity is assumed to affect the repository only through the effects of the seismic acceleration on the waste canisters. Over time, as a waste canister corrodes, the thickness of its walls will decrease, and thus, a progressively reduced level of seismic acceleration will be needed to fail the canister, either by exceeding the yield strength of the canister material or by buckling the canister via impact with the emplacement hole. Therefore, a relationship between the thickness of the canister walls with time and the likelihood of a seismic acceleration necessary to fail the canister was established. As discussed in Section 6.4, canisters were assumed to fail when the seismically-induced stress at the base of the canister exceeded the

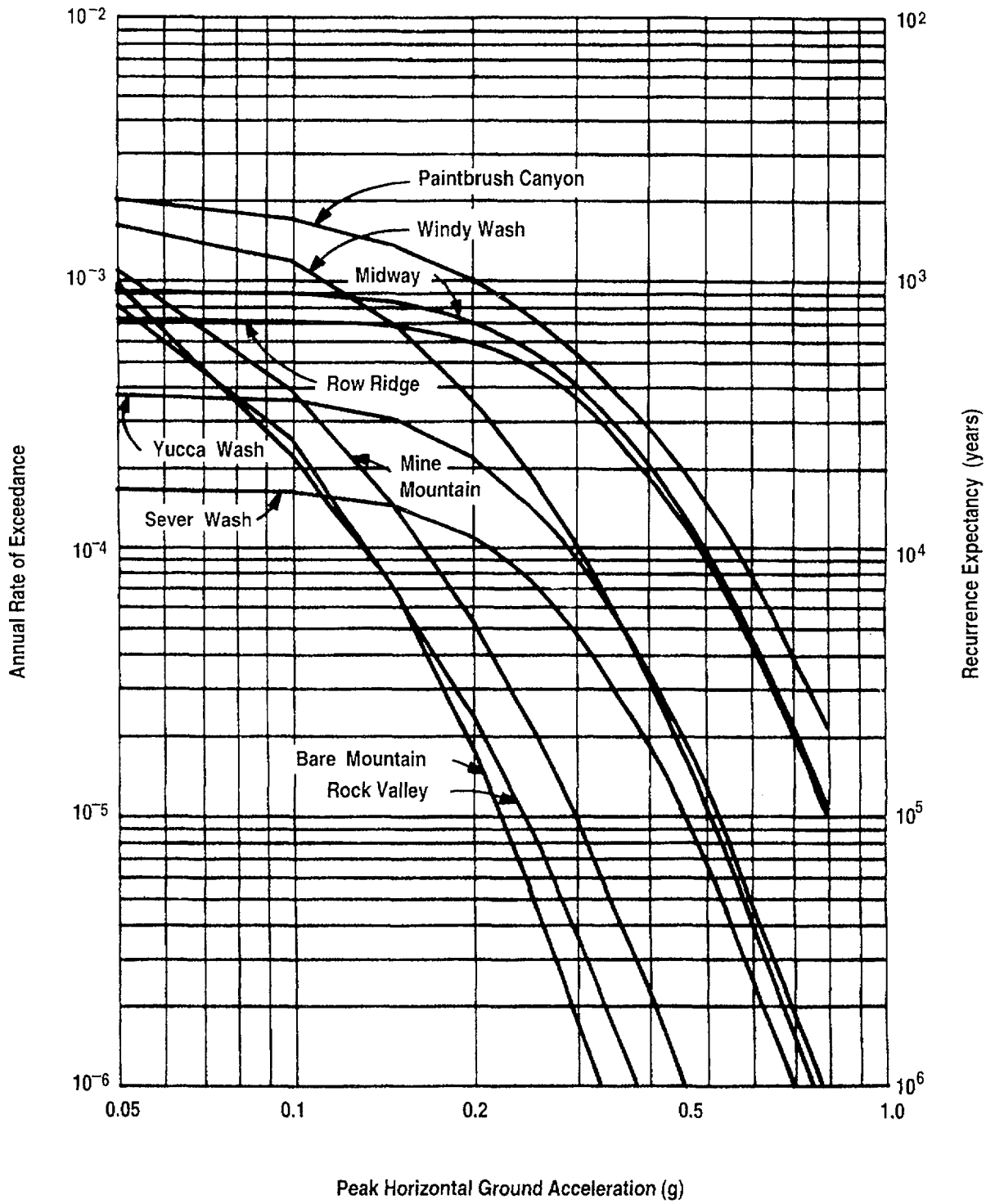

Figure 3–7 Annual probability of exceedance versus peak ground acceleration for several faults near Yucca Mountain (Adopted from URS/John A. Blume & Associates (1987).)

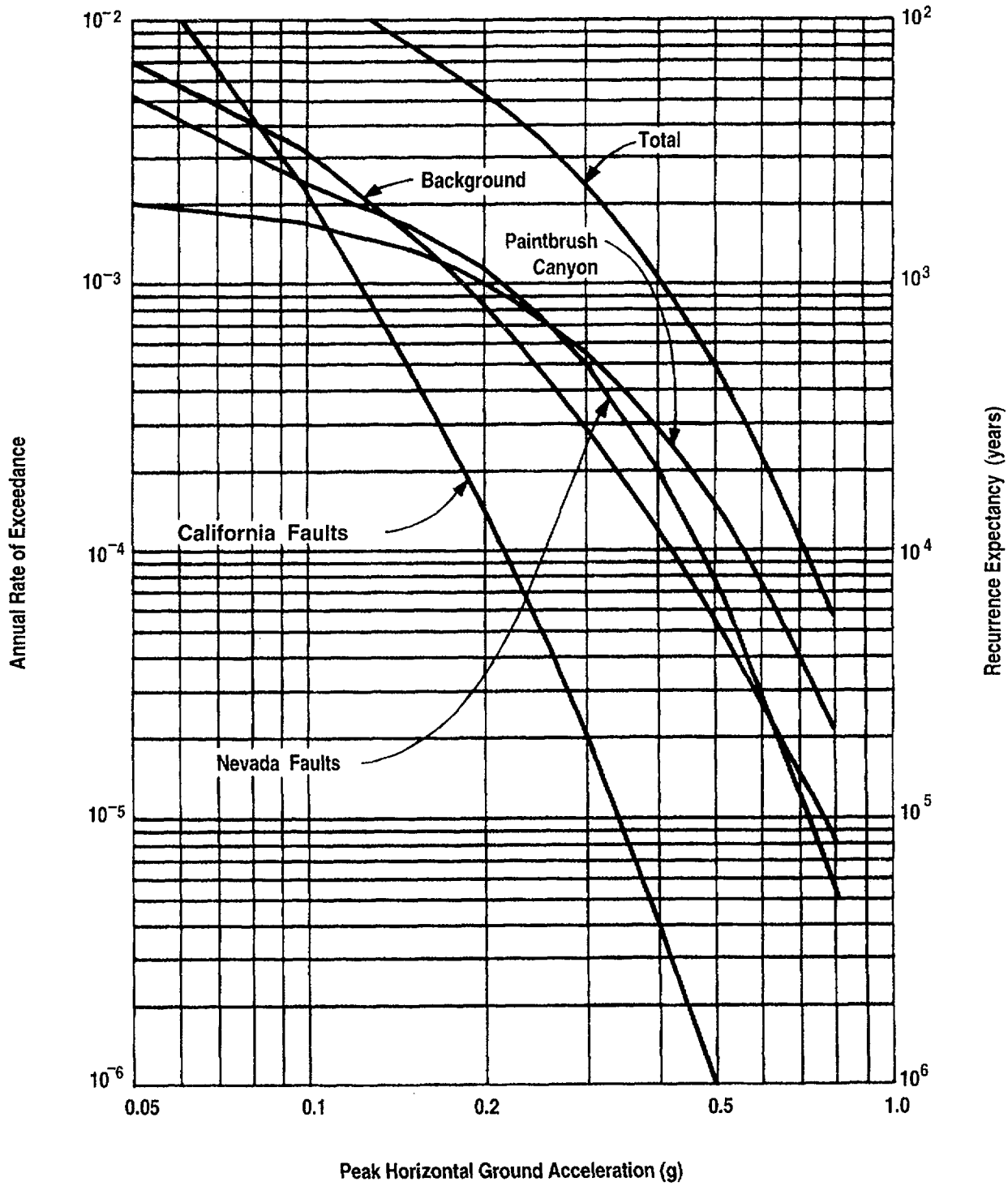

Figure 3–8 Comparison of annual probability of exceedance versus peak ground acceleration by location of faults (Adopted from URS/John A. Blume & Associates (1987).)

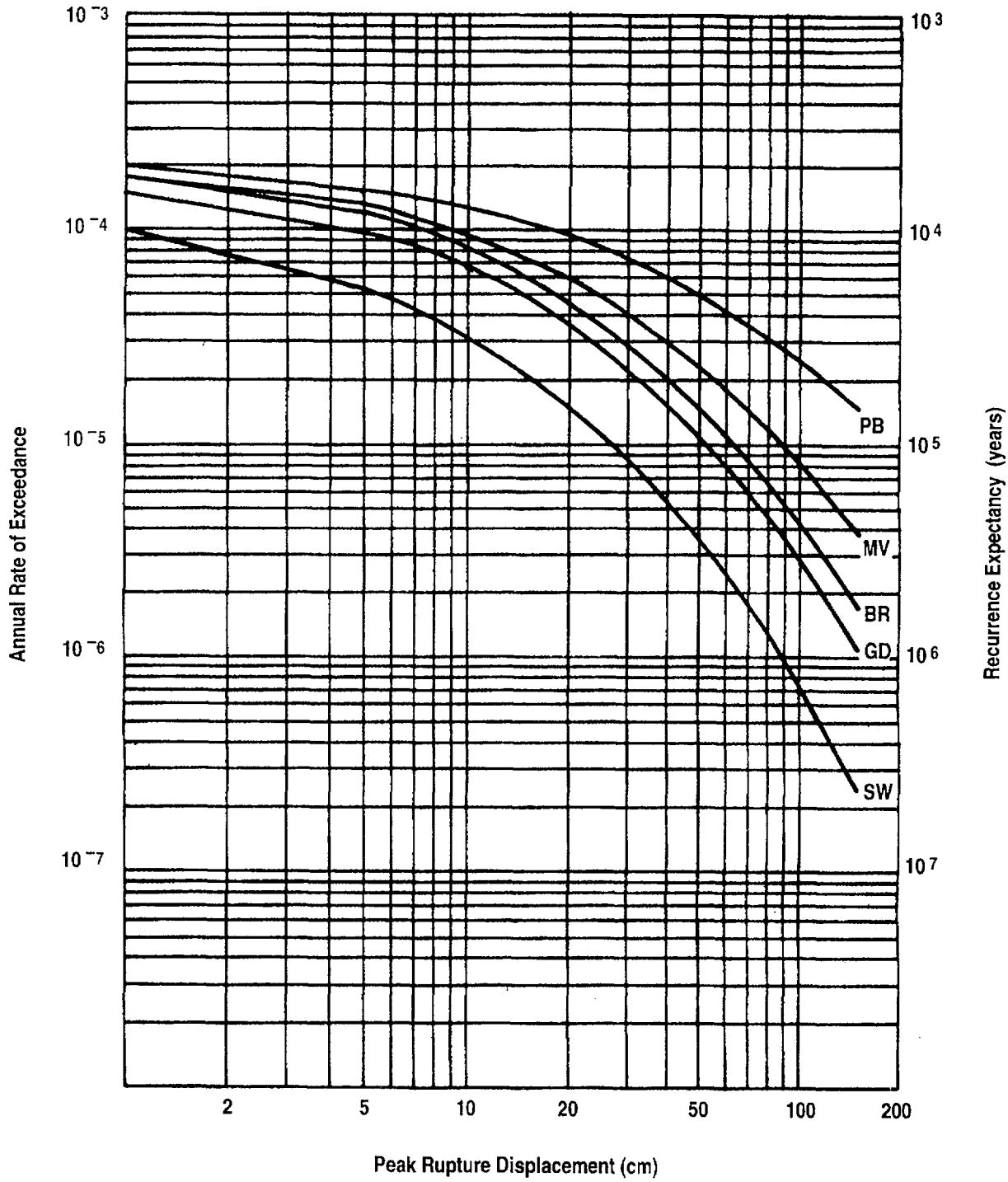

Figure 3–9 Annual probability of exceedance of peak surface rupture displacement for the Paintbrush Canyon (PB), Midway Valley (MV), Bow Ridge (BR), Ghost Dance (GD), and Sever Wash (SW) faults (Adopted from URS/John A. Blume & Associates (1987).)

yield strength of the waste canister material. First, a critical canister wall thickness was calculated (9.8×10^{-4} meters); a waste package canister with walls thinner than this would collapse under its own weight. Then, an acceleration necessary to fail a canister with walls of critical thickness was calculated (6.7×10^{-3} g). The recurrence rate for this level of acceleration is approximately equal to 0.02 per year, and therefore, the probability of seismic accelerations equal to or greater than this over the next 10,000 years in the Yucca Mountain region is estimated to be approximately 1.0. This is taken to be the probability of seismicity affecting the repository for this analysis.

3. *Climate Change*

Description: The present climate in which the Yucca Mountain site is located is classified as a midlatitude-desert climate, characterized by temperature extremes and annual precipitation of less than 150 millimeters. The paucity of precipitation in the region is believed to be caused by the rainshadow effect of the Sierra Nevada Mountains to the west of the site and the Transverse Ranges to the south. Rainfall in the area is sporadic, often occurring as showers, sometimes torrential, which can lead to local flooding. DOE currently estimates that perhaps less than 0.508 millimeters of the annual precipitation percolates to the deeper units of the unsaturated zone (DOE, 1988a; p. 27).

Current paleoclimatic data appear to indicate that there has been a general trend toward warmer and drier conditions in the southern Great Basin over the past 18,000 to 20,000 years, interrupted by episodes of cooler and wetter conditions lasting from a few hundred to perhaps 1000 years (Science Applications International Corporation, 1992). In general, the record of climatic conditions previous to this time back to the beginning of the Quaternary (2 Ma) is not well-preserved. However, analysis of calcitic veins at Ash Meadows in the Amargosa Desert and of vein calcite cores from Devils Hole near Ash Meadows indicate that the middle Pleistocene (500 to 750 thousand years ago) water table was tens to hundreds of meters above modern levels (Winograd and Szabo, 1988). Winograd and Szabo inferred the drop in the water table through the Quaternary as resulting from a combination of local erosion and climatic changes associated with the uplift of the Sierra Nevada and Transverse Ranges.

Potential impacts on radionuclide release and transport: Climatic changes over the next 10,000 years could have significant effects on the regional and local hydrologic system and therefore on the long-term performance of a repository at Yucca Mountain. A change to more arid conditions might lead to a further decrease in the frequency and intensity of precipitation in the region, as well as to an increase in evaporation. Such conditions might prove beneficial to repository performance.

A wetter, cooler climate could lead to increased infiltration at the site because of increased precipitation coupled with a reduction in evaporation. Such an increase in surface infiltration could lead potentially to an increase in the amount of ground-water flux through the unsaturated zone. If at sufficient levels, this increased flux could locally saturate formations above the repository horizon, leading to the formation of perched water tables, the transition from matrix flow to fracture flow, and an increased flux through the repository. Additional water could facilitate waste package corrosion, lead to faster dissolution of the UO_2 spent fuel matrix, and enhance the release of the radionuclides from the waste package canisters. Below the repository, transport from the repository to the accessible environment could be accelerated because of:

- Fracture flow, rather than matrix flow, through the unsaturated zone;
- A higher water table; and
- An increased hydraulic gradient in the saturated zone.

If the change to cooler climatic conditions is a presage to a period of glaciation, the annual precipitation rates in the Yucca Mountain region could increase dramatically. In the Pleistocene Ice Age, although the continental glaciers did not advance as far south as Yucca Mountain, increased precipitation associated with the change to a colder climate led to the formation of numerous lakes in the Great Basin province. One of these lakes, Lake Manly, estimated to be about 145 kilometers long and about 10 to 18 kilometers wide, formed in Death Valley (Thornbury, 1967). Presently, few of these lakes still exist, having

evaporated completely over time or shrunk dramatically in size.

The addition of large amounts of carbon dioxide, aerosols, and other trace gases to the atmosphere through man's activities has the potential for significantly altering future climate, especially in the near future (next 1000 years or so). Consideration of these anthropogenic contributions to potential climate change, with respect to the magnitude or probability of the change, were not included in the IPA Phase 2 analysis.

An NRC-sponsored elicitation of expert judgment of climatic conditions in the Yucca Mountain region over the next 10,000 years was conducted in 1993 (DeWispelare *et al.*, 1993). Data from this effort will be considered in future IPA analyses.

Probability of occurrence considerations: Both paleoclimatic data and climate models could be used in making climate predictions for the 10,000-year period of regulatory interest. Paleoclimatic data for the western U.S. may include lake-level records from present and former lakes, lake-bottom sediment cores, macrofossil assemblages from packrat middens, and stratigraphic pollen sequences (SAIC, 1992). When using such data in predictions of future climate, one assumes that the future variations in the climate system will be similar to those of the past. However, study of the past climate can yield only general indications of the future climate; explicit forecasts of the course of future climate are not possible, except as simple extrapolations of past behavior (Hunter and Mann, 1989). Examination of the paleoclimatic record can be used in the verification of modeling past climates and may serve to limit the range of variations expected in the future.

Climate models can be categorized into those that describe the slowly varying components of the climate system (e.g., the deep oceans, ice sheets) and those that model the fast-response components (e.g., the atmosphere, the upper layers of the oceans). Each of these component categories incorporate multiple temporal and spatial hierarchies that contribute additional uncertainties about the causes of past climate variations at a particular location and the likely consequences of future variations in the controls of the climate system (DOE, 1988b; p. 5–94). In attempting to predict future climate for 10,000 years, both types of climate models will be needed, as models of fast-response components provide a "snapshot" view of the climate system under a particular set of boundary conditions and state of slowly varying components (Hunter and Mann, 1989). At present, such integrated models are not available to provide estimates of future climate conditions at the spatial resolution necessary for a proposed repository site.

Given the current knowledge of climatic dynamics and the geological record of past climate changes, major climatic fluctuations may be likely within the next 10,000 years (Spaulding, 1985). Although methods of predicting long-term climatic variations (on the scale of 1000 to 100,000 years) do exist, the specific future variation of climatic parameters may not be entirely predictable (DOE, 1988b; pp. 5–91 – 5–98).

Probability for IPA Phase 2: The determination of a probability of climate change in the Yucca Mountain region over the next 10,000 years for use in IPA Phase 2 is predicated on the assumption that the variation in climatic conditions occurs slowly, such that the period of performance for the repository is short in comparison, and therefore, only a single "climate" will prevail during the period of performance. In making this assumption, "probabilities" can be assigned to a range of specific climatic conditions, which are then modeled in the consequence analysis using a particular data set of precipitation and temperature values. These parametric values are constant then throughout the modeled 10,000-year period of performance.

Given that a change in climate occurs, and that for the purposes of this scenario analysis, climate is represented by ranges in average annual temperature and average annual precipitation, four scenarios are possible under the "Climate Change" scenario class: warmer/drier; warmer/wetter; cooler/drier; and cooler/wetter, all relative to the current conditions.

In the IPA Phase 2 consequence analysis, described in Chapter 6, the "Current Climate" and "Climate Change" scenario classes were represented by distributions of infiltration rates however, the link between the temperature and precipitation ranges used in this scenario analysis

and the infiltration rates used in the consequence analysis was not made.

For this effort, probabilities were generated for the "Climate Change" and the "No Climate Change" EPs based on paleoclimatic data gathered in a review of available literature, with the majority of the data obtained from studies of plant microfossils contained in the radiocarbon-dated remains found in packrat middens in the NTS vicinity (Spaulding, 1985). These data were used to bound the potential future variation in average annual temperature and precipitation for the Yucca Mountain region, as well as to calculate the scenario probabilities for the two climate EPs.

The data used in this analysis are graphed in Figure 3-10. It should be stated that, as portrayed in the figure, the data reflect only the interpreted general trends in climatic conditions for the past 45,000 years in the Yucca Mountain region and do not show the true variation in these conditions. Data for the entire Quaternary Period were not compiled by the staff. Based on the results from Spaulding's work, it appears that while the average annual temperature in the Yucca Mountain region has ranged from several degrees Celsius (°C) below current levels to several degrees above over the past 45,000 years, the average annual precipitation levels were always higher than those of the present (although the data appear to show indications, particularly in the recent past, that further increases in temperature may actually serve to lessen precipitation at the site). Within the past 45,000 years, the greatest variance from current conditions appears to have occurred approximately 18,000 years ago, at the height of the Pleistocene Ice Age, when average annual temperatures had dropped 5 to 7°C below present levels and the average annual precipitation had increased to roughly 35 percent above current levels. Another interesting point is that there appears to have been a general decline in precipitation, from approximately 20 percent above current levels down to today's precipitation levels in the repository life timeframe of 13,500 years.

Probabilities for this analysis were determined by taking a simple ratio of the timespan encompassed by a particular climate relative to the total time (i.e., 45,000 years). This approach was taken although it was recognized that the timespan in which a particular climate has prevailed in the past is not related to the probability that the same climate (or any other) will occur or not occur in the future. Also, it was assumed arbitrarily that current climatic conditions included variations in the average annual temperature between 2°C below to 2°C above current levels and in the average annual precipitation of up to 15 percent higher or lower than at present. Variations beyond these levels were considered as constituting a change in climate.

Thus, for the 45,000 years before present (ybp) represented on the graph, the average annual precipitation appears to have been less than 15 percent above current levels from 45,000 ybp to 39,000 ybp, and again from 10,000 ybp to the present, while the temperatures were between 2°C below and 2°C above current. For the remainder of the 45,000 years (between 39,000 ybp and 10,000 ybp), the average annual precipitation ranged from 16 percent (with 20 percent as a high estimate) to 35 percent (with 40 percent as a high estimate) greater, while the average annual temperatures were 3 to 6°C cooler than at present. Therefore, the probability of "No Climate Change" was taken to be equal to 16,000 years/45,000 years, or 0.356, and the probability of "Climate Change" was taken to be equal to 1 - (0.356), or 0.644.

With respect to the four potential climate change scenarios identified previously, the data suggest that, given the definitions used in this analysis, only present climatic conditions and cooler/wetter conditions have prevailed in the Yucca Mountain region over the past 45,000 years. Data for the entire Quaternary Period were not compiled by the staff.

4. Exploration Drilling

Description: The Yucca Mountain site is located in a natural resource-rich region that includes current gold production and exploration for hydrocarbons. Gold has been mined within the site vicinity (at Bare Mountain to the west and at Wahmonie to the east) for over a century (Raney, 1990b) and world-class gold deposits are located within 25 kilometers of Yucca Mountain. Gold exploration and exploitation continues as five new mines and prospects have been located within 48

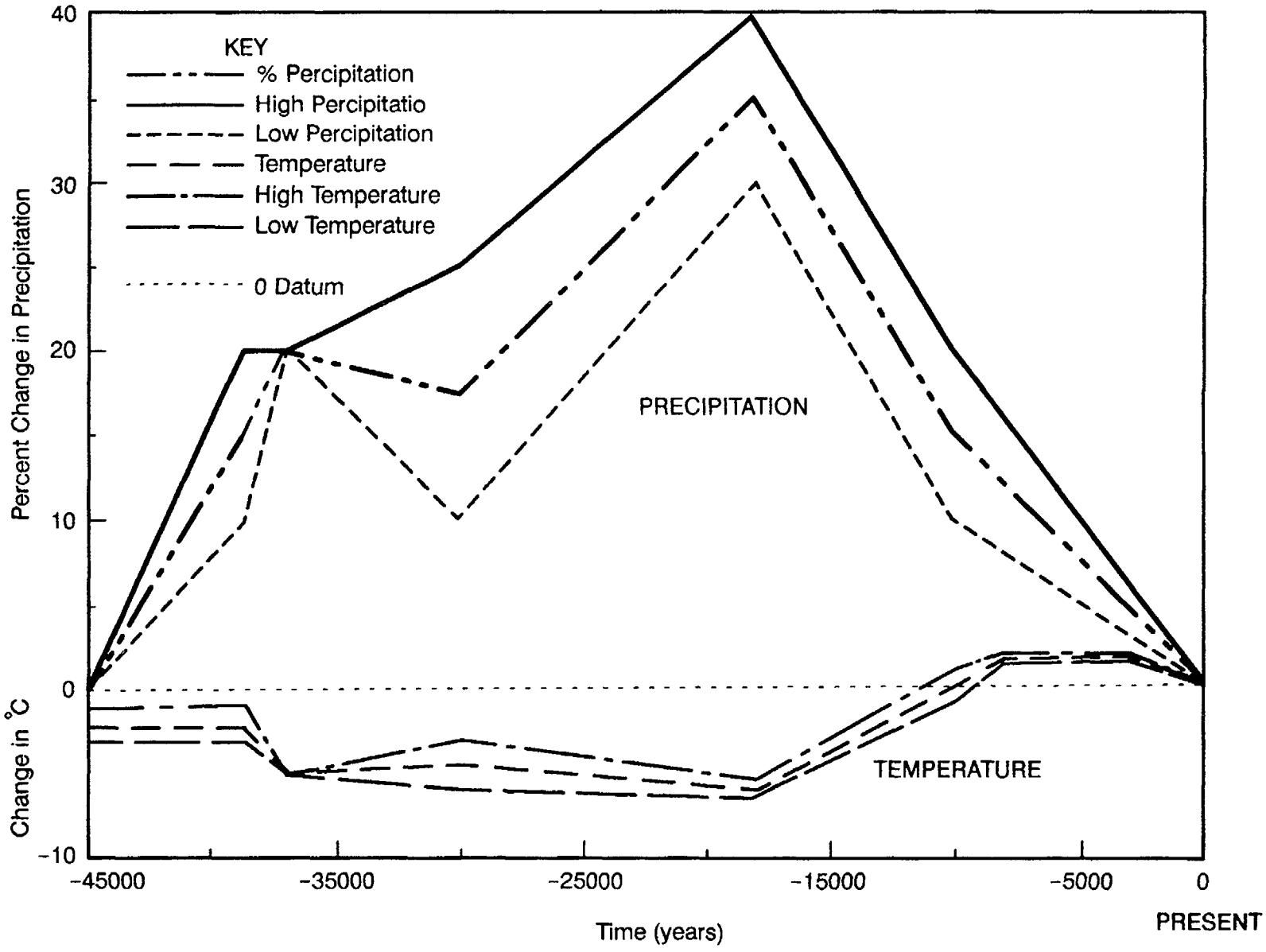

Figure 3–10 Precipitation and temperature variation over the past 45,000 years in the vicinity of the Nevada Test Site (Based on data from S ·lding (1985).)

kilometers of the proposed repository site between January 1988 and July 1990 (Raney, 1990b). The Railroad Valley petroleum deposits are located within 240 kilometers of the site (Garside *et al.*, 1988), and recent exploration for petroleum has occurred within 15 kilometers of Yucca Mountain. However, site characterization activities to date have not revealed any direct evidence of significant mineral or petroleum reserves at Yucca Mountain, although hydrothermal alteration is evident at the site (DOE, 1988b; p. 1–341).

Zeolitic clays are mined in playas south of the site, and significant quantities of zeolites compose part of the Calico Hills formation at the site (Vaniman *et al.*, 1984). However, it seems unlikely that zeolites at Yucca Mountain will become economically attractive because of their depth at the site and the wide availability of zeolites in more accessible locations throughout Nevada and the United States.

Geothermal waters are common in the State of Nevada (Garside and Schilling, 1979) and hot springs are evident within the vicinity of the site. However, in site characterization activities to date, only low-grade geothermal temperatures have been observed in ground water at or near the proposed repository site (DOE, 1988b; pp. 1–305 – 1–313; and Benson and McKinley, 1985).

Ground-water resources are known to be present at Yucca Mountain. DOE water wells presently pump water from the water table for testing and utilization within the DOE program, and this water may have commercial value in mining, agricultural, and residential applications.

Potential impacts on radionuclide release and transport: Future drilling at the site could lead to the inadvertent direct release of radionuclides from the underground repository to the accessible environment (in this case, the ground surface). Waste canisters may be intersected in the course of a exploratory drilling program, and as a result, canisters may be damaged, even punctured, by a drill bit. Under such a situation, spent nuclear fuel, irradiated waste package material, and contaminated host rock may be brought to the surface.

In addition, exploratory drilling for natural resources may have indirect impacts on the repository's ability to isolate waste. Such indirect impacts could include the creation of:

- Preferential pathways from the surface to the repository horizon for infiltrating waters; and
- Short-circuit radionuclide transport pathways through the unsaturated zone below the repository horizon for water-borne radionuclides, and from the repository to the surface for released gaseous radionuclides.

An additional concern is associated with the potential loss of significant amounts of drilling fluids into the geosphere, which may have adverse impacts on hydrologic flow through the repository and the geochemistry of the host rock (e.g., its sorptive capabilities).

The potential magnitude (i.e., severity) of these effects is related to the demand for the particular resource(s) being explored for or exploited, the depth and subsurface extent of the identified or inferred deposit(s), and the economic considerations involved. Such factors will directly impact the location and number of holes needed to exhaustively explore for or exploit the resource(s).

Probability of occurrence considerations: Estimates of the probability of future human intrusion at the Yucca Mountain site will be largely very subjective. For the most part, this is because of two factors:

- The lack of empirical or mechanistic models for determining the probability that a repository will be breached by human activity in the next 10,000 years; and
- The unpredictability of future human behavior, economic factors, and states of technology (Apostolakis *et al.*, 1991).

Despite the inability to predict the likelihood of future inadvertent human intrusion, EPs initiated by human activity, if found to be "sufficiently credible" under 10 CFR Part 60, will be included in assessments of compliance with the containment requirements of 40 CFR Part 191. Under 10 CFR Part 60, human intrusion ". . . may only be found to be sufficiently credible to warrant consideration if it is assumed that: (1) The monuments provided . . . are sufficiently permanent to serve their intended purpose; (2) the value to future generations of potential resources within

the site can be assessed adequately . . . ; (3) an understanding of the nature of radioactivity, and an appreciation of its hazards, have been retained in some functioning institutions; (4) institutions are able to assess risk and to take remedial action at a level of social organization and technological competence equivalent to, or superior to, that which was applied in initiating the processes or events concerned; and (5) relevant records are preserved, and remain accessible, for several hundred years after permanent closure" (10 CFR 60.2).

As the EPA believes that it will be impossible to develop a "correct" estimate of the probability of inadvertent human intrusion, Appendix B of 40 CFR Part 191 provides limits on the rates of inadvertent and intermittent drilling and the severity of the resulting consequences that need be considered (EPA, 1985; 50 *FR* 38089). The rate of drilling ". . . need not be taken to be greater than" 30 boreholes per square kilometer of repository area over 10,000 years for repositories located in or near sedimentary rocks and three boreholes per square kilometer per 10,000 years for repositories located in or near nonsedimentary rocks" (*op cit.*). These rates are believed to be based on average drilling rates determined from oil exploration in the Delaware Basin of the southwestern United States.

Probability for IPA Phase 2: For IPA Phase 2, it was assumed that the occurrence of future exploratory drilling is distributed randomly in space and time (and therefore can be approximated as a Poisson process). The rate of future inadvertent exploratory drilling was based on the guidance provided by EPA in Appendix B to 40 CFR Part 191 (EPA, 1985; 50 *FR* 38066–38089). Although sedimentary rocks underlie the site, the proposed repository horizon is in volcanic tuffs, and therefore, the EPA-recommended rate of three boreholes per square kilometer per 10,000 years was used.

For the purposes of this analysis, the repository area was defined to be 5.13 square kilometers (DOE, 1988b; p. 8.3.5.13–83), and therefore, the "expected" number of boreholes at the site over the next 10,000 years is 15.4. Further, if a Poisson distribution is assumed to describe the drilling, the probability of no boreholes being drilled (i.e., "No Exploratory Drilling") is approximately 2.3×10^{-7}, and therefore, the probability of one or more boreholes at the site (i.e., "Exploratory Drilling") is very nearly 1.0.

There are at least several problems with treating the probability of drilling in this way. First, the use of the EPA-derived drilling rate may not be completely applicable to the Yucca Mountain site or region, because it is believed that the EPA rate was derived from oil exploration drilling rates, whereas the Yucca Mountain region may more likely host exploration for precious metals. Apostolakis *et al.* (1991) calculated an example drilling rate for gold exploration using a common exploration technique for Nevada, which involves drilling a series of boreholes, and assuming a single gold-prospecting event every 100 years over the period of regulatory interest for the repository. This rate was equal to 7534 boreholes per square kilometer per 10,000 years.

Secondly, modeling drilling with a simple Poisson distribution precludes consideration of exploration programs that employ multiple boreholes in specific arrangements to appropriately assess a potential natural resource deposit(s). Finally, assuming that drilling is to be distributed randomly in space does not take into account topographical considerations (i.e., that drilling will likely take place preferentially at lower elevations on more level terrain (e.g., in drilling for water), rather than on the side or top of mountains, like Yucca Mountain).

Given that exploratory drilling occurs, the borehole could either intersect (for the IPA Phase 2 consequence analysis, "intersection" is equivalent to "penetration") a canister or merely excavate some of the surrounding host rock. The method used to calculate the likelihood of a random borehole intersecting a waste package canister in any one of the seven sub-areas of the modeled repository relative to any other is discussed in Section 6.3.

3.3.3 Combination of Events and Processes into Scenario Classes

Following screening, the remaining EPs ("Igneous Activity," "Seismicity," "Climate Change," and "Exploration Drilling") were combined to form scenario classes, as discussed in Section 3.2.4. T so-called "Latin square" is used to display all the possible combinations in Figure 3–11. In the far

left and top squares of the figure, the occurrence and non-occurrence of each initial EP are shown; the non-occurrence of an EP is represented by placing shading over the letter denoting the EP. Since there are four fundamental classes of EPs, 2^4 or 16 different combinations are possible. "Non-occurrence" should be interpreted as "not any occurrence;" e.g., since *D* represents drilling any boreholes within the perimeter of the mined facility projected to the surface, *D* represents no boreholes within that surface region over the 10,000-year performance period.

Figure 3–12 is similar to Figure 3–11 except the literal symbols for the EPs and their combinations are replaced with their assigned probabilities. In the IPA Phase 2 analysis, these initial EPs are assumed to be mutually independent, and therefore, the probability of the various scenario classes formed through these combinations is equal to the product of the constituent initial EPs (i.e., the probability of both event *A* and event *B* occurring is equal to the probability of event *A* occurring multiplied by the probability of event *B* occurring). In addition, in the figure, each row and column is summed.

Figure 3–13 is identical to Figure 3–12, except all combinations of the EPs (i.e. scenario classes) that have probabilities of occurrence less than 1 chance in 10,000 over 10,000 years are shaded. If the screening criteria for individual categories of events and processes in the EPA guidance were applied, these scenario classes would be screened out.

These figures present the information concerning the various combinations in an idealized, general format such that, for a particular scenario class, no conclusions can be drawn regarding:

- The number of times or the time(s) at which a particular EP will occur within the 10,000-year period of regulatory interest; or
- The order or sequence in which two or more EPs in the scenario class will occur within that same time period.

Instead, the calculated probability values refer only to the likelihood that a particular scenario class will occur in the Yucca Mountain region over the next 10,000 years. For example, the scenario class involving "Drilling" and "Seismicity" in the region (with "No Climate Change" and "No Igneous Activity") has the assigned probability of approximately 0.35 in the next 10,000 years. This is the probability of having any occurrence of both drilling and seismicity that will affect the site in the coming 10,000 years, and not the probability of having *x* episodes of drilling followed by *y* earthquakes of a given size, followed by *z* more holes being drilled or any such combination.

A manifestation, therefore, of the approach the staff has taken in its application of the SNL scenario methodology, particularly in defining the repository system boundaries as the staff did, is the issue of selecting the appropriate representative scenario(s) for the individual scenario classes. Addressing this issue will require answering:

- How many times a constituent EP will occur over the time period of regulatory interest;
- How the EP will manifest itself, once it does occur; and
- When during the period of interest the EP will occur(s).

It is likely that each of the various permutations of these three variables will affect the repository system differently, thus leading to a range in estimated radionuclide releases to the accessible environment. The approaches taken to modeling each of the scenario classes and their consequences are discussed in the following chapters of this report. This issue will need to be addressed explicitly in future staff work in this area.

3.3.4 Screening of Scenario Classes

EPA guidance set forth in Appendix B to 40 CFR Part 191 states that ". . . performance assessments need not consider categories of events or processes that are estimated to have less than one chance in 10,000 of occurring over 10,000 years" (EPA, 1985; 50 *FR* 38088). In its proposed conforming amendments to 10 CFR Part 60, NRC reaffirmed the application of the 1×10^{-4} in 10,000-years criterion to categories of events and processes, when it stated, "The term "categories" is used to refer to general classes of processes and events, such as faulting, volcanism, or drilling"

			V		V
		D	D	D	D
C	S	C S D V	C S D V	C S D V	C S D V
	S	C S D V	C S D V	C S D V	C S D V
C	S	C S D V	C S D V	C S D V	C S D V
	S	C S D V	C S D V	C S D V	C S D V

KEY

C - No climate change
C - Climate change

S - No seismic activity affecting the repository
S - Seismic activity affecting the repository

D - No human intrusion via exploratory drilling
D - Human intrusion via exploratory drilling

V - No magmatic activity affecting the repository
V - Magmatic activity affecting the repository

Figure 3-11 Combinations of events and processes into scenario classes

		P(Ⓥ) ≈ 0.97		P(V) ≈ 0.03		
		P(Ⓓ) = 2.3×10^{-7}	P(D) ≈ 1.0	P(Ⓓ) = 2.3×10^{-7}	P(D) ≈ 1.0	***SUM (approximate)***
P(Ⓒ) = 0.356	P(Ⓢ) ≈ 0.0	0.0	0.0	0.0	0.0	0.0
	P(S) ≈ 1.0	7.9×10^{-8}	0.35	2.5×10^{-9}	0.01	0.36
P(C) = 0.644	P(Ⓢ) ≈ 0.0	0.0	0.0	0.0	0.0	0.0
	P(S) ≈ 1.0	1.4×10^{-7}	0.62	4.4×10^{-9}	0.02	0.64
SUM (approximate)		2.2×10^{-7}	0.97	6.9×10^{-9}	0.03	1.0

KEY

P(Ⓒ) - Probability of no climate change
P(C) - Probability of climate change

P(Ⓢ) - Probability of no seismic activity affecting the repository
P(S) - Probability of seismic activity affecting the repository

P(Ⓓ) - Probability of no human intrusion via exploratory drilling
P(D) - Probability of human intrusion via exploratory drilling

P(Ⓥ) - Probability of no magmatic activity affecting the repository
P(V) - Probability of magmatic activity affecting the repository

Figure 3-12 Probabilities of scenario classes for IPA Phase 2 generated by combinations of probabilities of occurrence of constituent events and processes

		P(V) ≈ 0.97		P(V) ≈ 0.03		
		P(D) = 2.3×10^{-7}	P(D) ≈ 1.0	P(D) = 2.3×10^{-7}	P(D) ≈ 1.0	***SUM (approximate)***
P(C) = 0.356	P(S) ≈ 0.0	0.0	0.0	0.0	0.0	0.0
	P(S) ≈ 1.0	7.9×10^{-8}	0.35	2.5×10^{-9}	0.01	0.36
P(C) = 0.644	P(S) ≈ 0.0	0.0	0.0	0.0	0.0	0.0
	P(S) ≈ 1.0	1.4×10^{-7}	0.62	4.4×10^{-9}	0.02	0.64
SUM (approximate)		2.2×10^{-7}	0.97	6.9×10^{-9}	0.03	1.0

Note: Scenario classes with probabilities less than 1.0×10^{-4} over 10,000 years are shaded.

KEY

P(C) - Probability of no climate change
P(C) - Probability of climate change

P(S) - Probability of no seismic activity affecting the repository
P(S) - Probability of seismic activity affecting the repository

P(D) - Probability of no human intrusion via exploratory drilling
P(D) - Probability of human intrusion via exploratory drilling

P(V) - Probability of no magmatic activity affecting the repository
P(V) - Probability of magmatic activity affecting the repository

Figure 3-13 Scenario classes with generated probabilities greater than 1×10^{-4} in 10,000 years (Shading indicates scenario classes with probabilities less than 1×10^{-4} in 10,000 years.)

(NRC, 1986; 51 *FR* 22292). Therefore, use of the EPA criterion is not appropriate for scenario classes; however, if it were applied to the scenario classes shown in Figure 3–13, as suggested by Cranwell *et al.* (1990, p. 10), only 4 of the 16 classes would be retained (Table 3–4).

Table 3–4 Scenario Classes Remaining after Screening

Scenario Class	*Probability (over 10,000 yrs)*
Drilling + Seismicity	0.34
Drilling + Seismicity + Igneous Activity	1.0×10^{-2}
Drilling + Seismicity + Climate Change	0.61
Drilling + Seismicity + Igneous Activity + Climate Change	2.0×10^{-2}

Each of the four retained scenario classes would involve the occurrence of both drilling and seismicity at the Yucca Mountain site over the next 10,000 years. This is because, for the present analysis, the occurrence of both of these initial EPs have estimated probabilities approximately equal to 1.0.

It is also interesting to note that the base-case scenario class (i.e., the scenario class in which there would be no drilling, seismicity, igneous activity, or climate change) would be screened if the probability criterion were applied, as its assigned probability is approximately eight orders of magnitude below the EPA value. This result suggests that, given the currently assigned probabilities, conditions at the repository site over the next 10,000 years appear highly unlikely to remain as they are today.

For this scenario effort, no scenario classes were screened from the analysis. However, only a subset of the 16 scenario classes generated was modeled in the consequence analysis. Treatment of these scenario classes in the consequence analysis and the subsequent calculation of CCDFs for cumulative radionuclide releases to the accessible environment and for dose are discussed in the following chapters.

3.4 Discussion of Results

As noted, the staff has applied the SNL scenario selection procedure to generate scenario classes for consideration in the IPA Phase 2 consequence analysis (see Chapter 6). This section of the report summarizes the SNL procedure and documents the development of a final set of scenario classes and corresponding probability estimates used in the IPA Phase 2 analysis. From an initial list of potentially disruptive EPs, four were determined to be reasonably likely and warranting consideration of their possible effects on long-term repository performance: igneous activity (intrusive and extrusive), seismicity, climate change, and exploratory drilling. Estimates of their probability of occurrence over the next 10,000 years were developed, and these EPs are combined into 16 scenario classes with associated probabilities.

In applying the SNL scenario selection procedure, the staff found it to form an adequate basis for the development of scenario classes for the IPA Phase 2 analysis. The staff did consider that modifications were necessary, particularly the definition of explicit boundaries for the repository system, to meet the needs of the analysis and to keep the number of resultant scenario classes tractable. However, this does not detract from the adequacy of the methodology, in that other international programs that have applied the SNL procedure have also found modifications necessary to meet their specific programmatic needs and requirements (Andersson *et al.*, 1989; and Stephens and Goodwin, 1990). Cranwell *et al.* (1990) have, in fact, stated that "... the scenario selection methodology provides a general 'road map' for arriving at scenarios; the fact that [variations to] the methodology have been implemented is an indication of the flexibility of the methodology..." (*op cit.*, p. 15).

Suggestions for future work are discussed in Chapter 10.

4 FLOW AND TRANSPORT MODULE[1]

4.1 Introduction: Consequence Models for Flow and Radionuclide Transport

The Iterative Performance Assessment (IPA) effort provides, in part, a formal procedure for evaluating existing computer programs used to simulate ground-water flow and radionuclide transport; evaluating new concepts for flow and transport in unsaturated, fractured rock; and identifying performance assessment needs. IPA Phase 1 used some preliminary concepts regarding the Yucca Mountain site. This section will build on the ground-water IPA Phase 1 effort (see "Flow and Transport Models" (Chapter 6) in Codell *et al.*, 1992) using concepts that have been published since the Phase 1 effort concluded. Additionally this section will discuss the model used in estimating gaseous releases for inclusion into the complementary cumulative distribution function (CCDF) of repository performance (gaseous releases were analyzed as an auxiliary analysis in the IPA Phase 1 effort and were not included in the CCDF). The intent is to provide additional information for making modeling decisions and interpreting results. However, it needs to be pointed out that laboratory and field investigation of fluid flow in unsaturated, fractured rock can require significantly more time than improvements to computer programs; therefore, modeling capability in certain areas has progressed faster than parameter estimation and site characterization.

4.2 Flow and Radionuclide Transport Model for Ground-Water Releases

The IPA Phase 1 effort accounted for a number of important attributes of the Yucca Mountain site (e.g., stratigraphic changes below the repository in the unsaturated zone and differences between matrix and fracture flow). The IPA Phase 2 effort not only has maintained the important attributes of the Phase 1 study, but has added further modeling complexity such as:

- Saturated zone pathways to the accessible environment;
- Calculation of radionuclide concentration for dose assessment; and
- Distribution of mass flux between the fracture and matrix continua.

It is anticipated that additional complexity will provide insights into the performance of fractured rock as a geologic barrier, data requirements, and the capabilities of the computational methods used.

4.2.1 Site Concepts

The Yucca Mountain site is located on and immediately adjacent to the southwestern portion of the Nevada Test Site (see Figure 4–1). Yucca Mountain is a prominent group of north-trending, fault-block ridges. The terrain at the site is largely controlled by high-angle normal faults and eastward-tilted volcanic rocks. Slopes are locally steep (dip angle 15° to 30°) on the west-facing side of Yucca Mountain and along some of the valleys that cut into the more gently sloping (dip angle 5° to 10°) east side of the mountain (see Figure 4–2).

Stratigraphy

The hydrogeologic units of interest at Yucca Mountain are primarily comprised of ash-flow and ash-fall tuffs that originated from eruptions during the development of calderas. The amount of welding, fracturing, unit thickness, and chemical alteration varies greatly from one layer to the next; therefore, the hydrologic and transport parameters have the potential to also vary significantly from one layer to the next. Based on surface mapping and drill hole data, information on stratigraphic sequences and thicknesses for Yucca Mountain are presented in Ortiz *et al.* (1985). The Ortiz *et al.* report gives detailed stratigraphic information from the surface to the water table for a number of drill holes near the repository location and provides cross-sections at various locations of the site (see Figure 4–3). One particular cross-section, presented in

[1]The figures shown in this chapter present the results from a demonstration of staff capability to review a performance assessment. These figures, like the demonstration, are limited by the use of many simplifying assumptions and sparse data.

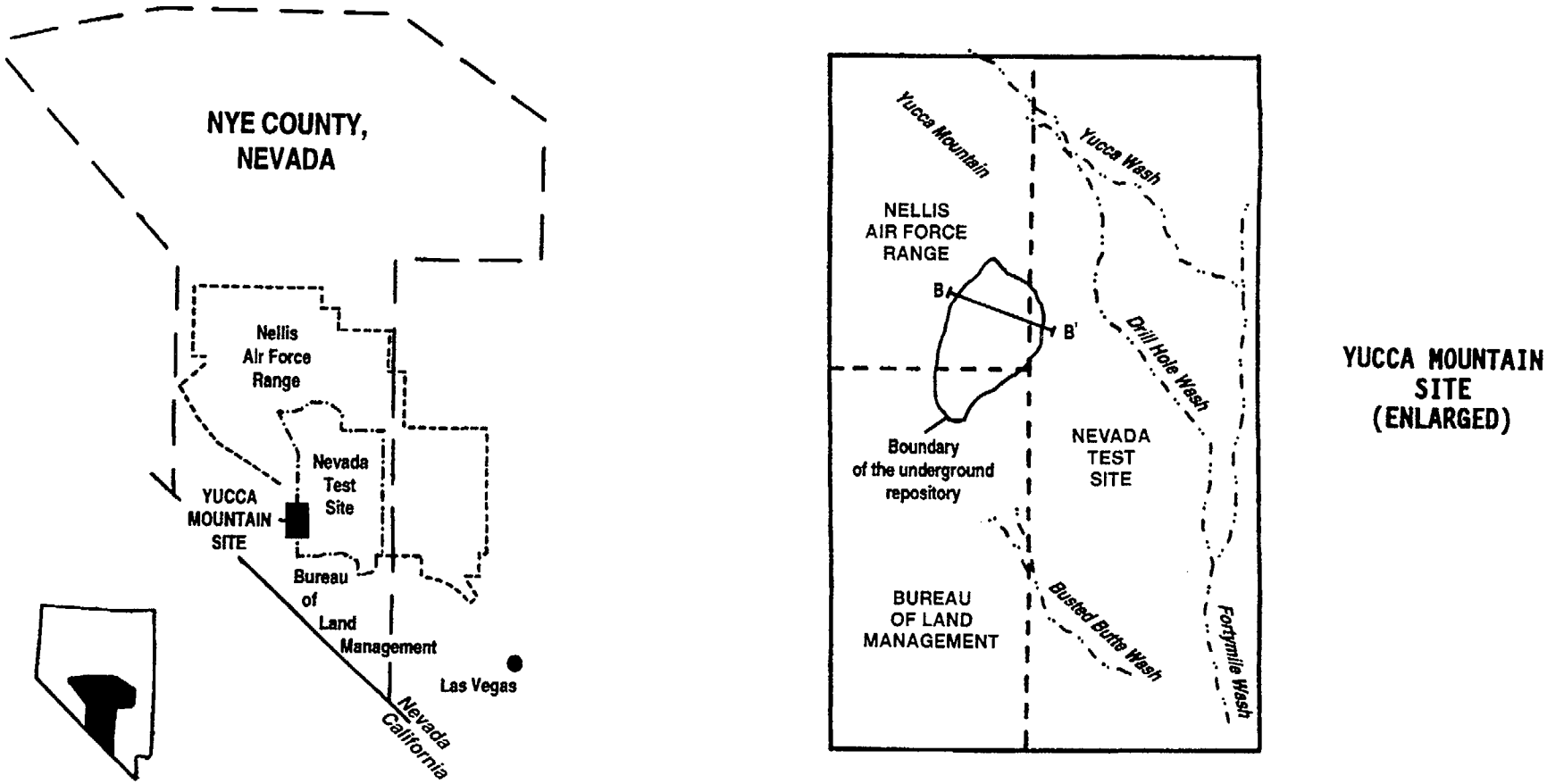

Figure 4–1 Location of the Yucca Mountain site (Adopted from DOE (1988b, p. 13).)

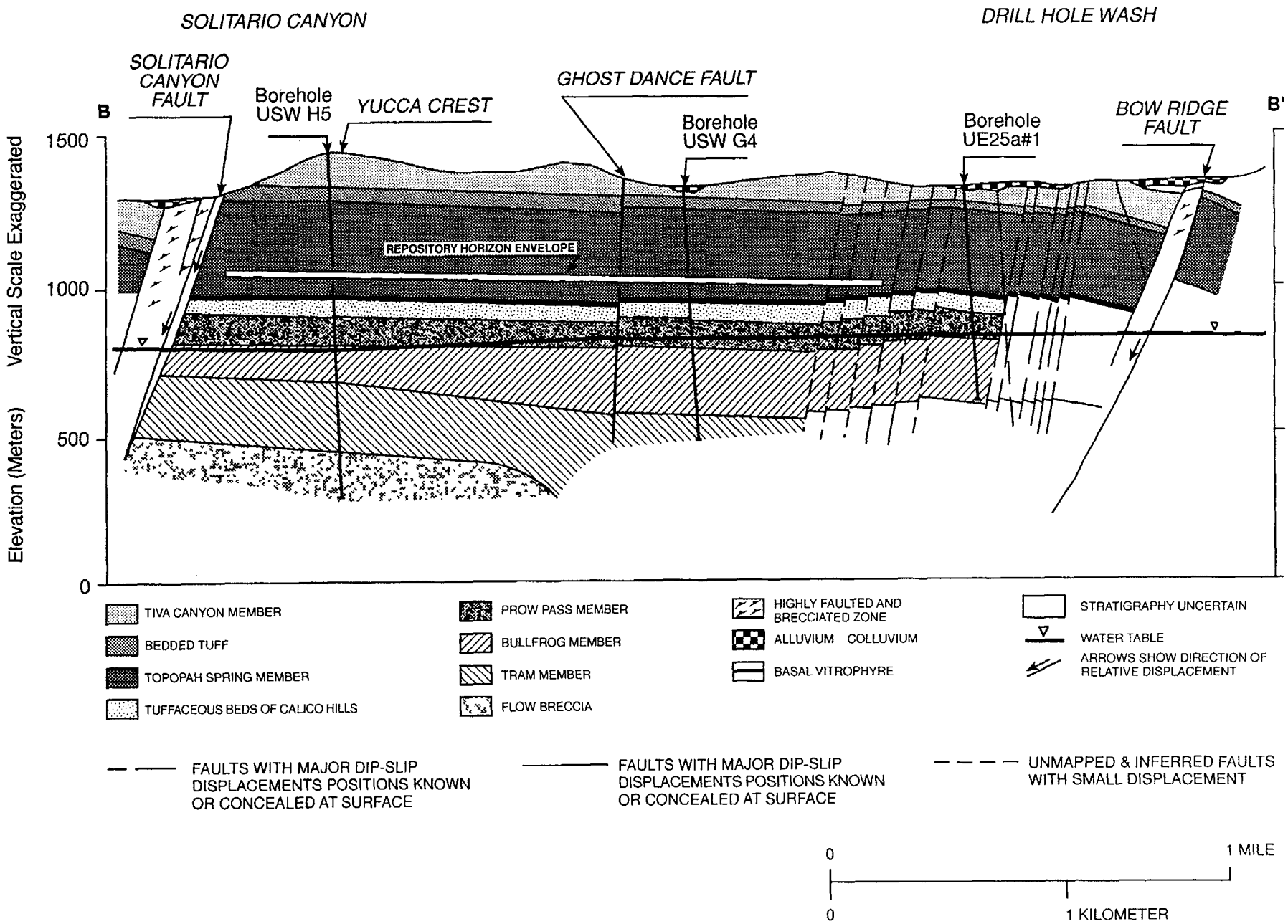

Figure 4–2 East-west geologic cross-section (along B–B′) for the Yucca Mountain site (Adopted from DOE (1988b, p. 19).)

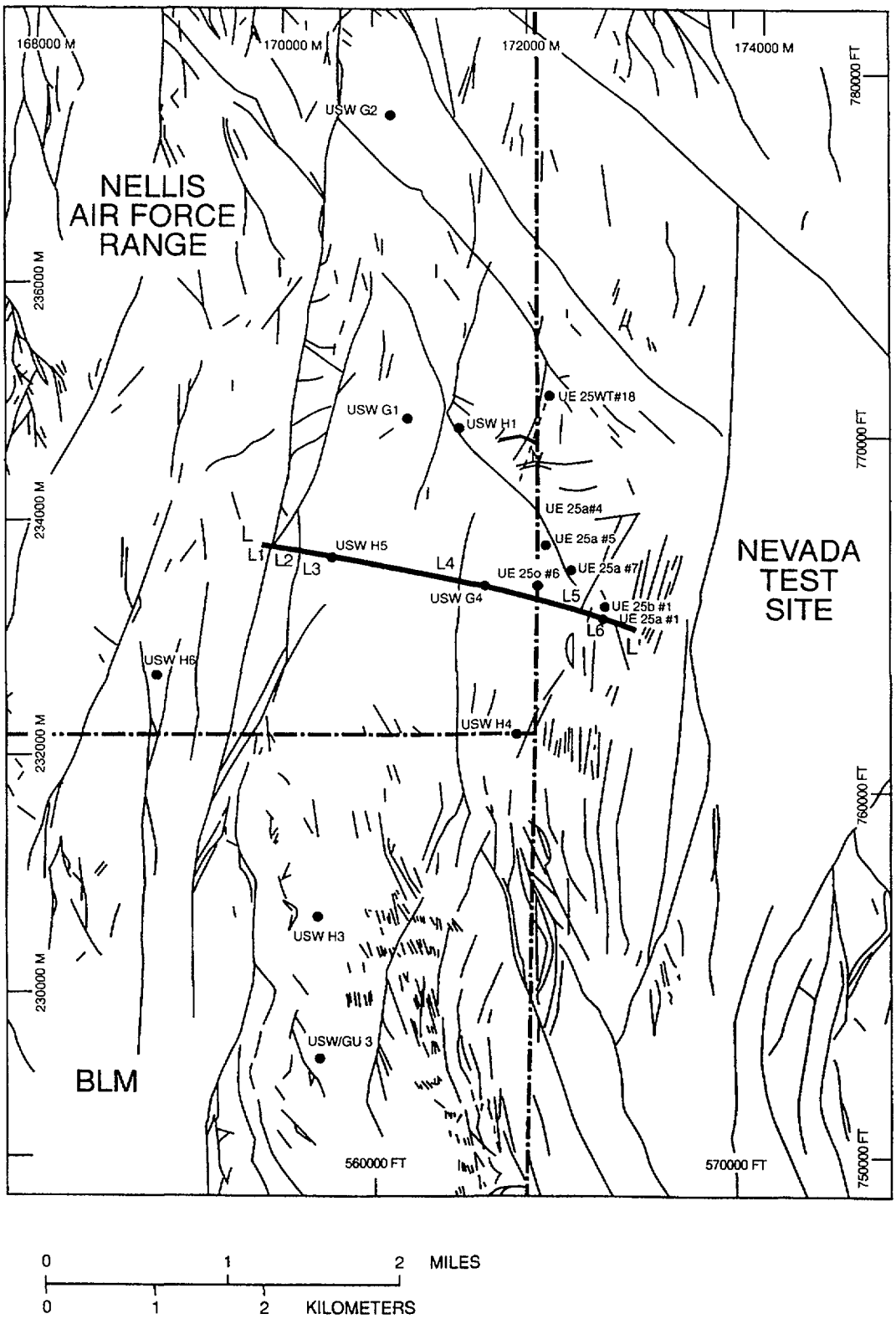

Figure 4–3 Locations of faults, drill holes (solid circles), and generated cross-sections (dotted lines) (Adopted from Ortiz *et al.* (1985, p. 17).)

Figure 4–4, has been the basis of preliminary studies attempting to better understand modeling limitations with respect to flow conditions associated with the unsaturated zone at Yucca Mountain (Barnard *et al.*, 1992; Prindle and Hopkins, 1990; and Dudley *et al.*, 1988). This cross-section possesses some of the primary features, of the Yucca Mountain site, anticipated to be important when calculating system performance. The important features are:

- Dipping strata with large contrasts in permeability between strata;
- Variation in the unit sequences and thicknesses between the water table and the repository horizon; and
- Variation in the distance from the suggested repository horizon to the water table.

Liquid Flow

Hydrologic data are rather limited for the Yucca Mountain site. The Peters report (1984) is a primary source of parametric data for recent modeling studies (Barnard *et al.*, 1992; Nitao and Buscheck, 1991; Prindle and Hopkins, 1990; and Dudley *et al.*, 1988) and for DOE's Site Characterization Plan (SCP) (see DOE, 1988a). Two important aspects of the hydrologic data, as reported in the SCP, are the contrast in matrix conductivity between hydrogeologic units (see Table 4–1) and the significant contrast between laboratory measurements and *in-situ* or field measurements for many of these units (see Table 4–2). This contrast, between laboratory and field measurements, could be indicative of the contribution of fractures to the saturated conductivity, which is more easily controlled in a small-scale laboratory measurement.

Generally, matrix data are very limited and provide little information to define defensible parametric ranges for use in performance assessments. The fracture data, being primarily derived from capillary theory rather than the results of hydrologic measurements, are even more limited than the matrix data. Recent modeling work by Nitao and Buscheck (1991) provides some insights on how matrix permeability affects fracture flow attenuation because of matrix imbibition. Although the Nitao work is based on preliminary field data and hypothetical fluxes, it clearly indicates the need to better understand fracture-matrix interactions and the need for more data to estimate parameters in both the fractures and the matrix.

Possibly the largest contributor to uncertainty in the fracture-matrix interactions is the assignment of the percolation rate. The SCP (DOE, 1988a; pp. 3–201 – 3–214) cites a number of studies that span a range of percolation rates (e.g., 0.015 – 4.5 millimeters/year). Recent analyses (Barnard *et al.*, 1992) using "representative" Yucca Mountain data and adopting a steady-state model wherein the fracture and matrix pressures are in equilibrium tend to support low values (0.01 millimeter/year) for percolation rates. However, the work of Nitao and Buscheck (1991) indicates that the time necessary to reach equilibrium can be significant and Ababou (1991, p. 2–8) has pointed out additional limitations of using mean values of percolation and simplified models for subsurface flow:

- The ground surface at Yucca Mountain is fractured since the "highly fractured" Tiva Canyon unit crops out throughout most of the repository (DOE, 1988a; p. 3–203);
- Rainfall occurs in bursts and the rainfall rate is far from periodic at any time scale accessible to observation;
- The interactions between rainfall intensity, infiltration, ponding, and runoff are not well-understood; and
- The linear theory of damping applied to the non-linear unsaturated flow equation may be overly inaccurate under certain conditions (such as Item Nos. (1) through (3) above).

A better understanding of transient effects, fracture-matrix interactions, and the effects of heterogeneity is necessary if defensible estimates of percolation are to be provided for performance assessments.

Gas Flow

One difference between disposal in the saturated zone as compared to disposal above the water table is the possibility for radionuclide migration via the gas pathway. Fractures, if dry and interconnected, could provide a fast pathway for gas

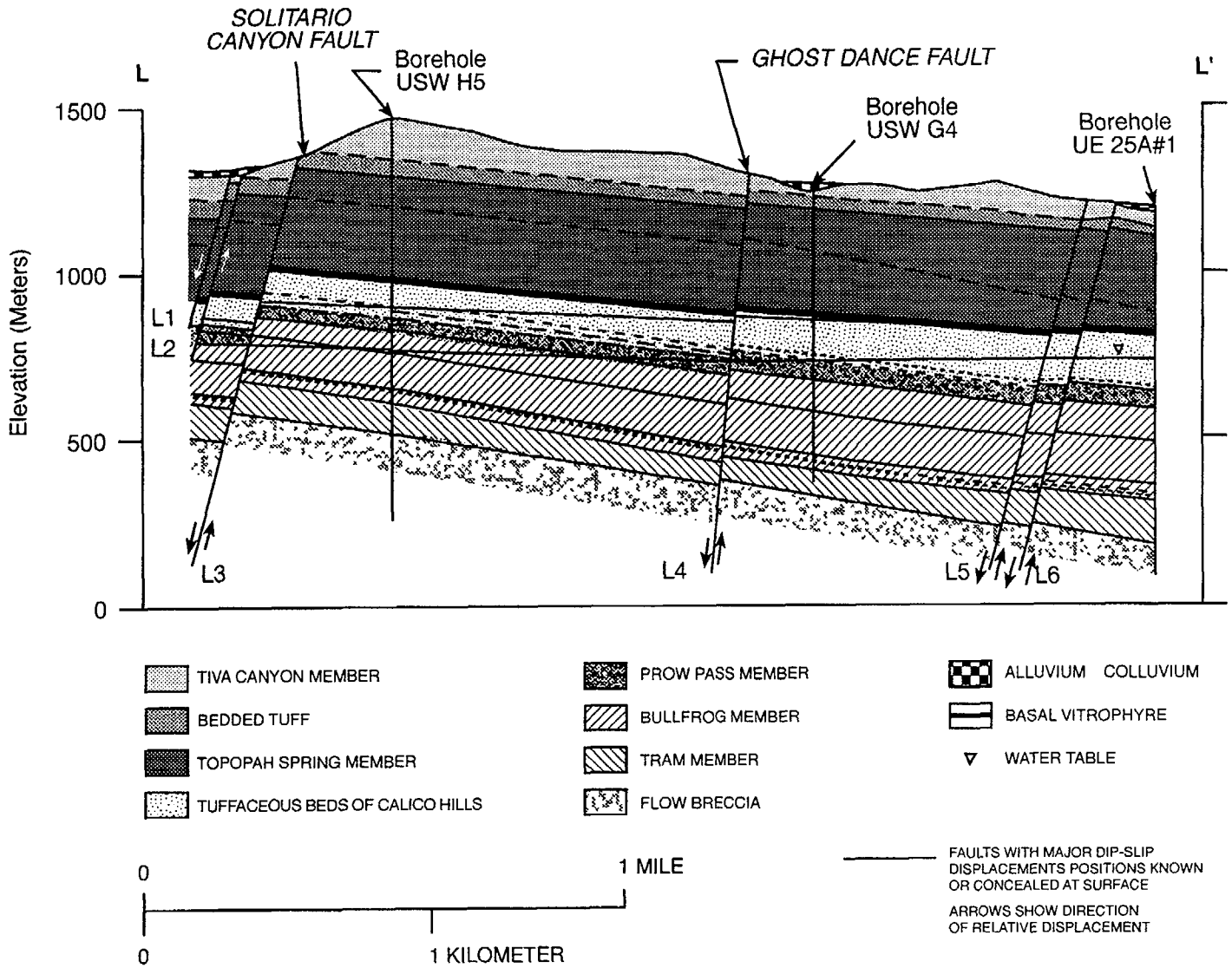

Figure 4–4 Cross-section L–L'. (See Figure 4.3 for location of cross-section in relation to Yucca Mountain. Adopted from Ortiz *et al.* (1985, p. 19).)

Table 4-1 Summary of Hydrogeologic Properties of Hydrogeologic Units within the Unsaturated Zone at Yucca Mountain (From DOE (1988a, p. 3-170).)

Hydrologic Unit	*Source of Data*	*Range of thickness (m)*	*Grain Density (kg/m^3)*	*Fracture Density[a] ($no./m^3$)*	*Matrix Porosity*	*Saturated Matrix Hydraulic Conductivity (m/sec)*
Tiva Canyon	b	0 - 150	No data	10 - 20	0.12	2.1×10^{-11}
(welded)	c	No data	2,490		0.08	9.7×10^{-12}
Paintbrush	b	20 - 100	No data	1	0.46	1.0×10^{-7}
(non-welded)	c	No data	2,350		0.40	3.9×10^{-7}
Topopah Spring	b	290 - 360	No data	8 - 40	0.14	3.5×10^{-11}
(welded)	c	No data	2,580		0.11	1.9×10^{-11}
Calico Hills	b	100 - 400	No data	2 - 3	0.37	5.0×10^{-8}
(non-welded, vitric)	c	No data	2,370		0.46	2.7×10^{-7}
Calico Hills	b	100 - 400	No data	2 - 3	0.31	9.0×10^{-11}
(non-welded, zeolitic)	c	No data	2,230		0.28	2.0×10^{-11}

[a]Scott *et al.* (1983).
[b]Montazer and Wilson (1984).
[c]Peters *et al.* (1984) and Peters *et al.* (1986).

Table 4-2 Summary of Hydrogeologic Characteristics, as Determined through Laboratory and Field Measurements, of Major Stratigraphic Units in the Vicinity of Yucca Mountain (From DOE (1988a, pp. 3-182 — 3-183))

***In-Situ* (field) Analyses**

Stratigraphic Unit	*Typical Character*	*Saturated Thickness*	*Transmissivity*[a] *(m^2/day)*	*Average Conductivity*[b] *(m/day)*	*Borehole Tested*
Topopah Spring	Moderately to densely welded tuff	167	120	0.7	J-13
Calico Hills	Zeolitized, nonwelded tuff, vitric tuff	148	(82)	0.5	UE-25b#1
Prow Pass	Nonwelded to moderately welded tuff	116	167	1.44	USW H-1
		135	150	1.1	USW H-1
		174	36 - 142	0.2 - 0.8	USW H-4
		150	(65)	0.4	UE-25b#1
		111	14	0.1	UE-25p#1
Bullfrog	Nonwelded to densely welded tuff	125	0.8	0.006	USW H-1
		119	70 - 276	0.6 - 2.3	USW H-4
		159	(65)	0.4	UE-25b#1
		132	(7)	0.05	UE-25p#1
Tram	Nonwelded to moderately welded ashflow and bedded tuffs	284	0.002	7.0×10^{-6}	USW H-1
		354	0.7	0.002	USW H-3
		352	70 - 276	0.2 - 0.8	USW H-4
		183	(3.3)	0.02	UE-25p#1
Lithic Ridge Tuff	Partially welded ashfall tuffs	594	0.001	2.0×10^{-6}	USW H-1
		110	0.1	0.001	USW H-3
		371	>10	>0.03	UE-25p#1

[a]Parentheses ( ) indicate approximate value because reported values reflect more than one stratigraphic unit.
[b]Obtained by dividing transmissivity by saturated thickness.

Table 4-2 (continued)

Laboratory (Core) Analyses

		Saturated Matrix		*Matrix Porosity*		
Stratigraphic Unit	*Typical Character*	*Conductivity (m/day)*	*No. of Samples*	*Percent*	*No. of Samples*	*Borehole Tested*
Topopah Spring	Moderately to densely welded tuff	3×10^{-7} to 2×10^{-4}	5	4 - 33	5	J-13
		7×10^{-7} to 5×10^{-4}	18	6 - 30	24	UE-25a#1
		8×10^{-7}	1	12	1	UE-25b#1
Calico Hills	Zeolitized, nonwelded tuff, vitric tuff	4×10^{-6} to 3×10^{-4}	6	20 -34	7	UE-25a#1
Prow Pass	Nonwelded to moderately welded tuff	6×10^{-5} to 1×10^{-4}	3	28 - 29	3	USW H-1
		2×10^{-5} to 1×10^{-3}	8	10 - 25	12	UE-25a#1
		6×10^{-7} to 1×10^{-3}	5	17 - 30	18	USW G-4
Bullfrog	Nonwelded to densely welded tuff	3×10^{-5} to 1×10^{-3}	10	19 - 34	9	USW H-1
		2×10^{-4} to 1×10^{-3}	3	17 - 34	3	UE-25a#1
		2×10^{-4} to 5×10^{-4}	2	24 - 27	6	USW G-4
Tram	Nonwelded to moderately welded ashflow and bedded tuffs	4×10^{-6} to 4×10^{-4}	9	18 - 26	9	USW H-1
Lithic Ridge Tuff	Partially welded ashfall tuffs	6×10^{-5} to 3×10^{-4}	2	9 - 17	2	USW H-1

phase radionuclides (e.g., ^{14}C). Air flow has been observed at some boreholes at Yucca Mountain (Weeks, 1987). Weeks has suggested that this phenomenon is caused by topographic and barometric effects combined with outcrops on the side of the mountain of rock units that intercept the boreholes.

Simulation work (Tsang and Pruess, 1987) has examined the effect of the thermal output of the repository on gas flow. Simulated gas pore velocities in fractures varied from 4.5 to 1174 meters/year (*op cit.*, p. 1963). Although these simulations were preliminary, the results indicate that further investigation may be needed to properly characterize boundary conditions and the fracture properties for gas flow.

Transport

The transport of radionuclides will be governed by properties associated with the transporting fluid (i.e., advection, dispersion, and diffusion) and properties associated with geochemistry (i.e., sorption and precipitation). The advective and dispersive components of transport are associated with the fluid flow and were highly dependent on the heterogeneous nature of the formation being studied. The presence of fractures can put increased demands on transport models. Although the presence of near horizontal strata or fractures can increase the horizontal/longitudinal spreading of radionuclides relative to isotropic media, the presence of vertical fractures could lead to contrary effects, depending on ambient moisture and the interplay between porous rock and fracture hydraulic properties (Ababou, 1991; p. 2–13).

Matrix diffusion in and out of fractures has been suggested as a possible mechanism for retarding transport (DOE, 1988b; p. 31). Consideration of this effect will require an understanding of the nature of the fracture surface (i.e., fracture coatings) that will affect the mass transfer at the fracture/matrix interface (Parsons *et al.*, 1991).

Sorption and precipitation of water-borne radionuclides will generally depend on the mineral surfaces present and the chemical composition in the ground water. The sorption properties of Yucca Mountain tuff can be significantly affected by the presence of zeolites. It has been suggested that model development should modify the hydrologic layering with a geochemical stratigraphy (s Figure 4–5) to account for geochemical variation (i.e., mineralization and ground-water chemistry) in the formation (*op cit.*). This type of more detailed geochemical stratigraphy provides a simple way to modify ground-water models with geochemical information.

4.2.2 Recent Modeling Studies

Parsons *et al.* (1991) reviewed a number of modeling studies relevant to Yucca Mountain. It is worthwhile to point out some simplifying assumptions that have been used in fluid flow simulations involving fractured tuff, such as: constant percolation rate; one-dimensional (1–D) vertical flow; steady-state conditions that imply pressure equilibrium between the fracture and matrix; fractures represented as a porous continuum; and transient flow with instantaneous pressure equilibration between the fracture and matrix. Some simplifying assumptions that have been used in transport simulations involving fractured tuff are: retardation calculated from a distribution coefficient (K_d); 1–D transport paths; and transport not occurring simultaneously in the fractures and matrix (*op cit.*). Many of the assumptions are because of computational constraints and limitations in characterization data (e.g., fracture properties and sorption parameters).

The above simplifications suggest that a better understanding is needed at both the fine-scale (phenomena that control fracture/matrix interactions and retardation mechanisms) and large-scale (accounting for multiple dimensions, spatial variability, and structural features such as faults). Recent work (Nitao and Buscheck, 1991; and Dykhuizen, 1990) has been examining different approaches to the fracture/matrix interaction. Nitao and Buscheck's work has examined a single fracture and quantitatively identified three distinct flow periods (predominantly fracture flow, flow primarily from the fracture into the matrix, and matrix flow) for flow in unsaturated, fractured tuff. There is, of course, a question of how best to incorporate modeling improvements of the fine-scale nature into performance assessments that need to address very large scales. Ababou (1991) in his review of modeling approaches to large-scale flow, has suggested that a compromi between direct high-resolution simulation of

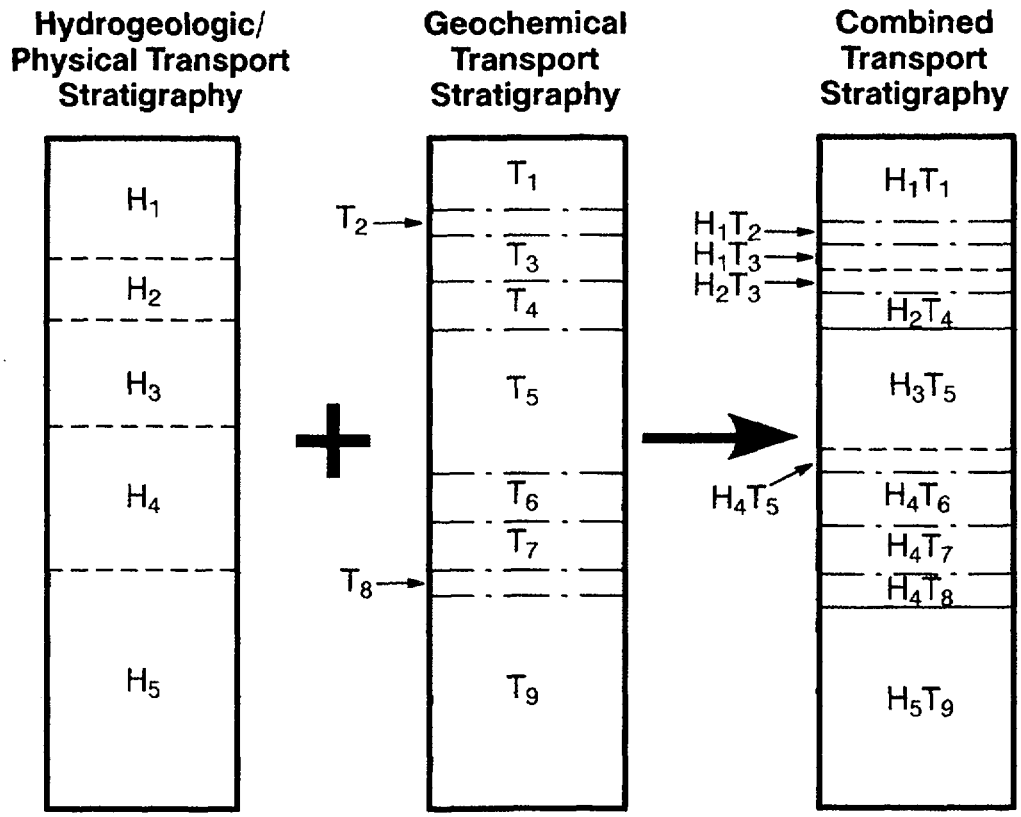

Figure 4–5 Hypothetical example of a "combined" transport stratigraphy that accounts for hydrologic and geochemical stratification (From Parsons *et al.* (1991, p. 76).)

fine-scale details and the indirect simulation approach based on uniform equivalent media models would be less computationally demanding and would capture a broad range of fine-scale to large-scale phenomena.

Additionally, the assignment of parameter values is oftentimes just as important as the underlying theory supporting the equations being solved. Ababou (1991, p. 7–1) has made the following important suggestion with respect to the interaction of modeling and data collection:

> "Realism dictates that the spatial structure of the least accessible material properties, such as the relative conductivity curves, be analyzed indirectly through correlations with more easily measured parameters. Therefore, auxiliary models need to be developed and tested in order to correlate the parameterized conductivity curves with say, void structure, porosity, and saturated conductivity."

It is important to understand the limitations and assumptions inherent with derived parameters (such as percolation) and their associated measurements (such as moisture contents). The rock properties desirable for a repository (i.e., low permeability, low percolation) also impose limitations on the ability to easily measure and quantify those same properties. As Ababou has pointed out above, a variety of models will be needed to assist the collection and interpretation of site information.

4.2.3 Site Conceptual Model

Despite the limitations and uncertainties described above, there are a number of published reports containing site information and parametric determinations to allow the development of site conceptual models and assignment of parametric values. The following section provides the details of the site conceptual model that includes the stratigraphy, boundary conditions, and parametric data.

4.2.3.1 Stratigraphy

The tilting hydrostratigraphy (generally dipping 7°) at the Yucca Mountain site results in significant differences in which hydrostratigraphic units are present at particular locations both in the unsaturated zone (between the repository horizon and the water table) and in the saturated zone (along the water table extending from a location directly below the repository to the accessible environment). The boundaries for the vertical (unsaturated zone) and near horizontal (saturated zone) flow systems are determined by the location of the water table. Therefore, assumptions regarding the location of the water table are important in identifying the hydrogeologic units present for the base case (undisturbed) and pluvial conditions (increased percolation). The assumptions and hydrogeologic units used for liquid flow are discussed below for the unsaturated zone, saturated zone, and pluvial conditions.

4.2.3.1.1 Unsaturated Liquid Flow

Ortiz *et al.* (1985) identified a number of reference stratigraphic units within the Paintbrush Tuff (Tiva Canyon welded unit, Paintbrush non-welded unit, and Topopah Spring unit); Tuffaceous beds of the Calico Hills (Calico Hills non-welded vitric unit, and Calico Hills non-welded zeolitic unit); and the Crater Flat Tuff (Prow Pass non-welded zeolitic unit, Upper Crater Flat non-welded zeolitic unit, Middle Crater Flat non-welded zeolitic unit, Bullfrog welded devitrified unit, and Tram non-welded unit) that can be used to identify where rock properties change within a particular tuff. Borehole stratigraphic data taken from Ortiz *et al.*, were used to identify hydrogeologic units and assign thicknesses below the repository. Tables 4.3 and 4.4 present information taken from Ortiz *et al.*, for selected boreholes at the Yucca Mountain site. For the purpose of defining the hydrogeologic units present in the unsaturated zone below the repository, stratigraphic information from the selected boreholes was used to represent the hydrogeology below seven distinct regions (or sub-areas) of the repository (see Figure 4–6). The seven selected boreholes depicted in Figure 4–6 were each associated with seven repository sub-areas (sub-area sizes were determined based on proximity to individual boreholes). The hydrogeologic units below each of the seven repository sub-areas were then assumed to correspond to its associated borehole stratigraphy, thus producing seven different hydrogeologic sequences over the entire repository (it should be noted that this approach assumed vertical flow in the unsaturated zone and ignored explicit site features such as the Ghost Dance fault).

The information contained in Tables 4.3 and 4.4 was simplified (i.e., rounding off thicknesses and neglecting very thin layers) to provide seven distinct hydrogeologic sequences for the unsaturated zone modeling (see Table 4–5).

4.2.3.1.2 Saturated Liquid Flow

The hydrogeologic units of the saturated zone, for this analysis, were assumed to correspond to the stratigraphy along the surface of the water table directly below the repository out to the accessible environment (5 kilometers). For the saturated zone, it was assumed that contaminant migration occurred only in the fractures and there would be minimal vertical mixing because of the relatively small volumetric flux in the unsaturated zone as compared to the volumetric flux in the saturated zone. This lack of vertical mixing and the low percolation rates result in the stratigraphic sequences along the water table being a reasonable representation for the portion of the saturated zone that affects radionuclide migration.

A map of stratigraphic changes along the surface of the water table (see Figure 4–7) in the area of interest was constructed. The map was built using available stratigraphic data from boreholes, water-table elevations, geologic maps, and stratigraphic cross-sections (see Czarnecki, 1984; Sc 1984; and DOE, 1988a). Therefore, to account better for structural effects, both hard and soft

Table 4–3 Elevations (Reported as Meters Above Sea Level) and Distances (in Meters) for Boreholes in the Vicinity of Yucca Mountain That Were Used to Define Hydrogeologic Units for the Unsaturated Flow Model (Based on Ortiz *et al.* (1985) and the assumption that the base of the repository is 60 meters above the base of the Topopah Spring unit.)

Information	*UE25a#1 Sub–Area 1*	*USW G4 Sub–Area 2*	*USW H4 Sub–Area 3*	*USE H3 Sub–Area 4*	*USW H6 Sub–Area 5*	*USW H5 Sub–Area 6*	*USW G1 Sub–Area 7*
Elevation of Wellhead	1199	1270	1249	1484	1302	1479	1199
Elevation of Water Table	730	730	730	732	776	775	730
Distance to Water Table	469	540	519	752	526	704	469
Thickness of Topopah Spring	317	336	294	245	297	331	317
Elevation of Base of Topopah Spring	798	860	878	1102	904	974	798
Distance from Base of Topopah Spring to Water Table	68	130	148	370	128	199	68
Distance from Base of Repository to Water Table	128	190	208	430	188	259	128
Distance from Base of Repository to the Surface (Elevation of the Base of the Repository)	341 (858)	350 (920)	311 (938)	321 (1163)	338 (964)	445 (1034)	341 (858)

Table 4-4 Hydrogeologic Unit Thickness (in Meters) and Location of Water Table (Denoted by: Thickness Above the Water Table/Thickness Below the Water Table) for Boreholes in the Vicinity of Yucca Mountain (Based on information provided by Ortiz *et al.* (1985).)

Hydrogeologic Unit	*UE25a#1 Sub-Area 1*	*USW G4 Sub-Area 2*	*USW H4 Sub-Area 3*	*USE H3 Sub-Area 4*	*USW H6 Sub-Area 5*	*USW H5 Sub-Area 6*	*USW G1 Sub-Area 7*
Alluvium	9	9	---	---	9	---	18
Tiva Canyon	50	27	53	107	49	125	---
Paintbrush	25	38	24	30	43	49	67
Topopah Spring	317	336	294	244	297	331	324
Calico Hills (vitric)	---	5	30	138	73	73	16
Calico Hills (zeolitic)	68 / 93	125 / 6	99	---	---	36	145
Prow Pass	51	51	19 / 18	2	53	34	2 / 37
Upper Crater Flat	98	91	162	88	2 / 24	56 / 11	98
Bullfrog	---	129	88	98	105	111	69
Middle Crater Flat	---	45	65	45 / 2	62	42	64
Tram	---	---	126	2	94	91	83

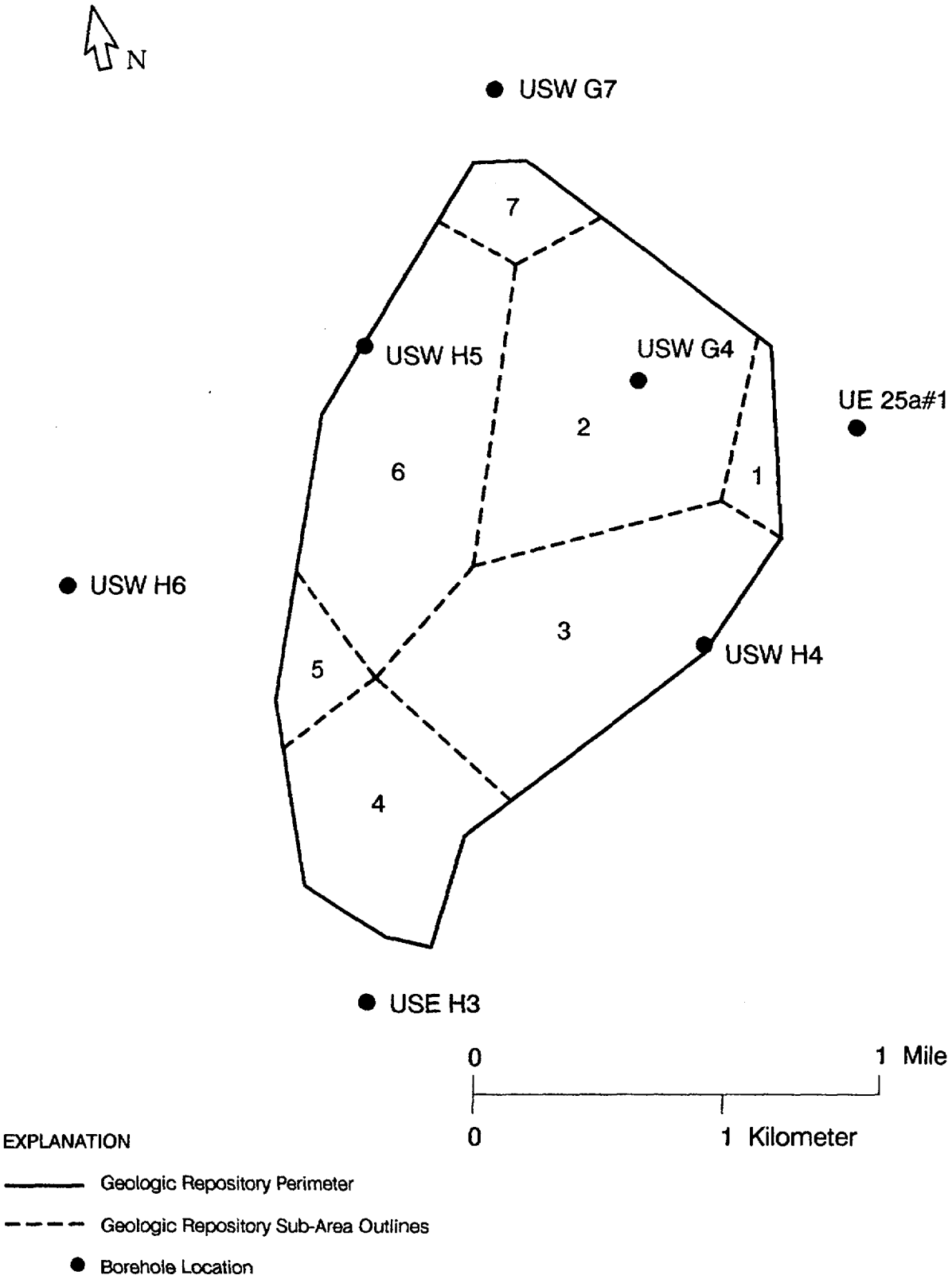

Figure 4–6 Location of seven selected boreholes used to define the hydrogeologic units for seven repository sub-areas

Table 4–5 Hydrogeologic Unit Thickness (in Meters) to be Used in the Unsaturated Flow Model (Base Case Scenario)

Hydrogeologic Unit	*UE25a#1 Sub–Area 1*	*USW G4 Sub–Area 2*	*USW H4 Sub–Area 3*	*USE H3 Sub–Area 4*	*USW H6 Sub–Area 5*	*USW H5 Sub–Area 6*	*USW G1 Sub–Area 7*
Topopah Spring	60	60	60	60	60	60	60
Calico Hills (vitric)	—	—	30	140	70	70	20
Calico Hills (zeolitic)	70	130	100	—	—	40	140
Prow Pass	—	—	20	—	60	30	—
Upper Crater Flat	—	—	—	90	—	60	—
Bullfrog	—	—	—	100	—	—	—
Middle Crater Flat	—	—	—	40	—	—	—
Distance to the Water Table	130	190	210	430	190	260	220

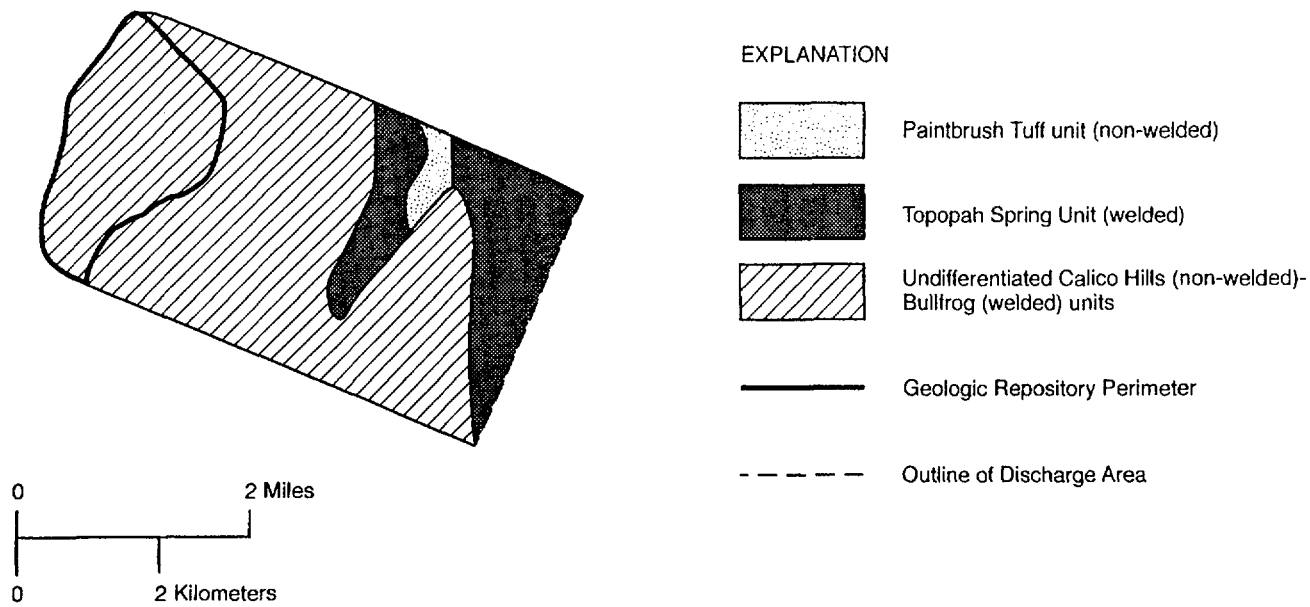

Figure 4–7 Depiction of changes in hydrogeologic units along the surface of the water table from beneath the proposed repository to the accessible environment (used for base case saturated zone model)

(interpretative) data were used to make this map. It is recognized that the interpretation of water-table stratigraphy, in Figure 4–7, is not the only possible interpretation, given the present geologic uncertainties. Future work will need to consider other possible interpretations.

This stratigraphic map was then used to determine unique hydrogeologic units (see Table 4–6 for numeric values) along the assumed saturated ground-water flow path for each of the repository zones identified for the unsaturated flow. The descriptions of the stratigraphic changes along the water table were interpreted for flow paths that assumed ground-water flows in a southeast direction from the repository. Although other interpretations of the direction of ground-water flow are possible, this interpretation agrees with most of the present interpretations found in the literature.

Additionally, as a result of data uncertainties and interpretation complexities, the interpretation of water-table stratigraphy contains no interpretations about stratigraphic units older than the Prow Pass unit. In Figure 4–7, the Prow Pass and older units occur underneath the site. It is recognized that units older than the Prow Pass unit probably occur above the water table, along the western and southern site boundaries. The simplification of using Prow Pass unit fracture properties to represent the fracture properties of the Prow Pass and older units is reasonable. It is anticipated that the rate of ground-water fracture flow over the long saturated flow path (5 kilometers) will be dominated by the fracture

Table 4–6 Length (in Kilometers) of Hydrogeologic Unit Sequences along the Saturated Flow Paths for Each of the Seven Repository Sub-Areas (Base Case Scenario)

Hydrogeologic Unit	*Sub–Area 1*	*Sub–Area 2*	*Sub–Area 3*	*Sub–Area 4*	*Sub–Area 5*	*Sub–Area 6*	*Sub–Area 7*
From the Water Table below the Repository							
Prow Pass	0.40	1.35	0.85	1.50	1.70	1.70	1.10
Calico Hills[a]	2.15	2.12	2.10	4.20	2.05	2.05	2.15
Topopah Spring	0.65	0.65	0.65	—	0.50	0.65	0.70
Paintbrush	0.30	0.25	1.35	—	—	—	0.25
Calico Hills	0.60	0.73	—	—	1.65	1.28	—
Topopah Spring	1.30	1.23	0.95	0.50	0.72	1.00	1.90
To the Accessible Environment							
Total Length	5.40	6.33	5.90	6.20	6.62	6.68	6.10

[a]Fractured properties of Calico Hills vitric and zeolitic tuff are assumed to be the same; therefore, no distinction is made between the two for the saturated paths that only consider fracture flow.

properties in units, outside the site boundary, that occur over the majority of the saturated flow path.

4.2.3.1.3 Pluvial Conditions

A pluvial scenario (increase in percolation resulting from wetter climatic conditions) was incorporated into the current modeling by assuming a higher range for percolation and an associated rise (100 meters) in the water table. These values are consistent with the initial values used in IPA Phase 1 calculations (see Codell *et al.*, 1992; p. 57) which were based in part on Czarnecki (1984). Additionally, an auxiliary analysis was performed that examined the amount of water-table rise for selected percolation rates attributed to various climatic changes. The auxiliary analysis (see Section 4.4.3) showed a variation in water-table rise (a few meters to 100 meters) for the range of climatic conditions considered.

The rise in the water table causes a decrease in the thickness of the unsaturated zone below the repository (see Table 4–7 for hydrogeologic unit thicknesses) and associated changes in the hydrogeologic units constituting the saturated flow path. The depths to the water table in a pluvial climate were assumed to be 100 meters less than the base-case depths. The stratigraphic changes used to determine hydrogeologic units for the saturated zone were based on a pluvial period as modeled by Czarnecki (1984), which projected the water table under Yucca Mountain to rise by 130 meters.

Since pluvial-period modeling effects are based on regional models they supply very little information on changes in hydraulic gradient and flow direction at a site scale. Therefore, it was assumed that the saturated flow direction and gradient would be the same as the base case. However, the hydrogeologic units along the water table for the pluvial case varied from the base case, because of the rise in the water table resulting in rock at higher elevations becoming saturated. Again, a map of stratigraphic changes along the surface of the pluvial water table was constructed. This map was then used to identify hydrogeologic units along the assumed saturated ground-water flow path for each of the repository zones identified for the unsaturated flow. The map was based on available stratigraphic data from boreholes, water-table elevations, geologic maps, and stratigraphic cross-sections (Spengler *et al.*, 1981; Bently *et al.*, 1983; Craig, 1991; Classen *et al.*, 1973; Thordarson, 1983; Lobmeyer *et al.*, 1983; Lahoud *et al.*, 1984; Healey *et al.*, 1984; Whitfield *et al.*, 1985; Thordarson *et al.*, 1985; Rush *et al.*, 1983; Scott and Bonk, 1984; Scott, 1984; Lobymeyer, 1986; Czarnecki, 1984; Czarnecki and Waddell, 1984; and DOE, 1988a). However, many less drill-hole data were available, because stratigraphic data above the water table could not be obtained for any of the U.S. Geological Survey water-table holes (WT holes). Therefore, the interpretation in Figure 4–8 (see Table 4–8 for numeric values) is less certain than the interpretation used in the base case. Again, it is recognized that the interpretation of water-table stratigraphy, in Figure 4–8, is not the only possible interpretation.

It is also recognized that the pluvial period was based on a 100-meter rise in the water table, whereas the saturated zone stratigraphy was based on a 130-meter rise. The saturated-zone stratigraphy (Figure 4–8) described above, which was based on a 130-meter rise, is considered to be a sufficient reflection of a 100-meter rise in the water table; therefore, no further work was done to refine the water-table-rise stratigraphy to 100 meters.

4.2.3.2 Boundary Conditions

The magnitude of ground-water flux leaving or entering the boundaries of a ground-water model is typically controlled through the assignment of pressure or flux boundary conditions. Understanding of these "inlet" and "outlet" boundary conditions is critical in the development of conceptual models and the interpretation of the results of ground-water models.

The upper or surface boundary condition for many ground-water models of the unsaturated zone is the percolation rate. As discussed above (see Section 4.2.1) the percolation rate is not a well-understood parameter; it can have large uncertainties because of spatial variability and transient conditions. The current analysis uses the same steady-state ranges for the percolation rate (0.1 to 5.0 millimeters/year for base case and 5.0 to 10.0 for pluvial conditions) that were used in

Table 4–7 Hydrogeologic Unit Thickness (in Meters) to be Used in the Unsaturated Flow Model (Pluvial Conditions)

Hydrogeologic Unit	*UE25a#1 Sub–Area 1*	*USW G4 Sub–Area 2*	*USW H4 Sub–Area 3*	*USE H3 Sub–Area 4*	*USW H6 Sub–Area 5*	*USW H5 Sub–Area 6*	*USW G1 Sub–Area 7*
Topopah Spring	30	60	60	60	60	60	60
Calico Hills (vitric)	—	—	30	140	30	70	20
Calico Hills (zeolitic)	—	30	20	—	—	30	40
Prow Pass	—	—	—	—	—	—	—
Upper Crater Flat	—	—	—	90	—	—	—
Bullfrog	—	—	—	40	—	—	—
Middle Crater Flat	—	—	—	—	—	—	—
Distance to the Water Table	30	90	110	330	90	160	120

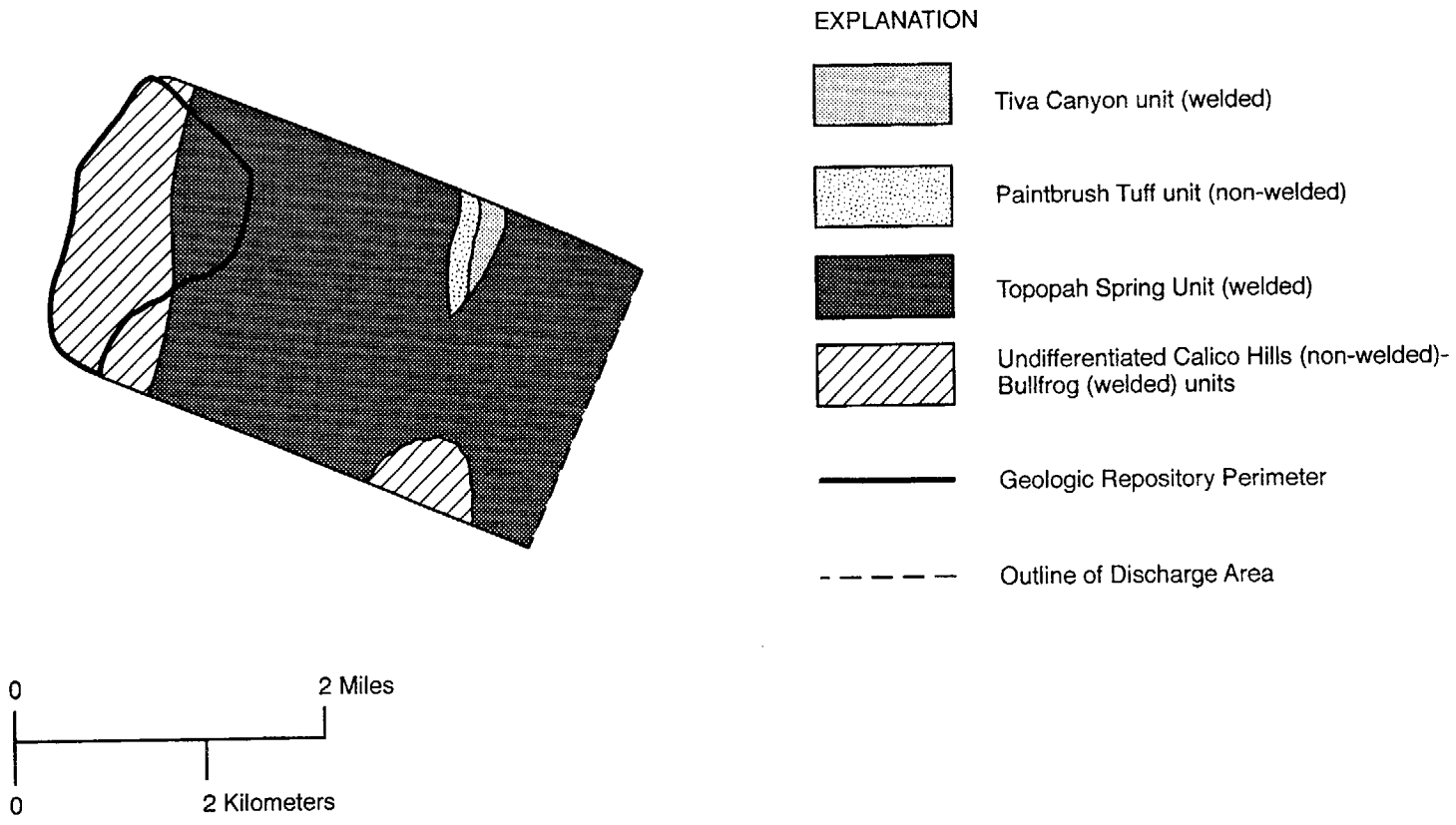

Figure 4–8 Depiction of changes, in hydrogeologic units, along the surface of the water table, under pluvial conditions (water-table rise of 100 meters) that was used for the saturated zone model

Table 4-8 Length (in Kilometers) of Hydrogeologic Unit Sequences along the Saturated Flow Paths for Each of the Seven Repository Sub-Areas (Pluvial Conditions)

Hydrogeologic Unit	*Sub-Area 1*	*Sub-Area 2*	*Sub-Area 3*	*Sub-Area 4*	*Sub-Area 5*	*Sub-Area 6*	*Sub-Area 7*
From the Water Table below the Repository							
Calico Hills[a]	—	0.38	0.28	0.90	1.22	0.90	0.10
Topopah Spring	3.05	3.65	—	3.70	—	—	3.60
Paintbrush	0.15	0.16	—	—	—	—	0.18
Tiva Canyon	0.30	0.22	—	—	—	—	0.30
Calico Hills[a]	—	—	—	0.30	—	—	—
Topopah Spring	1.90	1.92	5.62	1.30	5.40	5.78	1.92
To the Accessible Environment							
Total Length	5.40	6.33	5.90	6.20	6.62	6.68	6.10

[a]Fractured properties of Calico Hills vitric and zeolitic tuff are assumed to be the same; therefore, no distinction is made, between the two, for the saturated paths that only consider fracture flow.

the IPA Phase 1 effort (see Codell *et al.*, 1992; pp. 54 and 57). Future work will need to consider spatial variability, transient flow conditions, and further site characterization information, to provide better estimates on the range of percolation.

The current analysis is evaluating both the integrated discharge of radionuclides and the radionuclide dose. The calculation of dose requires a determination of the concentration of radionuclides in the ground water. Attributes of the "outlet" boundary condition are critical in determining the volume of water crossing the accessible environment boundary for a given time period. This volume of water is determined by multiplying the water velocity times the total pore area at the discharge point or accessible environment. The assumptions used to determine these quantities involved a number of assumptions that are described below.

4.2.3.2.1 Discharge Area

The discharge area refers to the vertical thickness and the lateral extent over which the radionuclide plume arrives at the accessible environment boundary. (In the determination of concentration, it was assumed that the radionuclides were uniformly mixed over the discharge area.) It was assumed there was no transverse dispersion of radionuclides. Therefore, the width of the plume was the lateral width of the repository (Figure 4–9). (Ignoring transverse dispersion over the long times simulated should have the conservative effect of producing higher concentrations of radionuclides at the accessible environment.) The determination of the vertical thickness was based on the assumption all radionuclide transport in the saturated zone occurred in fractures. Therefore, the range for this sampled parameter was determined from estimates of the vertical extent of fracture zones near the surface of the water table.

The vertical extent of fracturing was based on the interpretation of packer pump tests for well J–13 and radiation tracer logs for drill holes G–4, H–1, H–3, H–4, H–5, H–6, UE25b#1, and UE25p#1. In all these interpretations the thickness of the high-production zones was identified. It was assumed that high-production zones resulted from fracturing. This hypothesis was supported by an examination of fracture-hole data. In reaching interpretations of production-zone thickness, when more than one interpretation seemed reasonable, both interpretations were included for input into the simulations. This analysis yielded production-zone-thickness interpretations from 6 meters to 401 meters and averaged 70.2 meters. Table 4–9 contains the results of this analysis (Benson *et al.*, 1983; Bentley *et al.*, 1983; Blankennagel, 1967; Craig, 1991; Craig *et al.*, 1983; Craig and Robison, 1984; Craig and Johnson, 1984; Lahoud *et al.*, 1984; Lobmeyer *et al.*, 1983; Lobmeyer, 1986; Rush, 1984; Rush *et al.*, 1983; Thordarson, 1983; Thordarson *et al.*, 1985; and Whitfield *et al.*, 1984 and 1985). Values from this table were used to define a range for the thickness of the discharge area.

4.2.3.2.2 Discharge Velocity

The discharge velocity was calculated using the fracture permeability and the hydraulic gradient. The fracture permeability (see Section 4.2.3.3) is an input parameter based on laboratory measurements of rock cores, whereas the gradient was determined based on examination of head measurements in the Yucca Mountain area. The gradient was assumed to be constant (.0026). This was considered to be acceptable, since the ground-water gradient has a small dip over much of this area. It was also assumed that the gradient was not affected by variation in percolation rates in the unsaturated zone. This assumption is supported by observations that present day ground-water gradients and water-table elevations under Yucca Mountain are probably caused by percolation in high-elevation recharge areas, rather than from water percolating through the unsaturated zone at Yucca Mountain. Admittedly, a long-term change in local percolation rates at Yucca Mountain should be accompanied by a change in percolation rates in the recharge areas. This in turn should cause a change in water levels and ground-water gradients at Yucca Mountain. However, this type of detailed modeling and data is not presently available and therefore could not be incorporated into the analysis.

4.2.3.2.3 Discharge Radionuclide Concentrations

As discussed above, the product of the discharge area and the discharge velocity yielded the volume of water crossing the discharge point or the

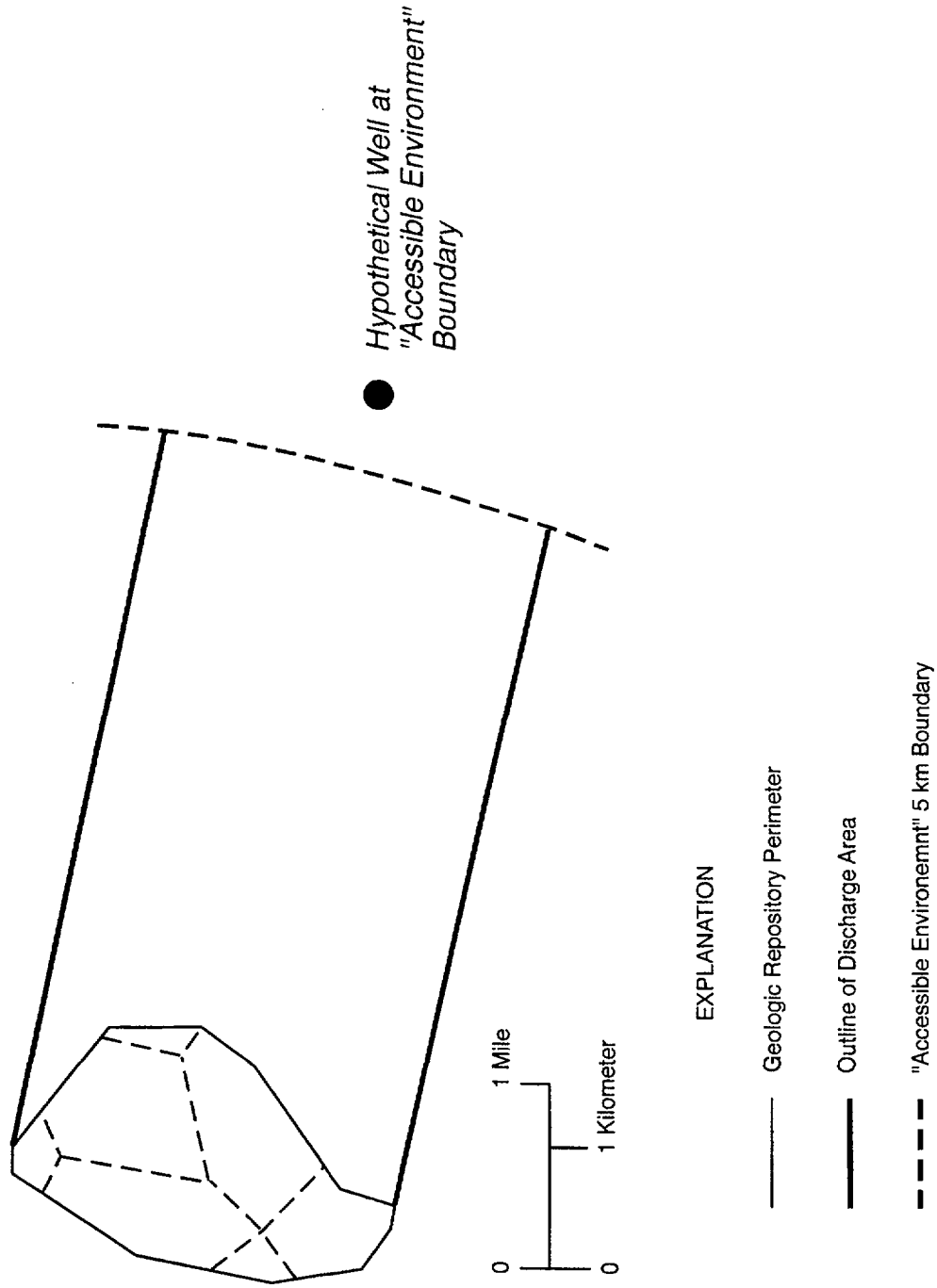

Figure 4–9 Depiction of the assumed radionuclide plume width used for calculating concentrations at a well located at the accessible environment boundary

Table 4–9 Permeability Zones Used to Determine the Range of Radionuclide Plume Depths for Transport in Fractures Within the Saturated Zone

Hole No.	*Hydrogeologic Units*	*Depth (m)*	*Thickness (m)*	*Test Flow Date*
G–4	Tram	890–900	10	1983
H–1	Prow Pass	572–563	81	1980
H–1	Prow Pass, Bullfrog	687–760	73	1980
H–1	Prow Pass	687–694	7	1980
H–1	Bullfrog	736–760	24	1980
H–3	Tram	809–841	32	1982
H–4	Prow Pass, Bullfrog, Tram	519–920	401	1982
H–5	Bullfrog	710–825	115	1982
H–5	Tram, Lava	1010–1090	80	1982
H–6	Bullfrog	616–631	15	1982
H–6	Tram	777–788	11	1982
J–13[a]	Topopah Spring	303.6–422.5	119	1963
UE25b#1	Calico Hills	471–490	19	1981
UE25b#1	Calico Hills, Prow Pass	471–620	149	1981
UE25b#1	Prow Pass	540–620	80	1981
UE25b#1	Bullfrog	799–810	11	1981
UE25b#1	Tram	875–881	6	1981
UE25p#1	Prow Pass	469–501	30	1983

[a]Interpretations of all tests from radioactive tracer logs, with the exception of Well J–13, which was from packer pump tests.

accessible environment. However, a minimum volume of ground water was used to dilute radionuclide concentrations at the discharge point. A minimum dilution volume of 1 million gallons/year was used in calculating radionuclide concentrations when the calculated discharge volume was less than this minimum amount. The 1 million gallons/year was considered consistent with the water usage of the population at the discharge point used to calculate doses. The minimum volumetric discharge amount has no effect on the calculation of integrated discharge for comparison with the U.S. Environmental Protection Agency's radiation protection standard—40 CFR Part 191[2] (*Code of Federal Regulations*, Title 40, "Protection of Environment").

4.2.3.3 Site Parameters

Site information is used to assign parametric values for the hydrologic models and the radionuclide transport models. The hydrologic parameters include permeability, matrix porosity, fracture apertures and density, and the van Genuchten parameters, whereas the transport parameters include dispersion length, K_d, and rock density. A discussion on the use of the site data and an application to the current modeling exercise is presented below, for each of the parametric topics previously listed.

4.2.3.3.1 Hydrologic Parameters

Peters *et al.* (1984) is the basis of hydrologic-parameter assignments in most of the recent modeling studies. The information reported in Peters *et al.* is the result of laboratory experiments, on tuffaceous core (fractured and unfractured), obtained from the Yucca Mountain site, used to measure (i.e., matrix porosity) and derive (i.e., permeability or conductivity, fracture aperture, and van Genuchten parameters) hydrologic parameters. The hydrologic-parametric values used in recent studies and the relevant values from the Peters' *et al.* report for hydrogeologic units present at Yucca Mountain are presented in Appendix B. Additionally, the parametric ranges and distributions used in the sensitivity analysis are reported in Appendix B.

Matrix Porosity: Matrix porosity values reported in Peters *et al.* (1984) were based on laboratory measurements. The parametric range for the sensitivity analysis used the wider range of either the reported results or plus and minus 25 percent of the mean value of the reported results. The assignment of a larger range than the reported results was done to more fully account for spatial variability and parametric uncertainty that may not be accurately reflected in the somewhat limited (two drill-holes) test results.

Matrix Conductivity: Saturated matrix conductivity values reported in Peters *et al.* (1984) were derived based on the laboratory measurement of volumetric flux (using a constant head method) and application of Darcy's Law. The wider range of either the reported results or of plus and minus 50 percent of the mean value reported in Peters *et al.* was used to represent the variability of the parameter in this analysis. As with the matrix porosity, a broader range was used to compensate for the limited data over the Yucca Mountain site.

The range in hydrologic measurements using small drill cores does not account for spatial variability within a hydrogeologic unit. The assignment of a hydraulic conductivity for a specific hydrogeologic unit needs to account for the correlation length of hydraulic conductivity over the thickness of a particular unit. Geostatistical analyses reported in the IPA Phase 1 effort (Codell *et al.*, 1992; p. F–1) indicated that there was no apparent spatial correlation of the core data for saturated hydraulic conductivity beyond the minimum separation distance of 10 meters. A correlation distance of 10 meters was assumed for the current analysis, to determine a range in hydraulic conductivity for each hydrogeologic unit.

A representative conductivity for a hydrogeologic unit was calculated, based on the number of correlated lengths present in a given unit (see

[2]Currently, a revised set of standards specific to the Yucca Mountain site is being developed in accordance with the provisions of the Energy Policy Act of 1992. The Energy Policy Act of 1992 (Public Law 102–486), approved October 24, 1992, directs NRC to promulgate a rule, modifying 10 CFR Part 60 of its regulations, so that these regulations are consistent with EPA's public health and safety standards for protection of the public from releases to the accessible environment from radioactive materials stored or disposed of at Yucca Mountain, Nevada, consistent with the findings and recommendations made by the National Academy of Sciences, to EPA, on issues relating to the environmental standards governing the Yucca Mountain repository. It is assumed that the revised EPA standards for the Yucca Mountain site will not be substantially different from those currently contained in 40 CFR Part 191, particularly as they pertain to the need to conduct a quantitative performance assessment as the means to estimate postclosure performance of the repository system.

Figure 4–10) and the variability in the parameter. To develop a range for the representative conductivity, 100 random samples were generated for each correlated length within an individual unit (for simplicity, the number of correlation lengths in a given unit was based on the smallest unit thickness in Table 4–5; for example, the Topopah Spring unit has 6 correlation lengths over the 60-meter length). The sampling range used for the 100 random samples was based on the parameter variability described above. Table 4–10 presents the resulting matrix representative conductivity ranges and the supporting input values.

Matrix Characteristic Curves: The parameters that describe the behavior of the fluid flow under partially saturated conditions were obtained (Peters *et al.*, 1984) by fitting water-retention data to the following form (Equation 4–1) of the van Genuchten equation:

$$S = (S_S - S_r)\left[\frac{1}{1 + |\alpha\, h|^{\beta}}\right]^{(1-1/\beta)} + S_r \quad , \qquad \textbf{(4–1)}$$

where:

S	=	saturation;
S_s	=	saturation at full saturation;
S_r	=	residual saturation;
h	=	pressure or suction;
α	=	fitting parameter; and
β	=	fitting parameter.

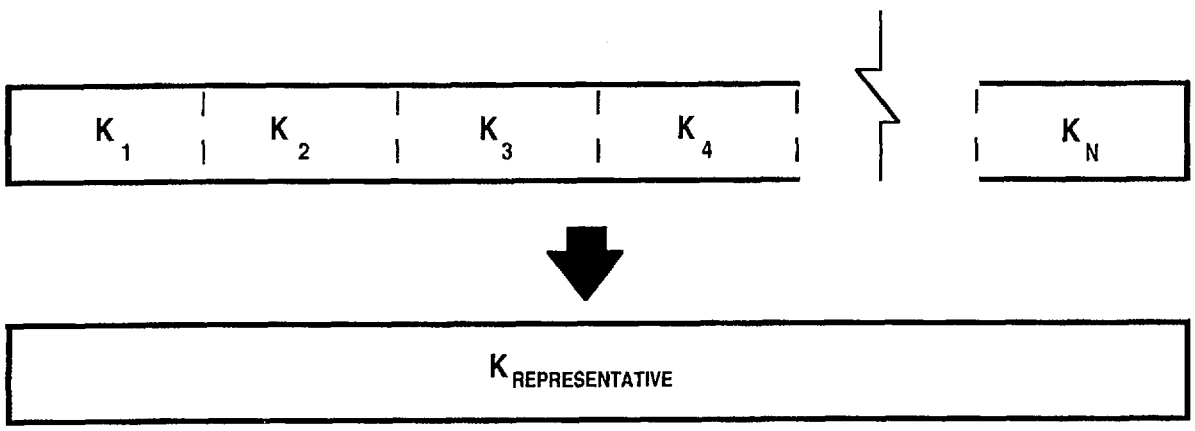

$$\frac{N}{K_{REPRESENTATIVE}} = \sum_{J=1}^{N} \frac{1}{K_J}$$

where:

N is the total number of correlation lengths present in the hydrologic unit

K_J is the conductivity value appropriate over one correlation length

Figure 4–10 Graphical representation of the correlation length of a hydrogeologic unit and its relationship to the calculation of a representative conductivity

Table 4–10 Matrix Representative Conductivities and Permeabilities (Permeabilities Given in Brackets) for the Indicated Hydrogeologic Units and the Values Used to Calculate the Representative Values Based on 100 Data Realizations and the Calculational Approach Presented in Figure 4–10

Hydrogeologic Unit	*Data Range*[a] *(mm/yr)*	*Number of 10 meter Correlation Lengths*	*Representative Range (mm/yr) [m²]*
Topopah Spring (welded)	.04 to 1.2	6	0.11 to .36 [3.6×10^{-19} to 1.2×10^{-18}]
Calico Hills (vitric, non-welded)	820. to 9,100.	2	1.2×10^{3} to 6.1×10^{3} [3.9×10^{-15} to 2.0×10^{-14}]
Calico Hills (zeolitic, non-welded)	7.6×10^{-4} to 5.0	4	.004 to .21 [1.3×10^{-20} to 6.7×10^{-19}]
Prow Pass (welded)	40. to 440.	2	58.0 to 300. [1.9×10^{-16} to 9.6×10^{-16}]
Upper Crater Flat (non-welded)	0.6 to 14.	6	1.6 to 4.6 [5.1×10^{-18} to 1.5×10^{-17}]
Bullfrog (welded)	72. to 200.	10	110.0 to 140. [3.5×10^{-16} to 4.4×10^{-16}]
Middle Crater Flat (non-welded)	0.6 to 14.	4	1.3 to 4.8 [4.1×10^{-18} to 1.6×10^{-17}]

[a]Based on actual ranges reported in Peters *et al.* (1984).

The two fitting parameters (α and β) control the shape of the characteristic curves (variation of saturation versus pressure, and variation of conductivity versus pressure or saturation) for unsaturated flow. These two parameters can physically be related to the size and distribution of pore space (larger pores will desaturate before smaller pores). A narrow distribution of pore space will result in desaturation occurring over a very small pressure range and thus will exhibit a relatively steep characteristic curve. A second van Genuchten equation (van Genuchten, 1980) based on the method of Mualem (1976) was used to represent the relationship of the conductivity and saturation, assuming the applicability of the desaturation curve (Equation 4–1) fitting parameters to the conductivity curve (Equation 4–2).

$$K_r = \sqrt{S_e}\left[1-\left(1-(S_e)^{\frac{1}{\lambda}}\right)^{\lambda}\right]^2 \quad \text{, and} \qquad \textbf{(4–2)}$$

$$S_e = \frac{S - S_r}{S_s - S_r} \quad , \qquad \textbf{(4–3)}$$

where:

S = saturation;
S_s = saturation at full saturation;
S_r = residual saturation;
S_e = effective saturation;
K_r = relative conductivity; and
λ = van Genuchten fitting parameter ($1 - 1/\beta$).

For this analysis, saturations were derived from flux considerations, using Equation 4–2; therefore, only the fitting parameter β was sampled. The parametric ranges for β were based on a 25 percent increase and decrease of values reported in Klavetter and Peters (1986) and supplemented by data ranges reported in Peters *et al.* (1984). Single values for the fitting parameter α were taken from Klavetter and Peters and were supplemented with average values from Peters *et al.*, where necessary. Finally, the residual saturation, S_r, for simplicity was assumed to be zero (this assumption is assumed to have a minimal effect on the analysis).

Fracture Porosity: Fracture apertures reported in Peters *et al.* (1984) were derived based on volumetric flow measurements and assuming the cubic law applied to steady-state laminar flow between parallel plates. These fracture apertures combined with fracture density were used to derive bulk-fracture porosity, as reported in Klavetter and Peters (1986). The bulk-fracture porosities were assumed to be constant in the current analysis.

Fracture Conductivity: Peters *et al.* (1984) reported on laboratory analyses of fractured tuff samples and the derivation of fracture properties based primarily on assuming the cubic law applied to steady-state laminar flow between parallel plates and determined the conductivity of a single fracture. Based on the Peters *et al.* analyses, Klavetter and Peters (1986) reported the fracture conductivities used to represent the initial range of unit properties. Bulk fracture conductivities (conductivity per unit area) were determined by multiplying the single fracture conductivity times the fracture area per unit area for each hydrogeologic unit. The wider range of either the reported results or plus and minus 50 percent of the mean values reported in Klavetter and Peters was used to represent the variability of the parametric range in this analysis. This was done to compensate for the limited data over the Yucca Mountain site and the lack of a range for conductivity, as reported in Klavetter and Peters.

The parametric range for a given hydrogeologic unit was subsequently used to calculate a representative permeability range for a given hydrogeologic unit, using the same procedure to account for spatial variability as was described above for matrix conductivity (see Table 4–11 for resulting representative ranges and supporting input values).

Fracture Characteristic Curves: It was assumed that unsaturated flow within fractures is governed by the same van Genuchten relationships described above for unsaturated matrix flow, in addition to the applicability of the steady-state laminar flow between parallel plates, as well as fracture apertures being sufficiently small so that capillary forces control fluid flow. The range for the fitting parameter β (see discussion under matrix characteristic curves above) was determined by increasing and decreasing by 25 percent the value reported in Klavetter and Peters (1986). Similar to the matrix value, the fitting parameter α was set to a single value corresponding to the value reported in Klavetter and Peters. Unlike the matrix values, which had separate values for each hydrologic unit, the fracture characteristic curves were the same for each unit.

4.2.3.3.2 Transport Parameters

Dispersion Length: The hydrodynamic dispersion process works to disperse contaminants along a flow path through mechanical dispersion and molecular diffusion. The dispersion length is a parameter used in transport equations to capture the spreading of a contaminant. This parameter, not without controversy, is a factor that compensates for a lack of knowledge of the conductivity field and therefore tends to exhibit a strong dependence on the scale over which it is estimated. For the current analysis, a range of 0.3 to 30.0 meters is used.

Retardation Factors: IPA Phase 1 used an element-specific retardation coefficient to represent the chemical reactions affecting radionuclide transport through the geologic medium. The IPA Phase 2 effort also uses a retardation coefficient type of approach (retardation coefficients are calculated from sorption coefficients or K_ds). A departure from the previous analysis is the assignment of K_ds to specific hydrogeologic units, when data were available to make the assignment. K_d values were selected, where appropriate, from Meijer (1990) and Thomas (1987). When information was not appropriate, values consistent with the Codell *et al.* report (1992) were used. The values were specific to the following hydrogeologic units:

Table 4–11 Fracture Representative Conductivities and Permeabilities (Permeabilities Given in Brackets) for the Indicated Hydrogeologic Units and the Values Used to Calculate the Representative Values Based on 100 Data Realizations and the Calculational Approach Presented in Figure 4–10

Hydrogeologic Unit	*Data Range*[a] *(mm/yr)*	*Number of 10 meter Correlation Lengths*	*Representative Range (mm/yr) [m²]*
Topopah Spring (welded)	20. to 100.	6	33. to 59. [1.1×10^{-16} to 1.9×10^{-16}]
Calico Hills (vitric, non-welded)	145. to 435.	2	170. to 360. [5.6×10^{-16} to 1.2×10^{-15}]
Calico Hills (zeolitic, non-welded)	145. to 435.	4	190. to 310. [6.2×10^{-16} to 9.9×10^{-16}]
Prow Pass (welded)	10. to 30.	2	12. to 25. [3.9×10^{-17} to 8.1×10^{-17}]
Upper Crater Flat[b] (non-welded)	145. to 435.	6	210. to 300. [6.7×10^{-16} to 9.8×10^{-16}]
Bullfrog[c] (welded)	10. to 30.	10	15. to 20. [4.9×10^{-17} to 6.4×10^{-17}
Middle Crater Flat[b] (non-welded)	145. to 435.	4	190. to 310. [6.2×10^{-16} to 9.9×10^{-16}]

[a]Based on wider range of either the actual range or plus and minus 50 percent of the mean value, as reported in Klavetter and Peters (1986).
[b]Based on Calico Hills.
[c]Based on Prow Pass.

Topopah Spring Member of the Paintbrush Tuff (Tpt); Calico Hills non-welded vitric (CHnv); Calico Hills non-welded zeolitic (CHnz); Prow Pass Member (PP) of the Crater Flat Tuff (Tcp); and Bullfrog Member (BF) of the Crater Flat Tuff (Tcb).

The K_d values for the matrix are presented in Appendix B along with a discussion on how the K_d values for the matrix were derived from the Meijer (1990) and Thomas (1987) reports. A range for sensitivity analysis was developed by assuming a log-uniform distribution and increasing and decreasing the K_d values by one order of magnitude, to develop the ends of the distribution. Sorption was assumed not to occur in fractures, because of the conceptualization that flow will be fast relative to the rates of sorption reactions. Therefore, K_d values in the fractures were all set to zero.

K_d values were used to calculate retardation factors via the following formula:

$$R_f = 1.0 + \frac{\varrho(1-n)}{\Theta} \cdot K_d \quad , \qquad \textbf{(4–4)}$$

where:

R_f = retardation factor;
K_d = distribution coefficient;
Θ = moisture content;
ϱ = grain density; and
n = porosity.

4.2.4 Computational Model Description (Liquid Flow and Transport)

The computational model, for use in the total-system performance assessment (TPA) computer code, used for representing liquid flow and subsequent transport of radionuclides, was developed to gain insights into the following processes and concepts:

- Matrix versus fracture flow;
- Variation in hydrogeologic unit thicknesses between the repository and the water table;
- Transport in the saturated zone; and
- Variation in geochemical retardation between different hydrogeologic units.

The implementation of these processes and concepts into a computational module for the current analysis involved the development of a calculational strategy, selection and development of a computer program(s), and determination of site representation. All of these topics will be discussed in more detail, to provide a better understanding of the representation of liquid flow and radionuclide transport in the current analysis.

4.2.4.1 Computational Strategy

As has been discussed in prior sections (see Section 4.2.3), the flow in the unsaturated zone (between the repository and the water table) is assumed to be primarily in the vertical direction, whereas the flow in the saturated zone, near the water table, has been assumed to be primarily to the south-east. Thus the flow representations, for both the saturated and the unsaturated zones, were assumed to be 1–D, with differing hydrogeologic units for the seven repository sub-areas (see Figure 4–11). The seven repository sub-areas were selected based on a need to represent the variation in hydrogeology below the repository and use stratigraphic information for selected boreholes at the site (Figure 4–6). Therefore, there are seven repository sub-areas, each connected to its own unsaturated and saturated zone hydrogeolgic sequences, similar to the representation presented in Figure 4–6.

The hydrogeologic sequences associated with the seven repository sub-areas define the flowpaths that are to be analyzed. These flowpaths are described as 1–D segments, because in part, of the 1–D nature of the flow and a calculational need for efficient simulation approaches that would be suitable to the numerous simulations that are required for sensitivity and uncertainty analyses. It was anticipated that a simple depiction, which still retained some realism with respect to site description, would be necessary for reasonable simulation times.

Additionally, the horizontal diversion of unsaturated flow, at the interface between hydrogeologic units with contrasting flow properties, and the transfer of liquid water, between fractures and matrix in the unsaturated zone, are two other aspects of unsaturated flow that have the potential to be computationally very demanding. Therefore, special consideration was given to the computational approach used to deal with these two issues. Rather than solve the flow equation explicitly, it was decided to use a "table look-up" (discussed below under computer program development) procedure to account for flow diversion above the repository and the interaction between matrix and fracture flow in the unsaturated zone.

4.2.4.2 Selection and Development of Computational Model(s)

The flow paths are assumed to be 1–D; therefore, the determination of the total amount of fluid flux in a given flow path and the partitioning of flux between the fracture and matrix is crucial. The *NEFTRAN II* (Olague *et al.*, 1991) computer program was selected to simulate liquid flow and radionuclide transport because of its ability to accommodate saturated and unsaturated flow and radionuclide transport, using a minimum amount of computer time. However, to account for the diversion of flow and transfer of fluid between the fractures and the matrix, a pre-processor was developed to determine the total incoming flux for each repository sub-area and the distribution of fracture versus matrix flow for each hydrogeologic unit present.

A detailed description of the pre-processor is required to fully understand the manner in which *NEFTRAN II* is implemented for the current

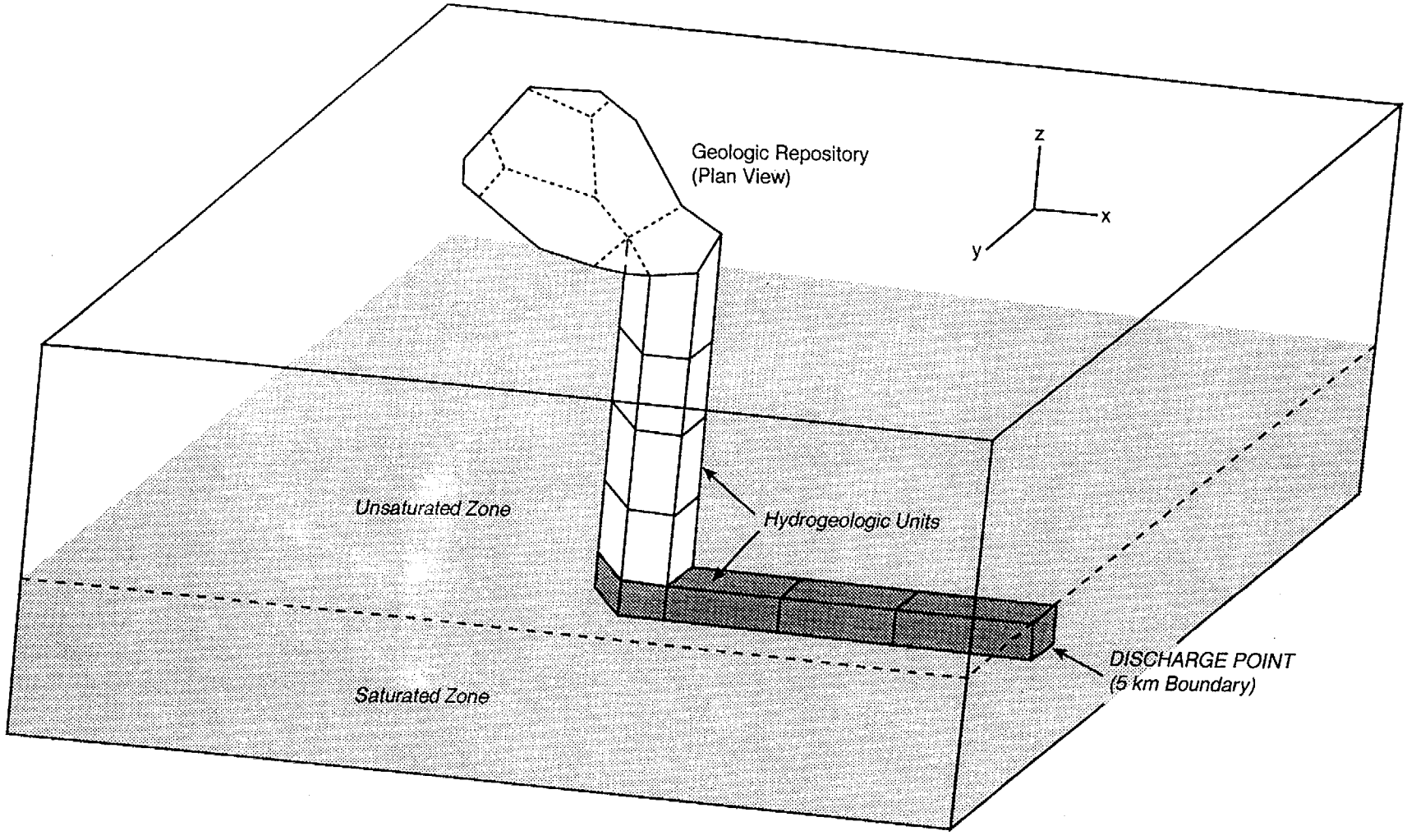

Figure 4–11 Illustration of a representative flow path for a sub-area of the repository, assuming one-dimensional flow in both the saturated and unsaturated zones

analysis. The pre-processor, hereafter referred to as *FLOWMOD*, performs the following primary functions:

- Determination of the areal flux;
- Determination of fracture flow; and
- Determination of retardation factors.

Determination of Areal Flux: The distribution of recharge at the repository depth is anticipated to have a degree of variation because of the tilting of the bedding planes, variation in hydraulic properties, and the amount of recharge. To quantitatively estimate the spatial distribution of percolation, a series of two-dimensional (2–D) simulations were conducted to develop an interpolation table for use within *FLOWMOD*. The 2–D simulations were performed using the *DCM3D* computer program (Updegraff *et al.*, 1991) and made use of the cross-sectional stratigraphy depicted in Figure 4–4 and parametric values (see Table 4–12) found in Klavetter and Peters (1986). *DCM3D* is a dual-continuum unsaturated flow simulator that represents liquid flow in fractures and matrix as separate but connected flow fields. The following flow equations are solved for the matrix and the fracture continuum, respectively:

$$C^m \frac{\partial p^m}{\partial t} = \nabla \cdot \left(\frac{k^m}{\mu} (\nabla p^m + \varrho g \nabla z) \right) - \Gamma + Q^m \,, \quad \textbf{(4–5)}$$

$$C^f \frac{\partial p^f}{\partial t} = \nabla \cdot \left(\frac{k^f}{\mu} (\nabla p^f + \varrho g \nabla z) \right) - \Gamma + Q^f \,, \quad \textbf{(4–6)}$$

where:

p^m = water pressure in the matrix continuum;
p^f = water pressure in the fracture continuum;
C^m = specific storage coefficient of the matrix continuum;
C^f = specific storage coefficient of the fracture continuum;
k^m = permeability of the matrix continuum (dependent on saturation);
k^f = permeability of the fracture continuum (dependent on saturation);
Q^m = volumetric source term for the matrix continuum;
Q^f = volumetric source term for the fracture continuum;
Γ = fracture to matrix transfer term;
ϱ = water density;
μ = viscosity of water;
g = gravitational coefficient;
z = z-direction distance; and
t = time.

A depiction of the hydrogeologic units and the types of boundary conditions applied to the cross-section is presented in Figure 4–12. Unit properties were assumed to be homogenous and isotropic for the all the cross-section simulations. To examine the spatial variation of the percolation, a number of steady-state simulations were performed over a range of percolation rates (.01 to 10.0 millimeters/year). The spatial distribution of recharge at the repository level resulting from these simulations was then used to develop a table (see Table 4–13) which was used to interpolate total flux amounts for each of the seven repository sub-areas (see Figure 4–6). Although this is a simple representation it accounts for a measure of flow diversion that is anticipated to occur for higher flux values. Future work will need to examine this phenomenon with more detailed modeling, which can take into account continuing site characterization activities (e.g., characterization of spatial variability of hydrologic properties, and location of and further understanding of the hydrologic significance of structures like major fracture zones or faults as sources of focused recharge).

Determination of Fracture Flow: The partitioning of fluid flux between the matrix and the fractures is dependent on a number of factors such as the total flux, hydraulic properties of the matrix and fractures, and spatial and temporal heterogeneities. For the present analysis, no attempt was made to account for the effects of spatial and temporal heterogeneities. The current analysis does account for the differences in hydrologic properties, between the fractures and the matrix, and the dependence of these properties on the flux. The sensitivity analysis required an efficient means to calculate fluid flow. Therefore a table interpolation approach was implemented within *FLOWMOD*. The interpolation table used in

Table 4–12 Hydrogeologic Parameters Used for Simulating Two-Dimensional Flow (see Figure 4.12) with *DCM3D*, to Analyze the Spatial Distribution of Percolation at the Repository Depth

Hydrogeologic Unit		*Permeability (m^2) [conductivity, mm/yr]*	*Porosity*	*Characteristic Curve–Fitting Parameters*		*Transfer Factor[a] (m^2) [No. Fractures]*
				α *(1/m)*	β	
Tiva Canyon (welded)	M[b]	9.7×10^{-19} [0.30]	.08	8.2×10^{-3}	1.6	N/A
	F[c]	5.5×10^{-16} [170.]	1.4×10^{-4}	1.3	4.2	1.6×10^{-15} [20]
Paintbrush (non-welded)	M	3.9×10^{-14} [1.2×10^{4}]	.40	1.5×10^{-2}	6.9	NA
	F	1.6×10^{-15} [490.]	2.7×10^{-5}	1.3	4.2	1.6×10^{-13} [1]
Topopah Spring (welded)	M	1.9×10^{-18} [0.6]	.11	6.0×10^{-3}	1.8	NA
	F	1.9×10^{-16} [59.]	1.1×10^{-4}	1.3	4.2	4.4×10^{-14} [24]
Calico Hills (non-welded, zeolitic)	M	2.0×10^{-18} [.06]	.28	3.0×10^{-3}	1.6	NA
	F	9.4×10^{-16} [290.]	4.6×10^{-5}	1.3	4.2	7.2×10^{-17} [3]

[a]Transfer factor based on assumption of regular planar fractions (equals $4n^2k_m$, where n is the number of fractures and k_m is the matrix permeability).
[b]Matrix.
[c]Fracture.

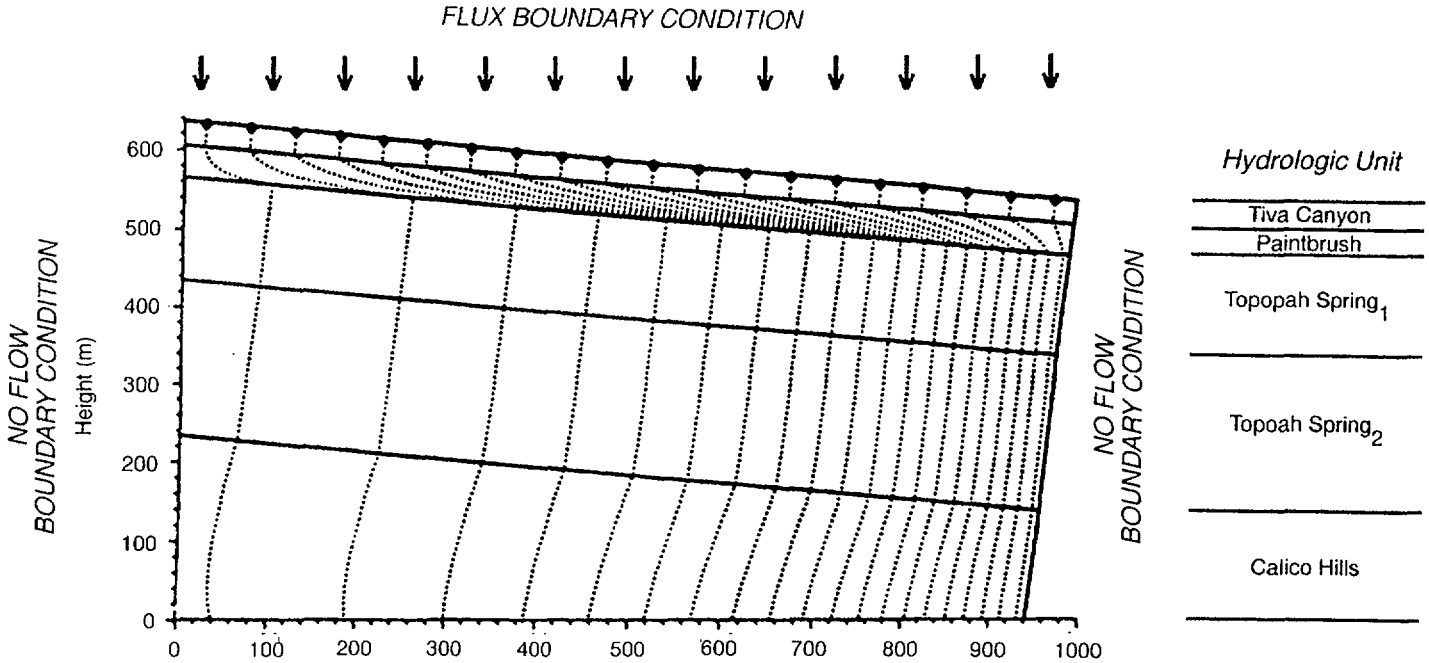

Figure 4–12 Depiction of the hydrologic units and boundary conditions used to evaluate the spatial variation of percolation at the repository depth

Table 4–13 Distribution of Percolation for the Seven Repository Sub-Areas, as Depicted in Figure 4–6

Surface Infiltration (mm/yr)	*Percolation at Repository Depth (mm/yr) for Each Sub–Area*		
	Sub–Areas 1 and 3	*Sub–Area 2*	*Sub–Areas 4, 5, 6, and 7*
0.01	0.01	0.01	0.01
0.05	0.06	0.05	0.04
0.10	0.13	0.09	0.07
0.20	0.26	0.18	0.13
0.30	0.38	0.25	0.18
1.00	1.25	0.80	0.60
2.00	2.25	1.80	1.60
10.0	10.5	9.80	9.50

determining the fraction of fluid flow was based on 1-D flow simulations, using *DCM3D*.

DCM3D was used to simulate 1-D unsaturated zone flow in a dual porosity medium (one fracture continuum and one matrix continuum) for a range of percolation rates. Steady-state flow was modeled for each of the hydrogeologic units, to determine the fraction of the total flow that was in the matrix as a percentage of the saturated conductivity of the matrix. A table, within *FLOWMOD*, was constructed for each unit, to determine the fraction of flow in the matrix. The table expressed the amount of matrix flow and the total flow as a fraction of the saturated conductivity of the matrix (see Table 4-14). The dimensionless aspect of the table allowed the same table to be used throughout the sensitivity analysis, where both the saturated conductivity and the percolation were sampled parameters. The table interpolation procedure determines the fraction of the total flow in the matrix. It was assumed that the remaining flow was in the fractures.

Retardation Factors: The retardation parameter was initially discussed in Section 4.2.3.3, under transport parameters. The retardation parameter is calculated within *FLOWMOD*, based on the K_d value (sampled in the sensitivity analysis); the grain density of the matrix (assumed to be a constant for each unit); porosity of the matrix (sampled in the sensitivity analysis); and the matrix moisture content (as mentioned previously, no retardation was assumed in the fractures, because, primarily, of the limited surface area of the fractures compared with the matrix). Of these values, the moisture content was the only value that required a calculation before determining the retardation factor. The moisture content for a given hydrogeologic unit was derived assuming a unit gradient in the unsaturated zone and using Equation (4-2). Retardation in the matrix above the water table (recall that transport in the saturated zone is assumed to occur entirely in the fractures and is thus unretarded) can vary because of a change of properties in the hydrogeologic units and changes in moisture content, caused primarily by changes in flux.

4.2.4.3 Site Representation

As discussed above, *FLOWMOD* does interpolations to determine the total flux entering each of the seven repository sub-areas and the distribution of flux in the matrix and the fracture continua. This information is then used by *FLOWMOD* to define a series of transport paths from each of the seven repository sub-areas to the accessible environment. The flow in a given hydrogeologic unit could be a combination of fracture and matrix flow; however, for computational simplicity, the fracture flow and the matrix flow are split into separate flowpaths. This approach for simulating the fracture and matrix flow precludes diffusive transport between fractures and matrix (i.e., matrix diffusion). This is likely to be a conservative assumption, because matrix diffusion is a potentially important retardation mechanism for fracture-dominated flow. Parametric uncertainty for the Yucca Mountain cases, and the possible importance of fracture coatings in reducing matrix diffusion, may diminish the importance of this phenomenon at the Yucca Mountain site.

Based on this approach, a flowpath over only one hydrogeologic unit would result in two transport paths (one for the matrix flow and one for the fracture flow). Because of the many hydrogeologic units that comprise the flowpaths from the repository to the accessible environment, there are a series of potential transport paths resulting from all the possible combinations of fracture and matrix flow (see Figure 4-13). *FLOWMOD* defines the transport paths for the flowpaths that have a non-zero flux and provides the input data necessary to simulate the transport of radionuclides with the *NEFTRAN II* computer program. Additionally, *FLOWMOD* distributes the repository releases from the source term according to the fraction of flux in a particular flowpath. For example, a flowpath that has 10 percent of the total flux will receive 10 percent of the source term. While this approach offers limited interaction between the fractures and matrix, it does account for the differing travel times and fluxes caused by fracture and matrix flow.

A common discharge point has been assumed (see Section 4.2.3.2) for all transport paths. Releases to the environment are obtained by summing all the individual releases from all the transport paths for each of the seven repository sub-areas.

Table 4–14 Variation of Matrix Flux Versus the Total Flux for Each of the Hydrogeologic Units Simulated at Yucca Mountain

Total and Matrix Flux (Expressed as Fraction of Saturated Conductivity, K_s) for the Indicated Hydrogeologic Units

	Topopah Spring	*Calico Hills (vitric)*	*Calico Hills (zeolitic)*	*Prow Pass*	*Upper Crater Flat*	*Bullfrog*	*Middle Crater Flat*
K_s (mm/yr)	.60	8,500.	.63	140.	1.0	140.	1.0
Total	.17	1.2×10^{-5}	.16	7.1×10^{-4}	.10	7.1×10^{-4}	.10
Matrix	.17	1.2×10^{-5}	.16	7.1×10^{-4}	.10	7.1×10^{-4}	.10
Total	.50	3.5×10^{-5}	.48	2.1×10^{-3}	.30	2.1×10^{-3}	.30
Matrix	.50	3.5×10^{-5}	.48	2.1×10^{-3}	.30	2.1×10^{-3}	.30
Total	.83	5.9×10^{-5}	.79	3.6×10^{-3}	.50	3.6×10^{-3}	.50
Matrix	.83	5.9×10^{-5}	.79	3.6×10^{-3}	.50	3.6×10^{-3}	.50
Total	1.25	8.8×10^{-5}	1.20	5.4×10^{-3}	.75	5.4×10^{-3}	.75
Matrix	.97	8.8×10^{-5}	.92	5.4×10^{-3}	.75	5.4×10^{-3}	.75
Total	1.67	1.2×10^{-4}	1.60	7.1×10^{-3}	1.00	7.1×10^{-3}	1.00
Matrix	.97	1.2×10^{-4}	.92	7.1×10^{-3}	.98	7.1×10^{-3}	.98
Total	3.33	2.4×10^{-4}	3.20	.01	2.00	.01	2.00
Matrix	.97	2.4×10^{-4}	.94	.01	.99	.01	.99
Total	6.67	4.7×10^{-4}	6.30	.03	4.00	.03	4.00
Matrix	.97	4.7×10^{-4}	.94	.03	.99	.03	.99
Total	11.67	8.2×10^{-4}	11.10	.05	7.00	.05	7.00
Matrix	.97	8.2×10^{-4}	.94	.05	.99	.05	.99
Total	16.70	1.2×10^{-3}	15.90	.07	10.00	.07	10.00
Matrix	.97	1.2×10^{-3}	.94	.07	.99	.07	.99

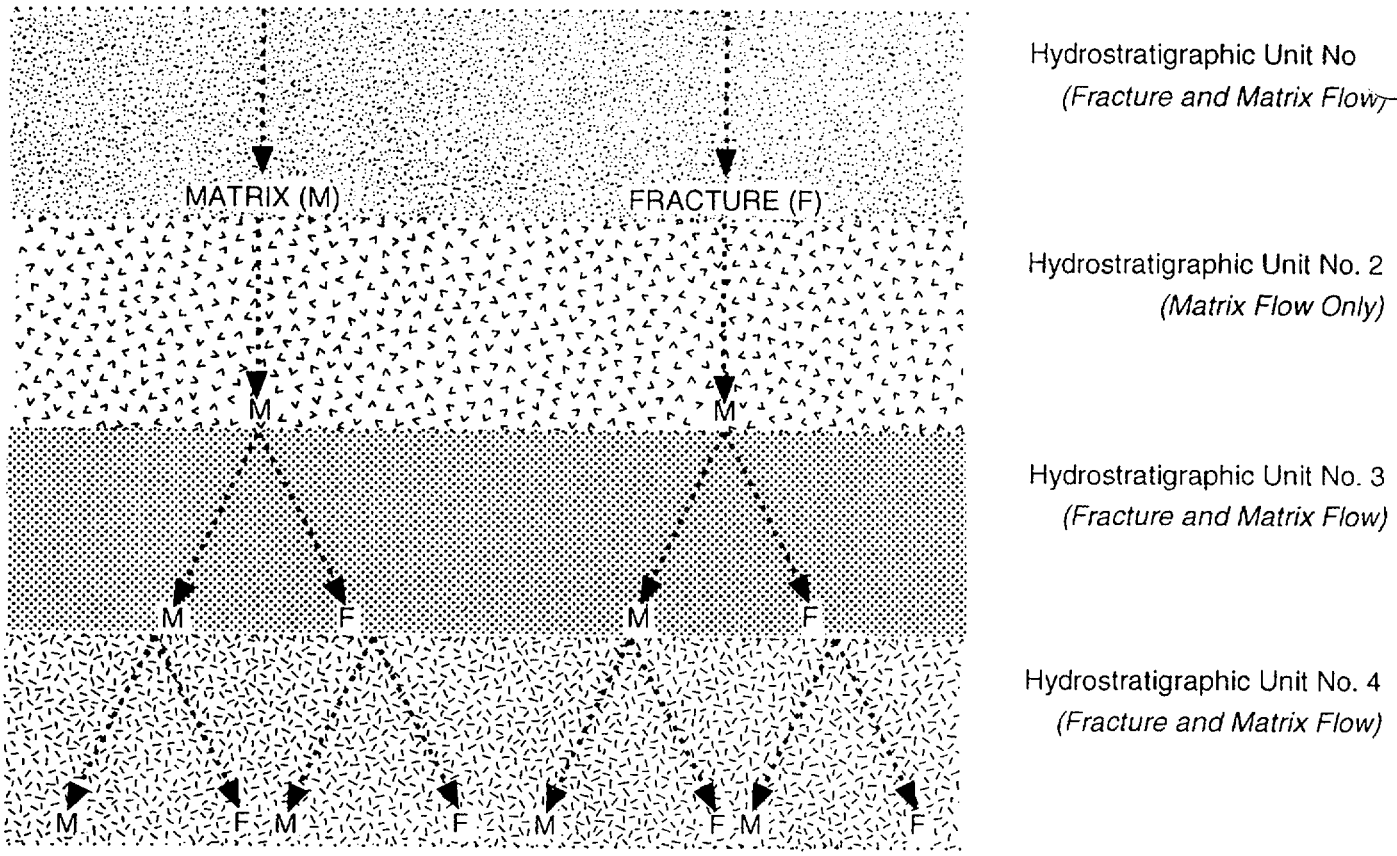

Figure 4–13 Depiction of the multiple transport paths, based on four different hydrogeologic units and the indicated combinations of fracture and matrix flow

4.3 Flow and Radionuclide Transport Module for Gaseous Releases

The elevated topography and unsaturated fractured stratigraphy of Yucca Mountain favor the existence of gas flows driven by thermal gradients. Such flows have been observed in relatively shallow holes (Weeks, 1987). Thermal gradient driven flows are expected to exist in the vicinity of the repository, particularly under the influence of the repository heat load. Such flows have been predicted by various models and researchers.

The conceptual and mathematical gas flow model chosen for IPA Phase 2 was the formulation of the steady-state flow equation as originally presented by Steven Amter and Benjamin Ross (Amter and Ross, 1990) of Disposal Safety Inc. (DSI), a DOE consultant. Because gas flow is expected to have relatively fast transients in comparison to changes in temperature gradients through conductive heat transfer, one can evaluate a series of steady-state flows at snapshots in time, as the temperature field develops, to emulate transient flow conditions. This was a major deviation in NRC's approach from the earlier DSI steady-state calculations. The NRC staff wrote its own computer code to solve the equations of flow, and in the process, made other significant modifications and improvements to the DSI model.

4.3.1 Governing Equations

The DSI model is based on single-phase flow of moist air in Yucca Mountain. The following assumptions are made in the derivation (see Amter and Ross, 1990):

- The gas behaves as an ideal gas.
- The gas is saturated with water vapor.
- Changes in partial pressure of water vapor are accommodated by changes in gas composition, with the total pressure remaining nearly constant.
- Gas viscosity is independent of pressure.

- All gas-filled voids in the matrix may be treated as a single porosity on time scales of years.
- The unsaturated zone stays at constant saturation.

The system is then described by three equations, a volume balance, a constitutive relation, and Darcy's Law. The full equation describing the system is then:

$$\nabla^2 h - m\nabla T \cdot \nabla h + \frac{1}{h_a}(\nabla h)^2 + \left[\frac{1}{T} + g\frac{\Omega_a - \Omega_v}{RT}\frac{dh_v}{dT} + \varrho'\left(\frac{1}{T} + m\right)\right]\frac{dT}{dz} + \left[\frac{1-\varrho'}{h_a} - \frac{g\,\Omega_a}{RT}\right]\frac{\partial h}{\partial z} - \frac{g\Omega_a}{RT} - \frac{\varrho'}{h_a} + \frac{1}{k}\nabla k \cdot (\nabla h - \varrho'\hat{z}) = 0 \quad , \tag{4-7}$$

where:

$$\varrho' = \frac{g}{RT}(h_v\Omega_v + h_a\Omega_a) - 1 \quad ;$$

$$m = \frac{1}{\mu}\frac{\partial \mu}{\partial T} + \frac{1}{T} + \frac{1}{h_a}\frac{dh_v}{dT} \quad ;$$

$$h_v = \frac{P_v}{g\varrho_0} \quad ; \text{ and}$$

$$h_a = \frac{P_0}{g\varrho_0} + z + h - h_v \quad .$$

The term ϱ' is the buoyant density of the air using the concept of "freshwater head." This concept is used in calculating stratified flows in surface water and ground water when dealing with two fluids that have only a small difference in density (e.g., salt water and fresh water, or hot and cold water). The terms h_v and h_a are the vapor-pressure and air pressure heads respectively, in cm.

Constant terms are defined as:

Ω_a	=	molar weight of dry air (28.96 g mol^{-1});
Ω_v	=	molar weight of water vapor (18.02 g mol^{-1});
R	=	gas constant (8.3144×10^7 g cm^2 s^{-2} mol^{-1} °K^{-1});
g	=	acceleration of gravity (980 cm sec^{-2});
P_0	=	reference pressure (880,521 dyn cm^{-2}); and
ϱ_0	=	reference fluid density (.001007 g cm^{-3}).

Other terms are defined as:

T	=	Temperature (degrees Kelvin (°K) from an externally calculated temperature field);
P	=	total pressure (dyn cm^{-2});
P_v	=	vapor pressure (calculated for temperature) (dyn cm–2);
μ	=	fluid viscosity (g cm^{-1} sec^{-1});
k	=	intrinsic gas permeability (cm^2); and
z	=	elevation (cm)

Boundary conditions on Equation (4–7) are no-flow on the sides and the bottom, and atmospheric pressure on the surface. The DSI model rationalized that the sides were modeled as topographic valleys that are air divides, much as the centerline of the mountain is a ground-water divide. No-flow at the bottom boundary was chosen because of either low-permeability rock or the presence of liquid water that would effectively cut off the air flow.

The DSI model linearized certain terms in Equation (4–7) in order to simplify the solution, and also because DSI did not have the necessary relationships for temperature dependence programmed into their model. The terms dh_v/dT and $d\mu/dT$ were replaced by their linearized equivalents taken at a reference temperature of 300°K. The term m was evaluated only at the reference temperature. They also eliminated some of the terms of Equation (4–7) altogether, namely those containing $(\nabla h)^2$ and $\partial h/\partial z$. The terms containing ∇k were included only where there were permeability contrasts.

The no-flow boundary conditions were simulated by setting flux to zero across boundaries:

$$q \cdot \hat{n} = -\frac{g\varrho_0 k}{\mu}\left[\frac{\partial h}{\partial n} - \varrho'\hat{z}\cdot\hat{n}\right] = 0 \quad , \qquad \textbf{(4–8)}$$

where n is the unit vector normal to the boundary. They chose to satisfy Equation (4–8) by setting the head at adjacent boundary nodes, so that the terms within the brackets were zero.

In a later improvement to the model, DSI (Ross *et al.*, 1992) developed a formulation that included atmospheric lapse rate (linear decrease in temperature with elevation) to determine the free atmospheric heads. Considering the atmospheric lapse rate and assuming a constant mole fraction of water vapor at all elevations resulted in the equation:

$$P = P_{atm}\left[1 + \frac{\lambda z}{T_a}\right]^{\frac{\Gamma}{\lambda}} \quad , \qquad \textbf{(4–9)}$$

where:

P_{atm} = atmospheric pressure at $z = 0$;
λ = the atmospheric lapse rate;
T_a = the air temperature at $z = 0$;

and

$$\Gamma = \frac{g}{R}\left[\Omega_a + \eta\,\frac{P_v(T_a)}{P_{atm}}(\Omega_v - \Omega_a)\right] \quad , \qquad \textbf{(4–10)}$$

where η is the relative humidity outside the mountain at $z = 0$.

This formulation was also adopted for IPA Phase 2.

DSI originally used a node-centered, explicit finite difference equation with Gauss-Siedel acceleration to solve the head field. Once the head field was solved, the velocity field was calculated from Darcy's Law, and particle tracking was used to calculate travel times from the repository to the earth's surface.

4.3.2 NRC Model

The goal of the IPA Phase 2 gas-flow-model development effort was to attempt to duplicate the DSI results and extend the model, if possible.

The NRC model improved on the original DSI model in several significant ways:

- Equation (4–7) was modeled with all terms except the one containing $(\nabla h)^2$ and $\partial h/\partial z$. Furthermore, several of the terms in Equation (4–7) were recast so that it was in a form more suitable for no-flow boundary conditions, using a block-centered finite difference scheme. The term:

$$\nabla^2 h + \frac{1}{k}\nabla k \cdot (\nabla h - \varrho'\hat{z}) \quad , \qquad \textbf{(4–11)}$$

expressed in two dimensions x and y, in relation to the downward unit vector, becomes:

$$\frac{1}{k}\left[\frac{\partial}{\partial x}\left(k\frac{\partial h}{\partial x}\right) + \frac{\partial}{\partial y}\left(k\frac{\partial h}{\partial y}\right)\right] - \frac{\varrho'}{k}\left[\frac{\partial k}{\partial x}\sin\theta + \frac{\partial k}{\partial y}\cos\theta\right] , \qquad \textbf{(4–12)}$$

where θ is the dip angle.

The finite difference model was set up in an orthogonal x–y grid, with the layers parallel to the y axis. The entire grid was tilted by the dip angle.

The advantage of the reformulation set up in Equation (4–12) is that the no-flow boundary condition can be expressed simply as zero permeability in the centered finite difference scheme.

- The NRC model did not linearize most of the terms, but instead included formulas for temperature dependency of h_v and viscosity. The relationship for vapor pressure was taken from the "Steam Tables" in *Thermodynamic Properties of Steam* (Keynan and Keyes, 1936). The relationship for viscosity was a quadratic-curve fit for dry air, with data coming from the *Handbook of Chemistry and Physics* (Weast, 1984). The finite-difference model was solved using an explici algorithm and Gauss-Seidel iteration, with ai acceleration factor.

- After initially testing its model, using the linear temperature profile developed by DSI, NRC decided to use a full 2–D temperature profile calculated from the equation for the time-dependent conduction of heat. Although, this model did not take multiphase processes into account, it did account for the growth of the isotherms as a function of time, and calculated the temperature profiles on the sides of the repository as well as above and below the repository.

Two forms of the temperature model have been used, to date. The first is a solution using Green's functions in a semi-infinite, uniform medium in two dimensions, with a fixed–temperature boundary condition at the earth's surface and an instantaneous heat source from a semi-infinite plane (Codell, 1984). A semi-infinite region was considered to best represent the repository; the isotherms will extend out great distances unaffected by boundaries, except at the surface and at contrasts in conductivity. The Green's function solution was for an instantaneous heat source. This was generalized to a time-dependent heat source, based on 10-year-old spent nuclear fuel using a convolution integral evaluated numerically with Simpson's rule quadrature. The geothermal gradient was added to the temperature calculated from the Green's function model. This model calculated temperatures for all locations needed by the flow model. Temperature gradients were calculated by finite-differencing of the nodal temperature.

Temperature distributions were also calculated using a semi-implicit finite difference model based on the Prickett-Lonnquist (Prickett and Lonnquist, 1971) model for aquifer drawdown. The advantage of this approach is that it lets the irregular surface boundary condition be represented explicitly, whereas the Green's function solution allowed the surface of the earth to be represented as flat, only. Another advantage is that the solution is no longer confined to uniform heat-transfer coefficients and heat capacities. The finite difference model also allows the simulation of the geothermal gradient more explicitly by input of a heat flux at the lower boundary of the model. A disadvantage of the finite difference model is that it is difficult to represent an infinite medium for heat conduction. This problem has been partially overcome by creation of a buffer zone around the computed area, to include a larger quantity of rock.

It must also be recognized that the DSI model has, thus far, been used to determine gas-flow pathways and travel times. The NRC model had to be capable of determining output flux of ^{14}C for dose calculations and the cumulative release for determining compliance with the performance requirements. This was accomplished by adding the following modifications:

- The capability to calculate the velocity fields for up to 10 different points in time after repository closing. This was done by providing a temperature input file with temperature distributions at up to 10 selected times and calculating the steady-state Darcy velocity field for each time. The particle tracing routine interpolated the velocity field tables through space and time. The tables were spaced at a few hundred years, for the first 1000, years and then by a few thousand years thereafter to more accurately reflect conditions during the initial period of rapid temperature change.

- A source of ^{14}C released within the engineered barrier system (EBS) in units of (curies/year) was provided to the model as input. In the particle-tracking routine, a fraction of the appropriate source term is attached to each particle released and the fraction remaining on that particle after radioactive decay is accumulated with other particles, according to the year in which the particle emerges into the atmosphere. This "bookkeeping" was required because particles released at different locations within the repository experience different travel times. The model approximates a continuous release from the repository by an instantaneous release of particles across the width of the repository, at the middle of discrete time intervals (every 50 years, for example).

- A file containing the calculated output flux (curies/year) is transferred as input to the dose-calculation model. The accumulated release over the performance assessment period is used as input to the CCDF, for that particular vector and scenario.

A logic diagram of the ^{14}C module is shown in Figure 4–14.

4.3.3 Application to Yucca Mountain

The gas-flow model was applied to Yucca Mountain using the simplified cross-section developed for the flow and transport-modeling tasks. The section was extended 600 meters on each side, to reach the natural no-flow boundaries needed to contain the entire flow field. This cross-section was further simplified by characterizing the stratigraphy as parallel layers at a 6° angle with the horizontal. The finite difference representation consists of 52 columns and 62 rows of nodes with DX = 50 meters and DY = 10 meters. The repository is 400 meters below the top of the land surface. The unsaturated stratigraphy was represented by five parallel layers, as follows, with their respective symbol and the assumed constant thickness in meters in parentheses: Tiva Canyon welded tuff (TCw, variable), Paintbrush non-welded tuff (PTn, 40 meters), Topopah Spring welded tuff (TSw, 340 meters), Calico Hills non-welded vitric tuff (CHnv, 50 meters), and Calico Hills non-welded zeolitic (CHnz, 60 meters). This representation of the repository cross-section is shown in Figure 4–15.

4.3.4 Parameters and Modeled Results

Ranges of the sampled parameters used to model gas transport at Yucca Mountain are shown in Table 4–15.

The values for bulk-fracture properties were determined through measurements of fracture aperature widths and counts of fractures per unit area (see Klavetter and Peters, 1986). As such, the accuracy is questionable. In addition, since there is no reduction in permeability because of moisture in the fractures, the staff has assumed that the full fracture conductivity is available for vapor flow. Also in the simulations, the two Calico Hills layers were treated as one layer and not separately sampled.

The temperature profiles for the simulation runs were determined from the means of the measured heat-transfer properties presented in the SCP (DOE, 1988a; Table 6–16). Only one temperature field was used for all gas-flow runs in the performance assessment simulations; however, as discussed later in this section, the effects of different thermal loadings on gas transport were also investigated using this model.

During the development of the model, runs were made with preliminary estimates of typical hydrologic parameters, to determine the sensitivity of the velocity field to the time varying temperature distribution. The permeabilities used for these calculations (in 10^{-16} square meters) were: 5.2 for Tiva Canyon (TCw); 16.0 for Paint Brush (PTn); 0.97 for Topopah Spring (TSw); and 9.7 for Calico Hills (CHn). The porosities and retardation coefficients were not used for the calculation of flux distribution. The results of the calculations are shown in Figures 4–16 to 4–19.

The vapor-flux distribution shown in Figure 4–16 is for vapor transport induced by the geothermal gradient alone, without the additional gradient created by the repository heat load. Most of the convective movement is contained in the upper layers of the stratigraphy, because of the higher permeability and the relief. Figure 4–17 shows vapor flux distribution at 500 years after permanent closure of the repository. This is near the time of highest thermal gradients in the host rock, and the greatest convective vapor movement is being induced. The vapor movement appears to be symmetric about the repository, implying that the heat load of the repository is the major influence at this time. Figure 4–18 shows vapor-flux distribution at 5000 years after repository closure. The magnitude of flux at the repository for 5000 years is about 20 percent of the flux for 500 years. The flux movement is still primarily influenced by the repository heat load, as shown by the arrows. Figure 4–19 shows fluxes at 10,000 years after permanent closure of the repository. The magnitude of flux at the repository for 10,000 years is about 10 percent of that for 500 years. The circulation pattern, however, is again starting to show the influence of topography and the geothermal gradient.

The gas-flow model also appears to be useful for investigating the effects of thermal loading. The same typical cross-section was used to compare gas travel times for a release at 500 years after closure for thermal loadings at areal power densities of 57 kilowatts (kW)/acre (the present

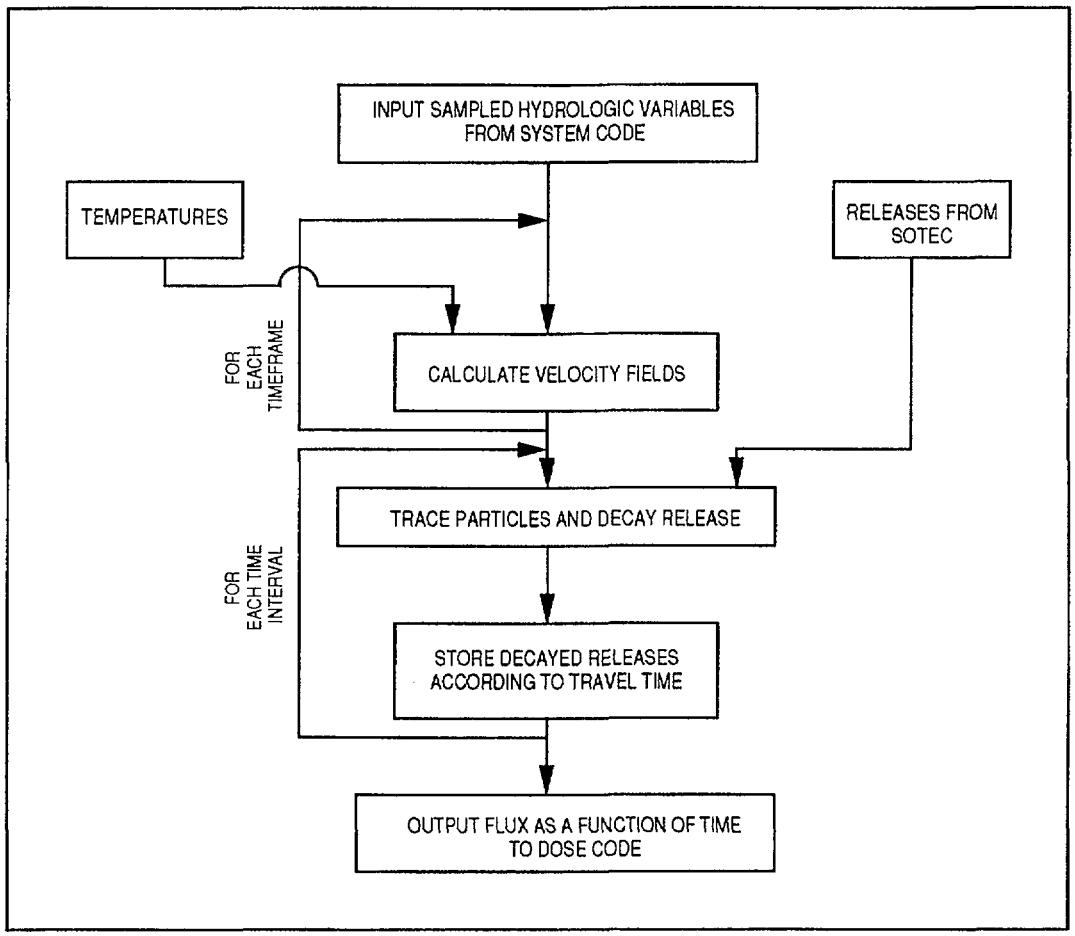

Figure 4–14 ^{14}C module logic diagram

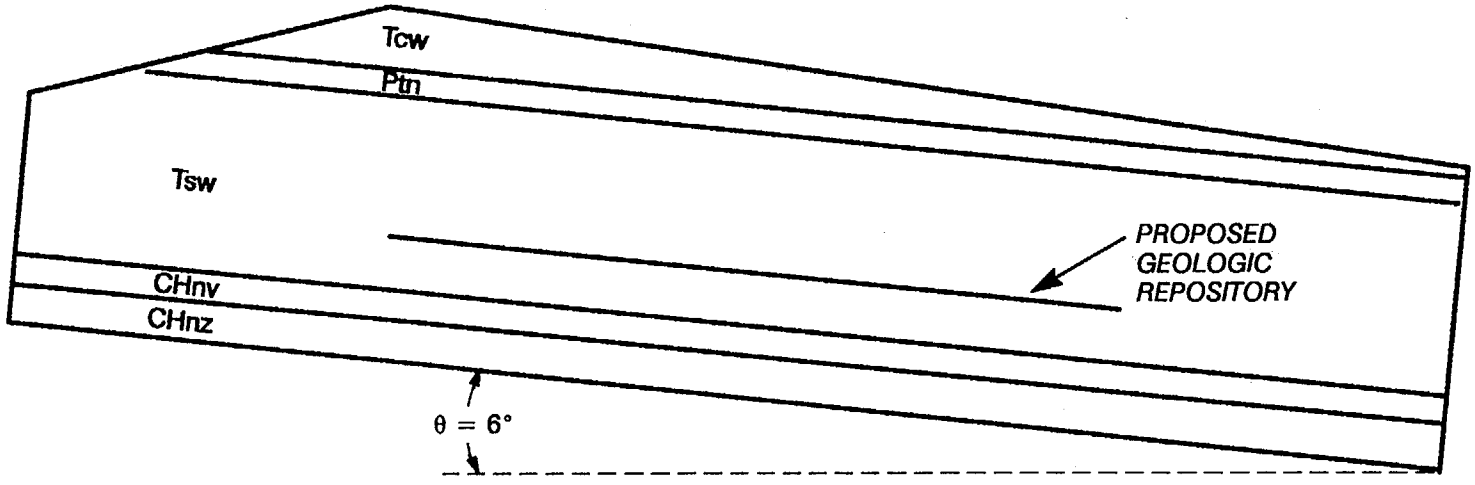

Figure 4–15 Modeled repository section (The hydrogeologic units depicted in Figures 4–15 through 4–22 are as follows: Paintbrush Tuff Members—Tiva Canyon welded unit (Tcw), Paintbrush non-welded unit (Ptn), and Topopah Spring unit (Tsw); and tuffaceous beds of the Calico Hills (non-welded vitric unit (CHnv) and non-welded zeolitic unit (CHnz).)

Table 4–15 Selected Hydrologic Parameters for Yucca Mountain

Stratigraphic Unit	*Permeability Range (m^2)*	*Porosity*	*Retardation Range*
Tiva Canyon (welded)	6.5×10^{-17} 5.5×10^{-15}	.00014	10 – 100
Paintbrush (non-welded)	1.6×10^{-16} 1.6×10^{-14}	.000027	10 – 100
Topopah Spring (welded)	3.2×10^{-17} 3.2×10^{-15}	.000041	10 – 100
Calico Hills (non-welded, vitric)	9.7×10^{-17} 9.7×10^{-15}	.000046	10 – 100
Calico Hills (non-welded, zeolitic)	9.7×10^{-17} 9.7×10^{-15}	.000046	10 – 100

design value[5]), 114 kW/acre and 28.5 kW/acre. The particle paths for these releases under the different loading conditions are the nearly vertical lines from the repository to the surface shown in Figures 4–20 to 4–22. The nearly horizontal lines that cross the particle paths are front lines that show the positions of particles along the different pathways at various times after release. Both porosity and geochemical retardation (assumed to be 10) were accounted for in the particle trackings. The actual average travel time for particles to reach the surface under the design loading condition of 57 kW/acre was 2100 years, resulting in an overall decrease because of radioactive decay of 22 percent of ^{14}C transport. The actual average travel time for a particle to reach the surface under the loading of 114 kW/acre was 980 years, resulting in an overall decrease of 11 percent. The actual average travel time for a particle to reach the surface under the loading of 28.5 kW/acre was 5900 years, resulting in an overall decrease of 55 percent.

A major assumption in the coupling of the source term model with the gas-transport model is that the ^{14}C moves directly from the waste package to the fractures in the host rock outside of the EBS. If the gas were to migrate first to the backfilled repository or even to pass through the repository on the way to the surface, travel times would be greatly increased because of the relatively large porosity of the backfill. Also, the fracture porosity of rock is used in the model, rather than the matrix porosity, which is much larger. The assumption is made that the gas stays in the fractures and does not migrate laterally on the way to the surface. It should be noted that if only 10 percent of the matrix porosity is available in the Topopah Spring unit for lateral migration, travel time through the unit would be increased by over three orders of magnitude. Although we consider our assumptions and our model to be conservative, we also consider that this assumed confinement of gas transport to the fracture, by possible fracture coatings, may be realistic.

[5]Kilowatts per acre is used in this report for easy comparison with the SCP rather than the metric equivalent of kilowatts per hectare.

4.4 Flow and Transport Auxiliary Analyses

Eleven auxiliary analyses conducted for this demonstration were performed to evaluate the appropriateness and limitations of various computational approaches and interpretations of data used in this study. These analyses are summarized below and discussed in detail in the appendices at the end of this document. They included: the evaluation of computer programs (*DCM3D* and *NEFTRAN II*); evaluation of the K_d assumption;

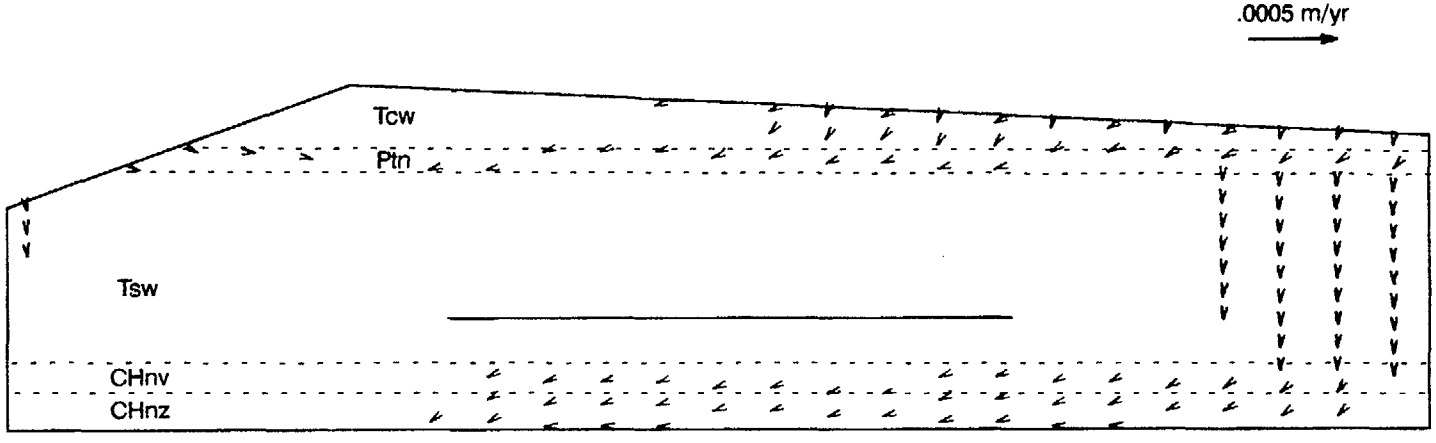

Figure 4–16 Vapor flux at ambient conditions

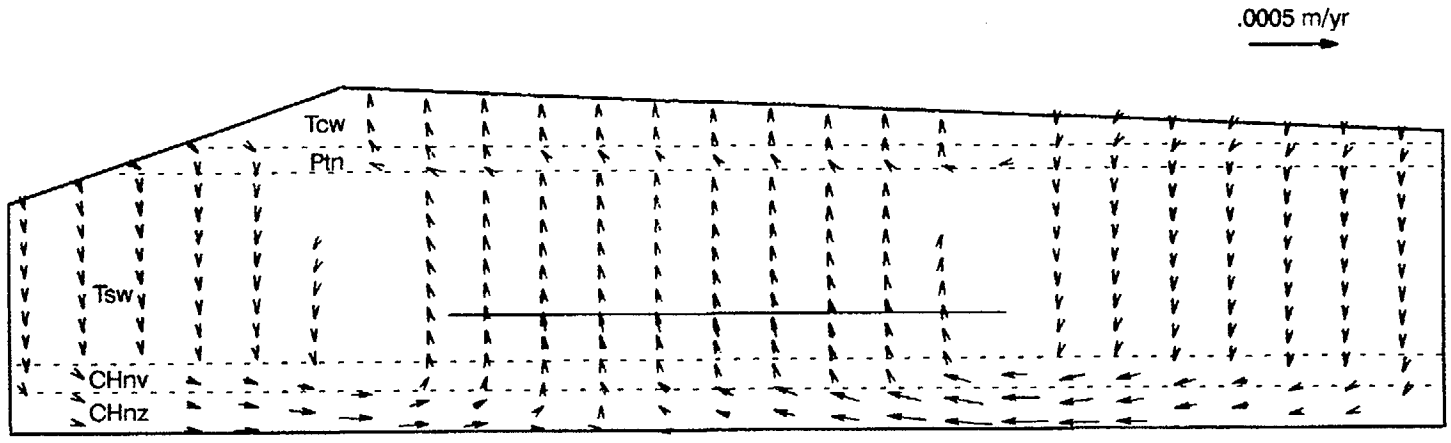

Figure 4–17 Vapor flux at 500 years after permanent closure of the geologic repository

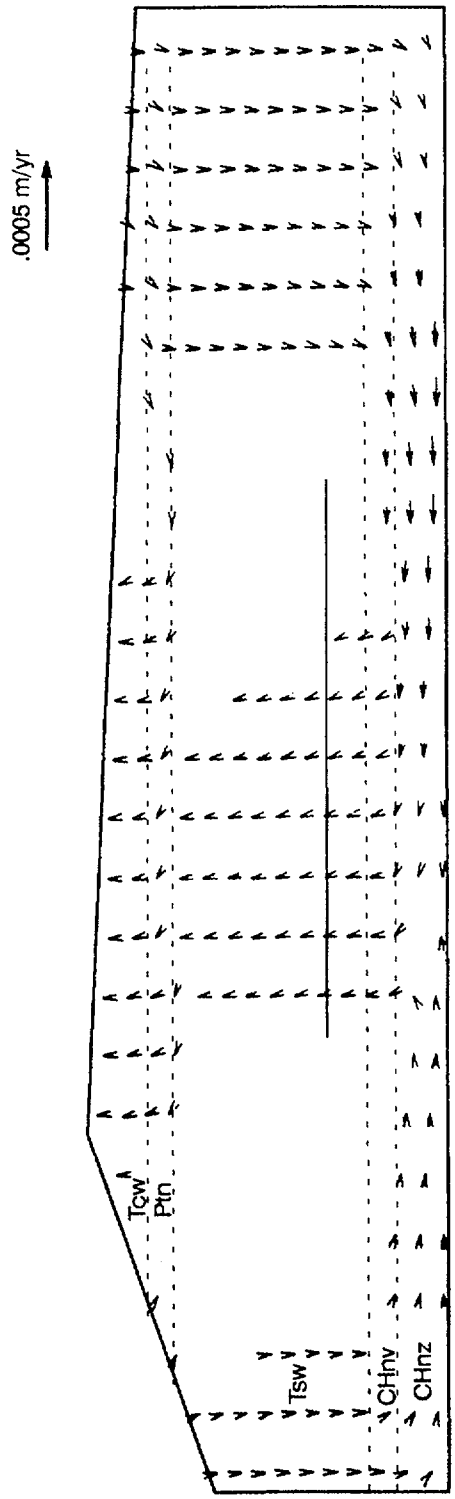

Figure 4–18 Vapor flux at 5,000 years after permanent closure of the geologic repository

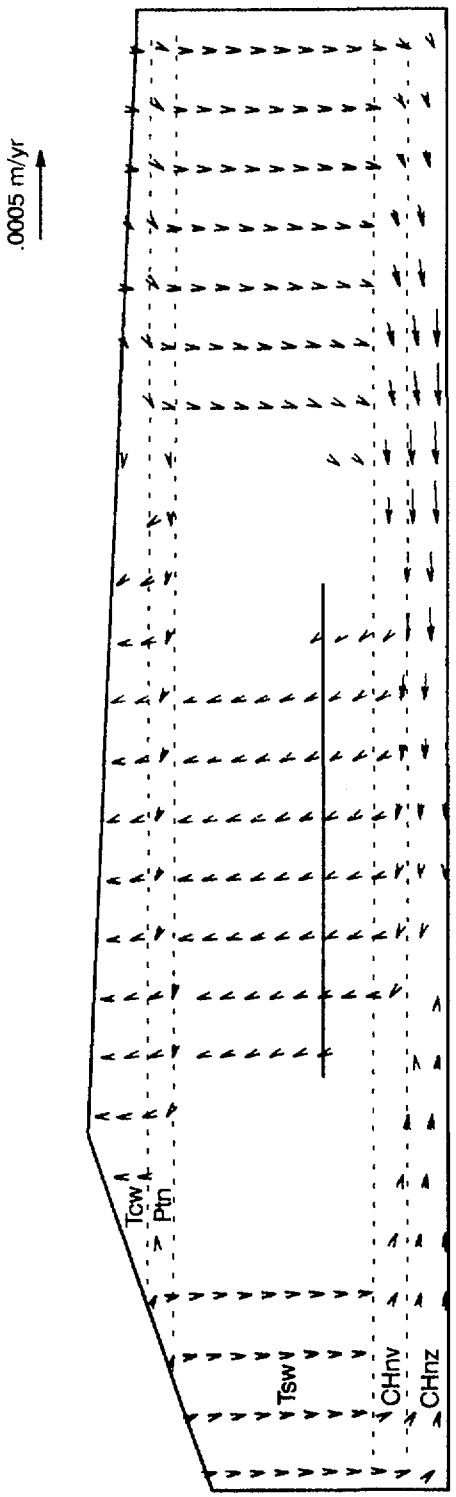

Figure 4–19 Vapor flux at 10,000 years after permanent closure of the geologic repository

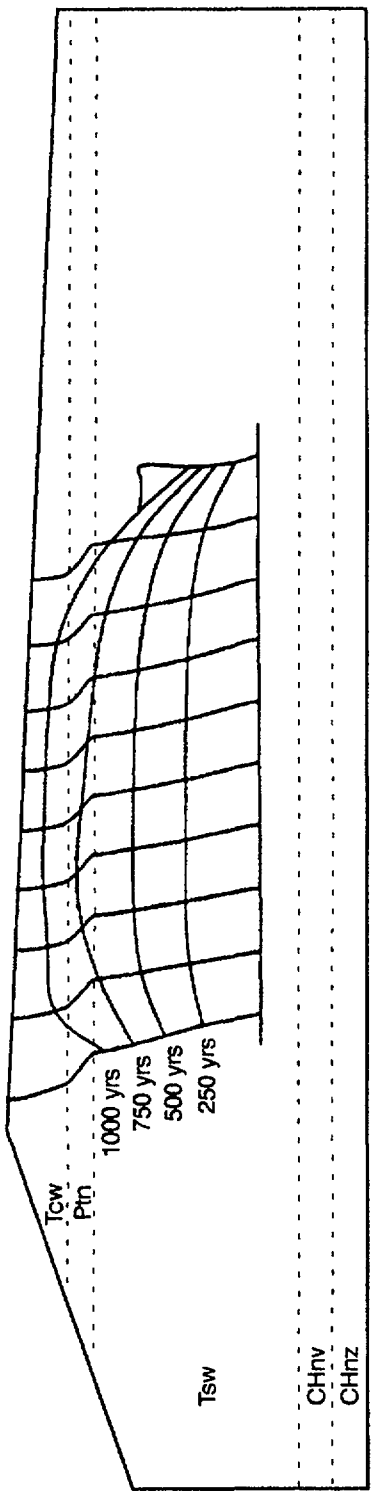

Figure 4–20 Paths and travel tim ˙r design thermal loading

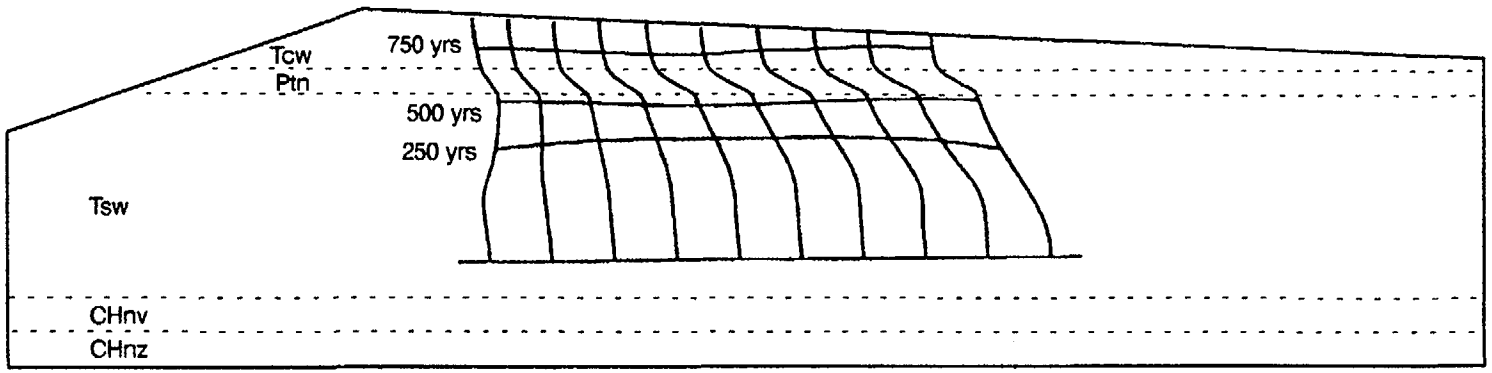

Figure 4–21 Paths and travel times for 2× the design thermal loading

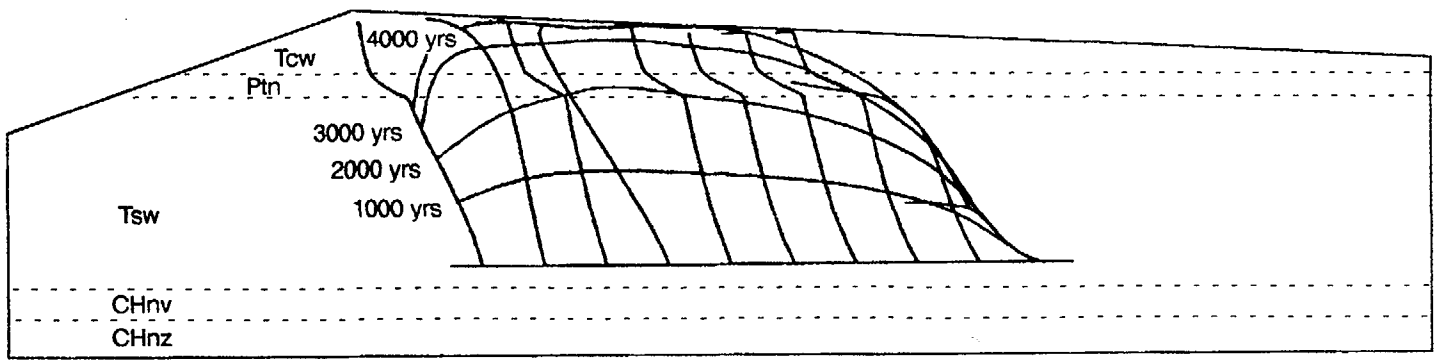

Figure 4–22 Paths and travel times for the design thermal loading

modeling of the saturated zone at Yucca Mountain, to determine flow paths and evaluate water table changes caused by climatic variation; evaluation of topography and transient conditions on percolation; evaluation of modeling considerations for unsaturated, fractured media; evaluation of the effects of hydrologic structures on 2–D, variably saturated flow; evaluation of ^{14}C transport in the unsaturated zone; and cation exchange.

4.4.1 Evaluation of the SNL Technology: Testing of the *DCM3D* Computer Code

Sandia National Laboratories (SNL), formerly under contract to NRC, developed a computer program for solving three-dimensional (3–D) ground-water flow problems in variably saturated, fractured porous media. To explicitly evaluate a fractured media, the program implements a dual-continuum approach that simulates the fractures and matrix as separate continua connected by a transfer term that depends on the unsaturated permeability of the porous medium (sometimes referred to as a dual-porosity approach). This approach, a departure from the more traditional composite characteristic curve approach, has not been previously used by NRC staff to simulate fluid flow at Yucca Mountain. An auxiliary analysis was conducted that compared *DCM3D* with other computer programs, to allow NRC staff to gain experience with *DCM3D* and better understand the implications of the dual continuum approach in the context of fluid flow in a fractured medium.

Because of the relatively recent interest in modeling fluid flow in partially saturated, fractured media it is difficult to find problems in the literature with which to evaluate the dual porosity concept. Despite this limitation, four test cases were used to provide some initial insights. The four cases involved:

- 1–D flow in a horizontal soil column (analytic solution available);
- 2–D flow in saturated-unsaturated soil (comparison with *PORFLO–3*);
- 2–D flow in a multi-layer unsaturated soil, based on a field experiment (comparison with *PORFLO–3, FLASH*, and *TRACER3D*); and
- 2–D flow through a layered, fractured, unsaturated rock (comparison with *NORIA*).

Overall, the comparison of *DCM3D* results for the four test cases compared well with the other computer programs and the analytic solution, indicating that the basic equations are correctly implemented. However, basic questions regarding the applicability of different approaches for simulating partially saturated flow in fractured rock have not been resolved by the testing provided by the four test cases. Many basic questions remain, such as:

- Anisotropic considerations of a fractured system;
- Representation of pressure equilibration between the matrix and fracture; and
- Transient effects.

Future work needs to examine problems that will provide more insights into differences in fracture-matrix interactions, because of different modeling approaches and assumptions.

This auxiliary analysis is discussed in greater detail in Appendix C.

4.4.2 Evaluation of the K_d Assumption

The system code of the present NRC performance assessment effort uses the K_d approach in estimating retardation of radionuclides. The relationship of K_d to retardation is:

$$R_f = 1 + \varrho \frac{K_d}{\theta} \quad , \qquad \textbf{(4–15)}$$

where ϱ is the bulk density, θ is the moisture content, and R_f is the retardation factor that is defined as the ratio of the velocity of ground water to that of the radionuclide. Freeze and Cherry (1979) state that this relationship is valid only when:

- The sorption reaction is fast and reversible; and
- The sorption isotherm is linear.

A sorption isotherm is the locus of points describing the concentration of radionuclide on

the solid as a function of the concentration of radionuclide in the liquid. Drever (1988) adds that for the relation to hold:

- The concentration of the radionuclide is small, compared with the total concentration of sorbing ions in solution.

In a system as complex as Yucca Mountain, it remains to be demonstrated that simplifications such as the K_d approach in estimating retardation are valid. This auxiliary analysis tests two of the three requirements described above. These requirements are that:

- The sorption isotherm is linear; and
- The radionuclide is in trace amounts relative to the total solute concentration.

The method of testing involves modeling sorption reactions in a 1-D flowing system. This modeling exercise simulates ion exchange involving sodium and potassium. The reaction considered is:

$$K^+ + NaX = KX + Na^+ , \qquad \textbf{(4–16)}$$

where X is the sorbing site on the solid. This system can be viewed as an analog for both the Na-K ion-exchange reactions involving zeolites and radionuclide-tuff reactions at Yucca Mountain. The computer code capable of simulating these processes is *PHREEQM*, an adaptation of *PHREEQE*, for use in mixing cell flowtube simulations. This code can simulate speciation and mass-transfer processes, including precipitation and dissolution; it also can simulate ion-exchange reactions, 1-D flow and transport, diffusion, and dispersion in a porous medium. The reaction written above describes the situation where a solution containing potassium flows through a column initially loaded with sodium. The potassium replaces sodium on the solid and this solute-solid interaction retards the movement of potassium down the column relative to that of water. In this study, the reverse of the reaction above is also simulated, where a solution containing sodium flows through a column initially loaded with potassium. This auxiliary analysis studies the effect of varying relative concentrations of sodium, potassium, and sorption site X, on the validity of the relationship between K_d and R_f. The equilibrium constant for the reaction potassium replacing sorbed sodium is arbitrarily given a value of 5 (i.e., > 1). The reverse reaction thus has an equilibrium constant that is the inverse of 5 (i.e., < 1).

Results

The results of the simulations are presented in the Table 4–16.

Conclusion

The requirement that the sorption isotherm be linear so that the retardation factor can be calculated from K_d is correct. However, the concentration front of the migrating ion can spread if dispersion or diffusion is significant. A linear isotherm results from the condition where the concentration of the migrating ion is trace relative to the competing ion. Linear isotherms do not result from the condition where the migrating ion is trace relative to the sorbing site. When the isotherm is nonlinear and convex up, the K_d value associated with the highest concentration of the migrating ion to be expected can be used to determine the retardation factor. This method does not work when the isotherm is concave up.

While dispersion tends to spread the concentration front of the migrating ion, ion exchange, where the corresponding nonlinear isotherm is convex up, tends to maintain a steep concentration gradient. On the other hand, ion exchange, where the corresponding nonlinear sorption isotherm is concave up, works in concert with dispersion, to spread the front.

This auxiliary analysis can be applied to the modeling of conditions and processes expected at Yucca Mountain. The assumption that all radionuclides will be in trace amounts relative to competing ions has not yet been proven. The waters at Yucca Mountain contain low concentrations of solute. Based on the solubility values from the SCP (DOE, 1988a; p. 4–100), uranium, neptunium, cesium, and technetium could be at concentration levels comparable to those in the uncontaminated waters. Furthermore, what constitutes a competing ion has not been established. Thus, in a solution with multiple species, the competing ion could be a major, minor, or trace constituent. Furthermore, at the low temperatures

Table 4–16 Results of K_d Simulations

	Concentrations (meq/l)						
Equilibrium Constant	*Migrating Ion*	*Competing Ion*	*Sorbing Site*	*Isotherm*	*K_d (ml/g)*	*Concentration Front Spread*	*Predictability of R_f from K_d*
>1	1	1	1	Convex Up	0.6–0.12	Least	Yes
>1	2	1	1	Convex Up	0.6–0.06	Least	Yes
>1	1	1	167	Convex Up	100–20	Least	Yes
>1	0.001	1	1	Linear	0.6	Least	Yes
<1	1	1	1	Concave Up	0.12–0.024	Most	No
<1	1	1	167	Concave Up	3.3–2	Most	No
<1	0.001	1	1	Linear	0.024	Least	Yes

at Yucca Mountain, certain ion-exchange reactions may be kinetically inhibited, thus allowing less thermodynamically favorable reactions to control the system. The questions concerning competing ions will have to be addressed by experimentation.

The simulations done in this auxiliary analysis involved the binary system Na-K. Consequently, changes in one component could affect the other, as shown when the two components were in comparable concentrations. When the one component was trace relative to the other, its addition to the system did not affect the other. This resulted in a linear isotherm, and constant K_d values along the column. However, Reardon (1981) has shown that variations in the concentrations of a major component can affect the partitioning (K_d) of a trace component. Thus, in a system as complex as Yucca Mountain, it is crucial that there be a demonstration that the (competing constituent) chemistry of the far field is relatively constant or predictable over the lifetime of the repository. Otherwise, the application of the K_d approach would be very difficult to defend technically.

This auxiliary analysis is discussed in greater detail in Appendix D.

4.4.3 Regional Flow Analysis

Simulation of flow in the saturated zone in the region containing Yucca Mountain in Nevada was undertaken as an auxiliary analysis for the IPA Phase 2. The primary purpose of the study is to gain experience in modeling large-scale saturated flow and to draw very preliminary inferences regarding the effects of certain selected conditions on the position of the water table. No effort, however, was made to make the analysis comprehensive; only data that were readily available were used. Some parameter values are taken from other published reports without verifying their accuracy. The analysis results should be considered as very preliminary and are likely to change when actual field data are used in simulations.

For this application, *PORFLOW* (Runchal and Sagar, 1989; and Sagar and Runchal, 1990), an integrated finite difference code, was modified to incorporate the free surface (water table) in a ground-water flow model. The model was set up in the *x–y* (horizontal) plane. Provision was made to allow for specification of recharge and discharge areas. A finite-difference grid (13161 computational cells) is imposed on a region approximately 200- by 200-kilometers. At this regional scale, the Yucca Mountain repository area is represented approximately by two grid nodes. In addition, to conduct more detailed saturated flow modeling in the vicinity of Yucca Mountain, a sub-regional model consisting of a finite difference grid (18,225 computational cells) is imposed on a region 50- by 50-kilometers around the proposed repository site. Boundary conditions for this sub-regional model consisted of fixed pressures that were read from the simulation results of the larger regional model. The hydrological data for the simulations are obtained from previously published studies that

themselves depended on numerical model calibration for their parameter values.

Recharge was assumed to occur on outcrops at higher elevations. Recharge areas included the Spring Mountains, Sheep Range, Pahranagat Range, Kawich Range, and Pahute Mesa (see Figure 4–23). Current recharge in these areas average from 25 to 50 millimeters/year. Discharge areas include Alkali Flats and the Furnace Creek Ranch, which were modeled as fixed-head boundaries. The entire modeled region was divided into eight zones, in which the hydraulic conductivity varied from 0.05 to 0.0035 meters/second. The model contains a low permeability zone northwest of Yucca Mountain for simulating the present-day high hydraulic gradient at that location. The actual cause of the steep gradient is not yet fully know.

Considering the present-day conditions, a steady-state solution to the flow system was obtained. The steady-state solution was then used as the starting point or initial state for simulating other conditions. The conditions simulated in the regional model include: (i) climatic change in the future, increasing the recharge at higher elevations by factors of 10, 20, and 30; (ii) increase of recharge in Fortymile Wash by a factor of 10; (iii) rise in water level at Alkali Flats discharge area by 10 meters; (iv) geologic activity (volcanic or tectonic) to the south of Yucca Mountain, creating a flow barrier 20 kilometers long; and (v) geologic activity to the north of Yucca Mountain, breaking the existing flow barrier. Most of the above conditions were simulated in a transient mode, so that the time variation of the water table could be studied.

Using the steady-state solution obtained from the regional model for the present-day conditions, a total of 10 additional simulations of volcanic dike intrusions in the vicinity of Yucca mountain were conducted, using the sub-regional model. These volcanic dikes were situated at various orientations directly below the repository site, as well as approximately 5 kilometers southeast of the site, to determine their impact on the ground-water flow.

Based on the regional analysis, the rise in the water table under Yucca Mountain because of various postulated conditions ranged from only a few meters to 275 meters. When the recharge at higher elevations was increased by a factor of 20, the water table under Yucca Mountain rose by 85 meters in about 700 years. Increase of recharge in Fortymile Wash by a factor of 10 raised the water table by about 100 meters. Backing up of ground water because of creation of a flow barrier south of Yucca Mountain resulted in a water table rise, under Yucca Mountain, of about 200 meters. The largest water-table rise of 275 meters was calculated when the flow barrier to the north of Yucca Mountain is removed. Figure 4–24 shows the results of the modeling of Condition (i), described previously, in which the water table rise at nodal points near Yucca Mountain and Fortymile Wash is plotted as a function of a multiple of the increased recharge rate into the regional model. Figure 4–24 does not include the effect of recharge into Fortymile Wash, which would cause an additional rise in the water table.

Results of the sub-regional model analysis of the intrusive volcanic dikes in the vicinity of Yucca Mountain showed water-table rises ranging from only a few meters to as much as 103 meters. For certain dike locations and orientations, the water table actually dropped several meters in the vicinity of the site. Figure 4–25 shows the simulated results of water-table rise, at the potential repository site, as a function of dike orientation, for the case in which the single intrusive dike extends vertically through the saturated zone directly beneath the repository site. The dike length is assumed to be 4 kilometers. The points on the plot represent the nodal points where the maximum water-table rise occurred, which in all cases was located somewhere along the fault. The maximum water-table rise for a single dike intrusion can be seen from Figure 4–25, to occur, for the dike orientation, approximately 75° counterclockwise from the east direction. The NRC staff has indicated that this particular dike orientation is the most likely to occur, because of the present faulting patterns in the Yucca Mountain area.

A number of assumptions were made in this study, with regard to the numerical model, as well as the data. These assumptions, which are discussed in the body of the report (Ahola and Sagar, 1992), should be kept in mind in interpreting the preliminary results given above. Specifically, with regard to the high water-table rises

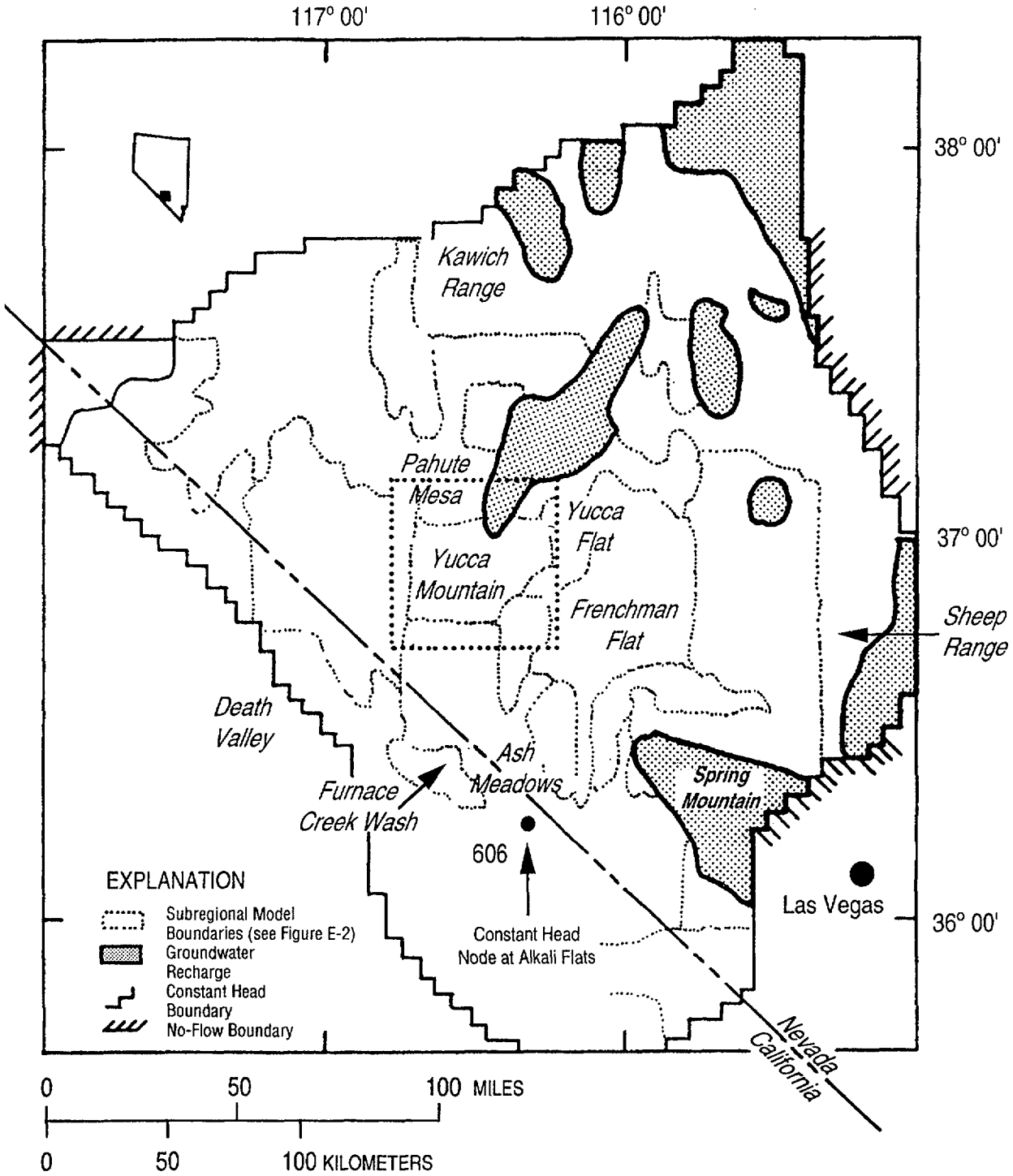

Figure 4–23 Location of recharge and discharge areas for the regional model

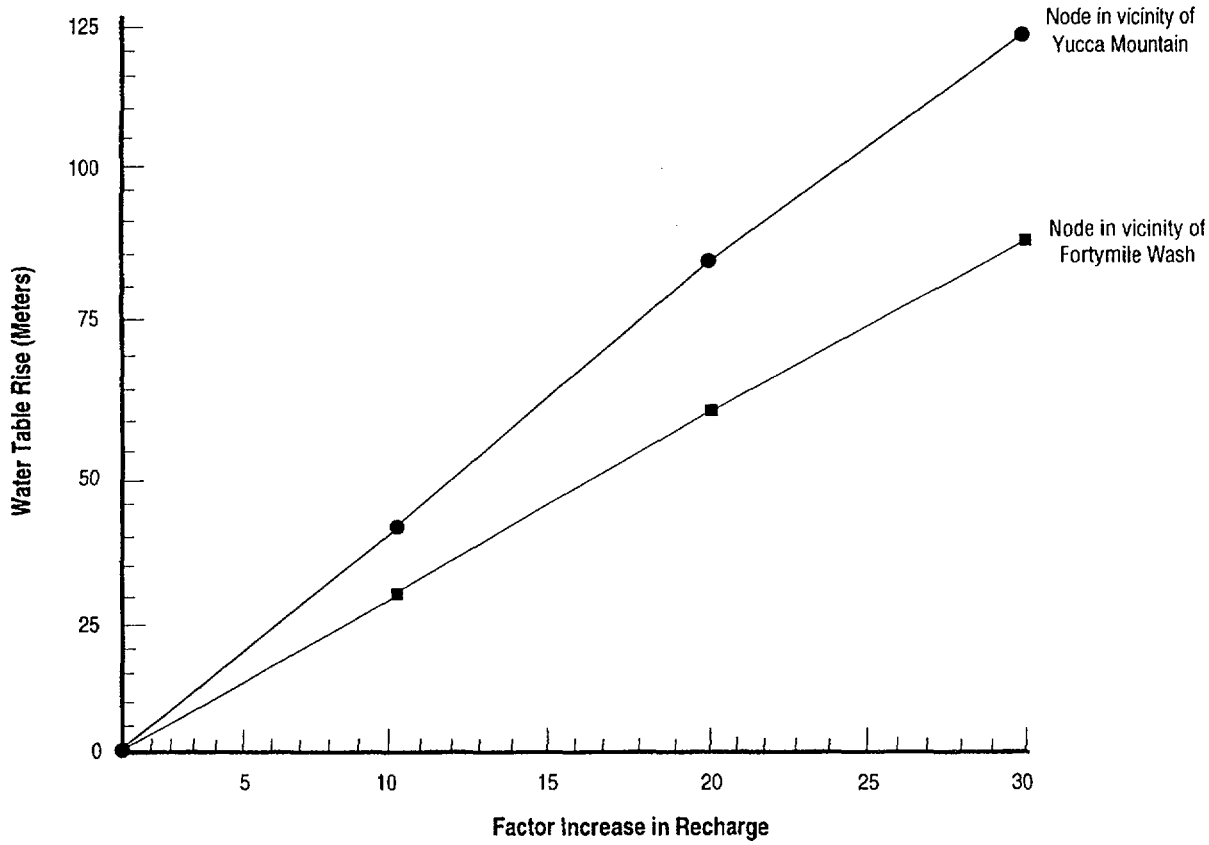

Figure 4–24 Water-table rise at Yucca Mountain as a function of increased recharge rate

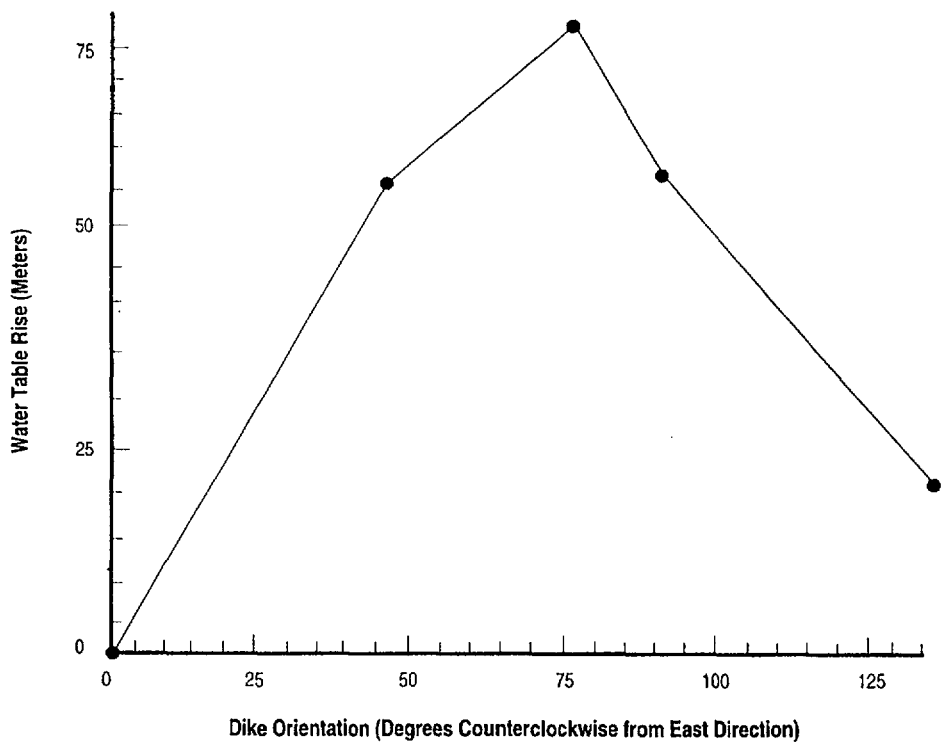

Figure 4–25 Maximum water-table rise at Yucca Mountain as a function of intrusive dike orientation (The volcanic dike is assumed to exist directly below the repository site and extend vertically through the saturated zone.)

predicted, the staff did not consider the formation of new discharge areas that such a rise may cause.

This auxiliary analysis is discussed in greater detail in Appendix E.

4.4.4 Effects of Stratification, Dip of Strata, and Sub-Vertical Faults

A numerical investigation of quasi-2-D unsaturated flow in a vertical cross-section with dipping strata and sub-vertical fault is reported in detail in the Center for Nuclear Waste Regulatory Analyses (CNWRA) report by Bagtzoglou *et al.* (1992) and a technical paper by Bagtzoglou *et al.* (1993). This work was performed as a part of IPA Phase 2 effort. The objectives and results of the work are summarized below.

IPA Phase 2 includes performance assessment of the total system and detailed auxiliary analyses of selected important features of subsystems. The main objectives of the auxiliary analyses in IPA are to provide support to simplifications made in performance assessment of the total system by obtaining better understanding of a subsystem through detailed analysis. Detailed analyses of flow in fully and partially saturated domains containing heterogeneous porous media and discrete fractures were planned as auxiliary analyses in the IPA Phase 2. Analyses of saturated flow in a region containing Yucca Mountain were reported in an earlier report (Ahola and Sagar, 1992), which discussed fluctuations of water table for various cases, including hypothesized changes in recharge/discharge conditions and stratigraphy. In the CNWRA report by Bagtzoglou *et al.* (1992), an analysis of the flow field in variably saturated zone has been developed to understand the effect of stratigraphic layering, presence of a fault zone, and the dipping of strata.

An analysis has been performed for a deep (approximately 530 meters) hard-rock system. Some of the data for the analysis were taken from the Yucca Mountain project reports, but were freely modified to enhance the effects that are being studied. However, at this stage, the report does not aim at analyzing unsaturated flow at the Yucca Mountain site. Hydraulic and stratigraphic parameters only resemble the Yucca Mountain site. For example, the depths to water table, the number of geologic strata, their dip angle, and the existence of a fault zone are characteristics used in the analysis that were based on information on Yucca Mountain. Whereas, the width of the faulting zone, the net percolation rate, and the hydraulic parameters of the matrix and fault media used in the analysis were based only partially on information on Yucca Mountain. Therefore, conclusions regarding suitability of Yucca Mountain for the proposed nuclear waste repository are not directly derivable from this analysis. Rather, the objective of this work is to help develop assumptions for the flow module in the total performance assessment system. Also, the investigation is limited to 2-D or quasi-2-D simulations in a vertical cross-section or 'thin slice,' with dipping strata intersected by a sub-vertical fault zone. The simulations are performed in a transient mode, to study the manner in which the solutions to the flow equation approach steady-state. Many other aspects of multi-dimensional flow in the unsaturated zone are worthy of detailed study. For a comprehensive review of variably saturated flow and field heterogeneity, see Ababou (1991).

In particular, the steady-state flow regime resulting from a 'wet' hydro-climatic scenario, corresponding to a net annual percolation rate of 50 millimeters/year was investigated. A hypothetical test problem was developed, to take into account, at least qualitatively: the effects of bedding (represented by five alternating layers); the presence of the sub-vertical Ghost Dance Fault (represented by a thin layer of very coarse material); and the effect of inclination of the beds (dipping six degrees eastward). A number of auxiliary tests were also conducted using variations on these hypothetical data. The main conclusions and results from this study, obtained with the aid of the *BIGFLOW* simulation code (Ababou and Bagtzoglou, 1993) and data processor, are as follows.

First, it was observed that initial-boundary conditions must be generated in a manner consistent with the hypothetical (and largely unknown) state of the system *in-situ*. More precisely, a method was devised for generating initial-boundary conditions that are consistent with: (i) the assumed input percolation rate; and (ii) the assumed material properties of the modeled cross-section. For instance, artificial boundary conditions are needed for the East-West and for the North-South lateral boundaries. This is because, in part, the cross-section is represented as a rectangular

domain bounded below by the water table, rather than a more complicated domain following the actual 'Yucca Mountain' topography. Artificial boundaries connecting ground surface to water table are also needed, particularly for the East-West faces.

Recognizing that there are no simple, natural, initial-boundary conditions that can be used for the more complex problems, a method of successive approximation was implemented. This method uses solutions of auxiliary flow problems to set up pressure conditions for the more complex problems. Unfortunately, for the 'thin-slice' simulations reported in this study, the results suggest that it is particularly difficult to design 'consistent' initial-boundary conditions in the case where the fault intersects lateral boundaries (in the case at hand, the North-South oriented fault intersected the North-South boundaries). An oscillating flow regime was obtained at large times, that is, after all initial transients died out, and this was done for both a horizontal and dipping stratigraphy. This process appeared to be localized in regions where the fault intersects these boundaries, although this requires further confirmation. This was shown to be an effect of the discrete-time nature of the equations being solved, and was eliminated by using extremely small time steps ($\Delta t \rightarrow 0$). The techniques used to identify these effects relied on detailed plots of global mass balance in terms of instantaneous net discharge rate and instantaneous rate of change of total mass. Large Δt yielded oscillations for both 2-D and 3-D flow systems, but seemed more consequential in 3-D (fault-cutting pressure boundaries).

Based on the parameters used, and simulations performed in this study, the following conclusions can be reached:

- The effects of stratification are important only for low net percolation rates and during the early parts of transient simulations;
- A dip angle of 6° to the East has a minimal effect on the pressure-head distributions (approximately 2 percent of the maximum pressure-head difference); and
- The flow behavior (ground-water fluxes and travel times) of a system consisting of highly contrasted matrix and vertical fault properties is greatly influenced by the ratio of the slopes of the matrix and fault unsaturated hydraulic conductivity curves.

Finally, the staff recognizes the need for introducing in future work, data that are more directly representative of the Yucca Mountain site. The stratigraphy should be refined regarding: the spatial configuration of geologic units; the orientation of the fault; the existence of a fault offset of the beds because of fault slip; the replacement of the exponential conductivity curve with the smoother van Genuchten-Mualem curve; the increase in contrast of some of the fault properties; a more refined mesh, to simulate a thinner fault zone; and generally a more careful selection of the unsaturated parameters of the fault and of the rock matrix in each geologic unit.

This auxiliary analysis is discussed in greater detail in Appendix F.

4.4.5 Exploration of Dual-Continuum Flow Modeling Concepts

To develop the ground-water flow and transport module, several different modeling approaches were attempted. One of the approaches required the staff to learn and experiment with *DCM3D*, a Dual-Continuum, three-dimensional (3D), Ground-Water Flow Code for Unsaturated, Fractured, Porous Media (Updegraff *et al.*, 1991). The *DCM3D* code is based on a dual-continuum model with matrix media comprising one porous equivalent continuum and fractures the other. It is attractive to use continuum codes to model ground-water flow at Yucca Mountain, because explicitly modeling individual fractures at the scale of Yucca Mountain at this time may not be possible or necessary.

At present, two main types of continua approaches are being used to model Yucca Mountain site unsaturated fracture and matrix ground-water flow; single continua and dual continua. Single continua approaches often use the same porosity values for both matrix and fractures, and a single characteristic curve to represent matrix and bulk fracture-matrix hydrologic properties (Klavetter and Peters, 1986). In contrast, dual-continuum models consist of two interconnected continua, with one continuum simulating flow through the rock matrix and the other simulating

flow through large numbers of fractures. The two continua are connected by a fracture-matrix transfer term allowing water to flow between the fracture and matrix continua. This enables a dual-continuum code to model the resistance to water movement between the matrix and fracture continua and may allow the code to simulate situations where a single-continuum approach could experience code-convergence problems.

A dual-continuum code may also be able to simulate conceptual models that single-continuum codes cannot. For example, in a single-continuum model of unsaturated fracture and matrix groundwater flow, when water saturation in the matrix reaches a level where bulk fracture flow occurs, faster velocities are computed, but with no change in direction. Therefore, this approach assumes that bulk fracture flow contains the same anisotropies as the matrix. However, individual fractures tend to be linear features with strong anisotropies. Therefore, for a single fracture it is reasonable to assume that irrespective of the flow direction in the matrix, flow in the fracture will be strongly influenced by the anisotropic properties of the fracture. Furthermore, when there are large numbers of fractures with similar linearities, a general fracture anisotropy may be created that is different from the rock matrix. This may be the case at Yucca Mountain, where faults and fractures are believed to be vertical or steeply dipping (DOE, 1988a; pp. 3–175, 3–179, and 3–185; and Barton *et al.*, 1989). Use of a dual-continuum code in this type of situation may be advantageous, because in a dual-continuum code, different anisotropies can be assigned to both the matrix and fracture continua.

In this auxiliary analysis, simulations using the *DCM3D* code demonstrate that the dual-continuum code *DCM3D* can model flow in two continua with different anisotropies, and that depending on the problem to be modeled, it may produce significantly different answers than a single continuum code.

This auxiliary analysis is discussed in greater detail in Appendix G.

4.4.6 Release and Transport of Potentially Gaseous Radionuclides Other than ^{14}C during Volcanism and Normal Operations

Several potentially volatile compounds of ^{99}Tc, ^{79}Se, and ^{129}I may be present in spent nuclear fuel. Because of the possibility of a gaseous pathway through the unsaturated rock at Yucca Mountain from the buried waste to the atmosphere, this auxiliary analysis investigated, using a series of conservative calculations, the phenomena by which volatile radionuclides could be released, and whether they posed enough of a threat to warrant further study.

Vapor pressure of possible volatile radionuclide compounds were taken from the available literature and estimated thermodynamic information. Given the estimated vapor pressures, a portion of the inventories of the volatile radionuclides could be released at normal repository operating conditions. The bulk of the inventories of these radionuclides would be contained within the structure of the spent nuclear fuel, however, and the vapor pressures of those inventories would be reduced. Barometric pumping caused by changes in atmospheric pressure was considered a possible mechanism for release of volatile radionuclides from breached waste-package containers. For temperatures and atmospheric pressure variations in the SCP design, the staff's conservative calculations estimated that less than 1 percent of the inventory of volatile radionuclides would be released from the waste packages to the geosphere in 10,000 years. The staff further estimated that most of the volatile compounds would become associated with liquid water in the rock rather than remaining in the gas phase.

The staff also estimated the effects of an intrusive basaltic dike causing temporary heating of the rock near waste packages. For a 10-meter-wide dike of 3000 meters length, the staff conservatively assumed that all volatile radionuclides in a 100 meter wide region would be driven off by the increased temperature. This represents an area approximately 6 percent of the total repository area for the SCP design. Even if all of the inventories of ^{99}Tc, ^{79}Se, and ^{129}I in 6 percent of the repository were released to the accessible environment, the total consequences would sum to only about 0.125 of the releases allowed under 40 CFR Part 191. On this basis, the staff concluded that

the releases were not large enough to warrant further study.

This auxiliary analysis is discussed in greater detail in Appendix H.

4.4.7 Evaluation of USGS Ground-Water Modeling for the Region That Includes Yucca Mountain

This section describes the major ground-water modeling work that has been performed by the U.S. Geological Survey (USGS) for the region of southern Nevada. Emphasis will be placed on the evolution of the subregional model originally developed by Czarnecki and Waddell (1984).

In the late 1970's,the USGS began an appraisal of the Nevada Test Site for potential disposal sites for high-level nuclear wastes. This work included regional geologic and hydrologic investigations, and a regional ground-water flow model was developed by Waddell (1982). Waddell produced a 2–D, steady-state, finite-element model that covered an area of about 18,000 square kilometers. This model extended from the Pahranagat Range and Las Vegas Valley on the east to Pahute Mesa and Death Valley on the west. The model included the Yucca Mountain area and almost all of the Nevada Test Site.

Following identification of the proposed Yucca Mountain site, Czarnecki and Waddell (1984) developed a subregional model within the hydrologic subbasin that includes the site. This model was derived using a parameter-estimation procedure developed by Cooley (1977, 1979, 1982). Czarnecki (1985) later revised and improved this model to help develop smaller site-scale models of ground-water flow and transport for the Yucca Mountain site. He initially prepared a steady-state base-case model and revised it to simulate the geohydrologic effects of increased recharge in the region. A transient version of the model was later used to evaluate scenarios related to the large hydraulic gradient located north of Yucca Mountain (Czarnecki 1990a). The work of Czarnecki and Waddell (1984), Czarnecki (1985, 1989, 1990a, 1990b), and Czarnecki and Wilson (1989) illustrates a methodical process for developing and improving numerical models of ground-water flow.

Because of the importance of the USGS regional modeling work, with respect to site characterization of the Yucca Mountain site, the NRC staff have acquired the subregional model of Czarnecki (1985) and the *MODFE* computer code. PC-based versions of the code and model have been prepared to facilitate staff evaluation. This evaluation is provided below, and serves as an example of how the staff can directly obtain and evaluate numerical codes and models developed under DOE's high-level waste program. In this way, the NRC staff can become more knowledgeable about codes and models during site characterization and before receipt of a potential license application.

Finally, the work of Czarnecki (1992) represents an important 10-year forecast of how future ground-water levels will be affected by human activities. After 10 years of site characterization, it will be possible to see how well the regional model has predicted the perturbations caused by pumping at Wells J–13 and J–12. It is expected that one of the many scenarios analyzed by Czarnecki will approximate actual ground-water withdrawals at the well sites, providing a test of how well the regional model represents present-day conditions in the flow system near Yucca Mountain.

This auxiliary analysis is discussed in greater detail in Appendix I.

4.4.8 Modeling Saturated Flow to the Accessible Environment

In the development of the ground-water flow and transport module, several different modeling approaches were attempted. *DCM3D* was used to analyze a dual-continuum approach for modeling a fractured, porous media. Using this code, a 1–D saturated zone flow model was built from the Yucca Mountain site, across that portion of the saturated zone simulated by the performance assessment flow module, to a location near the presently defined "accessible environment boundary" (10 CFR 60.2).

Simulations of ground-water flow and water-table elevation were conducted for a range of material properties. From these simulations, it was observed that:

- The slowest velocities and longest flow times were obtained from runs that used matrix properties. Seepage velocities were 1.3×10^{-6}

and 1.6×10^{-5} meters/year, resulting in extremely long calculated flow times of 3180 million years and 31.7 million years;

- The fastest velocities and shortest flow times were obtained from runs that used hydrologic properties from well tests. The average seepage velocity was 473 meters/year and the calculated flow time was 10.6 years; and

- A simulation of fracture flow that, like matrix property simulations, used low saturated hydraulic conductivities, produced faster flow velocities, and shorter flow times than matrix property runs. This simulation contained smaller porosity values than the matrix property runs and illustrates the importance of determining fracture porosity values, which at this time are hypothetically determined for bulk fracture property flow codes.

This auxiliary analysis is discussed in greater detail in Appendix J.

4.4.9 Geochemical Model for ^{14}C Transport in Unsaturated Rock

Under the unsaturated, oxidizing conditions expected for a geologic repository at the Yucca Mountain site, ^{14}C contained in spent nuclear fuel may be converted to carbon dioxide and be transported with moving gas to the atmosphere. There are several mechanisms that could facilitate the transport of gaseous radionuclides, including ^{14}C, to the atmosphere, and these are discussed in Section 5.6.

Carbon-14, as carbon dioxide, would interact with ions in the ground water and country rock, and would therefore be retarded with respect to the transport of inert gases. Since the temperature, gas flow, and water saturation of the rock will respond to the large amount of heat caused by the decaying nuclear waste, the chemical processes leading to retardation of gaseous ^{14}C will be complicated. The staff investigated the geochemical interactions of ^{14}C for a geologic repository in partially saturated rock. The ^{14}C transport model consists of three parts:

- A geochemical model describing the state of all carbon species in a representative volume of rock;

- A flow and transport model, for movement of total carbon through the system that consists of a number of connected volumes or "cells"; and

- A model of ^{14}C migration as a trace quantity in the general movement of total carbon.

For a simple 1-D example of vertical gas flow from the repository to the atmosphere, the staff reached the following conclusions:

- The results of the analysis show a significant redistribution of autochthonous carbon among solid, liquid, and gas phases, even in areas remote from the repository plane. Carbon remains predominantly in the aqueous solution, in spite of the fact that near-field heating results in a reduction of liquid saturation, abundant calcite precipitation, and increased equilibrium fractionation of CO_2 into the gas phase.

- Transport of ^{14}C released from the repository is generally retarded by a factor of approximately 30 to 40 because of immobilization in the liquid phase. In addition, ^{14}C released early during the period of solid calcite precipitation can be fixed for a long period before repository cooling leads to redissolution of the calcite.

This auxiliary analysis is discussed in greater detail in Appendix K.

4.4.10 The Exchange of Major Cations at Yucca Mountain

Zeolites are crystalline, hydrated aluminosilicates, which are characterized by an ability to readily exchange cations with aqueous solutions. The presence of zeolites is seen as an important barrier to the migration of radionuclides to the accessible environment. This auxiliary analysis was undertaken to address two questions related to the exchange of cations in Yucca Mountain.

The first question concerned the stability of zeolites. Using potassium/argon (K/Ar) dating techniques, WoldeGabriel *et al.* (1992) determined that the zeolites from boreholes in the Yucca Mountain vicinity range in age from 2 million years to 10 million years old. However, ion exchange involving potassium and sodium on zeolites has been shown to reach equilibrium in

about 2 days (Pabalan, 1991). How, then, can a mineral that can alter within a couple of days exist unchanged for at least 2 million years? To answer that question, simulations were performed in which pore water, whose composition approximates that found at Yucca Mountain, percolates through site-specific zeolite layers for a period of approximately 150,000 years. The simulation was intended to represent the chemical reactions that would take place between the cations dissolved in the pore water and the cations sorbed onto zeolites. If, in the simulation, the potassium ions attached to the zeolites become mobile, there would be reason to doubt the zeolites could be accurately dated using a K/Ar technique. If, however, the K is immobile, the K/Ar ratios would not be affected by ion-exchange reactions.

The second question to be answered by this analysis involved the determination of pore-water compositions from the unsaturated zone. Peters *et al.* (1992) describe methods of measuring pore water compositions from rocks of the unsaturated zone, plus the possible causes of changes in the compositions of the pore waters, due to the method of extraction (compression). Given that ion-exchange reactions involving zeolites are fast (Pabalan, 1991), can it be determined what the chemical composition of pore water from the unsaturated zone is if the composition of the zeolite in direct contact with the pore water is known?

The simulations performed to address the first question in this auxiliary analysis concerning the validity of K/Ar dating relied on the geochemical modeling code *PHREEQM* (Nienhuis and Appelo, 1990). This analysis involved simulating the flow of site-specific ground water through site-specific porous rock, at a site-specific rate. The simulation that was performed used mole fractions of Na, Ca + Mg, and K, derived from the zeolite compositions reported by Broxton *et al.* (1986). The flushing solution composition in the simulation approximates that of the site-specific water from Peters *et al.* (1992).

The results of this auxiliary analysis demonstrate that the K in the zeolites is relatively immobile. This is because of the large reservoir of K held in the zeolite, versus the amount of exchangeable cations in the liquid. There simply are not enough cations in the pore water to exchange with the K on the zeolites, and therefore the K remains immobile. Consequently, the K/Ar technique for determining the age of the zeolites should not be affected by ion exchange, given the low concentrations of cations in the ground water and slow flow rate in the vadose zone.

The simulations performed to address the second question in this auxiliary analysis required modeling the three ion-exchange reactions:

$$NaX + K^+ \leftrightarrows KX + Na^+ \quad , \qquad \textbf{(4–17)}$$

$$2Na^+ + CaX_2 \leftrightarrows 2NaX + Ca^{2+} \quad , \qquad \textbf{(4–18)}$$

$$2K^+ + CaX_2 \leftrightarrows 2KX + Ca^{2+} \quad . \qquad \textbf{(4–19)}$$

Equilibrium constants for Equations (4–17) and (4–18) were from Pabalan (1991). Equation (4–19) was derived by multiplying Equation (4–17) by 2 and adding the result to Equation (4–18). The equilibrium constant for Equation (4–19) was derived similarly.

By using the compositions of clinoptilolites from Yucca Mountain (Broxton *et al.*, 1986) and the equilibrium constants from Pabalan (1991) and this study for Equations (4–17) through (4–19), the relative concentrations of the exchangeable cations in the pore were calculated.

The results of the exercise demonstrate the wide variation in the pore-water chemistry which is possible in the vicinity around Yucca Mountain. In addition, this analysis has shown that the chemical composition of the pore waters in contact with the solids in the unsaturated zone may be different from the composition of the water in the saturated zone.

This auxiliary analysis is discussed in greater detail in Appendix L.

4.4.11 Considerations in Modeling Percolation at Yucca Mountain

The infiltration at Yucca Mountain could vary considerably because of topography, spatial variation in hydrologic properties, and the intensity and duration of the rainfall. The effect of these variations on the rate of percolation at the repository depth is uncertain. Detailed spatial and

temporal hydrologic modeling exercises have been proposed to provide insights on the impact of these variations.

The surface boundary condition for many modeling exercises is assumed to be a constant value over large areas. Although this type of assumption may offer a type of "average" behavior of percolation, a more explicit model which takes into account both the change in hydrologic properties and topography (e.g., alluvium in a wash), is needed, to better understand the effect this type of spatial variation has on percolation. Although very detailed topography of Yucca Mountain is readily available, site characterization is still quite limited in providing a detailed description of the hydrologic layering and structures below Yucca Mountain, to determine the effect on percolation (isolated areas of increased recharge may either be of benefit or detriment to performance, depending on whether the recharge intercepts the repository). Despite this characterization limitation, the current exercise was conducted to gain insights into the importance of this effect, examine the viability of modeling on a small spatial scale (meters to tens of meters), and gain experience on the recently developed computer program *DCM3D* (Updegraff *et al.*, 1991). A 2–D simulation based on detailed spatial variation and topography was conducted to analyze the affect on percolation. The simulation revealed an ability to concentrate recharge in the low-lying alluvium and indicated the numerical difficulties in examining this type of localized, focused recharge.

Likewise the duration of rainfall could have a significant impact on the determination of the amount of percolation at Yucca Mountain. Typically, surface boundary conditions assume a small annual, steady-state average infiltration rate. The effect of using an infiltration rate based on averaging rainfall over an entire year, as compared to using a transient infiltration rate, needs to be evaluated, to better understand any correlations with percolation and fracture flow. A 1–D simulation was conducted with transient infiltration rates, to examine the effect on percolation and fracture-flow rates.

The above two simulations experienced similar numerical difficulties simulating the infiltration of a sharp wetting front (either infiltration from a wet, high permeability alluvium in a wash into an underlying dry, low permeability unit or large episodic infiltration into a dry unit). The numerical difficulties were traced back to the manner in which pressures are evaluated at the grid block interface (either a linear interpolation or a Newton-Raphson iteration scheme). Numerical problems arose when very dry-node (meters of suction) and wet-node (near zero suction) pressures are interpolated to arrive at an interface pressure. When this situation occurs the saturated node increases in positive pressure (meters of pressure) before any appreciable water flows between the two nodes. This situation is a result of the interface pressure value remaining a large negative value, until the wet node attains the very large positive pressure to balance the high suction value of the dry node. This effect in the 1–D transient simulation resulted in large oscillations in the pressure, as the recharge front moved down the column. This type of behavior is considered to be an artifact of the numerics, rather than caused by the physical system. Upstream-weighting of the pressure interpolation scheme has been introduced into the *DCM3D* computer program, to correct this effect. This technique has corrected the observed aberrant behavior; however, further testing is needed to examine numerical dispersion effects before performing the above simulations again.

4.4.12 Comparison of *NEFTRAN II* to *UCBNE41*

NEFTRAN II, an SNL transport code (Longsine *et al.*, 1987), was compared to *UCBNE41* (Lung *et al.*, 1987). *UCBNE41* is a saturated 1–D transport code that uses an analytic solution. During the comparison an error in the internal documentation to the *UCBNE41* code was found and corrected.[4] The initial concentrations should be input in moles/cubic meter, not grams/cubic meter.

After making this change, the two computer codes compare well. Figures 4–26 to 4–28 compare the results of *NEFTRAN II* and *UCBNE41*, for a test case based on sample data set No. 3 in the *NEFTRAN II* documentation. Since *UCBNE41* requires a constant velocity, the initial velocity was maintained for all times. Sample data set No.

[4]H.C. Lung and W.W-L Lee were subsequently contacted and agree that the internal documentation for the code was in error. H.C. Lung is the author of *UCBNE41*. W.W-L Lee is NRC's contact at the University of California at Berkeley.

3 prescribes a doubling of the initial velocity at 50,000 years.

Other transport codes such as *UCBNE40*, *UCBNE50*, *UCBNE51*, and *UCBNE52* were not compared to *NEFTRAN II* in this study. However, they are very similar to *UCBNE41*. As transmitted to the NRC staff, all the codes in the *UCBNE40* and *50* series ask for initial concentrations in grams/cubic meter but do not accept the atomic mass as input. *UCBNE40*, *UCBNE50*, *UCBNE51*, and *UCBNE52* have therefore been altered to indicate that the initial concentrations should be input in moles/cubic meter, not grams/cubic meter. *UCBNE40* compiles correctly. *UCBNE50*, *UCBNE51*, and *UCBNE52* contain a non-ANSI (American National Standards Institute)-standard feature. They alter the value of a do loop variable inside the loop. This feature causes problems with some FORTRAN 77 compilers. This problem was documented, but not corrected. Fixing this problem would require reworking the entire looping structure of the program. The codes *UCBNE40*, *UCBNE50*, *UCBNE51*, and *UCBNE52* should be tested further before being used.

4.5 Conclusions and Suggestions for Further Work

A number of conclusions and recommendations resulted from: (1) the development and implementation of computational tools for calculating ground-water flow and radionuclide transport; (2) the analysis of results related to the conceptual models used for ground-water flow and radionuclide transport; and (3) the auxiliary analyses. A description of the more salient conclusions and recommendations relevant to ground-water flow and transport are presented below:

1—Examine modeling issues affecting percolation

Conceptual model assumptions with respect to percolation should have a major effect on water flux through a repository located in the unsaturated zone. One-dimensional approaches, like that used in the IPA Phase 2 analysis, can be very sensitive to assumptions regarding percolation. The modeling assumptions and uncertainties affecting percolation rates need to be analyzed to better understand their effect in relationship to the range assumed for percolation. Uncertainty in the percolation rate, in part, can be attributed to: variations in the infiltration rate; spatial variability of hydrologic properties within a hydrogeologic unit; variability in the thickness of the hydrologic units; and assumptions regarding fracture matrix interactions. The current analysis accounted for some of this uncertainty by use of a correlation length, to develop a representative permeability range for each hydrogeologic unit, use of different hydrogeologic unit sequences, and thicknesses attributed to different sub-areas of the repository, and the use of 2–D flow modeling results to interpolate spatial variation of percolation caused by the slope of the hydrogeologic units. These model abstractions were considered to be very important to the conceptualization of the flow problem and proved to be equally important to obtaining reasonable computer execution times for the TPA computer code. However a number of issues that are considered important to estimating percolation were not evaluated in IPA Phase 2. Issues that need to be examined further include: the relationship between highly transient rainfall and percolation estimates; the effect of topographic lows and fault zones as sources of increased recharge; how spatial variability in hydrologic parameters affect percolation; and the effect of fracture imbibition on percolation (also see *Recommendation 2*).

2—Examine modeling assumptions affecting fracture-matrix interaction

Modeling assumptions regarding the interaction between matrix and fractures are very important, because of differences in fluid velocities and retardation between the two flow systems. These differences are primarily caused by the fracture flow system having a very small bulk porosity (10^{-4} to 10^{-5}) and limited surface area of the fracture walls, compared with the large bulk porosity (.1 to .4) and large surface area associated with the pores of the matrix flow system. The IPA Phase 2 analysis used a dual-continuum approach that represented the fracture and matrix systems as separate but interacting continua.

Steady-state interaction between the two continua were modeled, assuming the fractures were planar, regularly spaced, and without a mineral coating affecting the movement of water across the fracture surface. Further simulation efforts could improve the understanding of conceptual

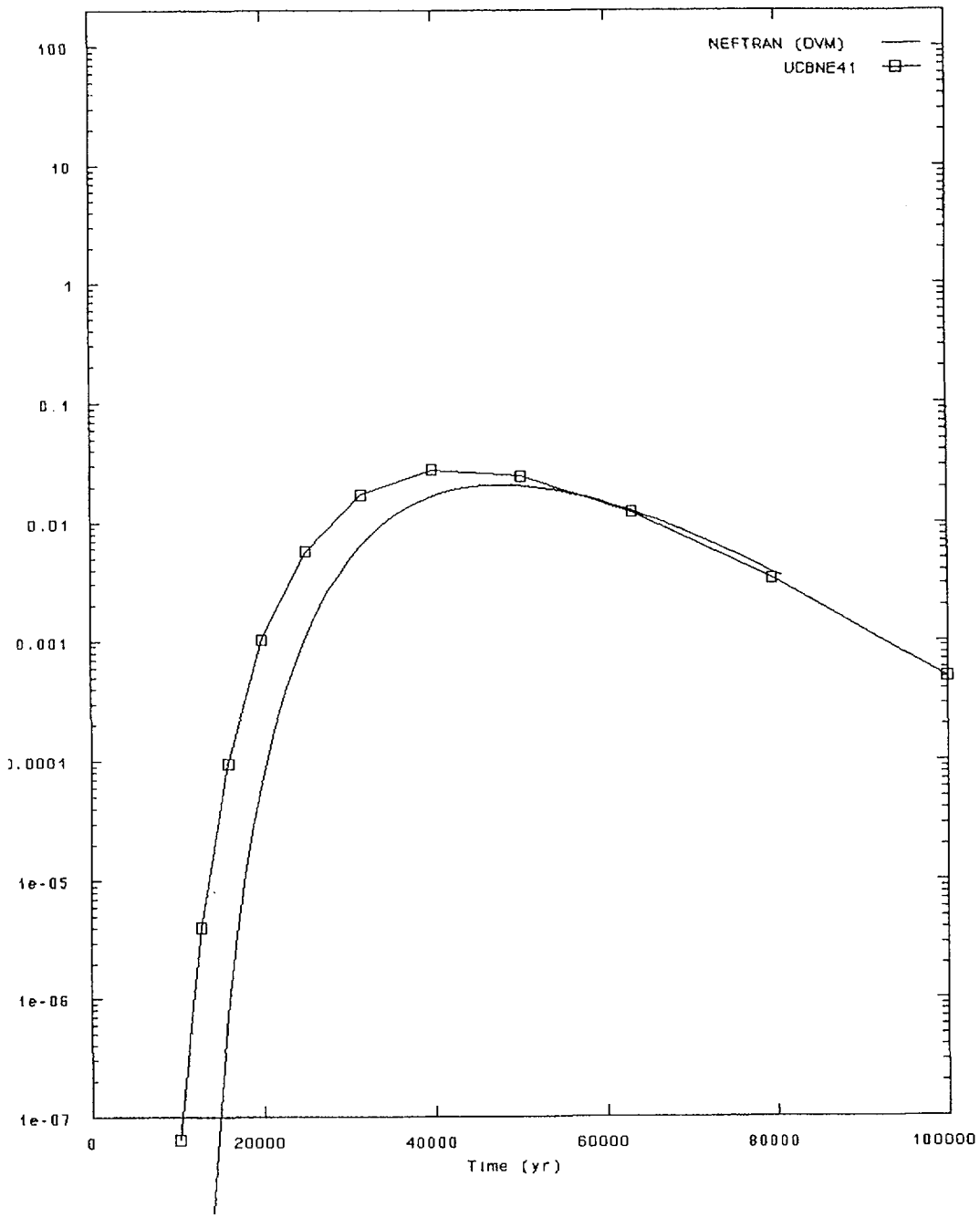

Figure 4–26 Discharge rates for ^{243}Am computed by *NEFTRAN II* and *UCBNE41*, in a benchmarking exercise

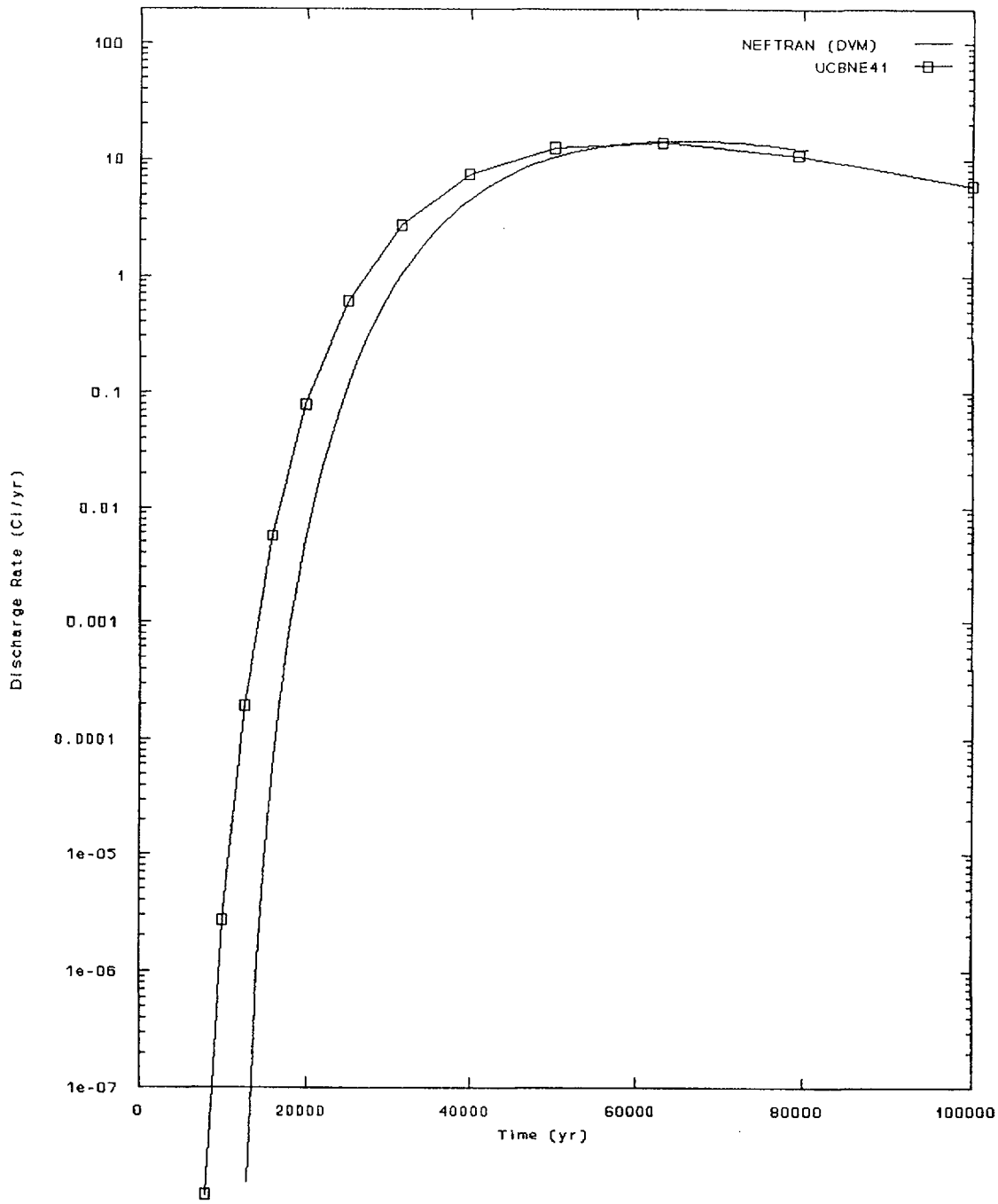

Figure 4–27 Discharge rates for ^{239}Pu computed by *NEFTRAN II* and *UCBNE41*, in a benchmarking exercise

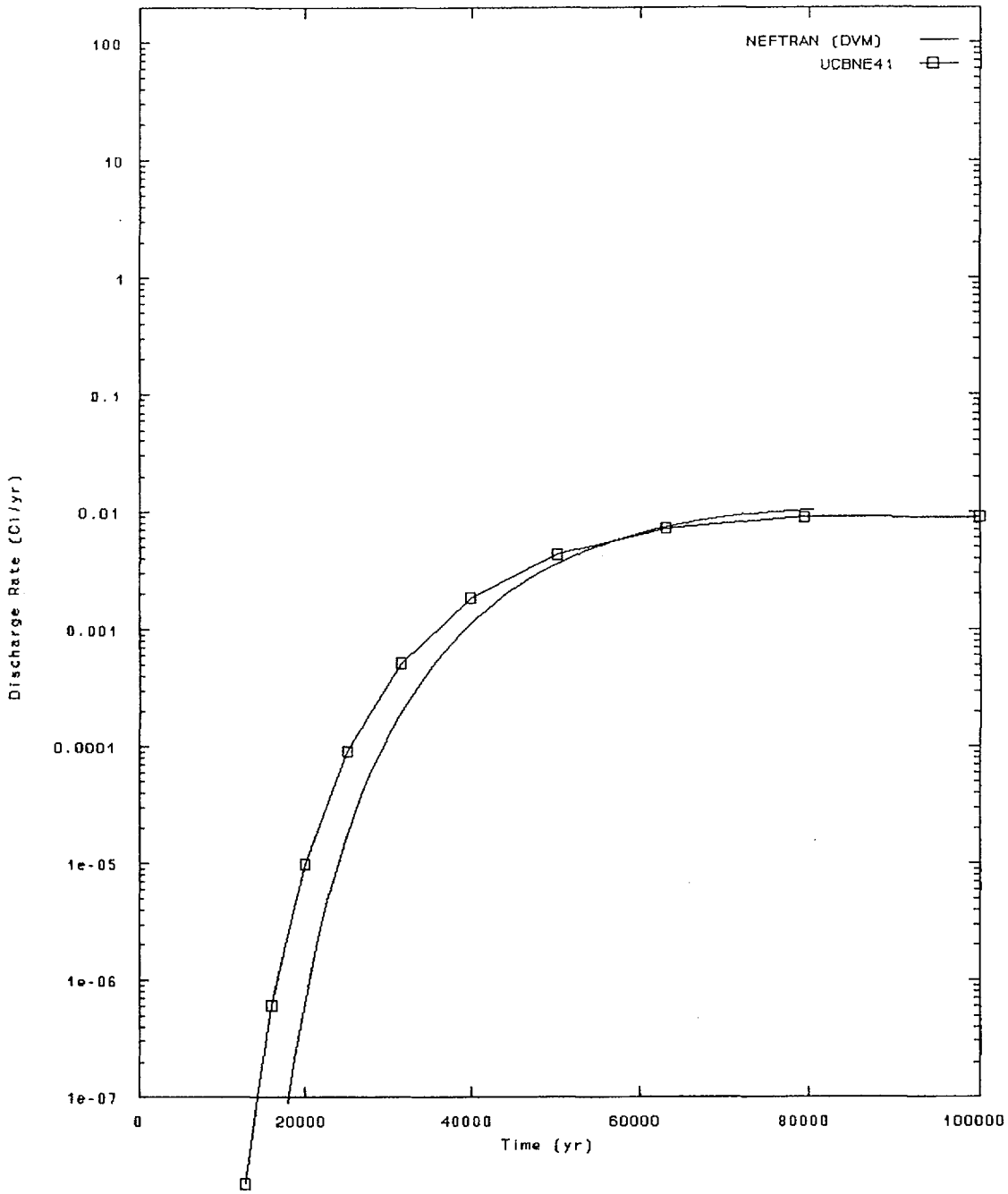

Figure 4–28 Discharge rates for ^{235}U computed by *NEFTRAN II* and *UCBNE41*, in a benchmarking exercise

modeling assumptions regarding small-scale interactions at the fracture-matrix interface (e.g., detailed simulations to examine the equilibration of pressure between the fracture and matrix, considering transient conditions and the effects of mineral coatings on fracture surfaces) and large-scale effects concerning the flow field within a hydrogeologic unit (e.g., examine how the small-scale effects propagate through a geologic unit). These further analyses can be used to modify current IPA models and revise parametric ranges.

3—Examine hydrogeologic features and heterogeneity in the context of providing a "short circuit" through the unsaturated zone

The IPA Phase 2 flow and transport analyses assumed that fluid flow and radionuclide transport could be represented through 1-D stream tubes for each of the hydrogeologic units. This representation does not account for possible "short circuiting" of the low conductivity matrix pathway via hydrogeologic features (i.e., fault zones) or fracture flow initiated by perched water forming in areas of heterogeneity. Two- and three-dimensional analyses could investigate the impact of fault zones and perched water on pathways through the unsaturated zone. If the impact were of sufficient magnitude, then additional pathways could be added to the flow and transport analysis in future IPA phases.

4—Examine the coupling of water in the gaseous and liquid phases

Although a number of characteristics of the flow system have been included in the abstracted models of the TPA computer models, a number of characteristics of the real system have not been included. The real problem is transient, 3-D, partially saturated flow with significant air and water-vapor movement in a fractured, porous medium complicated by potentially significant heat transfer and the associated flows of gas and liquid affecting the redistribution of moisture. How these phenomena can be approximated by simplifying assumptions and still provide an adequate representation for the calculation of system performance is poorly understood at this time and needs further investigation. Abstracted models need to be tested through simulation, comparing the results with those of the "complete" model, which includes the coupling of water movement in the liquid and gaseous phases, under non-isothermal conditions. Simulation efforts could examine the variation in moisture contents and fluid flux, through the repository, caused by vapor movement and condensation (this effect would be especially pronounced during the thermal phase of the repository). These results would provide more realistic fluid flux for the source-term and flow and transport modules.

5—Examine refinements in the saturated modeling to improve concentration estimates for dose calculations

The calculation of dose requires a determination of the radionuclide concentration. The concentration determination required an additional refinement of the transport model, beyond what is required for the calculation of integrated discharge, for comparison with the EPA standard. This determination required not only the integrated discharge of radionuclides, but the quantity of water associated with this discharge. For the current analysis, the contaminant plume was assumed to remain near the water table, and assumptions were made concerning the local population and its water usage. Additional refinements in these assumptions could require significant improvements in the current modeling approach for flow and transport and place greater demands on data requirements. Initial efforts should concentrate on compiling different approaches used for modeling saturated fractured rock and their relationship to field conditions at Yucca Mountain, as a guide for possible improvements to the current analysis.

6—Examine modeling assumptions affecting retardation in fractures

Radionuclide releases, in the liquid pathway, to the accessible environment were affected primarily by the presence of fracture flow. The IPA Phase 2 analysis conservatively assumed that there was no retardation in the fractures and did not consider the process of matrix diffusion in the modeling. Future work needs to evaluate the nature and magnitude of the conservatism of these assumptions and the relationship of fracture coatings in affecting these processes.

7—Access the usefulness of additional intermediate calculations for understanding the flow and transport results

The IPA Phase 2 performance measures were integrated discharge and radionuclide dose. Oftentimes, it is difficult to explain these results in the absence of other information on modeling results for individual modules (e.g., fluid flux or water velocity for the ground-water pathway, and release rates for the source term module). These intermediate results proved extremely valuable in both determining if the modules were performing as expected and in assisting the sensitivity analysis. It would be beneficial to further examine the modeling approaches and identify intermediate calculations that could be performed to provide further insights on model and system performance. For example, the current analysis used a dual-continuum model to represent the fracture-matrix system as separate but interacting continua that enabled a simple procedure to be implemented for performing intermediate calculations concerning fluid flow in the fracture and matrix continua.

Recommendations from the Auxiliary Analyses

The auxiliary analyses contributed to parametric values used in the TPA system code and to understand assumptions and limitations used to represent ground-water flow and radionuclide transport. The assignment of individual parametric values through an auxiliary analysis is not discussed here except in terms of impacting assumptions and limitations of the analysis. A brief description of the more salient conclusions and recommendations related to the auxiliary analyses are presented below (more complete descriptions can be found in the associated appendices):

(1) The representation of a fractured system can be accomplished via a discrete fracture model, a composite approach which attempts to average the matrix and fracture system, or a dual-continuum approach which treats the matrix and fracture as separate but interacting continua. Each of these representations have both benefits and disadvantages. Experimental information with respect to fracture-matrix interactions is extremely scant and is needed to provide insights on the applicability of these approaches.

(2) Ground-water flow modeling is affected by a number of assumptions at a very small scale (millimeters to centimeters) and at a large scale (tens of meters to kilometers). At a very small scale, assumptions with respect to characteristic curves (pore scale) can have dramatic impact on interactions between the matrix and fracture flow fields, in addition to assumptions regarding steady-state versus transient flow. At a large scale, there are a number of assumptions and features (topographic details that lead to spatial variation of recharge and discharge areas, discrete features such as a fault zone, spatial variability in hydrologic properties, and layering of geologic strata) that can have significant impact on the distribution of fluxes throughout the unsaturated zone. Further analysis is needed to better understand the impact of these assumptions on the overall repository performance.

(3) Several potentially volatile compounds of ^{99}Tc, ^{79}Se, and ^{129}I may be present in spent nuclear fuel. Conservative estimates of gaseous releases of these radionuclides during volcanism and normal operations were sufficiently low to not warrant further study.

(4) The transport of gaseous ^{14}C will be affected by variation in saturation, gas flow, and temperature, caused primarily by heat from decaying nuclear waste. Geochemical modeling of ^{14}C transport demonstrated a retardation factor of approximately 30 to 40, because of primarily transfer of carbon between the CO_2 in the gas phase and dissolved carbonate and bicarbonate in the liquid phase. Some ^{14}C might be trapped temporarily, in precipitating calcite during the period when temperatures are rising, and released from the calcite as it redissolves, as temperatures fall.

5 SOURCE TERM MODULE[1]

5.1 Introduction

The model used by the staff to calculate the source term in Iterative Performance Assessment (IPA) Phase 1 was that incorporated in the *NEFTRAN* (NEtwork Flow and TRANsport) computer code obtained from the Sandia National Laboratories (SNL) (see Longsine *et al.*, 1987). In this model, radionuclide releases would occur only after failure of the waste package canister,[2] characterized as a single failure time.

In IPA Phase 2, the staff developed its own computer code to calculate the source term. The *SOTEC* (Source Term Code) module (see Sagar *et al.* (1992)) deals with the calculation of aqueous and gaseous radionuclide time- and space-dependent source terms for the geologic repository. It does so by considering the variations in those physical processes expected to be important for the release of radionuclides from the engineered barrier system (EBS).

Three primary calculations are done in *SOTEC*: (a) failure of waste packages because of a combination of corrosion processes and mechanical stresses; (b) the leaching of spent nuclear fuel; and (c) the release of $^{14}CO_2$ gas from the oxidation of UO_2 and other components in spent nuclear fuel and hardware. The principal features of the staff's source term analysis are discussed below.

5.2 Overall Structure of the Source Term Code

5.2.1 Conceptual Model

The proposed geologic repository at Yucca Mountain will consist of a large number of waste packages placed in drifts and perhaps in boreholes. The repository environment will change with time, as a result of radioactive decay, leading to initial heating of the rock, followed by a long cooling period. The heating is anticipated to promote dramatic changes in the chemical and hydrologic environment surrounding the waste packages. Temperature and water flow rates will vary widely in both time and space. The geology of the mountain is of a fractured, porous rock material with high spatial variability. The problems with heterogeneity are increased because the type of water flow of greatest concern is fracture flow. The characteristics of the waste material such as age, burn-up, heavy metal inventory, and spent nuclear fuel versus defense vitrified waste (glass) will vary spatially in the repository. Environmental variables such as water flow rates, water saturation, water chemistry, and temperature will vary in time and in space in the repository.

The problem associated with heterogeneity are addressed in part in the source term module *SOTEC* by dividing the geologic repository into a number of zones, referred to as "repository sub-areas". Within each repository sub-area, all chemical, physical, and waste form properties are assumed to be identical. The release rate for each repository sub-area is then the release rate for an individual waste package in the repository sub-area times the number of waste packages in the repository sub-area. *SOTEC* calculates the performance characteristics for an individual waste package and extrapolates the result to the entire repository area.

Information concerning variability may come either from standard input parameters listed in Appendix A or from output files created by other modules of the total-system performance assessment (TPA) computer code. To limit the amount of input data and code complexity, the assumption is made that (except for temperature) a separation of parameters can be performed between spatial and temporal variations. For each parameter, the input appears as a time-variant repository average (or reference) value and a set of load factors for the individual repository sub-areas. *SOTEC* and the temperature code, *CANT2* (described in Section 2.1.3), consider only seven separate repository sub-areas. The small number of repository sub-areas is inadequate to describe a continuous distribution of failure times for the waste packages and the fractional release rate for the EBS. The concept of ensemble averaging to

[1]The figures shown in this chapter present the results from a demonstration of staff capability to review a performance assessment. These figures, like the demonstration, are limited by the use of many simplifying assumptions and sparse data.

[2]The term "waste package" is used here synonymously with "container" and "canister."

choose parameters that best represent all waste package canisters in discussed briefly in Section 5.3.5 and in greater detail in Appendix L.

5.2.2 Input to and Output from *SOTEC*

The structure and flow of the source term code is illustrated in Figures 5–1 and 5–2. Data are read into *SOTEC* from a series of files. Some of the file names are initially fixed, however the majority of file names are read from the main input files.

As noted in Chapter 2, many of the TPA modules can run in either the "internal" or the "external" mode.[3] In the internal mode, *SOTEC* reads from the file of input parameters produced by the Latin Hypercube Sampling (LHS) procedure. Many of the parameters in *SOTEC* that are read from the stand-alone input files are overwritten. Overwritten parameters represent either random parameters or system-wide input parameters. Figure 5–1 presents input and output files for *SOTEC*. Some of the output files for *SOTEC* are only written when operation is in internal mode.

All of the major output files written by *SOTEC* are designed to be read by other codes. The major output of *SOTEC* is the release rate, as a function of time, for each radionuclide for each repository sub-area. Additional outputs are:

- Waste package lifetimes for use in some of the other disruptive consequence models;
- The 1000-year inventory for each radionuclide, assuming radioactive decay only, with no other loss from the waste package;
- The cumulative release from the EBS of each radionuclide in each repository sub-area; and
- The failure times by corrosion necessary for evaluation of the model for seismic failure.

5.2.3 Structure of Calculations

The overall flow of the calculations in *SOTEC* is illustrated in Figure 5–2. Subsequent to reading the input files, *SOTEC* loops over time calculating corrosion penetration for each waste package as a function of time. Waste package failure times for each repository sub-area are recorded for use in the release-rate portion of the code. The corrosion portion of *SOTEC* is not coupled to the liquid release calculations and could be put in a separate code. In the corrosion calculations, the corrosion rate is estimated at the beginning of each time step. At the end of the time step, the total corrosion depth is compared with the critical thickness for buckling. If the remaining waste package thickness is less than the critical thickness, or if the remaining thickness is less than zero, failure is presumed to occur. Depending on input assumptions, the waste package may either fail completely, resulting in a flow-through system, or fail partially, with a specified maximum volume inside the failed waste package.

Calculation of liquid and gaseous releases begins with evaluation of the failure time and types for each repository sub-area. Individual waste packages in each repository sub-area can fail by three different mechanisms. The first type of failure is initial defectives, representing waste packages that were defective at the time of repository closure. Defective waste packages will begin releasing ^{14}C at time = 0 and begin releasing radionuclides in the aqueous phase once the waste package cools below the boiling point and begins filling with water. The second type of failure is by scenario. The scenario option fundamentally allows the TPA computer code, or the analyst, to specify a time of failure for a portion of the waste packages in each repository sub-area. The primary purpose is to facilitate evaluation of alternative scenarios besides corrosion/buckling failure of the waste packages. The scenario option can also be used by the TPA computer code to specify a waste package lifetime distribution independent of the corrosion calculations. The third type of waste package failure is by the corrosion/buckling mechanism discussed in Section 5.4.

After sorting out the type and timing of the failures in each repository sub-area, the liquid and gaseous release calculations begin. The calculations proceed by repository sub-area, with internal time and radionuclide loops in the liquid and gas-release modules. The calculations are set up to handle multiple chains of radionuclides and multiple isotopes of the same element.

[3] "Internal" versus "external" refers to the manner of code execution and the time at which the output files from the consequence modules are generated. In the internal mode, the modules are separate from the system code, and as a result, the cumulative releases can be generated and placed in files at any time before iteration of the system code.

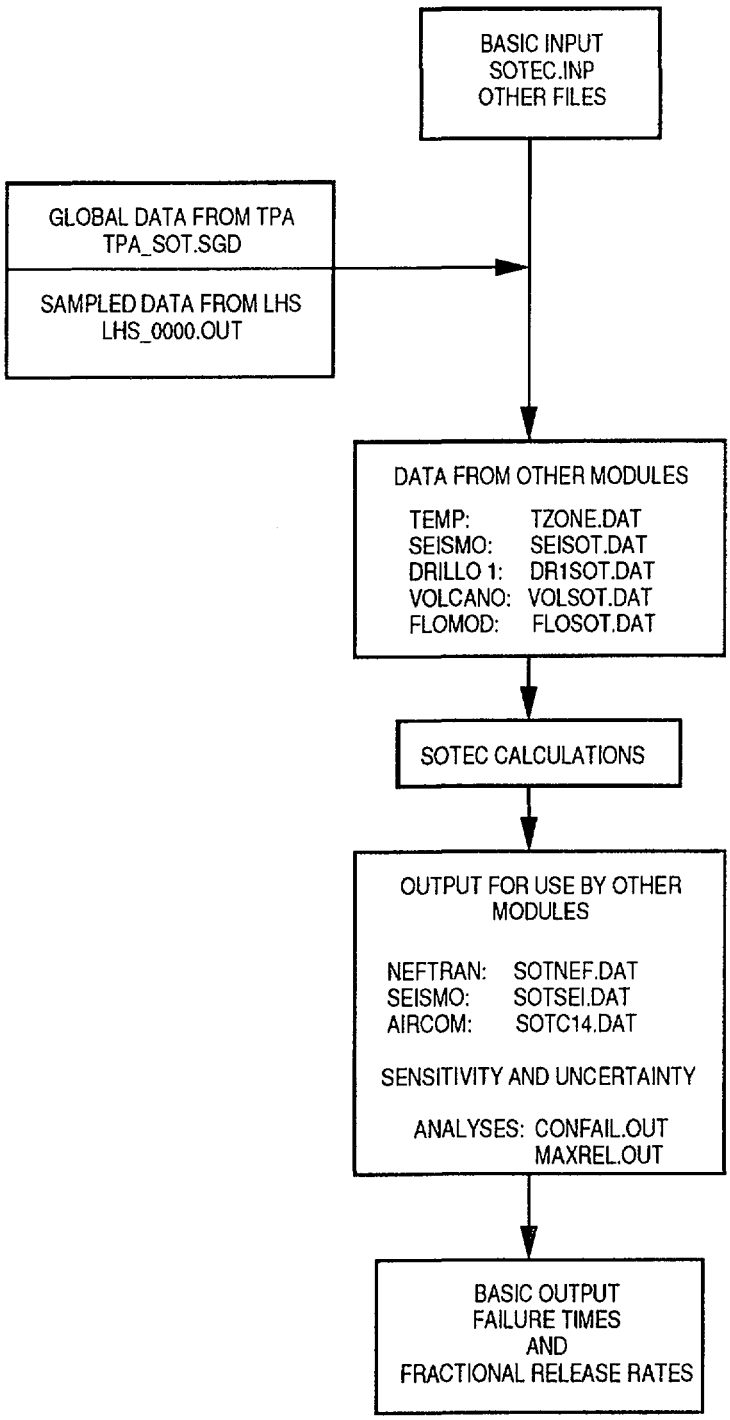

Figure 5-1 ***SOTEC*—Source term code input and output files**

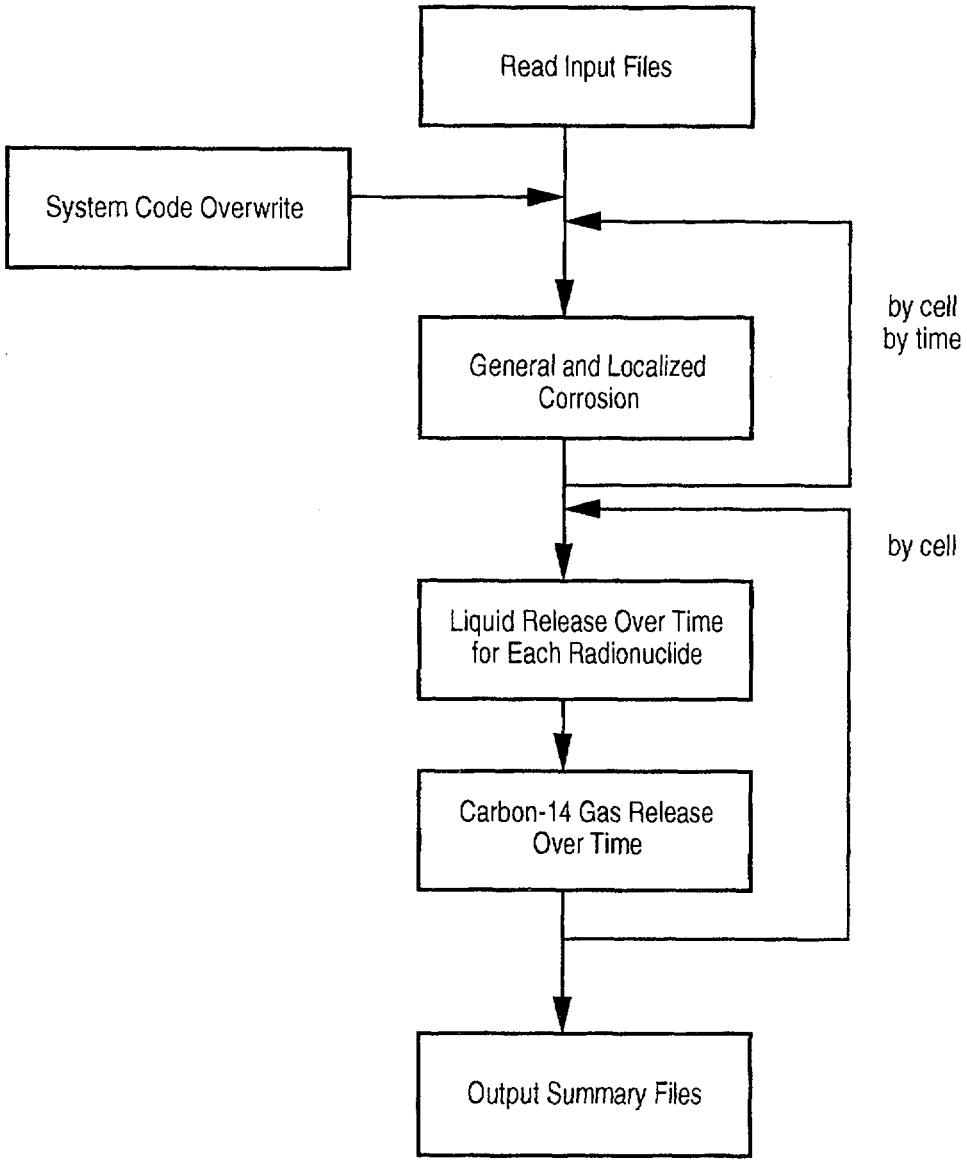

Figure 5–2 ***SOTEC*—Source Term Code**

Subsequent to the release calculations, the release rates are summarized by calculating cumulative release and interpolated to even grids for writing to file.

5.2.4 Radionuclide Inventory

The inventory of radionuclides included in the calculations of IPA Phase 2 were carefully screened from a large list of radionuclides, to include only the major contributors to cumulative release and dose. The primary objective of this screening was to reduce to a minimum the number of calculations in the computer programs, without substantially affecting the results.

Starting with a list of 37 radionuclides, the TPA computer code was run for 50 LHS vectors of the fully disturbed (*csdv*) scenario, and the results tabulated for cumulative release at the accessible environment and on-site dose to the farm family. A radionuclide was retained in the inventory if, in any of the 50 vectors, it contributed more than 1 percent of the U.S. Environmental Protection Agency (EPA) cumulative release limit[4] for that nuclide. The screening analysis also checked the maximum dose to the farm family, to see if any of the radionuclides that might have been screened out on the basis of cumulative release should have been kept on the basis of dose. In all cases, however, the cumulative release criteria were more restrictive than dose.

If a radionuclide screened out of the inventory was a parent to another radionuclide, the inventory of the progeny was adjusted upward to account for the decay of the parent. This was important for the radionuclide ^{238}Pu, which was screened out, and whose decayed inventory was added to that of the progeny ^{234}U. Table 5–1 presents the radionuclide inventory used in the Phase 2 analyses.

Table 5–1 Initial Radionuclide Inventory (in curies per metric ton of heavy metal (Ci/MTHM))

Nuclide	*Ci/MTHM*	*Nuclide*	*Ci/MTHM*
^{246}Cm	0.0258	^{226}Ra	3.67×10^{-7}
^{238}U	0.318	^{210}Pb	4.7×10^{-8}
^{245}Cm	0.126	^{137}Cs	7.66×10^{4}
^{241}Am	1640	^{135}Cs	0.35
^{237}Np	0.288	^{129}I	0.0295
^{243}Am	15.5	^{99}Tc	12.3
^{239}Pu	308	^{59}Ni	3.56
^{240}Pu	508	^{14}C	1.54
^{234}U	1.89	^{79}Se	0.381
^{230}Th	1.29×10^{-4}	^{94}Nb	0.793

5.3 Waste Package Environment

5.3.1 Introduction

The waste emplacement environment at Yucca Mountain is expected to be highly complex. Modeling for the IPA Phase 2 requires a relatively simple conceptual model for the interaction of the waste packages and their immediate environment. The following subsections discuss the thermal, hydrologic, and geochemical environment for the waste package, as conceived in IPA Phase 2.

5.3.2 Thermal Environment

The repository environment will change with time as a result of heat generated in the decaying waste. Heat will be transferred in the host rock primarily by thermal conduction, but heat transfer will be complicated by the evaporation and condensation of water, and the transport of air and water vapor. The movement of water vapor and liquid water will affect the hydrologic environment

[4]Currently, a revised set of standards specific to the Yucca Mountain site is being developed in accordance with the provisions of the Energy Policy Act of 1992. The Energy Policy Act of 1992 (Public Law 102–486), approved October 24, 1992, directs NRC to promulgate a rule, modifying 10 CFR Part 60 of its regulations, so that these regulations are consistent with EPA's public health and safety standards for protection of the public from releases to the accessible environment from radioactive materials stored or disposed of at Yucca Mountain, Nevada, consistent with the findings and recommendations made by the National Academy of Sciences, to EPA, on issues relating to the environmental standards governing the Yucca Mountain repository. It is assumed that the revised EPA standards for the Yucca Mountain site will not be substantially different from those currently contained in 40 CFR Part 191, particularly as they pertain to the need to conduct a quantitative performance assessment as the means to estimate postclosure performance of the repository system.

for periods of time after waste emplacement. The strengths of the thermal effects will be a function of the types of waste and the thermal loading per unit area. The repository temperature model for IPA Phase 2, discussed in Section 5.4.2, considers only heat conduction in a uniform semi-infinite medium, and does not take into account two-phase flow.

IPA Phase 2 considers only simplified aspects of the thermal environment for several of the models:

- *Onset of waste package corrosion*—The waste packages are assumed to remain dry, and no corrosion of the waste packages occurs before the temperature falling below the assumed boiling point, at the repository, of 96 degrees Celsius (°C).

- *Corrosion model parameters*—Several of the corrosion parameters in the model of Section 5.4.1 are temperature-dependent.

- *Carbon-14 source term model*—As described in Section 5.6.3, the release rate of gaseous $^{14}CO_2$ from the spent fuel waste form is temperature dependent. The rate of liquid release predicted by the model does not depend directly on the temperature.

5.3.3 Hydrologic Environment

The assumed disposal concept adopted in the IPA Phase 2 is one of vertically placed waste packages surrounded by an air gap, as discussed in the U.S. Department of Energy's (DOE's) 1988 Site Characterization Plan (SCP) (see DOE, 1988). One of the main intentions of this design is the isolation of the waste packages from liquid water, since there would be little or no direct contact of the waste packages with the surrounding rock. In an unsaturated environment, capillary suction should keep liquid water diverted away from the air gap and confine it to the rock.

If no liquid water could reach the waste packages, there would be little possibility of water-borne radionuclide releases to the geosphere, even if the waste packages failed. Gaseous radionuclides could still be released, however, as could releases in the case of disturbances such as human intrusion and volcanism. The reliance on engineered design to maintain the dryness of the waste packages has not been demonstrated, however, so the authors found it prudent to postulate mechanisms by which liquid water could reach the waste packages, and carry away dissolved radionuclides:

- *Dripping fractures*—Fracture flow in the rock could occur under conditions where infiltration exceeded the hydraulic conductivity of the rock matrix. Several mechanisms could lead to local saturation, such as perching along rock interbeds, fracture flow along continuous pathways from areas of local recharge at the surface, and the return of condensed water that had been evaporated by the waste heat. These phenomena are discussed more thoroughly in Chapter 4.

- *Direct contact of waste package with rock or rubble infilling material*—The air gap surrounding the waste package could be compromised if it were to become filled in with porous material from rock spallation or sedimentation. Another possibility would be the tilting of the waste package so that it leans against the side of the emplacement borehole.

- *Condensation of water onto surface of waste packages*—Minerals contained in the groundwater that might come into contact with the waste package surface could become highly concentrated, leading to a condition of vapor-pressure lowering (Walton, 1993). These highly concentrated mineral solutions might remain liquid at temperatures significantly above the boiling point of water. Furthermore, the solutions would probably be corrosive.

- *Immersion of waste package*—Perched water or a general rise in the regional water table could immerse the waste packages. Another possible mechanism for waste package immersion might be the mineralization of fractures near the waste packages, because of hydrothermal activity induced by repository heat or an external heat source. The plugged fracture might then allow the collection of infiltrating water that would otherwise drain The possibility of waste package immersion was not considered to be a credible scenario in the IPA Phase 2 analysis.

5.3.4 Interaction of Liquid Water with Waste Form: Direct Contact

The IPA Phase 2 model for release of dissolved radionuclides considers that there might be direct contact of dripping liquid water with some of the waste packages. Based on the infiltration of meteoric water, the carrying capacity of fractures and matrix in the vertical rock columns, and on horizontal diversions by the dipping bedding planes, the hydrologic models discussed in Chapter 4 are used to estimate an areally averaged rate of water carried by fractures. In some cases, all flow will be carried by the matrix, and consequently, there will be no release of dissolved radionuclides by direct contact of liquid water.

For the cases where there is fracture flow, dripping liquid water from fractures is likely to be non-uniformly distributed over the repository. There would be a wide distribution of amounts of dripping water, and many of the waste packages might never receive any. On average however, the total rate of water influx q affecting each waste package is likely to be no greater than the effective cross-sectional area A_e (or "funnel factor") of the emplacement hole times the average fracture infiltration rate I_f; that is:

$$q = A_e I_f \quad . \tag{5–1}$$

The effective cross-sectional area of the emplacement hole A_e is chosen to be a uniformly distributed random area between 0 and 0.4 square meters per waste package, based on a mean area for the borehole of 0.2 square meters. There are several reasons to believe that the flow rate of water affecting the waste packages would actually be far less:

- For partially saturated flow, openings are barriers to flow rather than conduits. Even in fractures and the emplacement borehole, capillary tension would likely restrict water to the fractures and borehole walls; and

- Dripping fractures would occur only occasionally, and drips might not land on the waste package or in places that would lead to corrosion or entry into the waste package.

5.3.5 Ensemble Averaging

For the sake of computational speed, the IPA Phase 2 analysis used a "lumped parameter" approach, in which the entire repository is represented by a relatively small number of waste packages. Since the repository source term, consisting of tens of thousands of waste packages (Johnson and Montan, 1990), is being represented by only seven repository sub-areas, with only one waste package per repository sub-area, there must be careful consideration given to the way in which the repository sub-areas represent the ensemble of waste packages.

Presently, the arithmetic average of external environmental parameter values (e.g., temperature, flow rate) for all waste packages in the repository sub-area is chosen for a representative waste package. Additionally, there is only one set of source term parameter values (e.g., corrosion parameters, solubilities) representing the corrosion, liquid, and gaseous release submodels per repository sub-area.

A demonstration of the conditions under which the lumped parameter approach might be valid is presented as an IPA Phase 2 auxiliary analysis in Appendix L. For solubility limited releases of single, long-lived radionuclides, the ensemble average cumulative release per waste package is represented exactly by the arithmetic averages of the flow rate per waste package $<q>$, the waste package failure time $<t_{fail}>$, and the waste package failure volume $<V_0>$. The waste package failure time, however, is a calculated parameter that is based on temperature and a number of corrosion parameters which might not be represented correctly by their arithmetic means.

The ensemble mean parameters for the congruent release case should be $<1/q>$ (the harmonic mean), $<t_{fail}/q>$, and $<V_0/q>$, which are much more complicated parameters. Use of the arithmetic average values of q, waste package-failure parameters, and V_0 may not necessarily give good results for radionuclides that are not solubility limited.

Numerical experiments with the release rate models themselves confirm that cumulative release of the long-lived solubility limited radionuclides is proportional to flow, which demonstrates that the arithmetic mean flow rate is the correct ensemble average to use for these

radionuclides. Release of congruently released radionuclides is not proportional to the flow rate, but for these radionuclides, the flow rate is relatively unimportant. As expected, numerical experiments with *SOTEC* showed a relatively low sensitivity of radionuclide releases to flow rate q, for congruently released radionuclides. The effects of using the arithmetic mean of V_0 and the parameters for the failure model has not been determined for IPA Phase 2.

5.3.6 Geochemical Environment

The waste package material, the waste itself, and the heat generated by the waste will affect the geochemical environment in a complex way. The IPA Phase 2 source term models do not explicitly consider changes in the geochemical environment, except to the extent these effects have been taken into account in choosing the parameter ranges for the submodels. The effects of heat on the geochemical environment presented in the IPA Phase 2 auxiliary analysis in Appendix K were explored in regard to the transport of ^{14}C in the gas phase. This auxiliary analysis was used to justify a range of retardation coefficients.

5.4 Waste Package Failure Modes

5.4.1 Corrosion Models

SOTEC considers the failure of waste packages from initial defects, corrosion, mechanical processes, and disruptions. For any given metal and set of environmental conditions, the corrosion potential is a major factor influencing the types of active corrosion processes and their rates. The importance of the corrosion potential is reflected in the philosophy and implementation of the corrosion routines in *SOTEC*. *SOTEC* assumes that the corrosion potential is a function of temperature and radiation dose rate:

$$E_{corr} = E_1 + A(T - 298) + \beta e^{-\lambda t} \quad , \qquad (5\text{–}2)$$

where:

A = empirical factor for temperature effect on corrosion potential (millivolts/degrees Kelvin—mV/°K);
β = empirical factor for radiolysis effect on corrosion potential (mV);
λ = average decay rate for gamma emitters in waste (year^{-1});
E_1 = reference corrosion potential (mV);
T = temperature (°K);
t = time (years); and
E_{corr} = corrosion potential (mV).

The equation for the corrosion potential assumes that the influence of radiolysis varies linearly with gamma dose rate, and that temperature affects the corrosion potential in a linear fashion. The impact of radiolysis appears as a maximum corrosion potential effect at time = 0, and declines with time, with radioactive decay of gamma emitters. The dependence of the corrosion potential on temperature and radiolysis is presumed to be obtained from independent theoretical analysis (e.g., Macdonald and Urquidi-Macdonald, 1990) or experimental data and translated into functional forms allowed in *SOTEC*.

Rates of pitting and crevice corrosion depend directly on the corrosion potential. When the potential is elevated above a critical value that is dependent on the type of metal, metal history, an solution composition, localized corrosion begins. The critical potential may be referred to as E_{pit}, E_{crev}, or E_{crit}, depending on the context and the type of corrosion involved. When the potential is lowered sufficiently, the localized corrosion pits generally repassivate. This is sometimes referred to as the repassivation potential or protection potential E_{prot}.

SOTEC currently allows only one critical potential for each of pitting and crevice corrosion and the critical potential is assumed to be a function of temperature, but not of solution composition.

5.4.1.1 General Corrosion

General corrosion is assumed to begin when repository temperatures drop below a specified (input) temperature. In the atmosphere, general corrosion is known to become significant when the relative humidity exceeds 80 percent. At the elevation of Yucca Mountain (approximately 1500 meters above sea level), this corresponds to a temperature of approximately 96°C, assuming conservatively that the air is 100 percent water vapor. Once corrosion begins, the corrosion rate is described by a generic power law equation (for more discussion, see Williford (1991)) of the form:

$$r = ae^{\frac{b}{cT}}\ t^d\, C_1^e\, C_2^f\ ,\ \text{when } T < T^o\ , \qquad (5\text{–}3)$$

where r is the corrosion rate, a, b, c, d, e, and f are empirical constants, T is absolute temperature, and t is time. Instead of concentrations C_1, C_2, etc., of aggressive species, the logarithm (to base 10) of the concentrations can be used. In some interpretations of this equation (e.g., Kubaschewski and Hopkins, 1962), b is the activation energy, and c is the gas law constant.

General corrosion is assumed to represent a passivated metal and as such is independent of the corrosion potential.

5.4.1.2 Crevice Corrosion

Crevice corrosion is affected by a number of coupled processes. These include mass transfer, production of metal ions within the crevice and hydrolysis. In the literature both the steady-state and transient models for crevice corrosion exist (see Watson and Postlethwaite (1990) as an example). However, for inclusion in *SOTEC*, such models are too complex and computationally time consuming. Therefore, a strategy to develop a simple parametric equation for crevice corrosion for use in *SOTEC* has been adopted.

Crevice corrosion has two characteristics: (1) critical potential for initiation and repassivation; and (2) propagation rate. Initiation time depends on the corrosion potential of the metal exceeding the critical potential for crevice-corrosion initiation.

The repassivation potential is taken to be a function of temperature:

$$E_{rc} = E_r + \zeta T, \qquad (5\text{–}4)$$

where:

E_{rc} = crevice repassivation potential (mV),
E_r = reference potential (mV); and
ζ = temperature-correction factor (mV/°K).

Subsequent to initiation, crevice corrosion is assumed to penetrate the waste package at a constant empirical rate r. The active corrosion rate can be estimated from an equation of the form:

$$r = \frac{i_a w}{\varrho z F}\ , \qquad (5\text{–}5)$$

where i_a is the active current density; w is the formula weight of the waste package material; ϱ is the material density; z is the ion valency; and F is the Faraday constant. *SOTEC* assumes a constant active corrosion rate.

5.4.1.3 Pitting Corrosion

Episodic evaporation and condensation of water on the surface of waste packages resulting in high concentration of aggressive ions makes them susceptible to pitting corrosion. Mechanistically, pitting corrosion is similar to crevice corrosion and it is possible to develop detailed models (Farmer *et al.*, 1991) for predicting critical pitting potentials or electrochemical conditions within the pit. Alternatively, heuristic stochastic models may also be developed (Henshall, 1992). For development of the *SOTEC* code, a strategy similar to that for crevice corrosion will be followed. Detailed models for pitting corrosion are still under development, and a constant propagation rate is assumed for pitting, in Version 1.0 of *SOTEC*.

Pitting corrosion is assumed to begin when the critical potential for pitting is reached. Pitting is assumed to begin immediately when the critical potential is exceeded. The critical potential is given by Equation (5–4). The rate of penetration by pitting is assumed to be identical to the rate in crevice corrosion, as described by Equation (5–5).

5.4.2 Temperature Model for Source Term

5.4.2.1 Introduction

Spent nuclear fuel will generate significant quantities of heat, leading to increases in the temperature of the waste package, fuel, and surrounding rock. The increase in temperature, in turn, will lead to changes important to the performance of the repository, such as chemical equilibrium and kinetics of the fuel and rock, mechanical changes to the host rock, waste package corrosion, and movements of gas and liquid. In the IPA Phase 2 analysis, temperature is taken into account explicitly in only three places; the gas velocity for the ^{14}C transport model; the onset of corrosion in

the source term model; and release of ^{14}C from the spent nuclear fuel under dry conditions.

The main purpose for program *CANT2* is to generate temperature for the surface of each waste package, to determine the time at which the temperature falls below the boiling point, assumed to be the onset of corrosion in the source term model. The temperature of the fuel inside the waste packages is calculated from the skin temperature for the ^{14}C source term model, by means of an empirical correlation (see Section 5.6.3.5.5).

5.4.2.2 Heat Transfer in Yucca Mountain

Heat transfer under both natural and repository modified conditions at Yucca Mountain will be complicated because of the unsaturated nature of the geologic media. Air circulates within Yucca Mountain under the influence of forces such as wind, barometric-pressure variations, and natural convection. Heat is transferred through conduction in the rock, and, to some extent, by the moving air, both as sensible and latent heat. Heat-transfer coefficients for conduction are sensitive to the degree of saturation of the rock, which can change both spatially and temporally. Close to the emplaced waste in the proposed repository, latent heat transfer and drying of the rock take on greater importance. Experiments (e.g., Ramirez and Wilder, 1991) and sophisticated mathematical models (e.g., Buscheck and Nitao, 1990) indicate deviations in temperature from model predictions based on conduction only, especially close to the emplaced waste. Furthermore, models of conductive heat transfer cannot predict the drying and re-wetting of the rock close to the waste packages. Models to predict two-phase heat and mass transfer are at the cutting edge of technology. In addition to the long computer run times associated with these models, there are a number of fundamental questions about how to treat two-phase flow through fractured porous media. Although it is possible to simulate two-phase flow at the scale of individual fractures, modeling of the waste package and larger scales must generally rely on the equivalent porous medium approach, to capture the effect of fractures in the matrix. Modeling of individual fractures is not feasible on the larger scale, because of both the large amount of computer resources that would be needed, and the lack of data on the location and characteristics of individual fractures.

5.4.2.3 Thermal Loading of the Repository

Under the design evaluated in IPA Phase 2, each waste panel would contain thousands of waste packages with different waste makeup (i.e., some will be vitrified defense wastes, most will be spent nuclear fuel, but of varying ages, from different types of reactors, and a range of burnups). Therefore, each waste package type will have a different heat output rate as a function of time.

5.4.2.4 NRC Temperature Model

The U.S. Nuclear Regulatory Commission temperature model is similar in some respects to the models of Altenhofen and Eslinger (1992) and also Johnson and Montan (1990). There are a number of significant enhancements that makes the present model more suited to our work in IPA Phase 2. It is very fast and efficient, so it could actually be incorporated into the system model if necessary (although it is not presently implemented this way).

As a first approximation of temperature of the waste packages within the repository, the report authors considered the following simplifying assumptions:

- Heat transfer is by thermal conduction only;
- The medium is homogeneous with constant thermal diffusivity;
- Waste packages are placed on a plane surface in a semi-infinite medium. The semi-infinite medium simulates a constant temperature at the surface of the earth, but extends infinitely in depth and laterally; and
- Heat output of each waste package as a function of time only.

The present model uses linear superposition of the temperature field for all waste packages in a panel, superimposed on the temperature field from all other panels represented as rectangular flat planes, as shown in Figure 5–3. Each waste package is represented as a solid rectangular parallelepiped with an instantaneous release of heat per unit volume. The heat source in each panel can vary from panel to panel. Convolution

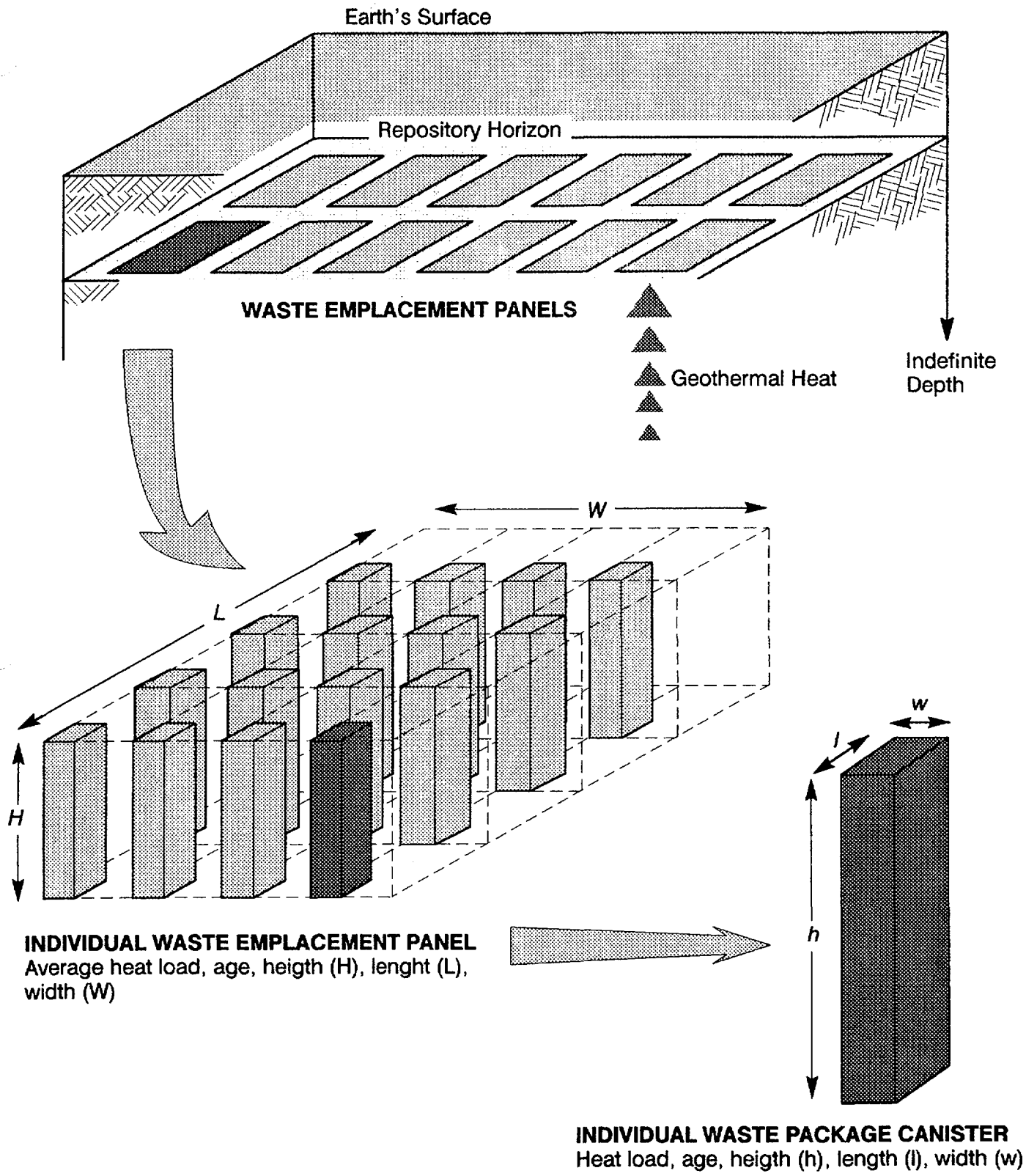

Figure 5–3 Representation of waste package canisters and waste emplacement panels in temperature model

of the instantaneous Green's functions for one waste package is performed numerically, to generalize the temperature to the time-varying heat source term.

Even with high efficiency, it would be very costly to evaluate all of the thousands of waste packages. Instead of calculating the temperature of all waste packages, the program samples a representative number in a Monte Carlo fashion from each panel. For the IPA Phase 2 study, there were a total of 66 waste packages sampled, approximately apportioned to the 17 waste panels according to the spent fuel load per panel. Since the geologic repository is divided into a small number of repository sub-areas (seven in IPA Phase 2), each repository sub-area consists of a whole number of waste panels. The present grouping of the waste packages and panels into individual repository sub-areas is shown in Figure 5–4.

The contribution to the temperature of a sampled waste package from the surrounding waste packages in the panel is simplified greatly by assuming that all waste packages are identical within a panel. The geothermal gradient is assumed to be a constant, so that the temperature of the rock (without the addition of repository heat) would be a function only of depth. In the model, the geothermal temperature addition is constant for each panel, based on the depth below the surface of the earth of the panel center. This temperature is then added to the temperature calculated for the individual waste package.

The temperature model considers only spent nuclear fuel waste. Heat loading, age of waste, and spacing of waste packages may vary between panels, but the model also assumes that all waste is buried instantaneously (i.e., there is no provision for temperature changes during the waste emplacement phase).

Green's Function Model for Individual Waste Package: The parallelepiped representing the waste package has a length equal to the actual cylindrical waste package, but its width and depth are adjusted so that the volume is equivalent to that of the cylindrical waste package. This parallelepiped shape allows the definition of a relatively simple analytical expression for temperature for an instantaneous heat release, whereas the expressions for a cylindrical waste package would be many times more complicated (Carslaw and Jaeger, 1959).

The temperature rise T' at any point x', y', z', and time t', in space relative to the center point of a single parallelepiped, can be calculated by the convolution of a Green's function, for an instantaneous release of heat and a function describing the rate of heat release:

$$T'(x',y',z',t') = \int_0^{t'} G_c(x',y',z',\tau)\, F_c(\tau - t')\, d\tau \ , \quad \textbf{(5–6)}$$

where x', y', z' is the position in the local coordinate system for each parallelepiped, t' is the time relative to the emplacement time for each parallelepiped, G_c is the temperature Green's function for an instantaneous unit release of heat, F_c is the heat-release rate as a function of time evaluated at time $(\tau - t')$, and τ is a dummy parameter of integration. T' is the temperature that would be produced by a single parallelepipe in complete isolation from all others.

For an instantaneous parallelepiped heat source of one Joule in an infinite medium, the Green's function G_c is defined:

$$G_c = \frac{1}{8\varrho C_p}\, G_x \cdot G_y \cdot G_z \ , \quad \textbf{(5–7)}$$

$$G_x = erf\left[\frac{\frac{L}{2} + x}{\sqrt{4kt'}}\right] + erf\left[\frac{\frac{L}{2} - x}{\sqrt{4kt'}}\right] ,$$

$$G_y = erf\left[\frac{\frac{W}{2} + y'}{\sqrt{4kt'}}\right] + erf\left[\frac{\frac{W}{2} - y'}{\sqrt{4kt'}}\right] ,$$

$$G_z = erf\left[\frac{\frac{H}{2} + z'}{\sqrt{4kt'}}\right] + erf\left[\frac{\frac{H}{2} - z'}{\sqrt{4kt'}}\right] .$$

where W, L, and H are the width, length, and height of the parallelepiped, respectively; ϱ = the

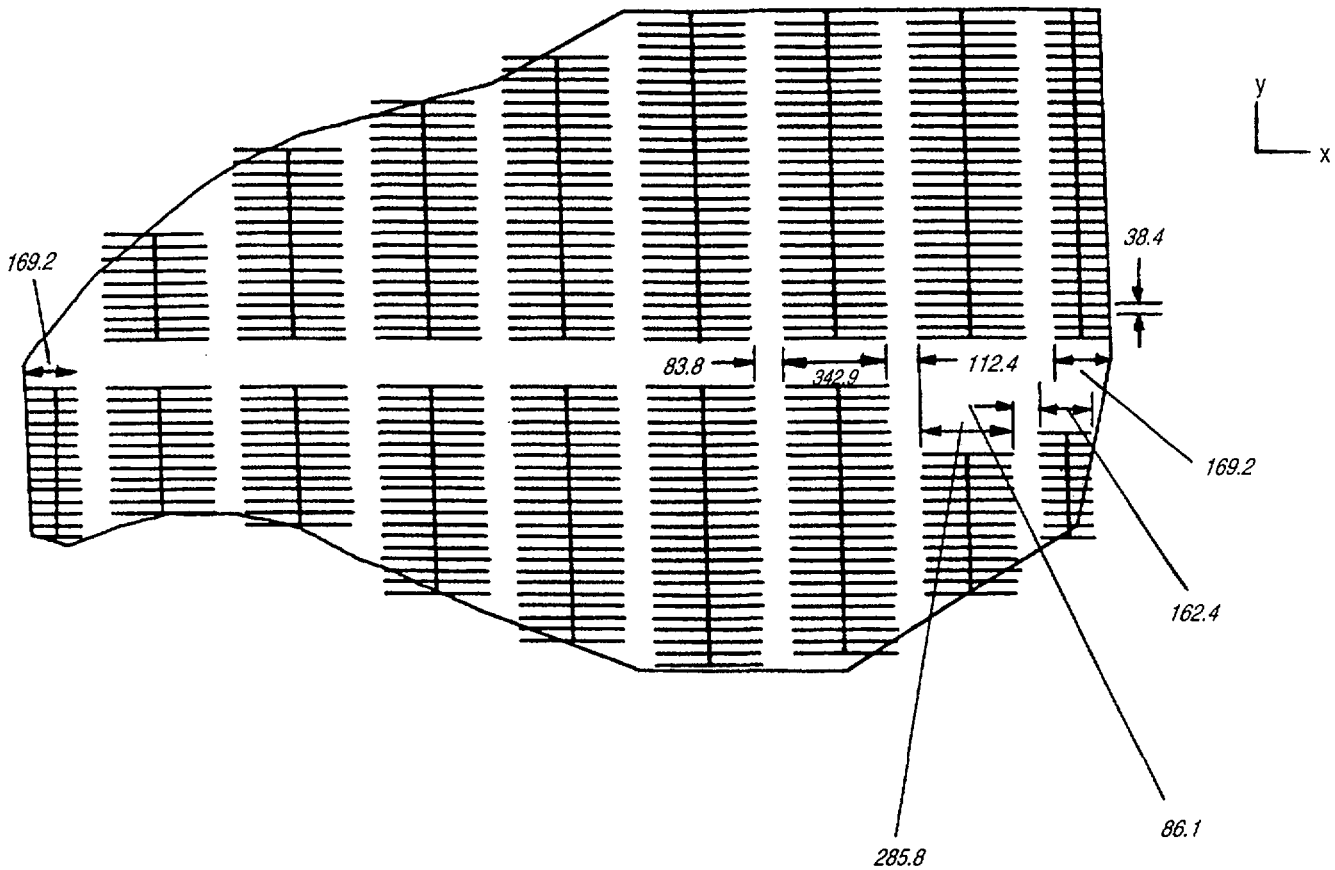

Figure 5–4 Grouping of waste package canisters and waste emplacement panels in temperature model (after Johnson and Montan, 1990)

bulk density of the rock; C_p = the heat capacity of the rock; k = thermal diffusivity of the rock; and *erf* is the error function. The temperature at any point x, y, z in space calculated from the contributions of all the other waste packages in the waste panel, would be:

$$T(x,y,z,t) = \sum_{i=1}^{N_{CL}} T_i'[x_i' - xy_i' - y, z_i' - z, t - t_i'] \quad ; \qquad \textbf{(5–8)}$$

where N_{CL} = number of waste packages in panel L; $x_{i'}, y_{i'}, z_{i'}$ is the location of the center of each parallelepiped; and $t_{i'}$ is the starting time (i.e., time of emplacement) for each parallelepiped.

All waste packages are assumed to be identical within a waste panel, but may vary from panel to panel. Equation (5–7) is used to define a table of temperature versus time and distance from the waste package. Although Green's function for the parallelepiped is not axially symmetric, the isotherms in the x-y plane around the parallelepiped are approximately circular a short distance from the waste package. These tables are then used to efficiently sum the temperature contributions for a large number of waste packages, using Equation (5–8).

Contribution of Other Waste Panels: The waste package temperature contribution from the other waste panels is calculated in a similar manner to the single panel in a waste package field. The panels are represented as rectangular flat plates. The temperature at the earth's surface is held steady, and is parallel to the repository plane.

The Green's function for temperature at any point x, y, z relative to the panel center (x'', y'', z'') contributed by a panel with an instantaneous heat load of one Joule is:

$$G_p = \frac{1}{4\sqrt{\pi k \varrho C_p}} \, G_{px} \cdot G_{py} \cdot G_{pz} \quad , \qquad \textbf{(5–9)}$$

$$G_{px} = erf\left[\frac{\frac{L_p}{2} + x''}{\sqrt{4kt}}\right] + erf\left[\frac{\frac{L_p}{2} - x''}{\sqrt{4kt}}\right] ,$$

$$G_{py} = erf\left[\frac{\frac{W_p}{2} + y''}{\sqrt{4kt}}\right] + erf\left[\frac{\frac{W_p}{2} - y''}{\sqrt{4kt}}\right] , \text{ and}$$

$$G_{pz} = \exp\left[-\frac{(z'' - z^*)^2}{\sqrt{4kt^2}}\right] - \exp\left[-\frac{(z'' + z^*)^2}{\sqrt{4kt^2}}\right] .$$

W_p and L_p are the width and length of the panel, respectively; ϱ = the bulk density of the rock; C_p = the heat capacity of the rock; k = thermal diffusivity of the rock; and z^* = depth of the repository below the surface of the earth.

The temperature caused by the panel for a general heat release rate can be calculated with the convolution integral:

$$T_p(x'',y'',z'',t'') = \int_0^{t''} G_p(x'',y'',z'',\tau'')\, F_p(\tau - t'')\, d\tau \; , \qquad \textbf{(5–10)}$$

where t'' is the time relative to the emplacement time for each panel, and F_p is the heat-release rate as a function of time evaluated at time $(\tau - t'')$, and τ is a dummy variable of integration. The temperature T_p is the temperature that would be produced by a single panel in complete isolation from all others.

The temperature at any point (x, y, z) calculated from the contributions of the individual panels would therefore be:

$$T_p(x,y,z,t) = \sum_{i=1}^{N_L} T_{pi}[x_{pi}-x,\ y_{pi}-y,\ z_{pi}-z,\ t-t_{pi}] \quad , \qquad (5\text{–}11)$$

where N_L = number of panels; x_{pi}, y_{pi}, z_{pi} is the location of the center of each panel; and t_{pi} is the starting time (i.e., time of emplacement) for each panel. The temperature at the sampled waste package locations is the sum of the contributions of the panel temperatures, the other waste packages, and the geothermal gradient.

5.4.2.5 Use of the Temperature Model

For the source term model, the staff is mainly interested in the waste package surface temperature, because that will determine the minimum time at which the waste package can be wetted by liquid water. The boiling point of water at the Yucca Mountain site is about 96°C, but this might vary slightly because of the tilt of the repository causing an elevation difference from one end to the other. Mineral concentrations in the repository water (especially if concentrated in minerals through evaporation) might also alter the boiling point. This "wetting time" is taken to be the time for the onset of corrosion leading to waste package failure and radionuclide release. The coolest point on the waste package's surface will be at its top, so this temperature is used to determine the minimum time for waste package wetting. Waste packages near the center of the repository stay above the wetting temperature for a longer period than those located at the edge of the repository. The temperature generated by this model is also used for ^{14}C source term modeling. The gas flow model used for the ^{14}C analysis (see Section 4.3) also is temperature-dependent, but uses a numerical solution different than the present model.

A total of 66 randomly selected waste packages were used to determine the temperature for the IPA Phase 2 source term model. The number of waste packages was apportioned between the 17 waste panels approximately proportional to the waste loading per panel. The panels were, in turn, arranged into seven repository sub-areas, as shown in Figure 5–4. Temperature for the onset of corrosion was taken as the arithmetic average of all waste packages within a repository sub-area.

5.4.2.6 Extent of Possible Errors in NRC Temperature Model

Some of these possible errors in the approach are discussed below:

- Heat transfer by conduction-only neglects heat transfer by two-phase flow of gas and liquid (i.e., the heat pipe). Neglecting these effects would underestimate heat transfer, possibly leading to predictions of higher temperature, which, in the present case, would be non-conservative because it could lead to later re-saturation and waste package failure from corrosion;
- Thermal properties of the host rock will be a function of water content, which will vary with time, irrespective of fluid movement. Also, the site consists of multiple layers of materials with differing heat-transfer properties;
- The conduction model does not account for heat transfer by convection or radiation across the air gap between the waste package and the host rock; and
- Averaging the waste package temperatures in a repository sub-area would likely overestimate the cooling time for those waste packages on the edge of the repository sub-area farthest from the center of the repository.

5.5 Structural Failure Models

5.5.1 Introduction

The structural failure considered for IPA Phase 2 is buckling failure of the corroded waste package. External dynamic loads from IPA Phase 2 scenarios may be superimposed onto emplaced waste packages, to predict buckling failure. The analytical expressions (Bazant and Cedolin, 1991; and Roark and Young, 1975) used uniform waste package temperature and uniform waste package thickness.

Consistent with structural engineering analysis practice, the waste package is assumed to be a long slender cylinder subject to both axial and radial symmetric loads. The cylinder is uncon-

strained in the radial direction. The stiffening effect contributed by the waste form inside the cylinder and the end plates is conservatively neglected. The material properties are assumed to be functions of temperature. Only static or quasi-static loads are considered.

In a typical buckling analysis, three types of bucklings are analyzed: elastic buckling, elastic-plastic buckling, and plastic buckling. For the IPA Phase 2 buckling analysis, only elastic buckling is considered, because this form of buckling occurs before elastic-plastic and plastic buckling, and it is conservatively assumed that after elastic buckling, corrosion of the buckled waste package would no longer contain the radionuclides inside the waste package. A safety factor (load factor) of 3 is normally used to account for the uncertainty and inconsistency experienced in the use of the elastic buckling formula.

5.5.2 Buckling Evaluation

For a *uniform radial external load* and for a safety factor of 3, assuming a uniform radial external load P_E, elastic buckling occurs when:

$$\frac{P_E}{3} \geq P_{cr} \geq \frac{E}{4(1-v^2)}\left[\frac{t}{R_o}\right]^3 , \qquad (5\text{–}12)$$

where:

P_E = external load (Megapascal—MPa);
P_{cr} = buckling load (MPa);
E = elastic modulus (MPa = 182,000 × [1 - 6 × 10^{-4} × (T - 20)]);
t = wall thickness;
T = current temperature (degrees Celsius—°C);
R_o = radius of cylinder; and
v = Poisson's ratio (0.25 × [1 + 4 × 10^{-4} × (T - 20)]).

The critical thickness t_c can be:

$$t_c = \frac{0.32(a)}{1-(a)} , \qquad (5\text{–}13)$$

where:

$$a = \frac{4P_E\,(1-v^2)^{\frac{1}{3}}}{3E} . \qquad (5\text{–}14)$$

For a *uniform axial external load* in the elastic range, with a safety factor of 3, buckling occurs when:

$$\frac{P_E}{3} \geq P_{cr} \geq \frac{1}{\sqrt{3}}\,\frac{E}{\sqrt{1-v^2}}\,\frac{t}{R} . \qquad (5\text{–}15)$$

The critical thickness is:

$$t_c = \frac{0.32(a)}{1-(a)} , \qquad (5\text{–}16)$$

where:

$$a = \frac{P_E\sqrt{(1-v^2)}}{\sqrt{3}E} . \qquad (5\text{–}17)$$

For a *uniform axial and radial external load*, buckling failure occurs when:

$$\frac{P_E}{3} \geq P_{cr} \geq \frac{0.92\,E}{\left[\frac{L}{R}\right]\left[\frac{R}{t}\right]^{2.5}} , \qquad (5\text{–}18)$$

where L = length of the cylinder.

Failure because of buckling is assumed to occur when the calculated critical thickness t_c is greater than the current (corroded) thickness or, equivalently, when the external load exceeds the critical buckling load.

5.6 Waste Dissolution and Radionuclide Releases

5.6.1 Introduction

Figure 5–5 shows a failed waste package, as represented in *SOTEC*. Water is assumed to enter the waste package and exit again, carrying dissolved radionuclides only (colloids are treated as a subcase of dissolved radionuclides and will be discussed further in Section 5.6.2.5). The model also accounts for radionuclides transported away

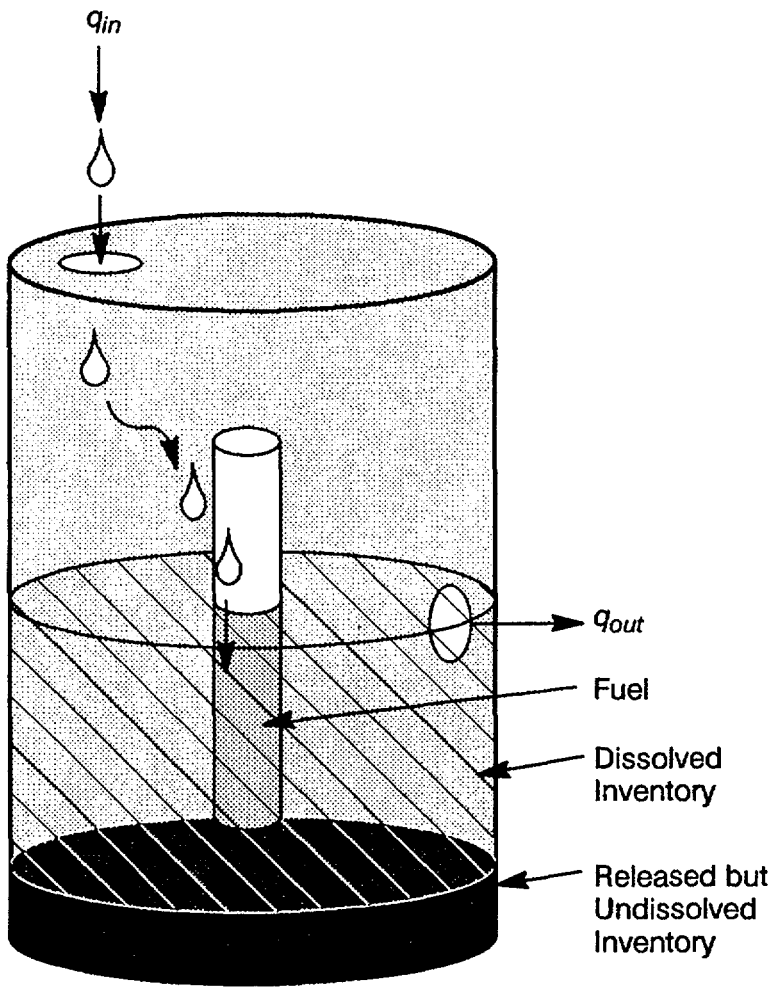

Figure 5–5 Dissolved radionuclide-release model

from the waste package by molecular diffusion through the adjacent rock.

Radionuclides are released from the spent nuclear fuel waste form at a rate determined by the alteration rate of the uranium dioxide fuel, as well as from crud, gap, grain boundary, and cladding. These compartments are shown in Figure 5-6 (see Apted, 1990).

Radionuclides can leave the waste package at a rate no greater than that allowed by the solubility of the element in the water. *SOTEC* allows for radioactive decay of each radionuclide and production from previous elements in the chain. The inventory of the unaltered uranium dioxide is calculated analytically by the Bateman equations (Bateman, 1910). The inventory of released radionuclides inside the waste package is calculated by numerical integration.

Molecular diffusion is accounted for in *SOTEC* by assuming a spherical source with no advection, and then adding the diffusive component to the advective component of transport out of the waste package. In the diffusion model, the inner surface of the sphere is held at the concentration of radionuclides in water inside the waste package. The concentration a fixed distance away from the waste form is held at zero. The diffusion model accounts for molecular diffusion, retardation, and radioactive decay, but does not allow for production from a parent radionuclide.

On waste package failure, water is assumed to begin entering the waste package at a rate q_{in}. There is no outflow until a critical value V_{max} in the waste package is exceeded, at which point the outflow is:

$$q_{out} = q_{in}\, k_q \left(\frac{V}{V_{max}} \right)^2 , \qquad (5\text{–}19)$$

where k_q is an arbitrary "weir" coefficient chosen so that the numerical integration of volume occurs smoothly and converges to steady state quickly once the maximum volume is reached; V is the volume of water; and V_{max} is the volume of water at which overflow occurs. For the present model, $k_q = 0.8$.

5.6.2 Waste Dissolution

5.6.2.1 Effective Waste Package Failure Time

No dissolved radionuclides can leave the waste package until it is perforated and water can enter and leave. The waste package fails from damage or corrosion at time t_{fail}. The temperature drops below the boiling point at time t_{cool}. The model assumes that no water can enter or leave the waste package until $t > t_{cool}$ and $t > t_{fail}$. The effective time at which fuel degradation can begin, t_{ftc}, is given by:

$$t_{ftc} = MAX\,(t_{cool},\ t_{fail}) , \qquad (5\text{–}20)$$

No dissolved radionuclides can leave the waste package until it is perforated and water can enter and leave.

Upon failure, water flowing into the waste package is assumed to come into intimate contact with the fuel. Radionuclides are released either instantaneously or congruently, with the alteration of the UO_2 fuel. On contact with water, those radionuclides being released congruently are released at a rate tied to the alteration rate of the UO_2 and the inventory of remaining radionuclides in the fuel. The leaching time t_{leach} is defined as:

$$t_{leach} = \frac{1}{(ff \times alt)} , \qquad (5\text{–}21)$$

Where *alt* is the fixed alteration rate of the wetted fuel, and *ff* is the fraction of fuel that is wetted at any time, *SOTEC* assumes that all fuel in the waste package will eventually be contacted and consumed, even though only part of it is wetted at any given time.

No alteration of the spent nuclear fuel occurs until t_{ftc}, and release from the spent nuclear fuel continues for t_{leach} years beyond t_{ftc}. The release stop time t_{lt} is defined as:

$$t_{lt} = t_{leach} + t_{ftc} . \qquad (5\text{–}22)$$

Subsequent to alteration of all the spent nuclear fuel, at time = t_{lt}, additional release from the waste package may continue from the released, but undissolved inventory (discussed in 5.6.2.2).

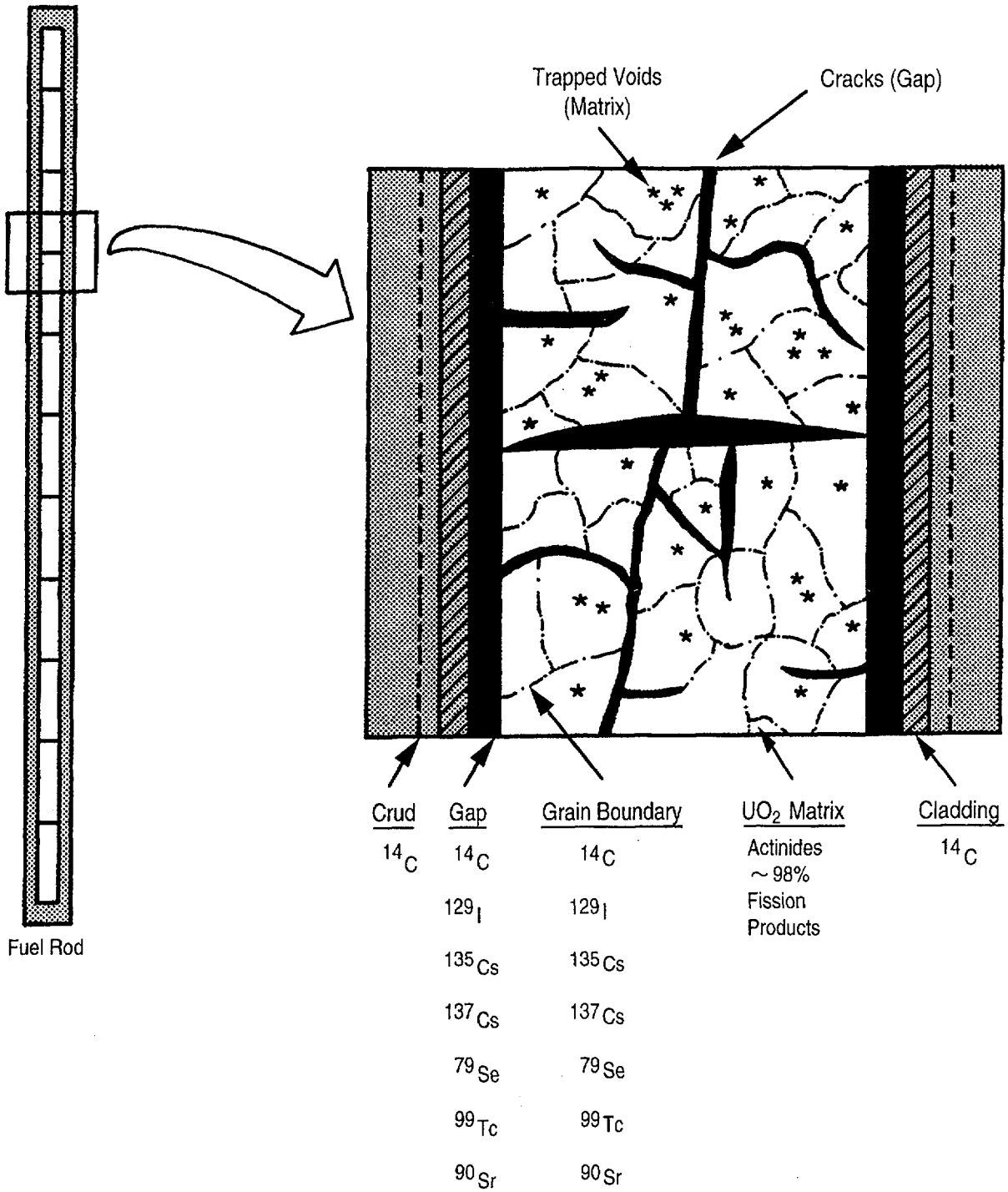

Figure 5–6 Locations of radionuclides in spent nuclear fuel

The model does not consider that oxidation of the fuel in the dry state affects liquid release. Ranges of solubilities used in the source term module are presented in Appendix A.

5.6.2.2 Solubility Limited Release

As the fuel is altered, it releases its radionuclide inventory at the alteration rate into the released but undissolved (RBU) inventory. This assumption is generally called the "congruent-release" mode, and assumes that the radionuclides are contained in the matrix of the UO_2. Radionuclides not contained in the matrix, but collected at the grain boundaries and in the cladding gap, are assumed to be part of the RBU inventory at the moment of failure.

Release of radionuclides from the waste package is possible only in the dissolved state. The inventory of all isotopes of an element are collected, and the model determines if the hypothetical concentration of that element is greater than or less than the solubility limit. If the hypothetical concentration exceeds the solubility, then the actual concentration of the waste package water is held at the solubility limit. Otherwise, the concentration of the waste package water is the RBU inventory divided by the volume of water V in the waste package. There is an assumed minimum volume of water of 1 liter in the waste package, to avoid division by zero. The concentration of the element in the waste package water is reapportioned to the isotopes, when determining the release rates.

The mass of each radionuclide remaining in the waste package water and RBU inventory is calculated by a material balance describing the inputs of:

- Radionuclide released from the fuel;
- Production from radioactive decay of another radionuclide;
- Losses from radioactive decay;
- Advective flow; and
- Diffusion.

5.6.2.3 Advective Mass Transfer

Advective mass transfer from the waste package occurs at the rate at which water leaves; that is,

$$W_{out,i} = C_i q_{out} ,$$

where C_i is the aqueous concentration of radionuclide i. The radionuclide concentration also is the boundary condition for the diffusive mass transfer from the waste package.

5.6.2.4 Diffusive Mass Transfer

The model assumes that mass can be transferred by molecular diffusion, irrespective of convective mass transfer from flowing water into and out of the waste package. Diffusive mass transfer is from an assumed spherical source into a domain unaffected by other waste packages and the flow rate of liquid water through the waste package and the surrounding rock. The boundary conditions are the concentration of water inside the waste package at the inner spherical boundary and zero concentration at the outer radius of the spherical boundary. The differential equation solved is:

$$K \frac{\partial C}{\partial t} = D \frac{1}{r^2} \frac{\partial}{\partial r} \left(r^2 \frac{\partial C}{\partial t} \right) - \lambda KC , \qquad (5\text{–}23)$$

where K is the retardation coefficient, C is the concentration, t is time, D is the coefficient of molecular diffusion, r is radius, and λ is the decay coefficient. The present formulation considers only decay of the radionuclide in question, and does not consider generation of the radionuclide from chain decay of other radionuclides.

The radius of the source sphere for diffusional mass transfer was chosen so that the surface area was equal to that of the cylindrical waste package. The spherical geometry with no advection allows a relatively simple solution either numerically or analytically, since it is one-dimensional. The present formulation for molecular diffusion is an approximation, since the waste package is not a sphere, and advective mass transfer is not considered in its solution. The staff believes that the formulation is conservative for the following reasons:

- The concentration of the inner boundary is held constant at the concentration inside the

waste package, neglecting the substantial barrier of the waste package, itself;

- Neglecting the production of the radionuclide from chain decay of other radionuclides causes the concentration gradient to be steeper than it would be if production from other chains were allowed (for those radionuclides in chains); and

- Setting the concentration at the outer boundary at zero causes the gradient to be steeper than if the effect of buildup from other waste packages were considered.

The numerical solution to Equation (5-23) is obtained in a finite difference grid with varying grid spacing. Diffusion coefficient and effective porosity may vary in each finite difference cell. Each solution requires the solution of N linear algebraic equations, where N is the number of increments in the finite difference grid. The equations are tri-diagonal, and several of the terms do not vary with time. The solution of the equations with the Thomas algorithm is quick and efficient (Lapidus, 1962).

The rate of change of mass m_i of each radionuclide in the waste package is determined by the following equation:

$$\frac{\partial m_i}{\partial t} = m_{i-1}\,\lambda_{i-1} - m_i\,\lambda_i - c_i\,q_{out} + w_i - w_{di}\ . \qquad \textbf{(5-24)}$$

The rate of release of radionuclide i from the fuel is defined:

$$w_i = m_i \times ff \times alt\ . \qquad \textbf{(5-25)}$$

The flux of radionuclide i leaving the waste package by molecular diffusion is calculated from the concentration gradient:

$$w_{d_i}(t) = 4\pi r^2 \epsilon D\,\frac{(C_{0_i} - C_{1_i})}{\Delta R_1}\ , \qquad \textbf{(5-26)}$$

where C_{0_i} is the waste package concentration, C_{1_i} is the concentration at the first grid point, and ΔR_1 is the grid spacing between the innermost two points. The diffusive flux $w_{d_i}(t)$ is subtracted from the inventory, when evaluating Equation (5-24) by numerical integration.

The parameters of water influx q_{in}, alteration rate alt, wetted fraction ff, diffusion coefficients, and maximum volume of water in the waste package V_{max} effectively allow the selection of several modes of potential release; e.g., a small V_{max} ensures the so-called "wet drip" case (Pigford *et al.*, 1992), whereas a large V_{max} leads to the "bathtub" case. Very low flow would correspond to the "moist continuous" case where the only mechanism for liquid release would be diffusion.

5.6.2.5 Treatment of Colloids

Colloidal radionuclides are potentially important at the Yucca Mountain site. Radionuclides such as plutonium have large inventories and are long-lived, but have generally low solubilities. Under conditions of a high alteration rate of the fuel matrix, there is evidence that they might form colloids when released from spent nuclear fuel (Wilson, 1990). *SOTEC* does not explicitly handle the release of colloids from spent nuclear fuel. A mechanistic treatment of the phenomena leading to growth of colloids from supersaturated liquids may be incorporated into the next update of *SOTEC*. In IPA Phase 2, colloids are considered to be part of the dissolved inventory, and are treated in the calculations by adjusting the solubility upwards.

5.6.3 Calculations of Gaseous Releases of ^{14}C

5.6.3.1 Introduction

Carbon-14 is a potentially important radionuclide at the partially saturated Yucca Mountain site because, in the gaseous form, it could migrate quickly to the atmosphere. Its abundance in spent nuclear fuel—roughly 10 times the present limit for cumulative releases of radioactive material—and its long half-life of 5720 years, contribute to the importance of the potential issue.

Carbon-14 is generated in nuclear fuel by the neutron activation of ^{14}N, ^{13}C, and ^{17}O contained in the fuel and other materials in the reactor core (Van Konynenburg *et al.*, 1984). The main reservoirs for ^{14}C are the cladding, the cladding/fuel gap and grain boundaries, and the fuel itself. There will be little ^{14}C in vitrified defense waste stored at the site.

Park (1992) estimates the inventories of ^{14}C in both spent nuclear fuels from boiling water reactors (BWRs) and pressurized water reactors (PWRs), as shown in Table 5-2. Currently, Park also estimates that there will be 70,000 MTHM of spent nuclear fuel in the repository, consisting of 22,500 MTHM of BWR fuel and 40,500 MTHM of PWR fuel. The inventory of ^{14}C is estimated to be 78,000 curies.

Van Konynenburg (1991) reports that the chemical forms of the ^{14}C inventories are uncertain, but that they are believed to exist partially as elemental carbon, carbides, and oxycarbides in the fuel, and as dissolved carbon and carbides in the metal. The form in the cladding oxide is unknown, but is at least partially in the reduced state.

Most of the ^{14}C in the fuel, cladding and hardware must first oxidize in order to be released in the gas pathway. Although elemental carbon is generally stable at low temperatures, thermodynamics in air favors the formation of gaseous compounds such as CO_2 and methane. Furthermore, carbon does not form protective oxide layers like corrosion-resistant metals. Van Konynenburg *et al.* (1987) noted that $^{14}CO_2$ was released from cladding in an oxidizing environment with a radiation level of 10,000 rad/hour and a temperature of 275°C. Kopp and Munzel (1990) showed $^{14}CO_2$ releases from ^{14}C-doped zirconium sheets at temperatures as low as 200°C, with virtually no radiation, and in an atmosphere of mostly argon with air and water impurities. In very pure argon, however, there was no measurable release of ^{14}C. The dependence of release on the O_2 content of the gas indicates that carbon was undergoing oxidation in the impure argon. Although kinetic considerations might restrict the formation of gaseous compounds of the ^{14}C in the fuel, the model conservatively assumes that any ^{14}C available to become oxidized is converted to $^{14}CO_2$.

The ^{14}C gas release component of *SOTEC* considers that $^{14}CO_2$ is released from the fuel, cladding, and hardware compartments on failure of the waste package. Several of the release mechanisms depend on the presence of oxygen. Although there may be small quantities of oxygen initially present in the waste package as impurity in the inert gas or as water, most of the oxidation would not occur before waste package failure.

The ^{14}C release model makes the following conservative or simplifying assumptions:

- There can be no release of gas before waste package failure;
- Cladding does not protect the spent nuclear fuel from oxidation;
- Once the waste package fails, it provides no resistance to the inflow of air or the outflow of CO_2;
- On waste package failure, a "prompt release fraction" of approximately 2.5 percent (Van Konynenburg *et al.*, 1991) of the total inventory is released from the waste package instantaneously;
- On waste package failure, cladding and structural metals undergo oxidation, and release ^{14}C at the rate that the metal oxidizes; and
- On waste package failure, oxygen diffuses into the spent nuclear fuel and oxidizes the ^{14}C to $^{14}CO_2$, which then diffuses out to the waste package.

The bases for the assumed release mechanisms are discussed in the following paragraphs.

5.6.3.2 Prompt Release Fraction

On failure of the waste package and cladding (no credit taken for the cladding integrity), a portion of the total ^{14}C inventory estimated at about 2.5 percent (Van Konynenburg *et al.*, 1991) would be released quickly (i.e., within a few hundred years). This inventory represents the ^{14}C held loosely on the cladding and in the cladding/fuel gap and grain boundaries. Experiments on ruptured spent nuclear fuel indicate that on cladding failure, 0.5 percent of the inventory is released from the fuel/cladding gap (Wilson, 1990). The initial layer of oxide and crud on the cladding is the other readily available inventory of loosely held ^{14}C. This layer holds a relatively elevated level of ^{14}C, some produced by activation *in-situ* but, some probably picked up from the circulating water within the reactor. The chemical form of this ^{14}C is uncertain, but experiments in which cladding was heated indicate that the release rate of ^{14}C appears to be controlled by a diffusion process from a layer of finite thickness.

Table 5–2 Adjusted ^{14}C Content in Spent Nuclear Fuel (in Ci/MTHM) (after Park, 1992)

Type	*Burnup (MWd/MTHM)*	*UO_2*	*Zircaloy*	*Hardware*	*TOTAL*
BWR	35,000	0.69	0.48	0.13	1.3
PWR	40,000	0.73	0.22	0.26	1.21
Average	——	0.72	0.31	0.21	1.24

Smith and Baldwin (1989) showed that as much as 2 percent of the spent nuclear fuel ^{14}C inventory was released in zircaloy cladding heated to 350°C for 8 hours. The release rate is an Arrhenius relationship consistent with diffusion out of a layer of finite thickness, with an activation energy of between 19 and 25 kilocalories/mole. However, the rate of release depended on the presence of air. In argon with a trace of air (50 parts-per-million oxygen), release rates were lower by a factor of about 10, indicating that the carbon was in a reduced state and had to be oxidized before being released.

If it is considered that the release of ^{14}C from the cladding oxide layer is governed by the diffusion mechanism, it is possible to estimate the upper bound of release rate for the temperature range of interest, approximately 350° to 100°C. One-dimensional molecular diffusion through the film of thickness $2L$ can be expressed by the partial differential equation:

$$\frac{\partial C}{\partial t} = D \frac{\partial^2 C}{\partial x^2} , \qquad (5\text{–}27)$$

where D is the diffusion coefficient, C is the concentration of $^{14}CO_2$, and x is the distance measured from the edge of the cladding toward the center. The boundary conditions that apply to Equation (5–27) are:

$$C = C_0 \; at \; x = 0 \; ,$$

$$\frac{\partial C}{\partial x} = 0 \; at \; x = L \; (center \; of \; film) \; .$$

Equation (5–27) has the following solution (Carslaw and Jaeger, 1959):

$$\frac{C}{C_0} = 1 - \frac{4}{\pi} \sum_{n=0}^{\infty} \frac{-1^n}{2n+1} e^{\frac{(2n+1)^2 \pi^2 \tau}{4}} \cos\left(\frac{(2n+1)\pi\zeta}{2}\right) , \qquad (5\text{–}28)$$

where $\tau = Dt/L^2$, $\zeta = x/L$, and L is one-half the cladding thickness.

For $Dt/L^2 = 1.5$, C/C_0 is close to unity, meaning nearly all $^{14}CO_2$ would have diffused out of the system. Relying on experimental data of Smith and Baldwin (1989), which indicate virtually complete release of ^{14}C from the oxide layer in 8 hours at 350°C, the fraction removed from the sample at other temperatures is related to the parameter Dt/L^2. Time to reach an equivalent concentration profile is inversely proportional to the diffusion coefficient; that is:

$$\frac{D_1 t_1}{L_1^2} = \frac{D_2 t_2}{L_2^2} , \qquad (5\text{–}29)$$

or for constant film thickness,

$$t_2 = t_1 \frac{D_1}{D_2} . \qquad (5\text{–}30)$$

The ratio D_1/D_2 can be related by the Arrhenius equation to be:

$$\frac{D_1}{D_2} = e^{-\frac{E}{R}\left(\frac{1}{T_2} - \frac{1}{T_1}\right)} \qquad (5\text{–}31)$$

The time for an equivalent release at lower temperatures is illustrated in Table 5–3, assuming $t_1 = 8$ hours, at 350°C, for $E = 19$ and 25 kilocalories/mole. R is the gas law constant, and the subscripts refer to the two different temperatures.

Table 5–3 Diffusion of $^{14}CO_2$ from Surface Oxide

Temperature (°C)	*t_2 (years) E = 19 (Kcal/mole)*	*t_2 (years) E = 25 (Kcal/mole)*
350	0.00091	0.00091
300	0.0035	0.0053
250	0.017	0.043
200	0.12	0.55
150	1.3	13
100	27	690
75	169	7800

Equation (5–30) was used to estimate t_2, for a range of activation energies and temperature.

Results presented in Table 5–3 indicate that for temperatures as low as 75°C, release of the ^{14}C by diffusion out of the oxide film would be nearly complete within 10,000 years, and possibly much less time. Furthermore, there may be sufficient oxygen present in an unfailed waste package as an impurity, or from the radiolysis of water to allow partial escape of $^{14}CO_2$ from the cladding into the waste package before failure. On the other hand, there are few direct data on $^{14}CO_2$ releases from zirconium at low temperature.

The observation that release from the cladding depended on the presence of oxygen indicates that the ^{14}C may be in a reduced state in the oxide film. The oxidation to $^{14}CO_2$ might depend on the combined effects of temperature, oxidizing environment, and ionizing radiation. Considering the uncertainties, the staff must assume a conservative model for release of ^{14}C from the oxide layer. In the present model, the entire quantity of ^{14}C in each waste package contained in the "prompt-release fraction"—2.5 percent of the spent nuclear fuel inventory—is assumed to be released to the geosphere at the time of waste package failure.

5.6.3.3 Cladding Integrity

Protection of the spent nuclear fuel by the cladding has been ignored in the IPA Phase 2 source term models for liquid and gaseous release. The staff believes this to be a conservative assumption, but it is difficult to prove, to the contrary,that the cladding would survive for long periods of time. Factors in favor of cladding integrity are:

- Cladding is usually a highly corrosion-resistant zirconium alloy (but some of the older fuel was clad in stainless steel); and
- Most fuel rods emplaced in the waste packages will be intact, but some will have a small number of undetected pinholes or cracks in the cladding, generally considered to be lower than 1 percent.

Factors in favor of loss of cladding integrity are:

- Under circumstances of sufficiently high temperature in an oxidizing environment to cause oxidation of the fuel to lower-density U_3O_8, fuel rods with cladding defects are known to split further. At temperatures abo 250°C, fuel oxidation was high enough to cause propagation of defects, but below 250°C, the defects were not observed to propagate (Einziger and Kohli, 1984). Those defected rods that do split allow oxygen to further oxidize fuel, causing the defect to spread down the length of the fuel rod. The waste package must first fail, to allow oxidation of the fuel and further splitting of the fuel rods;
- While cladding is highly corrosion-resistant, there are factors, such as hydride reorientation, that could lead to failure;
- Cladding could fail by mechanical breakage caused by handling errors, waste package buckling, or earthquakes; and
- The fuel rods will be pressurized up to 50 atmospheres, so the cladding will be under stress.

5.6.3.4 Release of ^{14}C from Oxidation of Cladding

The cladding oxidation layer is about 10 microns thick, initially. The cladding metal itself is on the

order of 0.5 to 1.0 millimeter thick, and contains the bulk of the ^{14}C in the cladding. The zirconium alloy generally used for cladding is highly corrosion-resistant, but in an oxidizing environment with elevated temperatures, could oxidize. Upon oxidation, the ^{14}C contained in the metal as elemental carbon, carbides, and oxycarbides could be released as $^{14}CO_2$.

Studies of zircaloy degradation in air have been performed in connection with dry-cask storage (Einziger and Kohli, 1984). The gain in weight of Zircaloy samples, attributed to oxidation, has been determined to proceed in two modes. The first mode, known as the "pre-transition" phase, shows weight gain proportional to the cube root of time until the oxide thickness reaches a critical value. The "post-transition" phase shows a linear weight gain, for oxide-layer thickness, greater than the critical value. It is most likely that the cladding reaches post-transition within the reactor core.

Post-transition cladding oxidation appears to follow an Arrhenius relationship (Garzarolli *et al.* 1980), that is:

$$\frac{\Delta w}{\Delta t} = AE^{-\frac{E}{RT}} \qquad \textbf{(5–32)}$$

where A is the coefficient, milligrams/square decimeter; E = activation energy, calories/mole; R = gas constant, 1.987 calories/mole/°K; and T = absolute temperature, Garzarolli *et al.* presents several empirical formulas for the post-transitional weight gain because of oxidation. Values of $A = 1.87 \times 10^7$ milligrams/square decimeter, and E = 22,200 calories/mole, were chosen from the formulas presented by Garzarolli *et al.* because they represented the most pessimistic model. The release model for cladding oxidation makes the following additional assumptions:

- $^{14}CO_2$ is released from the zircaloy at the rate that the metal oxidizes. Zirconium is a strong oxygen getter, so oxygen concentrations available to oxidize carbon would be limited until the zirconium oxidizes; and

- Other irradiated structural metal buried with the waste (other than the waste package itself) is conservatively included with the zircaloy cladding as a source of ^{14}C.

5.6.3.5 Release from UO_2

The largest inventory of ^{14}C is contained in the spent nuclear fuel tied up as solid solutions, elemental carbon, carbides, and oxycarbides. Investigations of the oxidation of grains of spent nuclear fuel indicate that the rate of oxidation is controlled by diffusion through at least two barriers; the grain boundaries, and the film of oxidized fuel surrounding each grain (Einziger and Buchanan, 1988). Irradiated spent nuclear fuel contains numerous cracks which allow gas to easily permeate the mass. The smallest scale of interest is the individual grains, that are on the order of 10 to 20 microns in diameter.

The model for release of ^{14}C from spent nuclear fuel makes the following assumptions:

- UO_2 oxidizes at a rate controlled by the diffusion of oxygen through the grain boundaries and film of higher oxide;

- The oxygen concentration at the oxide/fuel boundary will be zero because all oxygen is being consumed by fuel oxidation;

- ^{14}C can oxidize only after the fuel oxidizes;

- $^{14}CO_2$ will be released from the spent nuclear fuel at the rate that the spent fuel oxidizes;

- $^{14}CO_2$ must diffuse outward through the oxide film and grain boundaries; and

- Concentration profiles for both oxygen and $^{14}CO_2$ are at steady state, although the position of the boundary changes with time.

5.6.3.5.1 Fuel Oxidation Model

The present model assumes that the fuel mass in each waste package can be represented by two concentric spheres, as shown in Figure 5–7. The outer sphere represents the diffusion barrier for the grain boundaries, and has the equivalent spherical diameter of a fuel fragment, about 0.2 centimeter. The inner sphere represents the diffusion barrier through the oxide film on the surface of the fuel grain, with a diameter of about 20 microns. The boundary conditions for the model are zero oxygen concentration at the fuel/oxide

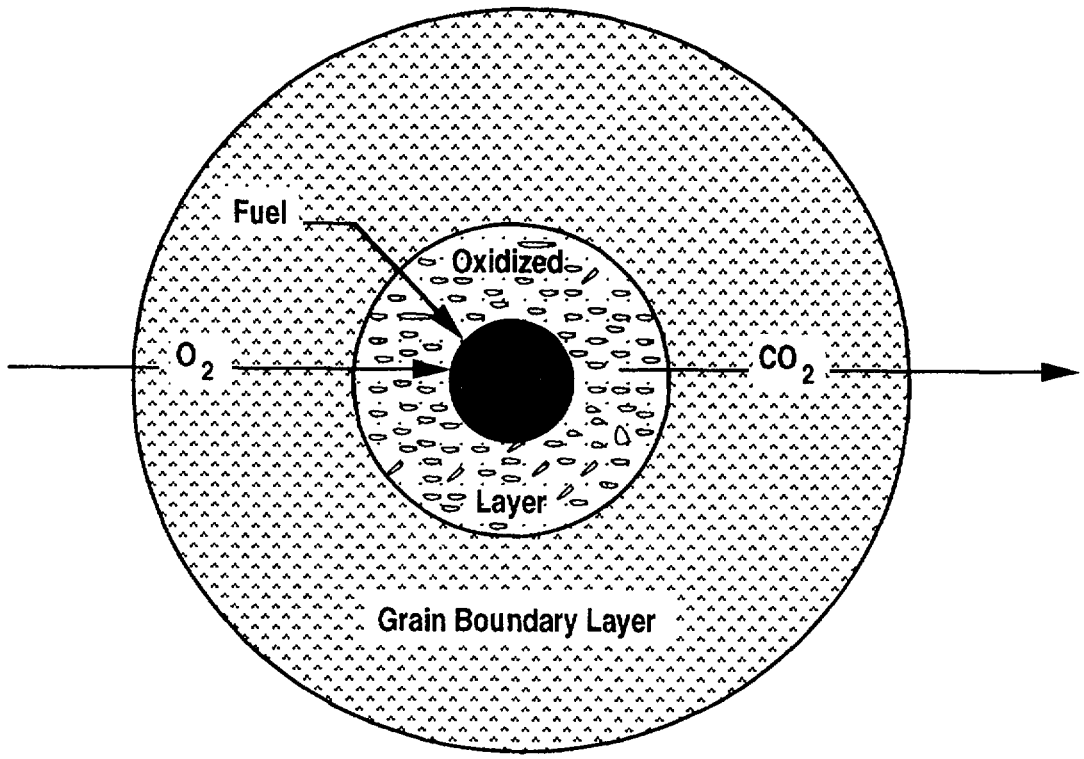

Figure 5–7 ^{14}C gaseous release model

interface and atmospheric oxygen concentration at the outer diameter.

Diffusion of oxygen through the fuel grain will be governed by the following partial differential equation:

$$\frac{\partial C}{\partial t} = \frac{1}{r^2}\frac{\partial}{\partial r}\left(r^2 D \frac{\partial C}{\partial r}\right), \qquad (5\text{–}33)$$

where C = oxygen concentration, t = time, r = radius from the center of the sphere, and D = diffusion coefficient.

The diffusion coefficient D is a function of temperature, and differs for the oxide layer and grain boundary layers. The boundary between the spent fuel grain and the oxide layer changes as the oxide layer grows, making this a moving boundary problem. The rate that the boundary recedes is governed by the diffusion rate of oxygen at the interface:

$$\frac{\partial r}{\partial t} = N_{ox}\frac{D}{\varrho_{ox}}\frac{\partial C}{\partial r}\bigg|_{r=r'}, \qquad (5\text{–}34)$$

where: r' = radius of fuel/oxide interface; D = diffusion coefficient in the oxide, square centimeters/year; and ϱ_{ox} is the density of the oxide, moles/cubic centimeter. The term N_{ox} is the conversion factor for UO_2, in terms of moles UO_2 oxidized per mole O reaching the boundary. X-ray diffraction analyses of samples of oxidized fuel indicate that for the temperature ranges likely to be encountered in the repository, most of the oxide formed will be U_4O_9, although stoichiometrically, the oxide appears to be U_3O_7, because of excess oxygen loosely held by the lattice (Einziger, 1992). For the purposes of the present analysis, N_{ox} will be taken to be 3 (i.e., 3

moles of UO_2 will be oxidized by 1 mole of O (1/2 mole O_2)).

5.6.3.5.2 Model for Oxygen and $^{14}CO_2$ Diffusion

The model for the release of $^{14}CO_2$ is similar to the UO_2 oxidation model. Diffusion of $^{14}CO_2$ through the fuel grain boundary layer and oxide layer will be governed by the following partial differential equation:

$$\frac{\partial C_c}{\partial t} = \frac{1}{r^2}\frac{\partial}{\partial r}\left(r^2 D \frac{\partial C_c}{\partial r}\right) - \lambda C_c \quad , \qquad (5\text{–}35)$$

where C_c = $^{14}CO_2$ concentration, t = time, r = radius from center of fragment, and λ is the decay coefficient for ^{14}C. The outer boundary conditions are:

$$C_c = 0 \; at \; r = R_1.$$

At the inner boundary, $^{14}CO_2$ enters the oxide layer from the just-oxidized fuel. The gradient of $^{14}CO_2$ concentration is adjusted to account for diffusion:

$$\left.\frac{\partial C_c}{\partial r}\right|_{r'} = \frac{3M}{4\pi r_0^3 D_0}\frac{dr}{dt} e^{-\lambda t} \quad , \qquad (5\text{–}36)$$

where M is the initial inventory of ^{14}C and D_o = diffusion coefficient in the oxide layer. The ^{14}C diffusion model depends on the UO_2 oxidation model, to provide the position of the moving boundary, and the source flux of $^{14}CO_2$, at the inner boundary, as the oxide layer grows. Release of $^{14}CO_2$ at the outer boundary of the fragment is calculated from the concentration gradient at that boundary:

$$q_{^{14}C} = 4\pi R_1^2 D_1 \left.\frac{\partial C_c}{\partial r}\right|_{R_1} , \qquad (5\text{–}37)$$

where q = the rate of release from the fragment, curies/year and D_1 = the diffusion coefficient in the boundary diffusion layer.

5.6.3.5.3 Numerical Solutions

A simple semi-analytical solution to Equation (5–35) was developed, which depends on the assumption that the O and $^{14}CO_2$ gradients are at steady state. At steady state, Equation (5–36) for O concentration reduces to:

$$\frac{\partial}{\partial r}\left(r^2 \frac{\partial C}{\partial r}\right) = 0 \quad , \qquad (5\text{–}38)$$

which has the general solution:

$$C = \frac{A}{r} + B \quad , \qquad (5\text{–}39)$$

where A and B are constants.

The boundary condition for oxygen is atmospheric concentration at the surface of the sphere and zero concentration at the boundary between the U_3O_7 and the fuel:

$$C = C_o, \text{ at } r = R_1, \text{ and}$$
$$C = 0, \text{ at } r = r'.$$

Between r' and R_o, diffusion coefficient D_o applies, and between R_o and R_1, D_1 applies. For a composite hollow sphere between r and R_1, therefore, the mass rate of oxygen transport to the surface of the fuel at steady state is:

$$flux = 4\pi R_1^2 D_1 \left.\frac{\partial C_c}{\partial r}\right|_{R_1}$$
$$= \frac{4\pi(C_o - C_1)}{\left[\frac{1}{D_o}\left(\frac{1}{r'} - \frac{1}{R_o}\right) + \frac{1}{D_1}\left(\frac{1}{R_o} - \frac{1}{R_1}\right)\right]} . \qquad (5\text{–}40)$$

The rate of growth of the film is related to the flux of oxygen. In terms of the oxidation rate of the fuel surface, Equation (5–40) becomes:

$$\frac{dr'}{dt} = \frac{(C_o - C_1)\, N_{ox}}{\left[\frac{1}{D_o}\left(\frac{1}{r'} - \frac{1}{R_o}\right) + \frac{1}{D_1}\left(\frac{1}{R_o} - \frac{1}{R_1}\right)\right] r'^2 \varrho_u} \quad , \qquad (5\text{–}41)$$

where:

C_0 = the concentration at the surface of the fuel, taken here to be zero; and

C_1 = concentration of oxygen at the surface of the fuel, taken here to be

the volumetric concentration in the atmosphere, 0.2 moles/22,400 cubic centimeters.

The rate of growth depends on R_0 and the diffusion coefficients D_0 and D_1, which are functions of fuel temperature. The temperature of the fuel is estimated from the temperature of the waste package (generated from the *CANT2* program externally) corrected with an empirical formula determined from a calculational exercise on fuel temperature shown in Figure 5-8 (O'Neal *et al.*, 1984). The growth of the oxide layer is calculated by numerically integrating Equation (5-41).

$^{14}CO_2$ generated at the oxide/fuel interface must diffuse out through the oxide and grain boundary layers to leave the fuel fragment. In the steady-state assumption, the gradient of $^{14}CO_2$ in the radial direction is steady, but because the ^{14}C decays radioactively, the gradient will be somewhat different than for a non-decaying substance. Although it is possible to have a separate model for diffusion of $^{14}CO_2$ at steady state, it would be much more complicated (involving series of Bessel functions) than the model necessary for the diffusion of the non-decaying oxygen. Numerical experiments on a somewhat simpler problem however, demonstrated that the error in neglecting the decay of ^{14}C in the diffusing layer was negligible, and therefore the rate of release of $^{14}CO_2$ to the waste package was taken as its rate of production at the oxide boundary.

5.6.3.5.4 Overall ^{14}C Model Conservatism

The ^{14}C release rate model is considered to be conservative for the following reasons:

- The protection of the spent nuclear fuel from oxidation afforded by the cladding is ignored in IPA Phase 2. Zircaloy is a highly corrosion-resistant material, and it is likely that it would protect the fuel, after waste package failure, for a substantial period of time. Protection of the fuel even for a few hundred years would have a substantial impact on the calculated release rate, because the greatest potential for release is the period during which the fuel temperature is highest;

- Most of the ^{14}C in the fuel, cladding, and hardware is likely to be in a reduced state, and must first become oxidized to be released in the gas pathway, although thermodynamics in air favors the formation of gaseous compounds such as CO_2. Although kinetic considerations might restrict the formation of gaseous compounds of the ^{14}C in the fuel, the model conservatively assumes that any ^{14}C available to be oxidized is converted to $^{14}CO_2$;

- The model assumes there is no resistance of $^{14}CO_2$ once it is released from the fuel fragment (i.e., there is no resistance for diffusion through the long length of the failed fuel rod, or through pinhole failures of the waste package). This conservatism is relatively less important for the far-field release calculations because of the long periods involved; that is, diffusion and barometric pumping could allow virtually all $^{14}CO_2$ to escape to the geosphere, even for relatively small failure holes. Resistance to release from the waste package might be more important in evaluating compliance with the EBS subsystem requirements set forth in 10 CFR 60.113, which are more sensitive to short-term rates of release; and

- A portion of the ^{14}C in the spent nuclear fuel may be in a chemical form that is not easily released. Experimental data in which spent nuclear fuel was heated to temperatures of up to 450°C in oxygen indicated that up to half of the ^{14}C remained in the solid, and was not released as $^{14}CO_2$ (Van Konynenburg, 1991).

5.6.3.5.5 Parameter Estimation and Model Verification/Validation

The ^{14}C source term model is based on an abstraction of many complex processes. At the present time, the model can only be compared to data on UO_2 oxidation. It relates UO_2 oxidation to diffusion through two layers of material and outward diffusion of $^{14}CO_2$ through the same two layers. The simplifying assumptions taken in the model are:

- The fuel is represented by concentric spheres of a single set of dimensions (i.e., the irregular shape of the fragments and grains is not taken into account);

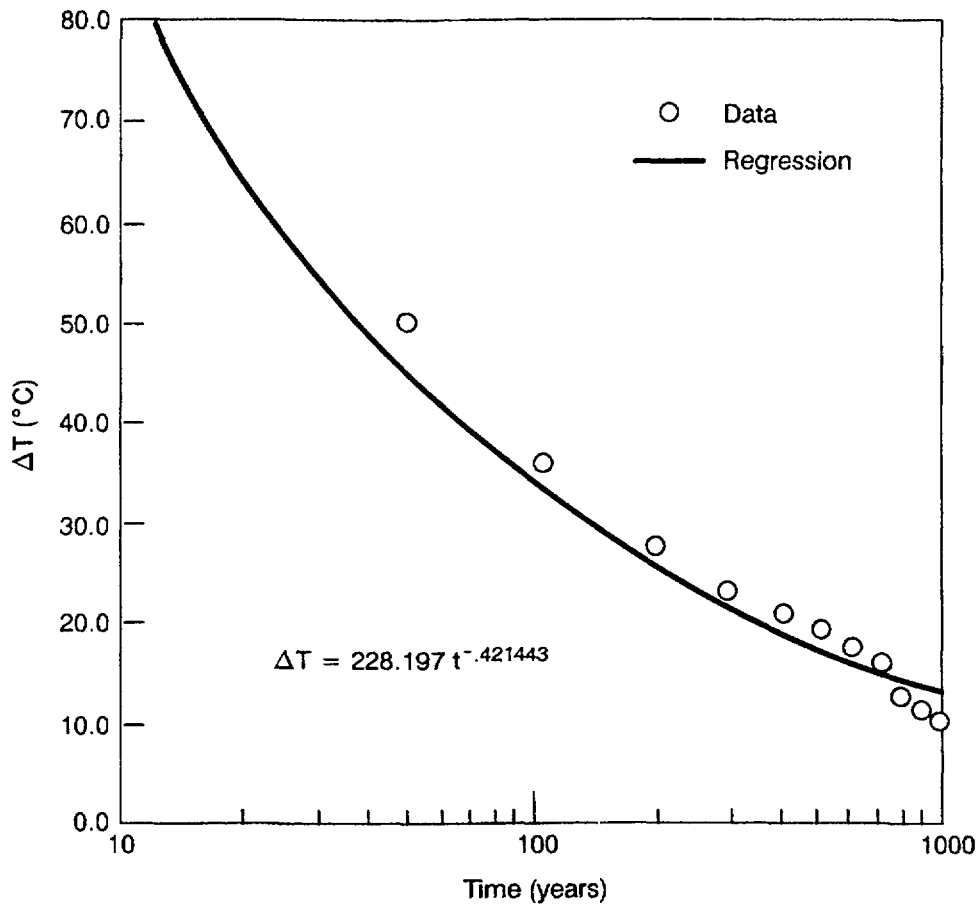

Figure 5–8 Fit of temperature difference between waste package skin and maximum fuel

- The current version of *SOTEC* allows only steady-state diffusion;
- No effects of the waste package or cladding on the diffusional processes are taken into account;
- The increase in surface area caused by oxidation of the grains is not taken into account; and
- Although there are some direct data on release of $^{14}CO_2$ from cladding and the grain/gap inventory, releases from the largest inventory in the fuel itself are lacking. There are data on UO_2 oxidation, but there are apparently no data available for release of $^{14}CO_2$ from fuel grain oxidation.

Nevertheless, the model was considered to be realistic enough that the parameters necessary for its implementation could be obtained from experimental data.

5.6.3.5.6 Data on Spent Nuclear Fuel Oxidation

Several investigators have collected data on the oxidation in air of spent and un-irradiated reactor fuel in connection with intermediate storage (Einziger, 1991, 1992; Einziger and Kohl; 1984; Einziger and Buchanan, 1988; Einziger *et al.*, 1991, 1992; Woodley *et al.*, 1989; and Thomas *et al.*, 1991). The main concern of these investigators was the degradation of the waste form for fuel in contact with oxygen at temperatures of several hundred °C (e.g., dry storage in air). The experimental programs concentrated on the physical changes to the fuel resulting from oxidation in failed rods rather than from the releases of radionuclides.

Quantitative data on fuel oxidation in air were basically of four types:

- Thermal Gravimetric Analysis (TGA);
- Dry-bath analysis;
- Ceramography; and
- X-ray crystallography.

In TGA, samples of spent nuclear fuel were exposed to air at fixed temperatures, and the gain in sample weight because of oxidation was recorded continuously, with an analytical balance. In the dry-bath tests, samples were kept in small crucibles held at fixed temperatures in an aluminum block, and weighed periodically outside the apparatus. The advantage of the dry-bath tests was that they could be performed for very long times, on the order of years, whereas the TGA experiments were limited to shorter periods, up to a few months.

Ceramography is the inspection of thin slices of spent nuclear fuel, to visually observe the growth of oxide films around individual fuel grains. These observations gave valuable, quantitative information about the sizes of fuel grains necessary for the implementation of the mathematical model and the rate of growth of the oxide thickness. In addition, ceramography gave qualitative information about the mechanisms of oxidation (e.g., the fact that the film of oxide appears to be growing at a consistent rate throughout the sample indicated that diffusion of oxygen through grain boundaries and cracks probably was much faster than the diffusion across the oxide layer, itself).

X-ray crystallography gave quantitative information on the chemical species of the oxide formed at different temperatures. Among the more interesting indications of X-ray crystallography was the observation that for temperatures below about 200°C, the oxide formed was primarily U_4O_9, even though it appeared to be U_3O_7 stoichiometrically (Einziger *et al.*, 1992).

5.6.3.5.7 Uses of the Data for Parameter Identification

Aside from identifying the chemical form of the oxide layer, only the quantitative data on grain size, growth of oxide film thickness, and sample weight were used, to determine the model parameters for fuel oxidation. Data on sample weight gain and film thickness at fixed temperatures were put into the form of "conversion fraction" of UO_2 to U_3O_7 versus time. The fuel oxidation model was then exercised to predict the conversion versus time of UO_2 grains to U_3O_7. The only model parameters that could vary were:

- Grain size (i.e., radius of inner sphere);
- Fragment size (i.e., radius of outer sphere);
- Diffusion coefficient through oxide layer at the reference temperature of 200°C;
- Diffusion coefficient through the grain boundary layer at the reference temperature of 200°C; and
- Activation energy for diffusion coefficient (considered to be equal for both layers).

The parameter identification does not at the present time take into account any differences between fragment sizes, grain sizes, or types of fuel.

Data on fuel conversion were collected in eight sets from TGA, Dry Bath, and ceramography, representing experimental periods from 700 to 12,000 hours, with the lower temperatures represented by the longer periods. Although data were available on whole-fuel fragments, as well as crushed fuel, only the whole-fragment data were used for the parameter identification for IPA Phase 2, because these samples were more like the actual spent nuclear fuel that would be in the repository.

The parameter identification was performed by manually varying the parameters and observing the agreement between predicted and observed conversion for the eight data sets. Parameters giving the best comparisons are given in Table 5–4.

Graphical results of the model/data comparison are given in Figures 5–9(a) through 5–9(h). Although there is a degree of scatter in the data, the model prediction is quite reasonable for the parameters chosen. Bear in mind that only one set of parameters was used to represent what are certainly nonhomogeneous samples.

5.6.3.5.8 Discussion

There are several facets of the model for ^{14}C release from the fuel matrix that could lead to errors. These factors are discussed below, and in the recommendations for further work, in Section 5.8:

- The IPA Phase 2 model considers only steady-state concentrations of oxygen and $^{14}CO_2$ in the fuel. Although it was possible to get a consistent fit of the model predictions to measured UO_2 conversion rates, there is some indication, from the transient modeling discussed in Section 5.6.3.5.1, that the coefficient for diffusion of oxygen through the grain boundaries should be relatively bigger than it appears in the steady-state model fit (Grambow, 1989). Thermal gravimetric analysis data on many samples indicate a period of very slow initial weight gain, followed by a substantially higher rate. This result has been interpreted as the transient diffusion of oxygen through the grain boundaries before oxidation of the grains. A transient model would be capable of simulating this phenomenon, but was not successfully completed for IPA Phase 2, because of problems with mass balance. The steady-state model used in IPA Phase 2 is incapable of simulating such a transient. At high temperatures where diffusion coefficients are large, there is relatively little difference between the conversion of large fuel fragments and crushed samples, indicating that the grain-boundary diffusion is fast. At lower temperatures, the difference between whole and crushed samples is much more evident. Although the steady-state model appears to fit the data well, it may, in fact, be portraying the transient diffusion as a much lower rate of conversion, especially at lower temperatures. This could lead to inaccurate predictions of conversion rates at low temperatures, for times much larger than the period of 12,000 hours, for the longest experiment;

- The IPA Phase 2 model assumes that the oxidizing fuel can be characterized by a single set of parameters. Actually, each sample of fuel oxidized in the laboratory consisted of grains of varying sizes, and material properties determined by their position in the fuel rod and distance from the pellet edge. Furthermore, the fuel would be expected to vary from one rod to the next, in the same core, and from one set of spent nuclear fuel to another, depending on such factors as reactor type, burnup, and fuel manufacturer; and

- The present model calculates an ensemble release rate from all waste packages, to feed into the gaseous transport model. Waste packages in different portions of the repository would be expected to have quite different gaseous release rates of $^{14}CO_2$, because of factors such as temperature, thermal loading, and age of the waste. Furthermore, the same factors would lead to gas-flow velocities varying from one portion of the repository to another, and these variations would be correlated to the variations in the $^{14}CO_2$ release rates.

Table 5–4 Model Parameters from Manual Identification

Model Parameter	*Value*
Grain radius (cm)	0.001
Fragment radius (cm)	0.1
Reference film diffusion coefficient (cm^2/yr)	5.256×10^{-4}
Reference grain diffusion coefficient (cm^2/yr)	5.942×10^{-3}
Reference temperature (°C)	200.0
Activation Energy (Kcal/mole)	32.0

5.7 Source Term Auxiliary Analyses

Two auxiliary analyses conducted for this demonstration were performed to evaluate the appropriateness and limitations of various computational approaches and interpretations of data used in this study. These analyses are summarized below.

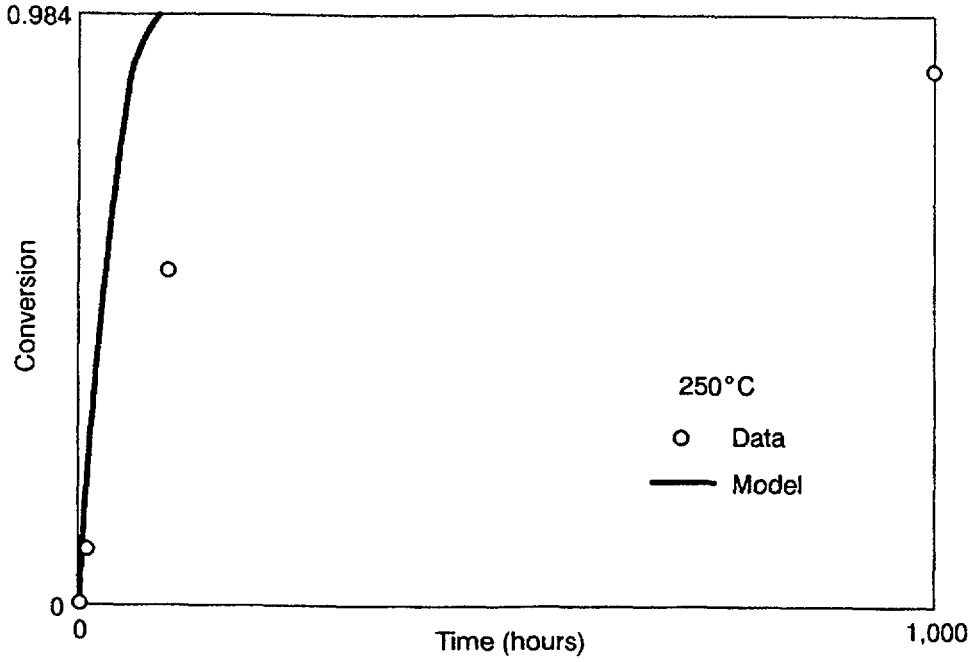

Figure 5–9a Model-prototype comparison, 250°C

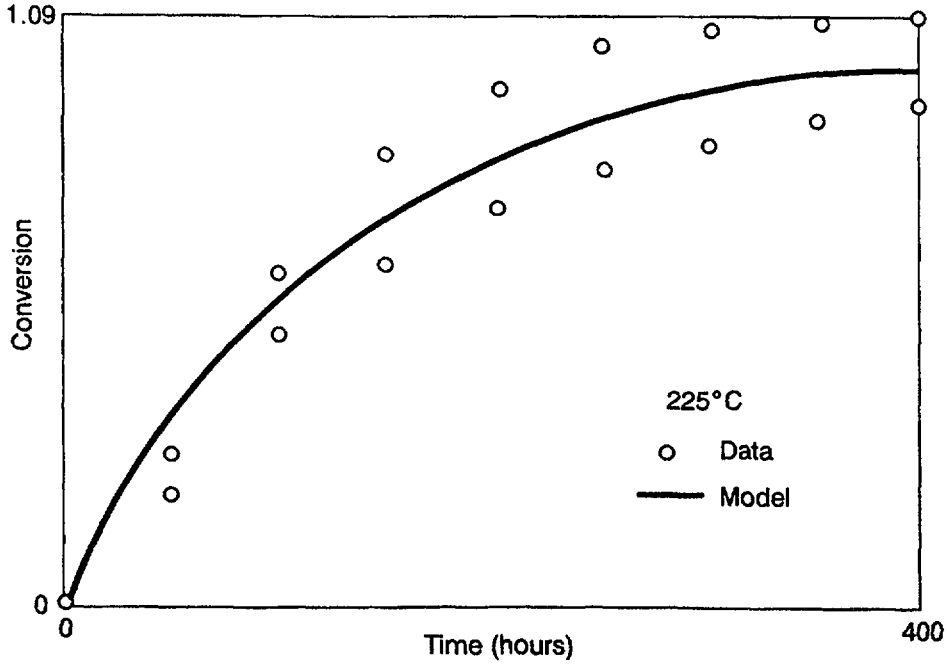

Figure 5–9b Model-prototype comparison, 225°C

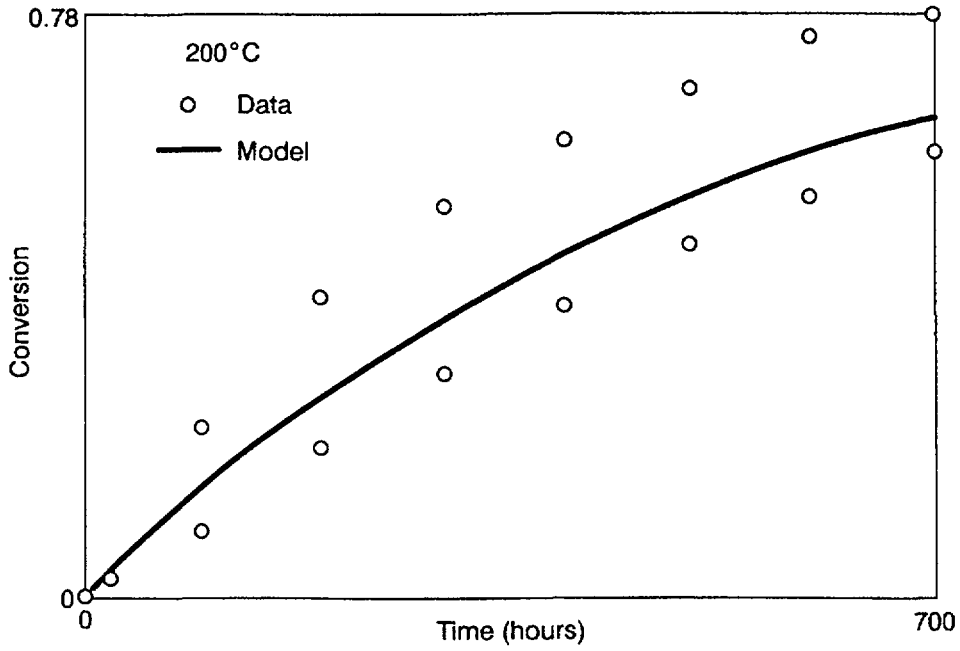

Figure 5–9c Model-prototype comparison, 200°C

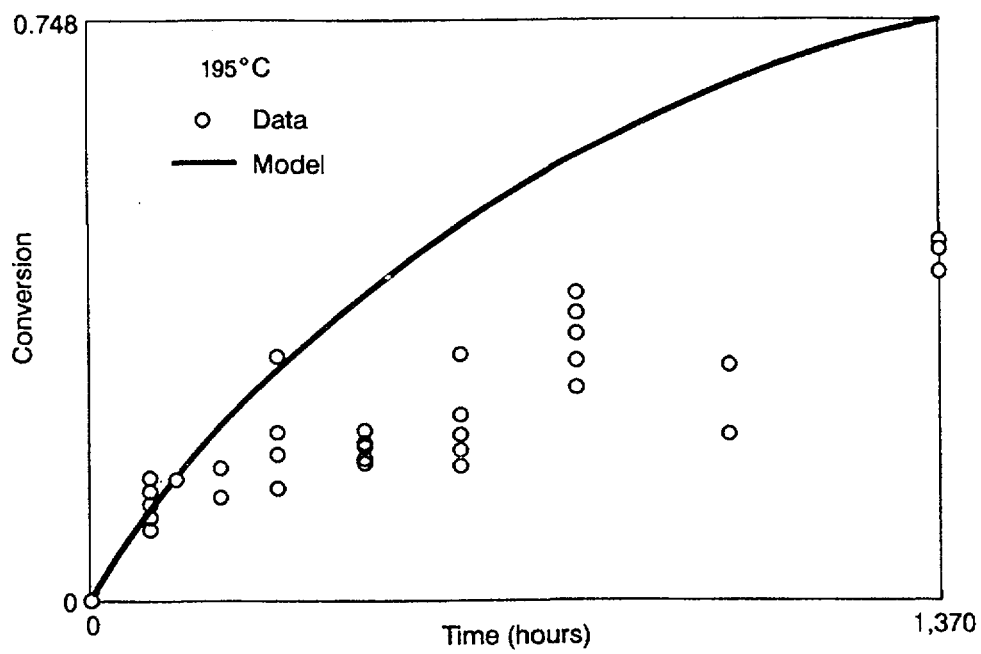

Figure 5–9d Model-prototype comparison, 195°C

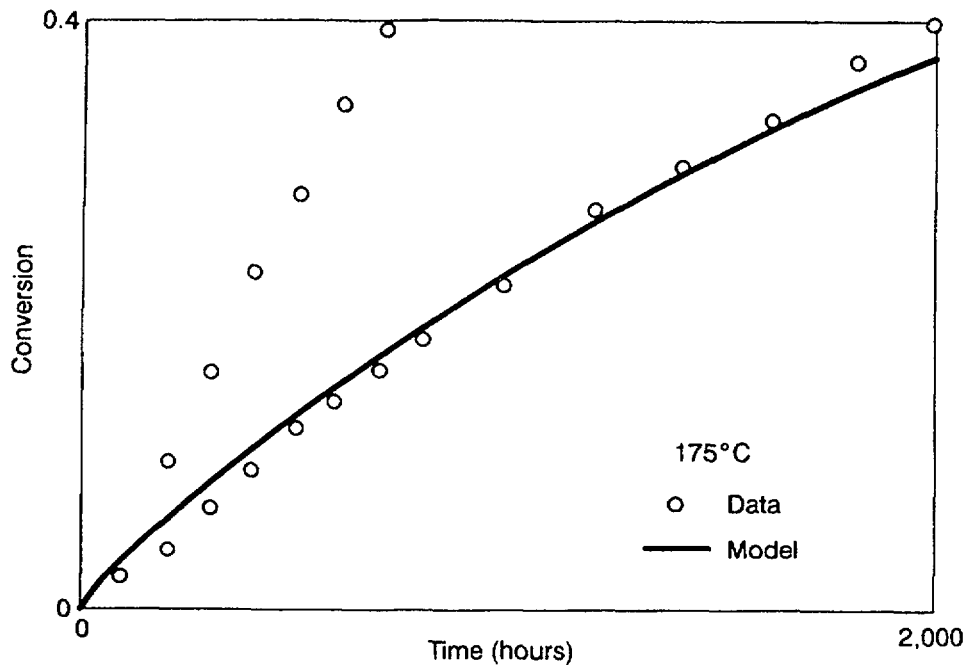

Figure 5–9e Model-prototype comparison, 175°C

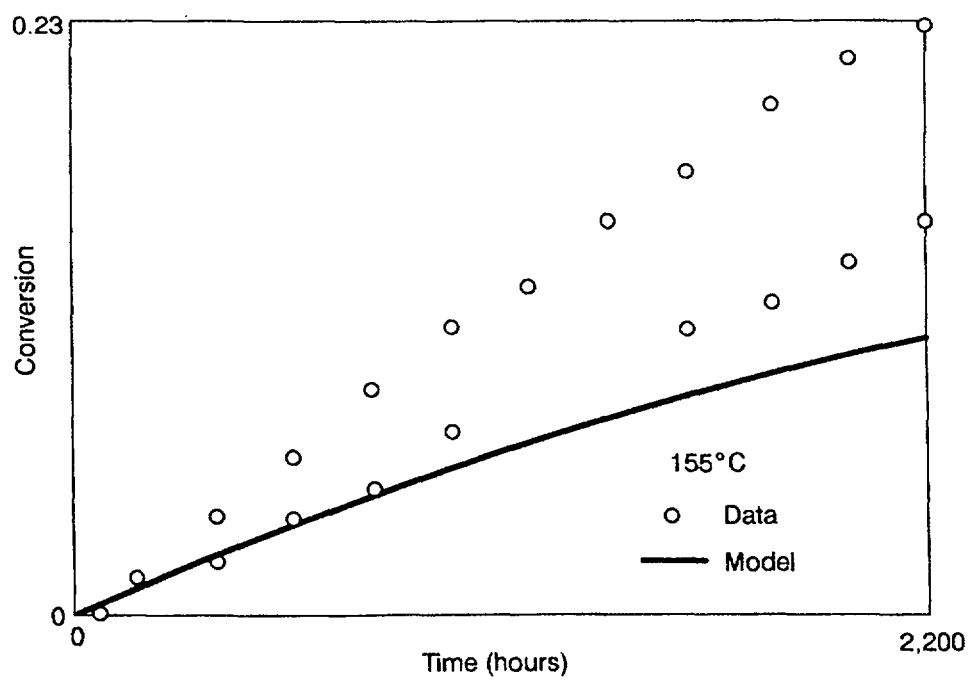

Figure 5–9f Model-prototype comparison, 155°C

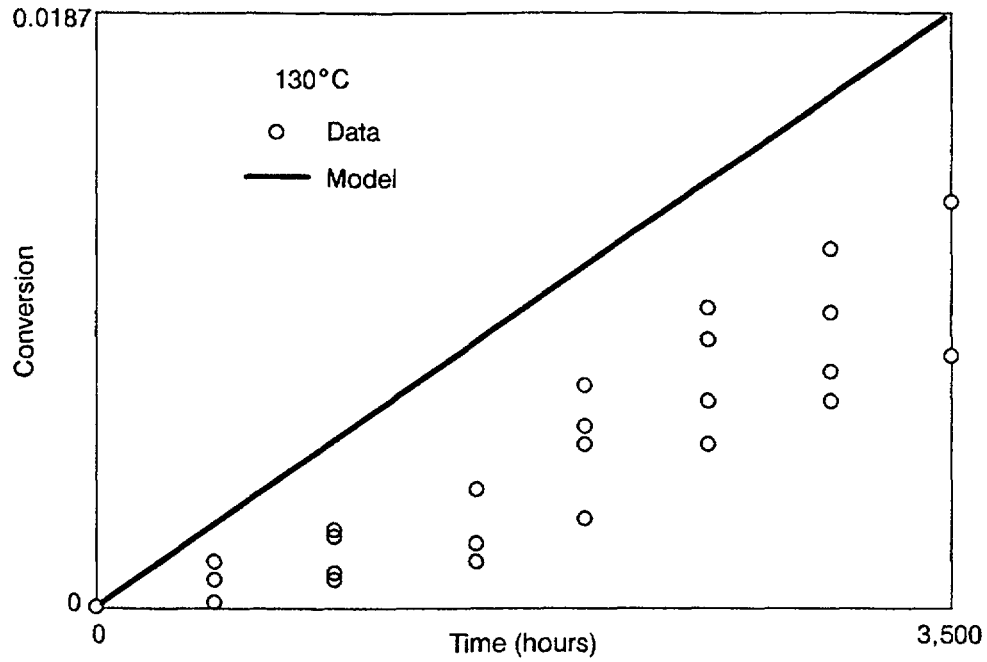

Figure 5–9g Model-prototype comparison, 130°C

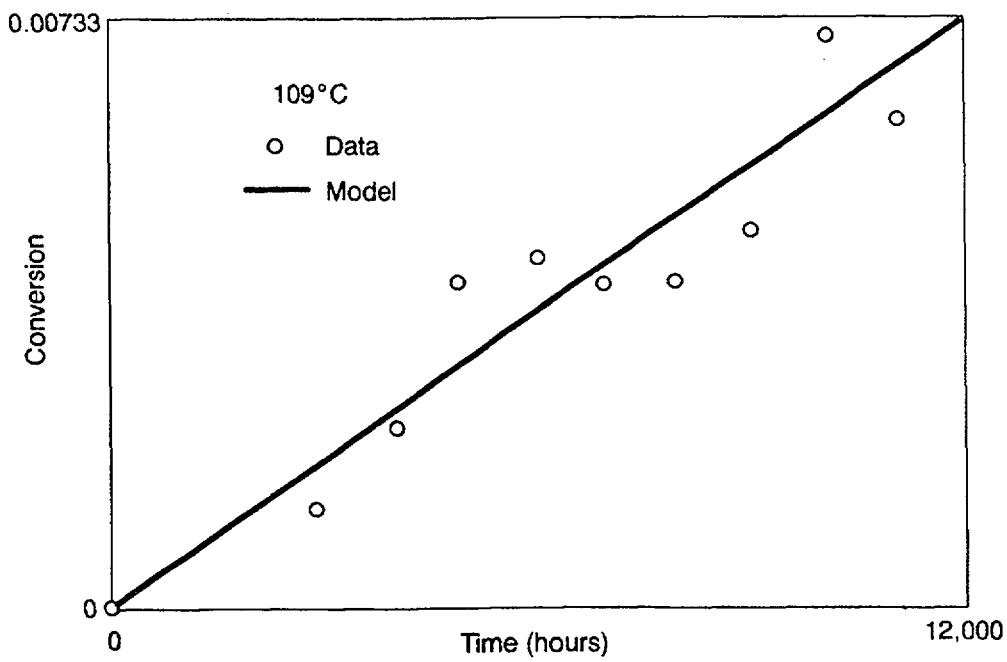

Figure 5–9h Model-prototype comparison, 109°C

5.7.1 Ensemble Averaging for Source Term Parameters

For the sake of computational speed in the systems model, the IPA Phase 2 analysis approximated the large number of individual waste packages by only seven repository sub-areas, with one waste package per repository sub-area. This analysis evaluates the way in which the averaging of a large number of waste packages can be accomplished with the least error. The demonstration of the effects of ensemble averaging of the parameters associated with the source term code was performed for a simplified case of only two radionuclides, one solubility limited and the other limited by congruent dissolution of the UO_2 fuel. Furthermore, both radionuclides were considered to have long half lives and the analysis did not consider decay daughters.

The staff concluded that for solubility limited releases of single, long-lived radionuclides, the ensemble average cumulative release per waste package would be represented by the arithmetic averages of the liquid flow rate q per waste package, waste package failure time, and the volume V_{fail} held by the waste package at the time of failure t_{fail}. The corresponding ensemble parameters for the congruent release case would be the harmonic mean flow rate per waste package, the mean of t_{fail}/q, and the mean of V_{fail}/q. There is presently no apparent way to choose the ensemble means of environmental parameters to use in the system analysis that would apply to all radionuclides.

This auxiliary analysis is discussed in greater detail in Appendix M.

5.7.2 Release and Transport of Potentially Gaseous Radionuclides Other than ^{14}C during Volcanism and Normal Operations

Several potentially volatile compounds of ^{79}Se, ^{99}Tc, and ^{129}I may be present in spent nuclear fuel. Because of the possibility of a gaseous pathway through the unsaturated rock at Yucca Mountain from the buried waste to the atmosphere, this auxiliary analysis investigated, using a series of conservative calculations, the phenomena by which volatile radionuclides could be released, and whether they posed enough of a threat to warrant further study.

Vapor pressure of possible volatile radionuclide compounds were taken from the available literature and also estimated thermodynamic information. Given the estimated vapor pressures, a portion of the inventories of the volatile radionuclides could be released at normal repository operating conditions. The bulk of the inventories of these radionuclides would be contained within the structure of the fuel, however, and the vapor pressures of those inventories would be reduced. Barometric pumping caused by changes in atmospheric pressure was considered a possible mechanism for release of volatile radionuclides from breached waste packages. For temperatures and atmospheric pressure variations in the 1988 SCP design, the staff's conservative calculations estimated that less than 1 percent of the inventory of volatile radionuclides would be released from the waste packages to the geosphere in 10,000 years. The staff further estimated that most of the volatile compounds would become associated with liquid water in the rock, rather than remaining in the gas phase.

The staff also estimated the effects of an intrusive basaltic dike causing temporary heating of the rock near waste packages. For a 10-meter-wide dike of 3000 meters length, the staff conservatively assumed that all volatile radionuclides in a 100-meter-wide region would be driven off by the increased temperature. This represents an area approximately 6 percent of the total repository sub-area for the 1988 SCP design. Even if all of the inventories of ^{99}Tc, ^{79}Se, and ^{129}I in 6 percent of the repository were released to the accessible environment, the total consequences would sum to only about 0.125 of the releases allowed under 40 CFR Part 191. The results of this analysis supported the staff's decision to neglect, for the time being, releases of volatile radionuclides other than ^{14}C in the Phase 2 analyses. This analysis, however, was based on preliminary models and data, and does not intend to foreclose further study of the issue of volatile radionuclides at Yucca Mountain.

5.8 Conclusions and Suggestions for Further Work

The following recommendations to improve the source term model came out of the work presented in Chapter 5:

1—Improve modeling of interaction between the waste and the near-field environment.

IPA Phase 2 analyses simplified treatments for the thermal, hydrological, and geochemical environments, based on the disposal concept of vertically placed waste packages surrounded by an air gap, as presented in DOE's 1988 SCP. Failure of the waste packages, by corrosion and transport of dissolved radionuclides from the waste package, is expected to depend on contact with liquid water. In IPA Phase 2, waste packages were considered to remain dry until their surface temperature dropped below the boiling point, and then assumed to come into contact with liquid water from dripping fractures and wet rock. Future models need: (1) plausible re-wetting mechanisms for dry rock; (2) the possible influx of liquid water such as dripping fractures; (3) condensation of water vapor on waste package surfaces, because of capillary and solution effects; (4) rise in the water table; and (5) water reflux, driven by repository or geothermal heat. Additionally, alterations to the hydrologic environment from climate change or hydrothermal processes, along with man-made changes, need to be factored into models for water influx. Models to determine accurately the contact of waste with liquid water will be highly design-specific to the repository concept finally adopted. Much of this work is expected to stem from confirmatory lab-scale and field-heater tests used to validate mathematical models of two-phase heat and mass transfer (Buscheck *et al.*, 1993). Since the experimental data must be necessarily of short duration and small-scale, relative to those of the repository, reliable mathematical models may be the only way to extrapolate results to greater times and distances. In this regard, the basis for the development of these models will rely on a mechanistic understanding of the processes and events related to waste package interaction with its environment.

2—Revise model for current DOE disposal concept.

IPA Phase 2 was based on the waste package concept described in DOE's 1988 SCP of single-walled packages placed vertically in boreholes, with an air gap between the waste package canister and the surrounding host rock. However, since the issuance of the SCP, DOE has developed a significant interest in more robust waste package concepts for both borehole and drift emplacement, including consideration of overpacked multi-purpose canisters for spent nuclear fuel. As part of its ongoing waste package Advanced Conceptual Design (ACD) (see TRW Environmental Safety Systems, 1993), DOE has identified various concepts for evaluation: (1) metallic multi-barrier containers; (2) metallic shielded containers; (3) small metallic multi-barrier containers; (4) nonmetallic multi-barrier containers; (5) overpacked multi-purpose canisters; (6) universal cask; (7) SCP single containers; and (8) defense HLW containers. Concurrent with the waste package ACD program, DOE is assessing the merits of various repository thermal loading strategies (i.e., cold, intermediate, and hot). Any decision regarding repository thermal loading should be integrated with the waste package concept. The behavior of the waste packages in the environment of the geologic repository will depend markedly on the concept finally adopted, the mode of emplacement (e.g., borehole or drift), and whether backfill or an air gap will be employed in the balance of the EBS design. The current models will have to be modified as DOE progresses in site characterization and makes decisions about its thermal loading strategy, waste package design, waste package materials, and additional engineered barriers.

3—Develop more mechanistic models for waste package corrosion.

Corrosion will be affected by a number of coupled processes that include heat and mass transfer, production of metal ions within the crevices and pits, and hydrolysis. Episodic evaporation and condensation of water on the surface of waste packages may result in high concentration of aggressive ions at temperatures well above the normal boiling point. The present version of *SOTEC* used in IPA Phase 2 considered simplified models for corrosion. General corrosion was assumed to begin when repository temperatures drop below boiling, and was described by a generic power law equation. Models of crevice and pitting corrosion assume an empirically derived temperature and radiation-dependent corrosion, critical and repassivation potentials,

and constant corrosion propagation rate. Needed improvements to *SOTEC* include codes abstracted from complex physics-based models, and inclusion of other localized corrosion modes, taking into account the geochemical environment and mechanical stresses. The models should also investigate the correlation between near-field chemical conditions, and corrosion and leaching.

4—Improve models for the effects of heat.

The present temperature model uses a semi-analytical approach for conduction-only. More realistic models could take heat and mass transfer in two-phase flow into account, to better estimate the temperature in the near field and the transfer of liquid water and water vapor (Buscheck, 1993), inputs needed to predict the onset of corrosion and the interaction of liquid water with the waste.

5—Take spatial and temporal variability into account in source term models.

For the sake of computational speed, IPA Phase 2 used an approach in which the entire repository was represented by only seven zones or sub-areas, within which all waste packages were of the same design and experienced the same environment. Future IPAs should deal with the difficult problem of spatial and temporal variability of material properties and external driving forces. If highly simplified models are required, then the IPAs should be able to demonstrate how spatial and temporal variabilities propagate through the system. IPA Phase 2 began to explore appropriate ensemble averages of the temporally and spatially varying input parameters for the simplified models.

An issue related to spatial and temporal variability is the distributed nature of some parameters. The distinction here is that the models might be able to account explicitly for known variations of parameters in space (e.g., temperature) and time (e.g., water flux). The distributed parameters cannot be completely characterized spatially or temporally, but should nevertheless be taken into account in the models. For example, *SOTEC* assumes that the oxidizing fuel can be characterized by a single set of parameters. The spent nuclear fuel, however, is highly heterogeneous, consisting of grains of varying size and material properties (Stout *et al.*, 1991). Improved source term models should take the variability of the properties of the spent nuclear fuel into account, either explicitly, or by defining effective input parameters that capture the variability without making the models too complex for total-system performance assessments.

6—Improve models for the release of gaseous ^{14}C.

For several reasons, the release of ^{14}C from the waste was one of the most important radionuclides identified in the IPA Phase 2 study: (1) ^{14}C can be released from the waste form as a gas whether or not there is liquid water involved; (2) the estimated inventory of ^{14}C in the spent nuclear fuel probably exceeds that which would be allowed under 40 CFR Part 191; and (3) there may be direct pathways for gaseous flow from the waste to the atmosphere through the unsaturated zone. *SOTEC* considers the release of gaseous $^{14}CO_2$ emanating from the waste form, tied to the oxidation of UO_2 from diffusing oxygen and escape of $^{14}CO_2$ through the oxidized film (Codell, 1993). There is little if any direct evidence of gaseous ^{14}C emanation from spent nuclear fuel, however, and the ^{14}C releases in *SOTEC* were based largely on speculation on the mechanisms for oxidation of the UO_2, and diffusion of $^{14}CO_2$ through the oxidized film and interstitial spaces.

A better model for gaseous ^{14}C emanations must await more definitive experimental data on spent fuel. Among the questions that await experimental results for the ^{14}C model are (Van Konynenburg *et al.*, 1987): (1) the chemical form of ^{14}C in the spent nuclear fuel; (2) the diffusion of the ^{14}C through the spent fuel matrix and the product of its oxidation, and the form of the diffusing substance (e.g., elemental carbon, CO, CO_2); (3) the variation in ^{14}C inventory in the different fuel assemblies, because of type of fuel, type of reactor and burn-up; (4) the rate of oxidation of ^{14}C in elemental or compound form; (5) the preferential locations of unoxidized ^{14}C in the fuel (e.g., along grain boundaries, within fuel grains); and (6) the effect of the state of UO_2 fuel oxidation on release (e.g., powdering of U_3O_8 at high temperature) (Tempest *et al.*, 1988).

Additional points concerning the model for $^{14}CO_2$ release are:

- The IPA Phase 2 model considers the release of gaseous $^{14}CO_2$ emanating from the waste based on steady-state diffusion of oxygen and $^{14}CO_2$. Although it was possible to get a

consistent fit of the model predictions to measured UO_2 conversion rates, there is evidence that transient diffusion may be important. Failure to include the transient diffusion of oxygen evident from the data could lead to inaccurate predictions of conversion rates at low temperatures. The model could be improved by considering transient diffusion.

- The Phase 2 model assumes that the oxidizing fuel can be characterized by a single set of parameters. The spent fuel, however, is highly heterogeneous, consisting of grains of varying size and material properties. Future IPA models should take the variability of the properties of the fuel into account explicitly.

- The present implementation of the model for the release of gaseous ^{14}C mixes the contribution from the seven repository sub-areas for use in the two-dimensional gas flow model. Since the release rate of ^{14}C is highly dependent on the temperature of the waste packages and the times of failure, this procedure might lead to needless errors in the release rate at the accessible environment. The procedure for calculating transport to the atmosphere should be revised to take into account the variations in release rate from the seven repository sub-areas.

7—Improve structural failure models.

Analytical expressions for buckling are only available for simplified geometries and loading conditions with static loads. A buckling model for a complex geometry and multiple and transient loads would require a complicated and computationally intensive simulation unsuited for IPA. The structural failure considered in IPA Phase 2 was for buckling of a highly simplified waste package weakened by corrosion, with external forces from seismic shaking. Structural failure depends on the engineering design, and the model should be adjusted accordingly, for changes. Once the engineering design has been finalized, the structural failure of the waste packages from dynamic and other forces could be analyzed deterministically by numerical and experimental techniques, and abstracted for IPA. These analyses would include the possible impact of mechanical fatigue of the waste packages from recurrent, low-intensity, seismic activity.

8—Consider modes of waste package failure other than corrosion.

Waste packages might also fail from mechanisms other than corrosion, such as seismic shaking, volcanism, and inadvertent human intrusion. Although IPA Phase 2 considered failure by drilling, volcanism and seismicity, the models were highly simplified. Improved models of seismic failure might take into account the range of frequencies of earth motion, and realistic dynamic modes of the waste packages. Models for failure by volcanism might take into account mechanisms of interaction between magma and the waste packages (e.g., corrosive gases and viscous forces). Improved models for human intrusion might consider the site-specific likelihood for exploratory drilling, shear forces from drilling fluids, and mechanisms that could bring radioactive material to the surface. These disruptive events could also have a significant effect on the other aspects of the repository performance.

9—Improve model for the dissolution of radionuclides from the waste form.

The chemistry within the waste package was treated in a highly simplified manner in IPA Phase 2. On waste package failure, water was assumed to infiltrate the waste package and come into intimate contact with the fuel. Radionuclides were released from the waste form to the inside of the waste package at a rate determined by the alteration rate of UO_2, and instantaneously from crud, gap, grain boundaries, and cladding. Transport out of the waste packages was limited by solubility of the nuclides. The models did not consider colloids explicitly; colloids were considered to be part of the dissolved inventory. The model could be improved by taking into account the formation and subsequent transport of colloids. Reflective of this interest, the NRC staff is presently conducting a literature survey of the role of colloids in the release and transport of radionuclides from vitrified waste forms and spent nuclear fuel. Improvements in the model for waste form dissolution should also consider speciation of the elements released to the water, the contribution of minerals from the groundwater and corrosion products from the waste package, the changing temperature, and other factors such as ionizing radiation. Subsequent iterations should also investigate models of spent

fuel dissolution based on electrochemical theories (Shoesmith and Sunder, 1992).

10—Improve model for transport of radionuclides from the waste package.

Mass transfer out of the waste package by flowing water and diffusion was included in IPA Phase 2, based on the 1988 SCP conceptual waste package. These transport mechanisms are highly specific to both waste package and overall repository design. Plausible mechanisms for transport from failed waste packages will need to take into account the design finally adopted by DOE. Both NRC and DOE total-system performance assessments considered rather simplistic idealizations for transport from the waste packages, such as bathtub or moist continuous cases (see Sagar *et al.*, 1992). However, in future assessments, the NRC staff plans to develop a more mechanistic model, which predicts the mass transport of radionuclides from the waste packages. The transport model, in conjunction with the waste form dissolution model, should consider the rates that water contacts and enters the waste package, interacts with the waste form, and transports radionuclides from the waste package by both advection and diffusion. The model should recognize that the suite of waste packages will represent a broad range of varying stages of degradation, with some completely intact and others significantly degraded from both anticipated and unanticipated processes and events. These conditions are progressive over the 10,000-year period of regulatory interest. Although conservatively neglected in *SOTEC*, the model could include recognition that degraded waste packages, including failed fuel (e.g., defective cladding), can still contribute to the isolation or controlled release of radionuclides, as demonstrated in static dissolution tests (Wilson, 1990).

11—Include models for other waste forms.

The NRC staff's first two IPAs focused on evaluating the performance of waste packages for spent fuel, recognizing that by the year 2030, spent fuel will constitute roughly 97 percent of the curie inventory of waste expected to be emplaced in a repository (DOE, 1992). However, this does not mean that the waste form resulting from the planned vitrification of existing defense-related HLW can be neglected as a potential contributor to the overall source term. Accordingly, in future IPAs, the staff should develop a source term model for the expected inventory of glass waste packages, with special consideration to the kinetics of glass dissolution, formation of secondary silicate mineral, colloid formation, and mass transport of radionuclides. Further, waste forms other than light water reactor spent fuel and defense-related glass may ultimately need to be considered if they are determined to be potentially significant sources. These may include any transuranic or greater-than-Class-C wastes.

12—Develop source term model abstractions for IPA.

Even though the analysis of the release of radionuclides to the geosphere from the waste form was highly simplified, the source term models and codes represented a large proportion of the overall complexity of IPA Phase 2. The recommended improvements listed above will further add to the complexity of the models. A substantial effort will be required to develop models that both take into account the complexity of the source term, yet are simplified enough to be practical for IPA.